ANNUAL REVIEW

INSTITUTE FOR MOLECULAR SCIENCE

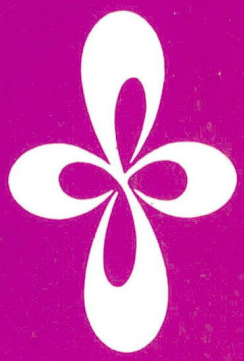

1986

ANNUAL REVIEW

INSTITUTE FOR MOLECULAR SCIENCE

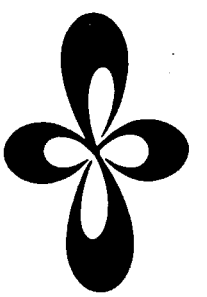

1986

Published by
Okazaki National Research Institutes
Institute for Molecular Science
Myodaiji, Okazaki 444, Japan
Phone 0564-54-1111
Telex 4537-475 KOKKEN J

IMS 1986

After celebrating the tenth anniversary in May 1985, IMS has made a new step toward further development of activity in its own works, in domestic joint programs with outside molecular scientists, and also in international cooperation projects. I expect that coming decade will be most prosperous era for IMS to bloom its scientific activity on the basis of high research potentiality cultivated during the past ten years and under the atmosphere full of an enthusiasm for scientific research.

We may say that the scientific activity of IMS proved fruitful in 1986. Since the success in test operation of our UVSOR (ultraviolet synchrotron orbital radiation) machine in November 1983, our staff has made efforts to improve its performance by attaching an undulator and a wiggler and also to set up various kinds of measurement systems attached to its beam lines. Because of the high stability and reliability of our machine, joint studies using UVSOR which officially started in April 1985 have made steady progress and have produced good fruits in the fields of photophysics, photochemistry, and molecular spectroscopy in the region extending from soft X-ray to far infrared. A supercomputer introduced in January 1985 is now in full operation and has made great contributions to development of computational molecular science. In addition to these I would like to mention that during the past year the research staff of IMS has added new scientific achievements of the very high order including ferromagnetic organic polymers, super-conductors of high critical temperature and others.

During the past year we have a good circulation of scientists between IMS and outside. I am happy to announce that Dr. N. Morita was appointed Associate Professor of Molecular Structure Laboratory as the successor of Professor S. Saito who had moved to Nagoya University.

Professor Per-Olov Löwdin completed his term of service as a foreign member of our Council at the end of last May. I would like to take this opportunity to express the sincere gratitude for his outstanding contributions to IMS. It is my great pleasure to have had Professor M. Eigen (Max-Planck Institute) and Professor R.G. Parr (The University of North Calorina) as new foreign members of our Council. I was delighted at the news that Professor Y.T. Lee of University of California, Berkeley who was staying at IMS as visiting professor from March to June, 1986 was awarded the Nobel Prize in Chemistry for 1986. I would like to extend my sincere congratulations to him for the great honour.

February 1987

S. NAGAKURA
Director-General

CONTENTS

ORGANIZATION AND STAFF

Organization

The Institute for Molecular Science comprises seventeen research laboratories – each staffed by a professor, and associate professor, two research associates and a few technical associates –, two research laboratories with foreign visiting professors, and six research facilities. The laboratories are grouped into five departments and one facility for coordination chemistry:

Department of Theoretical Studies	Theoretical Studies I
	Theoretical Studies II
	Theoretical Studies III[1)]
Department of Molecular Structure	Molecular Structure I
	Molecular Structure II[1)]
	Molecular Dynamics
Department of Electronic Structure	Excited State Chemistry
	Excited State Dynamics
	Electronic Structure[1)]
	Molecular Energy Conversion[2)]
Department of Molecular Assemblies	Solid State Chemistry
	Photochemistry
	Molecular Assemblies Dynamics
	Molecular Assemblies[1)]
	Synchrotron radiation Research[2)]
Department of Applied Molecular Science	Applied Molecular Science I
	Applied Molecular Science II[1)]
Coordination Chemistry Laboratories	Synthetic Coordination Chemistry
	Complex Catalysis

Research facilities are:

Computer Center
Low-Temperature Center
Instrument Center
Chemical Materials Center
Equipment Development Center
Ultraviolet Synchrotron Orbital Radiation (UVSOR) Facility.

1) Professors and associate professors are adjunct professors from universities.
2) Research Laboratories with foreign visiting professors.

Scientific Staff

Saburo NAGAKURA	**Professor, Director-General**

Department of Theoretical Studies

Tehoretical Studies I

Keiji MOROKUMA	Professor
Iwao OHMINE	Associate Professor
Koichi YAMASHITA	Research Associate
Chikatoshi SATOKO	Research Associate
Hideki TANAKA	Research Fellow (April '84–March '86), Technical Associate (April '86–)
Jun KAWAI	Graduate Student from Univ. of Tokyo* (April '85–)
Tadahiro OZAWA	Visiting Research Fellow from Kao Corp. (April '85–)

Theoretical Studies II

Hiroki NAKAMURA	Professor
Keiichiro NASU	Associate Professor
Kazuo TAKATSUKA	Research Associate
Hidemitsu HAYASHI	Research Associate
Akihiko OHSAKI	Technical Associate
Jun-ichi TAKIMOTO	Technical Associate
Masato NAKAMURA	IMS Fellow (April '86–)

Theoretical Studies III

Kichisuke NISHIMOTO	Adjunct Professor from Osaka City Univ. (April '85–)
Isao SHIMAMURA	Adjunct Associate Professor from Inst. of Phys. and Chem. Res. (April '84–March '86)
Koichiro NAKANISHI	Adjunct Associate Professor from Kyoto Univ. (April '86–)
Katsuhisa OHTA	Research Associate (–December '85)
Nobuaki KOGA	Technical Associate (–July '86), Research Associate (July '86–)
Masaki SASAI	Research Associate

Department of Molecular Structure

Molecular Structure I

Eizi HIROTA	Professor
Norio MORITA	Associate Professor (May '86–)
Chikashi YAMADA	Research Associate
Yasuki ENDO	Research Associate
Tetsuo SUZUKI	Technical Associate (–June '86)[1)]
Hideto KANAMORI	Technical Associate
Masatoshi KAJITA	Research Fellow (August '86–)
Tsutomu SHINZAWA	Graduate Student from Tokyo Inst. Tech.* (April '85–March '86)

Molecular Structure II

Shuji SAITO	Adjunct Professor from Nagoya Univ. (April '85–)
Hiroo HAMAGUCHI	Adjunct Associate Professor from Univ. of Tokyo (April '84–March '86)
Takayoshi KOBAYASHI	Adjunct Associate Professor from Univ. of Tokyo (April '86–)
Kentaro KAWAGUCHI	Research Associate

Takashi OGURA	Research Associate (August '86–)

Molecular Dynamics

Teizo KITAGAWA	Professor
Yasuo UDAGAWA	Associate Professor
Keiji KAMOGAWA	Research Associate
Kazuyuki TOHJI	Research Associate
Takashi FUJII	Technical Associate
Takanori MIZUSHIMA	Technical Associate (March '86–)
Hohi LEE	Technical Assistant (April '85–March '86)[2]
Noriyoshi KAKUTA	IMS Fellow (April '86–)
Shoji KAMINAKA	Graduate Student from Osaka Univ.* (April '86–)
Masatoshi NAKAGAWA	Graduate Student from Univ. of Tokyo* (April '86–)
Mutsumi HARADA	Graduate Student from Toyohashi Univ. of Tech.* (April '85–)
Akira ENDO	Graduate Student from Tokyo Metropolitan Univ.* (April '85–)
Takeshi MIKI	Graduate Student from Toyohashi Univ. of Tech.* (April '86–)

Department of Electronic Structure

Excited State Chemistry

Keitaro YOSHIHARA	Professor
Tadayoshi SAKATA	Associate Professor
Nobuaki NAKASHIMA	Research Associate
Kazuhito HASHIMOTO	Research Associate
Minoru SUMITANI	Technical Associate
Masahiro HIRAMOTO	Technical Associate
Hrvoje PETEK	Visiting Scientist (August '85–)
Nariaki HIROSHIGE	Graduate Student from Saga Univ.* (April '86–)
Yoshizumi KAJII	Graduate Student from Tokyo Inst. of Tech.* (April '85–)
Yoshinori YAMADA	Graduate Student from Toyohashi Univ. of Tech.* (April '86–)
Seiji AMAKUSA	Graduate Student from Nagoya Inst. of Tech.* (April '86–)

Excited State Dynamics

Ichiro HANAZAKI	Professor
Nobuyuki NISHI	Associate Professor
Iwao NISHIYAMA	Research Associate (–March '86)[3]
Masao TAKAYANAGI	Research Associate (October '86–)
Hisanori SHINOHARA	Research Associate
Masaaki BABA	Technical Associate (–February '86)[4]
Teruhiko NISHIYA	Graduate Student from Kyoto Univ.* (October '85–March '86), Technical Associate (April '86–)
Kazunori YAMAMOTO	Technical Associate
Kanekazu SEKI	Graduate Student from Univ. of Tokyo* (October '83–March'86)

Electronic Structure

Hisaharu HAYASHI	Adjunct Professor from Inst. of Phys. and Chem. Res. (April '84–March '86)
Noboru MATAGA	Adjunct Professor from Osaka Univ. (April '86–)
Hirochika SAKURAGI	Adjunct Associate Professor from Tsukuba Univ. (April '85–)

Ryoichi NAKAGAKI	Research Associate
Hiromi OKAMOTO	Research Associate (October '85–)
Takashi IMAMURA	IMS Fellow (April '85–June '86)
Yoshio FUKUDA	Visiting Research Fellow from Inst. of Phys. and Chem. Res. (April '84–March '86), Technical Assistant (April '86–)
Haruo ABE	Visiting Research Fellow from Inst. of Phys. and Chem. Res. (March '85–)

Molecular Energy Conversion

H.D. BIST	Visiting Professor from Indian Inst. of Tech. (August '85–May '86)
E. TIEMANN	Visiting Professor from Inst. At. Moleculphys., Univ. Hannover (FRG) (June '86–)
J. JESZKA	Visiting Associate Professor from Cent. Mol. Macromol. Stud., Pol. Acad. Sci. (Poland) (May '86–)

Department of Molecular Assemblies

Solid State Chemistry

Hiroo INOKUCHI	Professor
Inosuke KOYANO	Associate Professor
Kazuhiko SEKI	Research Associate (–July '86)[5]
Takashi IMAMURA	Research Associate (July '86–)
Shinzo SUZUKI	Technical Associate
Kenichi IMAEDA	Technical Associate
Hitoshi FUJIMOTO	JSPS Post-doctoral Fellow (April '86–)
Hiromichi YAMAMOTO	Graduate Student from Nagoya Univ.* (–March '86), Visiting Research Fellow (April '86–)

Photochemistry

Katsumi KIMURA	Professor
Kosuke SHOBATAKE	Associate Professor
Yohji ACHIBA	Research Associate (–March '86)[6]
Kiyohiko TABAYASHI	Research Associate
Katsuhiko OKUYAMA	Research Associate (August '86–)
Kenji SATO	Technical Associate (–September '86)[7]
Atsunari HIRAYA	Technical Associate (October '84–)
Haruo SHIROMARU	IMS Fellow (April '84–)
Nobuo HAYASAKA	Visiting Research Fellow from Toshiba Corp. (May '86–)
Marcus J.J. VRAKKING	Visiting Graduate Student from Eindhoven Univ. of Technology (September '85–April '86)

Molecular Assemblies Dynamics

Yusei MARUYAMA	Professor
Masatoshi SATO	Associate Professor
Tamotsu INABE	Research Associate
Masashige ONODA	Research Associate
Hajime HOSHI	Technical Associate (March '86–)
Naomi HOSHINO	Technical Associate (July '86–)
Hatsumi URAYAMA	Graduate Student from Ochanomizu Univ.* (–March '86)[8]
Yuji MATSUDA	Graduate Student from Univ. of Tokyo* (April '85–)
Shin-ichi SHAMOTO	Graduate Student from Kyoto Univ.* (April '86–)
Toshifumi NISHII	Visiting Research Fellow from Mitsubishi Petrochemical Co., Ltd. (–March '86)[9]

Molecular Assemblies

Hiroyoshi SUEMATSU	Adjunct Professor from Tsukuba Univ. (April '86–)
Nobuaki WASHIDA	Adjunct Associate Professor from National Inst. for Environmental Studies (April '85–)
Takehiko MORI	Research Associate
Shin-ichi NAGAOKA	Research Associate

Synchrotron Radiation Research

M. BAER	Visiting Professor from Soreq. Nucl. Res. Cent., Israel (September '85–June '86)
J. Robb GROVER	Visiting Professor from Brookhaven National Laboratory, U.S.A. (June '86–)
J.M. LEE	Visiting Associate Professor from Chonbuk Natl. Univ., Korea (April '86–)

Department of Applied Molecular Science

Applied Molecular Science I

Hiizu IWAMURA	Professor
Koshiro TORIUMI	Research Associate
Shigeru MURATA	Technical Associate
Katsuya ISHIGURO	Graduate Student from Nagoya Univ.* (April '85–)

Applied Molecular Science II

Soichi MISUMI	Adjunct Professor from Osaka Univ. (April '85–)
Tsutomu MIYASHI	Adjunct Associate Professor from Tohoku Univ. (April '86–)
Noboru KOGA	Research Associate
Hiroki OSHIO	Research Associate

Coordination Chemistry Laboratories

Kazuo SAITO	Director

Synthetic Coordination Chemistry

Sigeo KIDA	Professor
Shin-ichi ISHIGURO	Associate Professor
Kazuhiko OZUTSUMI	Research Associate
Masayoshi MIKURIYA	Research Associate
Honoh SUZUKI	Graduate Student from Tokyo Inst. of Tech.* (April '86–)
Eiji ASATO	Graduate Student from Kyushu Univ.* (April '86–)
Makoto HANDA	Graduate Student from Kyushu Univ.* (April '86–)
Kei-ichi SATOH	Graduat Student from Niigata Univ.* (October '86–)

Complex Catalysis

Kazuo SAITO	Professor
Taro SAITO	Adjunct Professor from Osaka Univ. (April '86–)
Shigenobu FUNAHASHI	Adjunct Associate Professor from Nagoya Univ.
Takamitsu KOUZUMA	Graduate Student from Kanazawa Univ.* (April '86–)

Coordination Bond

Humihiko TAKEI	Adjunct Professor from Tokyo Univ. (April '86–)
Shozo TERO	Adjunct Associate Professor from Tohoku Univ. (April '86–)

Research Facilities

Computer Center

Keiji MOROKUMA	Director
Hiroshi KASHIWAGI	Associate Professor
Umpei NAGASHIMA	Research Associate

Shigeyoshi YAMAMOTO	Technical Associate

Low-Temperature Center

Hiroo INOKUCHI	Director
Toshiaki ENOKI	Research Associate

Instrument Center

Ichiro HANAZAKI	Director
Iwao YAMAZAKI	Associate Professor
Keisaku KIMURA	Research Associate
Naoto TAMAI	Research Associate
Katsuhiro SUMI	IMS Fellow (Sept. '86–)

Chemical Materials Center

Hiizu IWAMURA	Director
Hidemasa TAKAYA	Associate Professor
Kazushi MASHIMA	Research Associate
Tetsuo OHTA	Technical Associate

Equipment Development Center

Eizi HIROTA	Director
Tadaoki MITANI	Associate Professor
Yoshihiro TAKAGI	Research Associate
Yoshiki WADA	IMS Fellow (April '85–)

Ultraviolet Synchrotron Orbital Radiation Facility

Hiroo INOKUCHI	Director
Makoto WATANABE	Associate Professor
Toshio KASUGA	Associate Professor
Hideo NAKAGAWA	Adjunct Associate Professor from Fukui Univ. (April '84–March '86)
Hisashi KOBAYAKAWA	Adjunct Associate Professor from KEK (April '86–)
Hiroto YONEHARA	Research Associate
Kazutoshi FUKUI	Research Associate (Sept. '85–)
Teruo HOSOKAWA	Visiting Research Fellow from NTT (April '85–)

Technical Staff

Akira UCHIDA	Technical Division Head
Keiichi HAYASAKA	Technical Section Chief
Kusuo SAKAI	Technical Section Chief
Satoshi INA	Computer Center (Unit Chief)
Fumio NISHIMOTO	Computer Center
Takaya YAMANAKA	Instrument Center
Shunji BANDOW	Instrument Center
Kiyonori KATO	Low-Temperature Center (Unit Chief)
Taeko MAEDA	Chemical Materials Center
Kazuo HAYAKAWA	Equipment Development Center (Unit Subchief)
Hisashi YOSHIDA	Equipment Development Center
Masaaki NAGATA	Equipment Development Center
Toshio HORIGOME	Equipment Development Center (Unit Subchief)
Norio OKADA	Equipment Development Center
Mitsukazu SUZUKI	Equipment Development Center

Nobuo MIZUTANI	Equipment Development Center
Shinji KATO	Equipment Development Center
Osamu MATSUDO	UVSOR Facility (Unit Chief)
Toshio KINOSHITA	UVSOR Facility
Masami HASUMOTO	UVSOR Facility
Jun-ichiro YAMAZAKI	UVSOR Facility
Eiken NAKAMURA	UVSOR Facility

* Carries out graduate research at IMS on the Cooperative Education Programs of IMS with graduate schools.
1) Present Address: Kobe Steel Limited, Wakihama-cho 1-3-18, Chuō-ku, Kobe, Hyōgo 651
2) Present Address: Chisso Petrochemical Corp., Goikaigan 5-1, Ichihara, Chiba 729-21
3) Present Address: Opto-Electronics Res. Lab., NEC Corp., Miyamae-ku, Kawasaki 213
4) Present Address: Dept. of Chemistry, Faculty of Science, Kobe Univ., Nada-ku, Kobe 657
5) Present Address: Department of Materials Science, Hiroshima Univ., 1-1-89, Higashi-Senda, Naka-ku, Hiroshima 730
6) Present Address: Department of Chemistry, Tokyo Metropolitan Univ., 2-1-1, Hukazawa, Setagaya, Tokyo 158
7) Present Address: Wako Institute, Honda Co., Wako 351-01
8) Present Address: Institute for Solid State Physics, Univ. of Tokyo, 7-22-1, Roppongi, Minato-ku, Tokyo 106
9) Present Address: Mitsubishi Petrochemical Co., Ltd., Toho-cho 1, Yokkaichi 510

Foreign Visiting Staff

Zurong Shi	Academia Sinica Inst. of Chemistry, China	May 18, 1985–May 14, 1986
M. C. Chang	Sun Cheon Natl. Univ., Korea	Jul.–Aug., 1985 Dec. 1, 1985–Jan. 31, 1986 Jun. 23–Jul. 6, 1986
Pierre Laszio	Univ. of Liege, Belgium	Aug. 26–Oct. 6, 1985
R. Chen	Dalian Inst. Chem. Phys., China	Aug. 27–Nov. 26, 1985
Edgar A. Silinish	Pysico-Energetic Institute, Academy of Science of Latvian SSR, USSR	Sep. 25–Dec. 23, 1985
Kyung H. Jung	KAIST, Korea	Dec. 21, 1985–Feb. 20, 1986
B. S. Lee	Inha Univ., Korea	Jan. 4–Mar. 3, 1986
Yuan-T. Lee	Univ. of California, Berkeley, USA	Mar. 1–Jun. 15, 1986
Jeremiasz Jeszka	Centre of Molecular and Macromolecular Studies, Polish Academy of Science, Poland	May 27–Nov. 26, 1986
Chantal Daniel	C.N.R.S., France	May 30–Dec. 1, 1986
J. Robb Grover	Brookhaven National Laboratory, USA	Jun. 6, 1986–Apr. 30, 1987
Martin R. Willis	Nottingham Univ. U.K.	Jun. 15–Sep. 12, 1986
Hee S. Yoo	Chungbuk Univ., Korea	Jul. 1–Aug. 31, 1986
Sang-Oh Oh	Kyungpook National Univ., Korea	Jul. 1–Aug. 31, 1986
Xin Sun	Fudan Univ., China	Jul. 17–Dec. 2, 1986

COUNCIL

Saburo NAGAKURA **Director-General**

Councillors

Chairman	Kenichi FUKUI	President, Kyoto Institute of Technology
Vice-Chairman	Hiroaki BABA	Professor, The Research Institute of Applied Electricity, Hokkaido University
	Hideo AKAMATU	Professor Emeritus, The University of Tokyo and IMS
	Masao FUJIMAKI	President, Ochanomizu University
	Ryuichi HIRANO	Professor Emeritus, The University of Tokyo
	Namio HONDA	President, Toyohashi University of Technology
	Soichi IIJIMA	President, Nagoya University
	Shô ITÔ	Professor, Tohoku University
	Masao KAKUDO	President, Himeji Institute of Technology
	Tetsuji KAMETANI	President, Hoshi University
	Masatoshi MORITA	Chief Executive Officer, Toyota Central Research & Development Laboratories, INC
	Minoru ODA	Director-General, The Institute of Space and Astoronautical Science
	Yoshihiko SAITO	Professor, Keio University
	Susumu SUZUKI	Director, The Research Institute for Iron, Steel and other Metals, Tohoku University
	Ikuzo TANAKA	President, Tokyo Institute of Technology
	Yutaka TOYOZAWA	Director, The Institute for Solid State Physics, The University of Tokyo
	Yasutada UEMURA	Professor, Science University of Tokyo
	Per-Olov LÖWDIN	Professor, University of Florida and Professor Emeritus, Uppsala University (–May '86)
	George C. PIMENTEL	Professor, University of California, Barkley (–May '86)
	Manfred EIGEN	Head of Department, Max-Planck Institute of Physical Chemistry and Professor, Technical University of Göttingen (August '86–)
	Robert Ghormley PARR	Professor, University of Northcarolina (August '86–)

The Council is the advisory board for the Director-General. Two of the councillors are selected among distinguished foreign scientists.

Professor Emeritus

Professor Hideo AKAMATU, ex-Director-General of IMS, was named the first professor emeritus of this institute in September, 1982.

Distinguished Research Consultants

Kenichi FUKUI	President, Kyoto Institute of Technology; Professor Emeritus, Kyoto University
Masao KOTANI	Professor Emeritus, The University of Tokyo
Yonezo MORINO	Professor Emeritus, The University of Tokyo; Director and Supreme Consultant, Sagami Chemical Research Center

Administration Bureau

Katsuhiko KURIOKA	Director-General, Administration Bureau (–March '86)
Kiyoshi INOUE	Director-General, Administration Bureau (April '86–)
Minoru OKAMOTO	Director, General Affairs Department
Seigo MIURA	Director, Finance and Facilities Department (–March '86)
Hozumi KISHIYAMA	Director, Finance and Facilities Department (April '86–)
Hideo ISHIKAWA	Head, General Affairs Division
Shigeyoshi ONO	Head, Personnel Division
Takeru YAMAKAWA	Head, Research Cooperation and International Affairs Division
Kaichi ONUMA	Head, Budget Division
Yasutaro NAGATA	Head, Accounts Division
Hirohiko URA	Head, Construction Division
Shoichi SATO	Head, Equipment Division (–March '86)
Motokazu FURUYA	Head, Equipment Division (April '86–)

BUILDINGS AND CAMPUS

The IMS campus covering 62,341 m^2 is located on a low hill in the middle of Okazaki City. The inequality in the surface of the hill and growing trees are preserved as much as possible, and low-storied buildings are adopted for conservation of the environment. The buildings of IMS are separated according to their funcitons as shown in the map. The Research Office Building and all Research Facilities except for the Computer Center are linked organically to the Main Laboratory Building by corridors. Computer Center, Library, and Administration Buildings are situated between IMS and the neighboring National Institute for Basic Biology and National Institute for Physiological Sciences, because the latter two facilities are common to these three institutes.

The lodging facility of IMS called Yamate Lodge, located within 10 min walk, has sleeping accommodations for 19 guests and two families. Since June 1, 1981 a new lodging facility called Mishima Lodge has been opened. Mishima Lodge, located within four minutes' walk east of IMS can accommodate 30 guests and ten families. Scientists who visit IMS as well as the two other institutes can make use of these facilities. Foreign visiting scientists can also live at these lodgings with their families during their stays.

The Institute for molecular Science

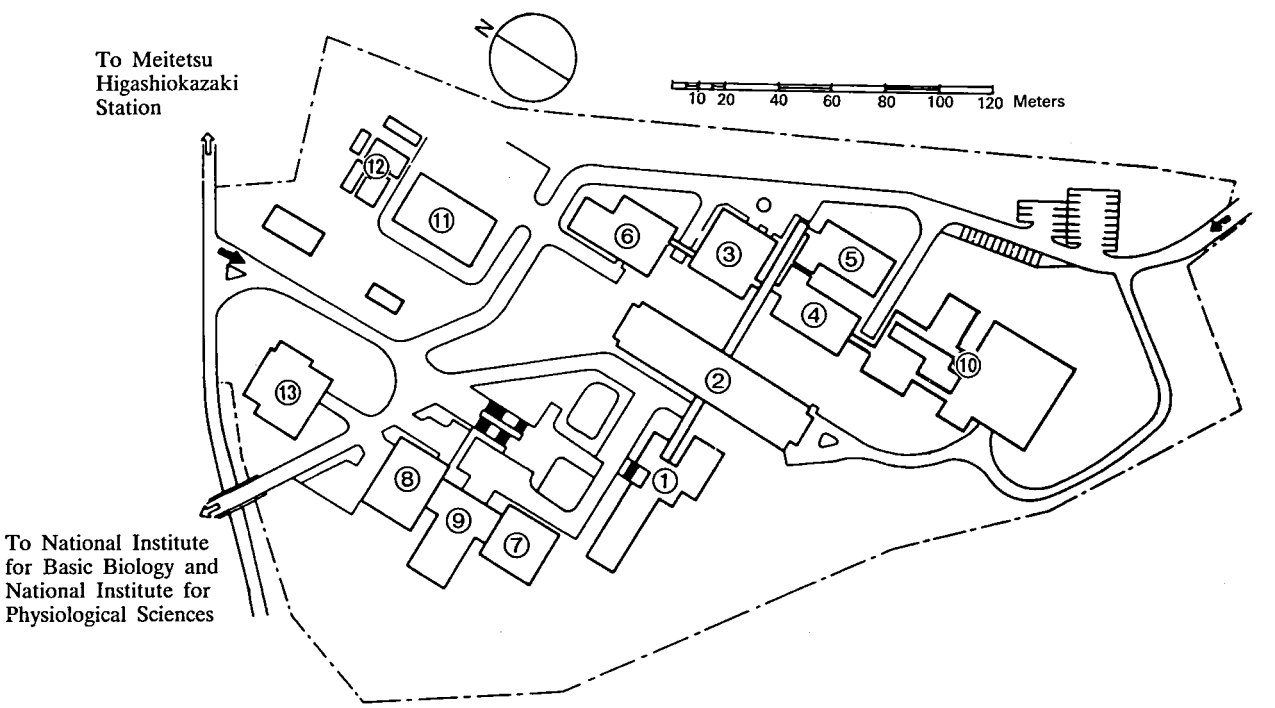

1. Research Office Building
2. Main Laboratory Building
3. Equipment Development Center
4. Instrument Center
5. Chemical Materials Center
6. Low-Temperature Center
7. Computer Center
8. Library
9. Central Administration
10. UVSOR Facility
11. Power Station
12. Waste-Water Disposition Facilities
13. Faculty Club

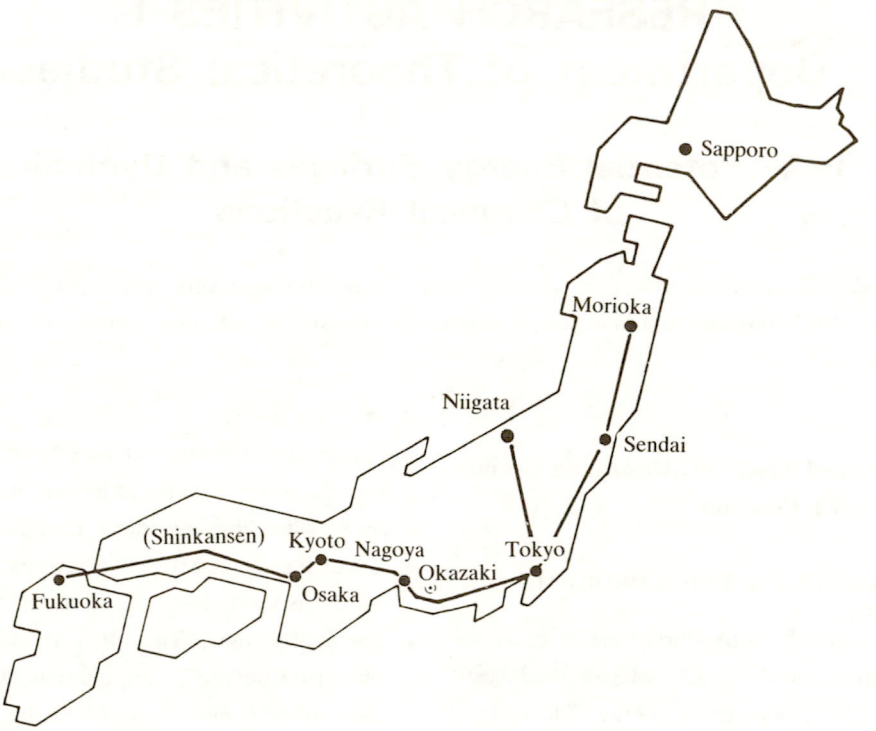

Okazaki (population 280,000) is 260 km southwest of Tokyo, and can be reached by train in about 3 hours from Tokyo via New Tokaido Line (Shinkansen) and Meitetsu Line.

The nearest large city is Nagoya, about 40 km west of Okazaki

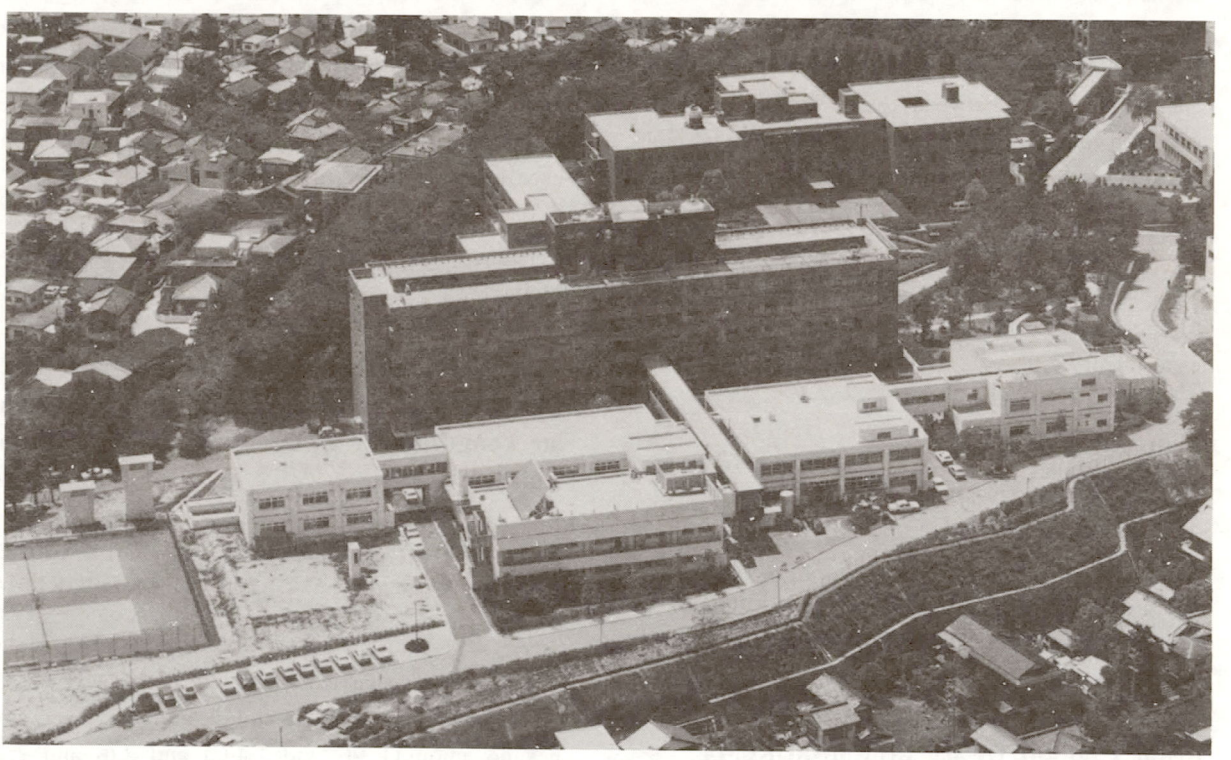

RESEARCH ACTIVITIES I
Department of Theoretical Studies

I-A Potential Energy Surfaces and Dynamics of Chemical Reactions

Dr. Katsuhisa Ohta, Research Associate who had worked in collaboration with the electronic structure group, left IMS in October, 1985. We have continued our theoretical studies on the potential energy surfaces and dynamics of chemical reactions.

I-A-1 Theoretical Study of Absorption Spectra for the K + NaCl Reaction

Koichi YAMASHITA and Keiji MOROKUMA

Photon absorption spectra during the reaction between the K atom and the NaCl molecule are investigated theoretically. The potential energy surface of the ground ($1^2A'$) and the electronically excited states ($2\text{-}4^2A'$ and $1^2A''$) are determined by the MRSD-CI method with the effective core potentials. The density of KClNa in configuration space of the ground state is obtained from classical trajectory calculations on the ab initio fitted potential surface. The absorption intensity is assumed to be proportional to the density of KClNa trajectory and the square of transition dipole moments at the respective geometries. The vertical energy difference between the ground and excited potential energies correspond to the transition frequency. Some structures seen in the spectra are interpreted in terms of characteristic features of the ground as well as the excited electronic states and the collision dynamcis on the ground state potential energy surface. The results are discussed in connection with the recent experiment.[1)]

Reference

1) T.C. Maguire, P.R. Brooks and R.F. Curl, *Phys. Rev. Lett.*, **50**, 1918 (1983).

I-A-2 Ab Initio Potential Energy Surfaces of the Electronically Excited Na Atom with the O_2 Molecule

Koichi YAMASHITA and Keiji MOROKUMA

The potential energy surfaces of the reaction between the 3^2S or 3^2P state Na atom with the O_2 molecule are investigated by ab initio configuration interaction calculations. The MRSD-CI method is applied with the DZP basis set. For the Na atom, the effective core potential is used. The MO's for CI calculations are obtained from the $^2\Sigma^-$ ground state SCF calculations. In the case of collinear approach, the interaction of the ground state O_2 molecule with $Na(3^2S)$ produces $1^2\Sigma^-$, and that with $Na(3^2P)$ produces $2^2\Sigma^-$ and $1^2\Pi$. These states are correlated adiabatically to the product ground state, $NaO(^2\Pi) + O(^3P_g)$, with the high energy barriers due to avoided crossings between the ionic state, $Na^+ + O_2^-$. A large collision energy is needed to promote the reaction on these potential energy surfaces. The ionic state, $Na^+ + O_2^-(^2\Pi_g)$, correlates to $2^2\Pi$, which is the most stable in the interaction region and have a lower barrier to the products. The results are used to discuss the mechanism of the recent experimental observation.[1)]

Reference

1) H. Schmidt, P.S. Weiss, J.M. Mestdagh, M.H. Covinsky and Y.T. Lee, *Chem. Phys. Lett.*, **118**, 538 (1985).

I-A-3 Stereo-Electronic Effects on Intramolecular Long-Distance Electron Transfer in Radical Anions

Nobuaki KOGA, Katsuhisa OHTA, Gerhart L. CLOSS *(Univ. of Chicago, U.S.A.)*, **and Keiji MOROKUMA**

As an extension of our previous study on the topics,[1)] we have carried out ab initio UHF MO + 2×2 CI calculations on 1,3- and 1,4-dimethylenecyclohexane anion (1,3-C and 1,4-C) and 2,6- and 2,7-dimethylenedecaline anion (2,6-D and 2,7-D) with the

STO-3G and the 4-31G basis set in order to evaluate the trans annular interaction matrix element for electron transfer. The order of the matrix element calculated with the 4-31G basis set is in agreement with experiments: 1,3-C > 1,4-C > 2,7-D > 2,6-D. It has been also found that the magnitude of this interaction is highly dependent on geometry, conformation and methylene rotational angle. The calculations on simpler model systems such as CH_2-$(CH_2)_n$-CH_2^- gave illuminating insight into the stereo-electronic effect. For instance, the matrix element as a function of the dihedral angle about the central CC bond from 0° to 180° in n=4 chain gave a maximum at 180° and a minimum at 0°; the interaction is the strongest, when all the conformations are trans. The calculations of n=1, 2, and 3 chains gave the similar trend of stereo-electronic effect. This stereo-electronic effect has been interpreted in terms of an orbital interaction scheme.

Reference
1) K. Ohta, G.L. Closs, K. Morokuma, and N.J. Green, *J. Am. Chem. Soc.*, **108**, 1319 (1986).

I-A-4 Origin of Exo Selectivity of Norbornene. An Ab Initio MO Study

Nobuaki KOGA, Tadahiro OZAWA *(IMS and Kao Corp.)*, **and Keiji MOROKUMA**

It is an often asked question why exo addition is preferred for norbornene and its derivatives in reactions such as hydroboration, epoxidation, and cycloaddition. In order to analyze the factors that govern the exo selectivity, we have determined the transition states for both exo and endo addition of BH_3 to norbornene with an ab initio MO method. The transition state optimization with the energy gradient method with the 3-21G basis set shows that the activation barrier for exo attack is 5.3 kcal/mol, which is lower than that for endo attack by 8.8 kcal/mol, in agreement with the experimentally observed trend of exo preference. We have also estimated the activation energy differences between exo and endo attack due to the staggering effect proposed by Houk et al., the endo deformability proposed by Morokuma et al. and Gleiter et al., and the steric effect and found them to be 2.2, 5.5, and 1.0 kcal/mol, respectively. This estimation indicates that exo selectivity originates mainly from the endo deformability, assisted by staggering effect at the transition state.

I-B Theoretical Studies of Moleculer Structure and Spectroscopy

Theoretical studies in the last several years have been providing useful information as to the structure and spectroscopy of transition species. We are pleased to continue to participate in such activities in collaboration with experimental groups within and outside IMS.

I-B-1 A Molecular Orbital Study of Protonated N_2O

Koichi YAMASHITA and Keiji MOROKUMA

[*Chem. Phys. Lett.*, **131**, 237 (1986)]

The structures of isomers of protonated N_2O in the ground state are determined by the ab initio MP2 gradient method with a 6-31G* basis set. Calculations at the MP4SDQ/6-311G** level predict that the O-protonated N_2O is the most stable isomer and is lower in energy by 7.1 kcal/mol (with zero point corrections) than the N-protonated form. The rotational constants and the OH stretching frequency predicted for the O-protonated isomer are fairly in agreement with the recent observation.[1] These findings indicate that the ion which observed experimentally is the O-protonated isomer. The singlet and triplet biradical intermediates, which connect the two isomers, are found to be around 80 kcal/mol higher in energy than the N-protonated N_2O, and this suggests that the N-isomer is experimentally observable.

Reference
1) T. Amano, *Chem. Phys. Lett.*, **127**, 438 (1986).

I-B-2 Ab Initio Configuration Interaction Study on the Vibrational Structure of the FHF^- Ion

Koichi YAMASHITA and Keiji MOROKUMA

Ab initio configuration interaction calculations are performed to investigate the vibrational structure of the FHF^- ion. The SDCI method is applied using the DZP basis set augmented with an anion p function on the F atom. The Davidson's formula is used to estimate the contribution from quadruple excitations. The potential energies are evaluated as a function of the symmetric and anti-symmetric stretching normal coordinates. Variational calculations are carried out on the SDQCI/DZP+Ap potential surface fitted to a polynomial of normal coordinates. The results do not change a qualitative feature of the fundamental, overtone and combination bands predicted by Almlof[1] at the SCF/DZP level; the effect of correlated wavefunction seems to be rather small on the vibrational structure of the ion. A disagreement between these theoretical predictions and the recent gas phase observation[2] of FHF^- is then still an open-question.

References
1) J. Almlof, *Chem. Phys. Lett.*, **17**, 49 (1972).
2) K. Kawaguchi and E. Hirota, *J. Chem. Phys.*, **84**, 2953 (1986).

I-B-3 Ab Initio Calculations of the Dipole Moments in Low-Lying Electronic States of the CCN Radical

Koichi YAMASHITA and Keiji MOROKUMA

The dipole moments in the four low-lying electronic states ($X^2\Pi$, $A^2\Delta$, $B^2\Sigma^-$ and $C^2\Sigma^+$) of the CCN radical are investigated by ab initio calculations. The geometries of the radical in each electronic states are determined at the level of MRSD-CI as well as SCF with the DZ and DZP basis sets. For the electronically excited states, the MRSD-CI/DZP dipole moments are calculated to be around 3.0 D. However, a significantly small dipole moment, ~0.6 D, is predicted for the ground state. This result is consistent with a failure of observing the signals of microwave-optical double resonance for the ground state CCN.[1]

Reference
1) T. Suzuki, S. Saito and E. Hirota, *J. Chem. Phys.*, **83**, 6154 (1985).

I-B-4 Study of Correlation Effects on Stretching Force Constants of The $H_3N\cdots LiF$ Lithium–Bonded and $H_3N\cdots HF$ Hydrogen–Bonded Complexes

Zdzistaw LATAJKA*, Henryk RATAJCZAK* *(*Univ. Wrocław, Poland)*, **Keiji MOROKUMA, and W.J. ORVILLE-THOMAS** *(Univ. Salford, UK)*

[*J. Mol. Str. (Theochem)*, in press]

All quadratic, cubic and quartic force constants associated with high and low vibrational modes of the $H_3N\cdots HF$ hydrogen-bonded and $H_3N\cdots LiF$ lithium-bonded complexes have calculated employing the Møller-Plesset perturbation theory to the second order (MP2) with the 4-31G** basis set.

I-B-5 Nuclear Quadrupole Coupling Tensors for Hydrazine, Methylhydrazine, and 1,2-Dimethylhydrazine as Determined by Microwave Spectroscopy and Ab Initio Calculation

Kaoru YAMANOUCHI*, Shigeki KATO*, *(*Univ. of Tokyo)*, **Keiji MOROKUMA, Masaaki SUGIE**, Harutoshi TAKEO**, Chi MATSUMURA**,** *(**Natl. Chem. Lab. Ind.)*, **and Kozo KUCHITSU***

[*J. Chem. Phys.*, in press]

The nuclear quadrupole coupling constants for the ^{14}N nuclei in hydrazine (HY) and the two conformers of 1,2-dimethylhydrazine (DMH) were determined by a least-squares analysis of the observed hyperfine structures as follows (in MHz): $\chi_{aa} = 4.14(8)$ and $\chi_{bb} = -2.15(15)$ for HY, $\chi_{aa1} = 2.92(30)$, $\chi_{bb1} = 1.35(32)$, $\chi_{aa2} = 2.38(33)$, and $\chi_{bb2} = -4.69(35)$ for the inner-outer conformer of DMH, $\chi_{aa} = 2.84(30)$ and $\chi_{bb} = 0.32(43)$ for the outer-outer conformer of DMH. The coupling constants for HY, DMH, and the inner and outer conformers of methylhydrazine were evaluated by ab initio calculations. Configuration interaction calculations were also performed for HY. The calculated coupling constants were compared with the observed ones and used to derive the principal values of the coupling constants by a procedure developed in the present study. The characteristic dependence of the χ tensors on the conformational structure demonstrates practical utility of an ab initio calculation of hyperfine structures for a spectral analysis.

I–C Structure and Reaction of Transition Metal Complexes

One of our initial goals of theoretical studies of transition metal complexes has been to understand theoretically a full catalytic cycle consisting of several elementary reactions. This goal is becoming near with our study of Wilkinson catalysis cycle.

I-C-1 Mechanism of Hydrogenation Reaction by Wilkinson Catalyst: An Ab Initio MO Study

Nobuaki KOGA, Chantal DANIEL, Jin HAN*, Xiao-Yuan FU* *(*Beijing Normal Univ. and IMS)*, **and Keiji MOROKUMA**

In order to determine the energetics and identify the structures of intermediates and transition states involved in the hydrogenation of ethylene by Wilkinson catalyst, we have carried out ab initio RHF MO calculations for the reactions:

$Rh(Cl)(PH_3)_2 + H_2 + C_2H_4$ **(1)** $\rightarrow Rh(Cl)(H)_2(PH_3)_2 + C_2H_4$ **(2)** $\rightarrow Rh(Cl)(H)_2(C_2H_4)(PH_3)_2$ **(3)** $\rightarrow Rh(Cl)(C_2H_5)(H)(PH_3)_2$ **(4)** $\rightarrow Rh(Cl)(PH_3)_2 + C_2H_6$ **(5)**

The relative energies of complexes are calculated to be 34.7 kcal/mol for **1**, 8.7 kcal/mol for **2**, 0.0 kcal/mol for **3**, 16.4 kcal/mol for **4**, −12.6 kcal/mol for **4a**, the most stable isomer of **4**, and −9.9 kcal/mol for **5**. The calculated activation barriers for **3** → **4** and **4a** → **5** are 18.4 and 14.4 kcal/mol, respectively. The catalytic process **1** to **5** is totally exothermic by 43.7 kcal/mol and does not require a large activation barrier. The rate-determining step consists of the insertion of ethylene, **3** → **4**, followed by the isomerization of the ethyl complex. An energetically more reliable MP2 calculation suggests that these two steps may actually take place as one combined step.

I-C-2 Origin of Alkenyl Group Distortion in $Ti(C(SiH_2CH_3)=CH_2)X_2^+$: Donative Interaction of SiC σ and CH Bonds with Ti Vacant d Orbitals

Nobuaki KOGA and Keiji MOROKUMA

We have optimized the structure of $Ti(C(SiH_2CH_3)=CH_2)(Cl)_2^+$ by an ab initio MO method and found a distorted alkenyl group with a small TiCSi bond angle, a long SiC^γ bond and a short $Ti\ldots C^\gamma$ distance, all of which are in good agreement with the experiment[1] on $Ti(C(Si(CH_3)_3)=C(C_6H_5)(CH_3))(Cp)_2^+$. The calculated $C^\gamma H$ bond is also long, indicating the presence of an agostic interaction between Ti and $C^\gamma H$. Evidences have been found showing that the alkenyl group distortion is a consequence of the donative interaction from the SiC σ bond to a Ti vacant d orbital, assisted also by the CH → Ti d agostic interaction. The origin of this SiC...M interaction is the same as that of CH...M agostic interaction. Therefore, the CSi...M interaction found here may be called the $^\beta$SiC agostic interaction.

Reference

1) J.J. Eisch, A.M. Piotrowski, S.J. Brownstein, E.J. Gabe, F.L. Lee, *J. Am. Chem. Soc.*, **107**, 7219 (1985).

I-C-3 Formaldehyde Insertion into Ruthenium-Hydride: A Theoretical Study

Shinichiro NAKAMURA *(IMS and Mitsubishi Chem. Ind.)* **and Keiji MOROKUMA**

Formaldehyde insertion reaction into ruthenium-hydride has been studied with an ab initio MO method. This reaction is an important key step toward ethylene glycol and methanol formation in the catalyzed hydrogenation of carbon monoxide. The structure and the relative energy have been calculated for $H_2Ru(CO)_3(CH_2O)$, $HRu(CO)_3(CH_2OH)$ and $HRu(CO)_3(OCH_3)$ and for the transition states connecting them.

I–D Development and Application of the Local-Density-Functional Methods

The local-density-functional (LDF) methods are quite convenient for the study of such systems as solids, surfaces, and large clusters. On the base of the electronic structures by the LDF methods, we study the stable geometry and dynamical processes of surfaces, clusters and the final state interaction effect on high energy spectra.

I-D-1 Many Body Effects on the Dynamical Properties of Metal Clusters

Chikatoshi SATOKO

Dynamical properties of clusters have been studied by many methods such as a self-consistent harmonic method, molecular dynamics, and Monte-Carlo methods. For strongly anharmonic system such as melting, the self-consistent harmonic approximation has been done in the Born-Mayer pair interaction between metal atoms. The calculated melting points were, however, too high to fit with experimental values. One reason is that the self-consistent harmonic approximation does not describe the cooperative moiton of each atom. Another reason is that the pair potential obtained from experimental data of the infinite solid is not suitable for the small system. Therefore other methods are required for studies of the melting of the metal fine-particles.

To get the correct interaction between metal atoms we introduce the adiabatic potential which is calculated from the sum of electronic total energies of the Hubbard Hamiltonian and core repulsive energies. To study the collective motion we try to carry out the molecular dynamics. Stable structures of alkali atom clusters at 0 K are obtained up to the number of the 20 atoms. When the temperature is raised, the movement of atoms in the alkali-metal cluster seems to be in several groups. The number of atoms in each group corresponds to the magic numbers 2 and 8 of the alkali-metal clusters. This behavior is considered to be characteristic of the many-body interaction between the metal atoms.

I-D-2 Stabilities of Clusters Si_n and C_n — Static Properties —

Chikatoshi SATOKO

Recently molecular beam mass spectroscopies show some clusters to be more stable. Interactions between Si atoms and C atoms are not only more than three-body ones, but also s-p hybridization ones. We introduce a simple Hamiltonian to study stable geometries of the Si and C clusters. Parameters in the Hamiltonian are determined from calculated electronic structures of the small clusters by the LCAO-Xα method.

It is very complex to find minimum points of the total energy in the large cluster. We obtain stable geometries by the Car's dynamical method which is very useful to study the lowest state in a large dimensional space. The optimized stable geometries of the silicon cluster from Si_2 to Si_{20} are determined. The stable cluster Si_6 has the close structure with the result of the LCAO-Xα-Force calculations. The stable cluster Si_7 has the distorted-pentagon structure which may grow to the amorphous silicon in the crystal growth. We calculate fragmentation energies which are defined as the difference between the binding energies of the clusters n and n-1. The clusters, Si_4 and Si_{11}, have more stable structures than the others.

We calculate stable geometries of C_n($N<21$) and C_{60} clusters in the same way. The stable clusters from C_3 to C_6 are linear. The dependence of bond lengths on the size of the cluster shows the Peiels distortions. The stable cluster C_7 is not linear, but circular. The cluster C_{60} is optimized in the distorted soccer boll which is made of the assembly of C_{10} clusters.

I-D-3 Chemisorption Process of the Transition Metal Atoms on the Si(111) Surfaces

Chikatoshi SATOKO, Shuhei OHNISHI *(NEC Corp.)* **and TIAN Zeng-ju** *(Fudan Univ. and IMS)*

Studies on electronic structures of the interface between a metal and a semiconductor are important for the formation mechanism of the Schottky barrier height

and the Ohmic contacts. Recently initial stages of the silicide formation process have been observed by many experiments such as the photoemission spectra, Auger, EXAFS and so on. The experimental results show that the silicide formation process is greatly dependent on the chemical species of the transition metal: Ni atoms make two-dimensional super-lattice on the Si(111) surface, while metal Cr atoms are reactive and intermixing with the silicon at the room temperature. To elucidate the microscopic mechanism of the silicide formation we calculate the electronic structure and forces acting on the transition metal and the Si atoms by the LCAO-Xα-force cluster method.

The calculated results show that the complex behaviors of the silicide formation are understood by the occupation number in the d-orbitals dπ, dσ, dδ of the transition metal atoms. The d-orbitals interact with the surface dangling bond of the first layer Si atoms when the metal approaches to the surface. The strong antibonding orbital dσ is not occupied for the Cr metal-, but for the Ni atoms. Therefore the Cr atoms easily penetrate under the surface, while the Ni atom is not. Further calculation is now in progress.

I-D-4 Chemical Effects on the Hidden Satellite of Potassium Kα X-ray Spectra

Jun KAWAI *(Univ. of Tokyo and IMS)*, **Chikatoshi SATOKO, and Yohichi GOHSHI** *(Univ. of Tokyo)*

[*J. Phys. C.*, in press]

X-ray emission spectra have characteristics to reflect the electronic structure or chemical state of matter. Satellite structures in x-ray emission spectra have attracted considerable interest because of the large correlation effects in the final hole states. The intensity ratio of the satellite to the main peak is given by a function of the covalent parameter of the core hole in the sudden approximation. Roughly speaking the larger the covalent parameter in the final state, the weaker the intensity of the satellite. In the observed K Kα X-ray spectra the relative intensities of the satellite increase in the order of the compounds K_2TiF_6, K_2SO_4 and KSCN. The K 3p core orbital in the initial and final states of these compounds is studied by the DV-Xα method. The K 3p orbital of these compounds is localized at the K site in the initial state. In the final state the K 3p-hole state of the K_2TiF_6 is delocalized between the K3p and F2s orbitals. The resonance between the K3p and F2s orbital levels accounts for this enhanced increase of the covalency in the final state. The satellite intensities in these compounds are understood by the order of the final state covalency of the K 3p states.

I-D-5 LCAO-Xα-Force Study on Stable Structures of Si_6 and Si_{10} Clusters

Susumu SAITO *(NEC Corp. and Institute for Solid State Physics)*, **Shuhei OHNISHI** *(NEC Corp.)*, **Chikatoshi SATOKO, Satoru SUGANO** *(Institute for Solid State Physics)*

[*J. Phys. Soc. of Japan*, **55**, 1791(1986)]

Stable structures of the Si_6 and the Si_{10} microclusters have been calculated using LCAO-Xα-force method. The calculated structures of the Si_6 and the Si_{10} clusters resemble a regular octahydron and a tetrahedron, respectively. In both clusters, triangles in these clusters contract by 20% in length compared to those of the crystal (111) surface. This contraction attributed to the interaction between dangling bonds is important for silicon clusters of any size. Condensed silicon atoms with the diamonds structure bond covalency each other. Bond-energy concept may be reasonable for such a covalent bond material. To gain the number of the bonds, silicon clusters have a tendency to take structures as many rings as possible. The structure of Si_6 cluster, which is the smallest unit having a ring-like structure, is thought to be stable.

I–E Photochemical Reaction in Gas and Liquid Phases

To understand the chemical reactions in gas and liquid phases, we need to know not only the electronic and dynamic properties of reacting molecules, but also the nature of reactant and solvent molecular interactions such as solvation mechanism. We have made the following three studies for this purpose; (i) Nonadiabatic coupling between the excited and ground states of polyenes, (ii) the energy dissipation mechanism of the excited molecules in liquid phases and (iii) the structure of the solvent and solute interactions (hydration structure).

I-E-1 Energy Dissipation Mechanism of the Optically Excited Molecules in Solvents; A Trajectory Study for a Photoisomerization Process of the π Conjugated Molecule in Ar and Water

Iwao OHMINE

[*J. Chem. Phys.*, in press]

The energy dissipation mechanism of an optically excited molecule in solution is studied by using a classical molecular dynamics (MD) calculation. We choose ethylene in Ar or water as a model system and perform the MD calculation to analyze the solvent response to the optically excited ethylene motions that are large in magnitude and high in frequency. It is found that the energy dissipation is very fast; it is in the order of a picosecond in water and of a few to a few tens of picoseconds in Ar. The energy decay rate strongly depends on each ethylene mode and on the nature of solvent-solvent interaction. Due to the characteristic form of water-water interaction, that is strong and sensitive to the mutual geometrical changes, a large water kinetic fluctuation occurs. The ethylene motions couple to this water fluctuation efficiently transferring the ethylene energy to the water libration energy, that is immediately distributed into the various inter and intra water modes. A multistep collision process leading the energy flow from the ethylene internal vibration → the ethylene rotation → the solvent molecule motion, not accounted for in the gas-like models such as Isolated Binary Collision model, is a pathway for the fast energy dissipation in Ar and water. We also employ simple model of an oscillator in Ar to make a detail analysis of the energy decay mechanism, especially of its dependence on the oscillator amplitude, the solvent-solvent interaction and the solvent density.

I-E-2 A Theoretical Study of Extremely Large Fluctuations of Water Kinetics

Hideki TANAKA and Iwao OHMINE

We have found that there exist extremely large water kinetic fluctuations. A water molecule in water solution exhibits large fluctuations of the order of 10~20 kcal/mole in the potential energy (i.e. the interaction energy sumed over all surrownding water molecules j; $\Sigma_j V_{ij}(r)$) and only small fluctuations of the order of kT in the kinetic energy. Many physical quanties such as power spectra and bonding pattern relating to these fluctuations are analized. In order to study the cause of such fluctuations, we have made a model that yields similar fluctuations and found that the repulsive forces in the water-water molecular interactions are essential for their existence. A discussion are made in the extremely fast energy transfer mechanism from photo-excited molecules to the water solvent molecules through the coupling with these extremely large water kinetic fluctuations.

I-E-3 Integral Equation and Monte Carlo Study on Hydrophobic Effects; Size Dependence of Apolar Solutes on Solute-Solute Interactions and Structures of Water

Hideki TANAKA

Hydrophobic effects for various solute sizes have been investigated by RISM equation and Monte Carlo simulation. It is shown that coulomb interaction among water molecules is one of the origin of the association of solute molecules. The degree of association depends on the solute size. For a large apolar solute, the structure of water is enhanced, resulting in the exo-

thermic hydration and the negative entropy change in hydration. For a solute comparable with the water size, the hydrogen bonds among water molecules are strengthened but net hydrogen bonds number does not increase. These results are also confirmed by the analysis of the geometric patterns formed by the hydrogen bond network. It is shown that the ordered structure of water in the solution of the large solutes gives rise to the larger enthalpy of the hydration, and thus they are more soluble in water than the smaller solutes.

I–F Studies of Chemical Reaction Dynamics

Two directions in this research area have been again pursued this year. One is the semiclassical theory in phase space and the other is the hyperspherical coordinate approach. This year the latter has enjoyed a nice marriage with the RIOS approximation by the collaboration with IMS visiting professor Michael Baer.

I-F-1 Semiclassical Theory in Phase Space for Molecular Processes III: Electronically Nonadiabatic Transitions in Multi-Dimensional Systems

Kazuo TAKATSUKA and Hiroki NAKAMURA

[*J. Chem. Phys.* in press]

A theory for electronically nonadiabatic transition in a multi-dimensional system is presented in the scheme of phase space quantum theory. The previously proposed phase space distribution function called DCF (dynamical characteristic function) is generalized to this case and coupled equations of motion are derived for this new DCF. Semiclassical approximation to these equations is analyzed, and the physical picture is clarified for the propagation of the semiclassical DCF based on wave packets. A sudden approximation applied to a series expansion of solution is shown to produce a multi-dimensional generalization of the first order Magnus approximation for nonadiabatic transition amplitude. It is also suggested to incorporate the more sophisticated formulae into propagation of the semiclassical DCF.

I-F-2 New Implementation to Approximate Quantum-Mechanical Treatment of Atom-Diatom Chemical Reactions

Hiroki NAKAMURA, Akihiko OHSAKI and Michael BAER *(Soreq Nucl. Res. Center and IMS)*

[*J. Phys. Chem.* in press]

A new approximate quantum-mechanical treatment of 3-D atom-diatom chemical reactions is proposed by combining the reactive infinite order sudden approximation (RIOSA) and the collinear-type hyperspherical coordinate approach. Using the hyperspherical coordinate analysis of potential energy surface and noticing the physical significance of potential ridge, we can determine the matching parameter of the RIOSA without ambiguity at each γ, defined as the angle between diatomic molecular axis and atom-diatom relative translational coordinate vector. This solves the "arbitrariness" problem associated with the matching line within the RIOSA. It is also shown that one can have a better understanding of the reaction mechanisms by calculating eigenvalues as a function of hyperradius for each γ. Some numerical examples are presented to demonstrate these features.

I-F-3 Quantum Infinite Order Sudden Approximation for Ion-Molecule Reactions: Treatment of the He + H_2^+ System

Michael BAER *(Soreq Nucl. Res. Center and IMS)*, **Hiroki NAKAMURA and Donald J. KOURI** *(Univ. of Houston)*

[*Int. J. Quant. Chem.* in press]

In this work the ion-molecule reaction He + H_2^+ (v_i) $\rightarrow$ HeH^+ (v_f) + H (v_i=0–7, v_f=0–2) was studied quantum mechanically in the energy range 1.3 eV $\leq$ E_{tot} $\leq$ 1.8 eV. The calculations were carried out employing the Reactive Infinite Order Sudden Approx-

imation (RIOSA). The two features characteristic of this system in the above energy range, namely the strong enhancement of the reaction rate with the initial vibrational energy (at a fixed total energy) and the relatively weak dependence of the cross sections on translational energy, were found to be well reproduced in the numerical treatment. The results also revealed the existence of two mechanisms of the exchange process: one is the ordinary mechanism and the other is probably related to the spectator stripping model.

I-F-4 He + H_2^+ Ion-Molecule Reaction: A Comparison between Experimental and Quantum Mechanical Results

Michael BAER *(Soreq Nucl. Res. Center and IMS)*, **Shinzo SUZUKI, Kenichiro TANAKA, Inosuke KOYANO, Hiroki NAKAMURA, Zdenek HERMAN** *(J. Heyrovsky Inst. of Phys. Chem. and Electrochem. and IMS)* **and Donald J. KOURI** *(Univ. of Houston)*

[*Phys. Rev.* **A34**, 1748 (1986)]

In this work a comparison between new experimental and quantum mechanical results is performed for the reactions $He+H_2^+(v_i) \rightarrow HeH^+(\Sigma v_f)+H$; $v_i=0\sim4$ in the energy range $1eV \leqq E_{tot} \leqq 2eV$, where E_{tot} is the total (vibrational + relative translational) energy including the zero point energy. It was found that the two features which characterize this system, namely the strong enhancement of the reaction rate with initial vibrational energy (at fixed total energy) and the relatively weak dependence of the cross-sections on translational energy are moderately well reproduced by the quantum mechanical infinite order sudden approximation.

I–G Dynamic Processes of Electronically Highly Excited States of Simple Molecules

Understanding the mechanisms of the various dynamic processes involving superexcited states of molecules is our ultimate purpose. Preliminary studies of dissociative recombination of H_2^+ reported last year have been extended. Theoretical analysis of multi-photon auto-ionization process of NO is now undertaken as a new project.

I-G-1 Dissociative Recombination of H_2^+, HD^+ and D_2^+ by Collisions with Slow Electrons

Keiji NAKASHIMA *(Kyushu Univ. and IMS)*, **Hidekazu TAKAGI** *(Kitasato Univ.)* **and Hiroki NAKAMURA**

[*J. Chem. Phys.*, in press]

Using the multi-channel quantum defect theory (MQDT), dissociative recombination of H_2^+, HD^+ and D_2^+ via the two-electron excited superexcited state $^1\Sigma_g(2p\sigma_u)^2$ is studied for each specified initial vibrational state v_i ($\lesssim 4$) of molecular ions at low electron energies $0.02eV \lesssim E \lesssim 1.0eV$. The necessary basic physical quantities, electronic coupling V(R) and quantum defect as a function of internuclear distance R, are obtained from our previous scattering calculations. As a by-product we have also obtained the singlet scattering d-wave partial cross sections for the various vibrational transitions of molecular ions by electron impact. It is found that the Franck-Condon like factor between vibrational state and dissociative continuum is most decisive in characterizing the overall magnitude and energy dependence of the cross sections. Even the vibrational transitions occur predominantly via the dissociative superexcited state. This suggests that the preionization mechanism of the states of the $^1\Sigma_g$ symmetry is very different from that of $^1\Sigma_u$ and $^1\Pi_u$ in the vicinity of ionization threshold.

I–H Photodissociation of a Triatomic Van der Waals Complex and Rotational Rainbow Effect

A nice collaborative work was done with the experimental group of Professor Kimura of IMS.

I-H-1 Anomalous Rotational-State Distribution of NO A State in UV Photodissociation of Rare Gas-NO van der Waals Complexes. Rotational Rainbow Effect

Kenji SATO, Yohji ACHIBA, Hiroki NAKAMURA and Katsumi KIMURA

[*J. Chem. Phys.* **85**, 1418 (1986)]

An explicit cross section formula for photodissociation of a triatomic molecule was derived and expressed in terms of the scattering matrix and the Franck-Condon like factor. With a half-collision approximation and a certain assumption about the Franck-Condon factor, the photodissociation cross section has been shown to be proportional to a partial cross section for rotationally inelastic atom-diatom collision. The partial cross sections are calculated by the close-coupling method with the use of a model potential which mimics the potential for the relevant ArNO system. These calculations strongly support that the experimentally observed anormalous rotational state distribution is a manifestation of the rotational rainbow effect. Figure 1 shows the calculated rainbow states plotted against the square root of the collision energy and the square root of the reduced mass.

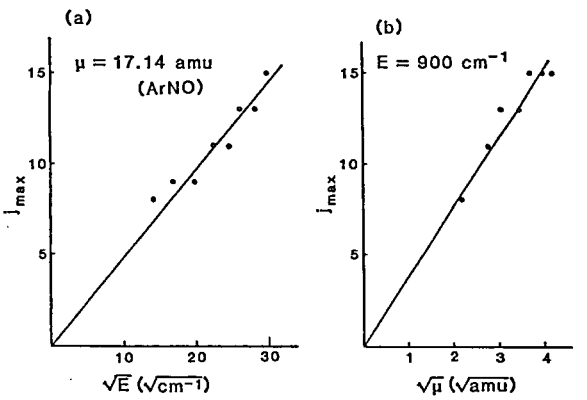

Figure 1

I–I Unified Theory for CDW, Superconductivity and Superfluidity in Strongly Coupled Electron-Phonon Systems

To clarify effects of extremely strong electron-phonon coupling on many-electron systems, we have started theoretical studies for CDW, superconductivity and superfluidity from a unified point of view based on the polaron model.

I-1-1 Many-Polaron Theory for Superconductivity and CDW in a Strongly Coupled Electron-Phonon System with Quasi Two-Dimension

Keiichiro NASU

The phase diagram of a two-dimensional N-site N-electron system (N≫1) with a site-diagonal electron-phonon (e-p) coupling is studied in the context of polaron theory, so as to clarify the competition between the superconducting (SC) state and the CDW state. The Fermi surface of noninteracting electrons is assumed to be a complete circle with no nesting type instability in the case of weak e-p coupling, so as to focus on such a strong coupling that even the standard "strong coupling theory" for superconductivity breaks down. Phonon clouds moving with electrons as well as a frozen phonon are taken into account by a variational method, combined with a mean-field theory. It covers the whole region of three basic parameters characterizing the system: the inter-site transfer energy of electron T, the e-p coupling energy S and the phonon energy ω. The resultant phase diagram is given in a triangular coordinate space spanned by T, S and ω. In the

adiabatic region $\omega \ll$(T,S) near the T-S line of the triangle, each electron becomes a large polaron with a thin phonon cloud, and the system changes discontinuously from the SC state to the CDW state with a frozen phonon as S/T increases. In the inverse-adiabatic limit $\omega \gg$(T,S) near the ω-vertex of the triangle, on the other hand, each electron always becomes a small polaron, and the SC state is always stable than the CDW state, because the retardation effect is absent. Thus, the polaron shrinks its radius and the SC region expands in the triangle, as T/ω decreases. It is found, for the first time, that the energy gap of the SC state for given T and S becomes maximum at the intermediate region $\omega \sim$ T, indicating the importance of the polaron effect. The collective excitation within the gap of the SC state is also studied by the random-phase approximation, and is found to change its nature continuously from the pair-breaking excitation to the superfluid type one as S/T increases.

I-I-2 The Vibrational Modes around Soliton in Strong-Coupled One-Dimensional Electron-Lattice Systems

Xin SUN *(Fudan Univ. and IMS)*, **Chang-qin WU** *(Fudan Univ. and IMS)* **and Keiichiro NASU**

The vibrational properties of the strong-coupled 1d electron-lattice systems are distinct from the weak-coupled systems. While weak-coupled systems have only four localized vibrational modes around the soliton, and there is no gap between acoustic and optical extended vibrational modes. The strong- coupled systems can possess two more localized modes around soliton, and a gap will appear between acoustic and optical branches when the coupling constant λ exceeds the critical value $\lambda_c = 0.21$. Furthermore, in the weak-coupled case, the width of soliton is much larger than the lattice constants, then the discrete lattice can be considered as a continuum, and the soliton is easily sliding along the chain by the driving of vibrations. However, in the strong-coupled case, the width of soliton is comparable with the lattice span, the mismatch between soliton configuration and discrete lattice will cause a barrier for soliton hopping. The stronger the coupling is getting, the less mobile the soliton will be. Each localized mode can exist in a certain extent of λ, and the whole extent $[0,2/\pi]$ of λ will be divided into seven regions, in each region, the disposition of localized modes and the dispersion curve of the extended modes including acoustic and optical branches have been figured out in this work.

I-J Theory for Resonant Raman, Hot Luminescence and Ordinary Luminescence with Nonradiative Process

To study the dynamics of lattice relaxation of optical excitations in solids and molecules, we derive an unified theory that can describe all components of the resonant secondary radiation; resonant Raman scattering, the hot luminescence and the ordinary luminescence. We are especially interested to clarify how the lattice relaxation occurs when the excited states are created by a two photon process not by the one photon process.

I-J-1 Hot Luminescence and Resonant Raman Scattering from the Two-photon Excited States in F center

Keiichiro NASU and Shinji Muramatsu *(Utsunomiya Univ.)*

A theory for the time-resolved secondary radiation from the F center excited by a pico-second two-photon pulse is formulated on the basis of a vibronic model. It includes 1s gound state, 2s and 2p excited states with a pseudo-Jahn-Teller type electron-phonon interacton. The transient behavior of the intensity of the radiated photon, in a pico-second time region, is calculated as a function of time interval between the excitation and the detection. A special attention is paid for the difference from the hot luminescence spectrum previously obtained by the one-photon excitation. It is shown that the crossing between 2s and 2p states also clearly appears in the hot luminescence due to this two-photon excitation.

I–K Theoretical Studies of Some Photochemical Reaction Mechanisms

I-K-1 A MO Study of 1,3 Hydrogen Shift of Amidine, Formamide, and Formic Acid at their Excited States

Hidetsugu TANAKA *(Osaka Inst. Tech)* **and Kichisuke NISHIMOTO** *(Osaka City Univ. and IMS)*

The effects of the electronic excitation and the hydrogen-bonding interaction on 1,3 hydrogen shift of amidine, formamide, and formic acid are investigated theoretically by means of ab initio calculations. The present calculations show that the energy barrier of 1,3 shift at the ground state is high (ca. 60 kcal/mol), whereas, at the $^1\pi\pi^*$ state, it reduces to ca. 15 kcal/mol. This is because there exists the orbital interaction effective to the 1,3 shift at the $^1\pi\pi^*$ state. Considering the hydrogen-bonding interaction with water molecule, the energy barrier becomes lower (ca. 25 kcal/mol) at the ground state, while that at the $^1\pi\pi^*$ state becomes high (ca. 23 kcal/mol).

I-K-2 Solvent Effect on the Hydrogen-Bonding Interaction between Adenine and Uracil

Yoshihisa OHTA *(Osaka City Univ.)*, **Hidetsugu TANAKA** *(Osaka Inst. Tech.)*, **Yoshihiro BABA** *(Osaka Inst. Tech.)*, **Akihiro KAGEMOTO** *(Osaka Inst. Tech.)* **and Kichisuke NISHIMOTO** *(Osaka City Univ. and IMS)*

[*J. Phys. Chem.* **90**, 4438 (1986)]

The stability of the adenine-uracil hydrogen-bonded systems of the Watson-Crick and the Hoogsteen pairs in vacuo and in aqueous solution is investigated by means of ab initio MO calculations and calorimetry. The calculated hydrogen-bonding energies of the Watson-Crick and the Hoogsteen pairs in vacuo are -58.8 and -51.4 kJ·mol^{-1}, respectively. The heat of mixing of adenine and uracil in aqueous solution is measured at 298.15 K and the enthalpy change obtained is -12 kJ·mol^{-1}. The calculated formation energies of the hydrated Watson-Crick pair and Hoogsteen one from the hydrated adenine and uracil by means of ab initio MO calculations are -8.3 and $+5.5$ kJ·mol^{-1}, respectively. These calculated values may be reasonable compared with the experimental ones.

I-K-3 Studies in a Model System on the Effect of Hydrogen Bonding at Heteroatoms of Oxidized Flavin on its Electron Acceptability

Kichisuke NISHIMOTO *(Osaka City Univ. and IMS)*, **Hiroo FUKUNAGA** *(Osaka City Univ.)* **and Kunio YAGI** *(Inst. Applied Biochem.)*

[*J. Biochem.* in press]

The effect of hydrogen bonding at hetero atoms of the oxidized flavin on its electron acceptability was studied by the *ab initio* molecular orbital method. The calculations were carried out for all possible lumiflavin-H_2O complexes and for some of lumiflavin-formamide complexes. Calculated data showed that the magnitudes of hydrogen bonding energy at the hetero atoms are in the order of N(3)H > O(14) > N(5) > N(1) > O(12). It was found that the atomic orbital coefficient of the lowest unoccupied molecular orbital is the largest at N(5) and that hydrogen bonding at N(1), N(5), O(12), and O(14) increases the electron acceptability of the oxidized flavin at N(5), while hydrogen bonding at N(3)H decreases it.

I-K-4 Theoretical Study of Soliton Dynamics of a Finite One Dimenisonal Hydrogen-Bonded System

Yoshiki KASHIMORI *(Osaka City Univ.)*, **Fuchun CHIEN** *(Osaka City Univ.)*, **and Kichisuke NISHIMOTO** *(Osaka City Univ. and IMS)*

[*Chem. Phys.* **107**, 389 (1986)]

The dynamical behavior of a model for a finite one dimensional hydrogen-bonded system has been studied by numerical calculation (RKG method). The present study shows that there exists a threshold level of the proton-proton interaction, below which the soliton will not form in the finite system. The threshold value seems to be too large in the previous model. However,

when we take into consideration a higher order interaction between the nearest-neighbor protons, the width and the energy of the soliton becomes quite reasonable. Thus, when such a condition is fulfilled, a soliton might appear under normal physiological conditions.

I-K-5 Theoretical Study on Electron Impact Mass Spectrometry. III. *ab initio* MO Study on the Fragmentation of Propylamine

Takae TAKEUCHI *(Nara Women's Univ.)*, **Masao YAMAMOTO** *(Nara Women's Univ.)* **and Kichisuke NISHIMOTO** *(Osaka City Univ. and IMS)*

[*Mass Spectr.* **34** in press]

In order to elucidate the fragmentation mechanism of propylamine following the low energy electron bombardment, the potential energy curves have been calculated by means of *ab initio* MO methods (STO-3G/4-31G). The present study indicates that the fragmentation due to C_α-C_β bond cleavage is the main process at the low energy.

I-L Computer Simulation of Liquid Mixtures

Our research activity in this area is in two different directions. One is the computer simulations on aqueous solution models which are based on quantum mechanical molecular orbital calculations. The other is the computer simulation of model mixtures of Lennard-Jones fluids-systems with a more empirical potential.

I-L-1 Effect of Pressure on the Internal Energy of Lennard-Jones Mixtures

Koichiro NAKANISHI *(Kyoto Univ. and IMS)*

[*Physica* **139 & 140**, 148 (1986)]

Molecular dynamics calculations have been carried out for Lennard-Jones fluid mixtures simulating an athermal solution. The excess internal energies of mixing U^E have been obtained as a function of molar composition at 120 K and reduced number densities between 0.5 and 1.5. The pressure range involved is from essentially zero up to 40 000 atm. The U^E values at constant density (volume) show a large pressure dependence. They change sign from positive to negative as the pressure increases. Thus, it is found that the mixture is probably not athermal except for some limited situation.

I-L-2 PVT Relation and Density-Dependent Local Composition for Super-Critical and Sub-Critical Fluid Mixtures of Lennard-Jones Molecules

Koichiro NAKANISHI *(Kyoto Univ. and IMS)*, **Yoshinori ADACHI** *(Nagoya Inst. Tech.)* **and Ichiro FUJIHARA** *(Osaka Ind. Univ.)*

Molecular dynamics and Monte Carlo calculations have been carried out for Lennard-Jones fluid mixtures in order to investigate the following three problems. They are (1) the PVT relationship for the LB-2-1 model and its two pure components in a wide range of pressure and temperature, (2) the dependence of local compositions on the density (pressure) for the LB-2-1 model above and below the critical point, and (3) the effect of attractive interaction on the local compositions for the LB-2-1 and related models. It is found that computer simulation can give the PVT relationship of model fluids which might be used for that of real fluids and their mixtures with appropriate parameter value. It is also revealed that the density dependence of local compositions is fairly large especially at lower temperatures. Finally, new results for the local composition in LB-2-1 model coincide with those reported recently in the literature.

I-L-3 Molecular Interaction between Fluoroalcohol and Water

Ken-ichi KINUGAWA *(Kyoto Univ.)* **and Koichiro NAKANISHI** *(Kyoto Univ. and IMS)*

Molecular orbital calculations have been carried out for two fluoroalcohols (1,1,1-trifluoro-2-propanol and 1,1,1,2,2,2-hexafluoro-2-propanol) and their supermolecular systems with water. The results have been used to prepare a new pair potential between fluoroalcohol and water, the functional form of which is of a conventional 12-6-3-1 type with appropriate rigid-rotor model. For a reference, similar procedure has also been applied to 2-propanol+water system. Molecular dynamics simulations are in progress by using these potentials together with MCY potential for water dimers.

RESEARCH ACTIVITIES II
Department of Molecular Structure

II–A High Resolution Spectroscopy of Transient Molecules and Ions

During the course of chemical reactions many transient molecules and ions appear as intermediates. Because of their high reactivities, i.e. their short lifetimes, these transient species have remained to be explored and some of them have even escaped detection. Many of these molecules have open-shell electronic structure, which characterizes them as free radicals. Unpaired electrons in a molecule cause splittings in high resolution spectra of such species through fine and hyperfine interactions, and, when properly analyzed, these splittings provide us with information on the electronic properties of the molecule which is not obtainable for molecules without unpaired electrons. High resolution spectroscopy not only provides molecular constants of transient molecules at very high precision, but also allows us to unambiguously identify chemical species occuring in reaction systems and to unravel the details of reaction mechanisms, in particular, when it is combined with some time-resolved detection methods. The present project will also be of some significance in related fields such as astrophysics and environmental sciences, and even in semiconductor fabrication.

II-A-1 The Microwave Spectrum of the Thiomethoxy Radical CH_3S

Yasuki ENDO, Shuji SAITO, and Eizi HIROTA

[*J. Chem. Phys.*, in press]

The pure rotational spectrum of the thiomethoxy radical CH_3S was observed for the first time in the millimeter-wave region. The radical was produced in a 0.5 m long free-space cell by the reaction of CH_3SH with 2450 MHz microwave discharge products of CF_4. The rotational transitions were observed to be split into doublets by spin-orbit interaction, and each component of the doublets further into K structures spread over several hundred MHz by vibronic Coriolis interaction and vibronic (2,2)- and (2,−1)-type interactions which are characteristic of a symmetric-top molecule in an orbitally degenerate ^2E electronic state. The magnetic hyperfine structure due to the three protons was clearly resolved and was analyzed by taking into account the pseudodipolar interaction which had not been considered previously. Ground-state molecular parameters were determined by least-squares analyzing the observed spectrum, and the C-S bond length was estimated to be 1.791 Å from the observed B rotational constant while assuming an appropriate structure for the methyl group.

II-A-2 The Microwave Spectrum of the PF_2 Radical in the $\tilde{X}^2B_1$ Ground Vibronic State

Shuji SAITO, Yasuki ENDO, and Eizi HIROTA

[*J. Chem. Phys.*, in press]

The microwave spectrum of the PF_2 radical in the $\tilde{X}^2B_1$ ground vibronic state was observed by using a source modulation spectrometer. The radical was produced in a free-space absorption cell by a dc glow discharge in a mixture of PF_3 and CF_4, and 260 spectral lines were observed in the frequency region of 63-181 GHz and were assigned to 37 rotational transitions. The observed lines were least-squares analyzed to determine the rotational constants, centrifugal distortion constants, spin-rotation coupling constants with centrifugal distortion correction terms, and magnetic hyperfine coupling constants for both the phosphorus and fluorine nuclei. The ε_{aa} spin-rotation coupling constant was found to be very small: −30.041 MHz, suggesting that excited electronic states contributing to ε_{aa} are all high lying or their contributions have canceled each other. The r_0 structure of PF_2 was calculated from the observed rotational constants: r_0(P−F)=1.5792 (18) Å and θ_0(FPF)=98.48 (21)° with uncertainties in parentheses. The vibrational frequencies were estimated from the observed centrifugal

distortion constants to be ω_1=864 (14), ω_2=365.3 (11), and ω_3=848 (24) in cm^{-1}. The T_{cc} dipolar hyperfine coupling constants give the spin density of the unpaired electron orbital to be 92.1% and 8.1% at P and each of F, respectively, whereas the a_F Fermi coupling constants lead to the s characters of 1.64% and 0.18% at the two atoms.

II-A-3 Infrared Laser Kinetic Spectroscopy of a Photofragment CS Generated by Photodissociation of CS_2 at 193 nm: Nascent Vibrational-Rotational-Translational Distribution of CS

Hideto KANAMORI and Eizi HIROTA

Carbon monosulfide fragments generated by CS_2 photodecomposition at 193 nm were examined by time-resolved observation of their vibration-rotation spectral lines with infrared diode laser kinetic spectroscopy. The CS molecules were found to be initially spread over a wide range of vibrational and rotational levels which could be of access with available energy, for both the triplet and singlet channels leading to sulfur atoms in the ^3P ground and ^1D excited states, respectively. The analysis of the observed line shape has allowed us to obtain information also on translational energy of CS fragments and to distinguish the contributions of the two channels. The branching ratio was thus estimated to be approximately one to one.

II-A-4 The Microwave Spectrum of the SiF_3 Radical

Mitsutoshi TANIMOTO *(Sagami Chem. Res. Center)*, **Shuji SAITO, and Eizi HIROTA**

We have observed the N=22←21 and 25←24 transitions of the SiF_3 radical in the 330 and 375 GHz regions, respectively.[1] The radical was produced by a glow discharge in Si_2F_6. Each transition was found to be split into more than 100 hyperfine and K components; the structure was too complicated to be readily analyzed. Therefore, the measurement was repeated so as to minimize overlapping of lines by reducing the line width. The observation was extended to cover the N=21←20 and 23←22 transitions at 315 and 345 GHz, respectively. Each transition was found to consist of many component lines spread over more than 250 MHz. The analysis is being made to derive the rotational, fine, and hyperfine constants.

Reference

1) M. Tanimoto, S. Saito, and E. Hirota, *IMS Ann. Rev.* 1985, II-A-15.

II-A-5 The Microwave Spectrum of the HCCO Radical

Yasuki ENDO and Eizi HIROTA

The pure rotational spectra of the HCCO and DCCO radicals were observed by submillimeter-wave spectroscopy. The radical was produced by either the O+acetylene or the F+ketene reaction; the former was found to be about twice as efficient as the latter and was employed to generate DCCO using C_2D_2 as a precursor. The observed spectra were fitted to the pattern expected for a very near prolate symmetric-top molecule. The rotational constants listed in Table I, which were derived from the spectra, indicate that the HCC angle is bent to 138.7°, while the CCO group is linear. As shown in Table I, the observed spin-rotation splitting exhibited an anomalous K dependence, which was ascribed to an interaction with a low-lying excited electronic state.

Table I. Rotational constants and spin-rotation interaction constants of the HCCO and DCCO radicals (in MHz)[a]

Constant	HCCO	DCCO
A	1 243 000 (45 000)	652 100 (3 600)
B	10 896.788 (41)	9 926.800 8 (104)
C	10 766.466 (39)	9 755.231 6 (126)
ε_{aa}[b]	−247 827 (74)	−112 201 (34)
ε_{bb}	−43.1 (27)	−30.62 (85)
ε_{cc}	13.8 (27)	10.20 (69)
$\lvert\varepsilon_{ab}+\varepsilon_{ba}\rvert/2$	1 619 (53)	275 (31)
t[b]	0.564 93 (97)	0.247 246 (171)

a. Values in parentheses denote 2.5 standard deviations and apply to the last digits of the constants.
b. Effective ε_{aa} constant was assumed to have the K dependence of the form $\varepsilon_{aa}(K)=\varepsilon_{aa}/(1+tK)$: t is a dimensionless quantity.

II-A-6 Microwave Kinetic Spectroscopy of Reaction Intermediates: O+Ethylene Reaction at Low Pressure

Yasuki ENDO, Soji TSUCHIYA *(Univ. of Tokyo and IMS)*, **Chikashi YAMADA, Eizi HIROTA, and Seiichiro KODA** *(Univ. of Tokyo)*

[*J. Chem. Phys.*, in press]

A microwave spectroscopic method has been developed to study elementary reactions in real time through *in situ* observation of rotational spectra of reaction intermediates such as free radicals with lifetime as short as 1 ms (II-B-1). This method was applied to the $O(^3P)$+ethylene reaction in order to assess the roles of (a) vinoxy+H and (b) CH_3+CHO channels in the initial process. The reaction was initiated by irradiating an N_2O/C_2H_4 mixture containing a trace amount of mercury with the 253.7 nm mercury resonance line, and the time evolution of vinoxy, HCO, and H_2CO was followed by measuring their microwave absorption intensities as functions of time. The branching ratio was thus determined to be 0.4±0.1 and 0.5±0.1 for (a) and (b), respectively, at the sample pressure of 30 mTorr. The present result agrees with those obtained by Hunziker et al.[1] using much higher pressures of samples, but is not compatible with the observation of Buss et al.[2] that (a) is dominant in collision-free conditions.

References

1) H.D. Hunziker, H. Kneppe, and H.R. Wendt, *J. Photochem.*, **17**, 377 (1981).
2) R.J. Buss, R.J. Baseman, G.He, and Y.T. Lee, *J. Photochem.*, **17**, 389 (1981).

II-A-7 Microwave Spectroscopy of the ClSO Radical

Shuji SAITO, Yasuki ENDO, and Eizi HIROTA

We have previously reported the observation of the microwave spectrum of ClSO and preliminary molecular parameters derived therefrom.[1] Since then, the measurement was extended to cover five branches, $^rQ_0$, $^rQ_1$, $^pR_1$, $^rR_0$, and $^rR_1$, which included 22 rotational transitions split into 111 fine and hyperfine components. Of these components, 107 lines were analyzed by the least-squares method to yield molecular parameters listed in Table I. The standard deviation of the fit was 28.7 kHz, which was of the same order of magnitude as the experimental error.

The present values of the Fermi contact term 3.24 MHz and of the T_{cc} dipolar term 29.07 MHz may be compared, respectively, with the ESR values, −2.5 and 35.6 MHz, reported for the radical trapped in a polycrystalline matrix.[2] The discrepancies are attributed, at least in part, to the omission of the nuclear quadrupole effect in analyzing the ESR data. The s-character of the unparied electron orbital at the Cl nucleus is estimated from the Fermi term to be 0.06%. This result and the observed dipolar interaction tensor are all consistent with the ClSO radical being a π radical in the ground electronic state.

References

1) S. Saito, Y. Endo, and E. Hirota, *IMS Ann. Rev.* II-A-12 (1980).
2) K. Nishikida and F. Williams, *J. Magn. Reson.*, **14**, 348 (1974).

Table I. Molecular Constants of the ClSO Radical (MHz)[a]

A	32 823.640 (37)	a_F	3.24 (47)
B	4 553.944 (16)	T_{aa}	−17.37 (20)
C	3 992.354 (20)	T_{bb}	−11.699 (91)
Δ_N	0.002 611 (35)	T_{ab}	∓2.1 (16)[b]
Δ_{NK}	−0.021 88 (81)	χ_{aa}	−52.57 (49)
Δ_K	0.600 4 (54)	χ_{bb}	22.65 (22)
δ_N	0.000 475 3 (81)		
δ_K	0.014 4 (86)		
ε_{aa}	−799.757 (61)		
ε_{bb}	−85.563 (28)		
ε_{cc}	3.538 (31)		
$(\varepsilon_{ab}+\varepsilon_{ba})/2$	±36.18 (29)[b]		

a. Values in parentheses denote one standard deviation and apply to the last digits of the constants.
b. Signs should be taken in the same order.

II-A-8 Detection of the Silyl Radical SiH_3 by Infrared Diode-Laser Spectroscopy

Chikashi YAMADA and Eizi HIROTA

[*Phys. Rev. Lett.*, **56**, 923 (1986)]

The silyl radical SiH_3 has been detected in a silane-discharge plasma through the observation of the ν_2 band by infrared diode-laser spectroscopy. The band was observed to consist of two inversion-doubling components, $1^- \leftarrow 0^+$ and $1^+ \leftarrow 0^-$, and the analysis of the observed spectrum yielded molecular constants in the v_2=0 and 1 states. The barrier height to the inversion has been calculated from the observed band origins to be 1868 cm^{-1}. The same analysis yielded the height of the pyramid to be 0.465 Å, which was

combined with the observed rotational constant B_0 to calculate r(Si−H)=1.468 Å and θ(HSiH)=110.5°.

II-A-9 Magnetic Interactions in HCF and HSiF Studied by Sub-Doppler Spectroscopy

Tetsuo SUZUKI and Eizi HIROTA

[*J. Chem. Phys.*, in press]

The $\widetilde{A}^1A''(000)$-$\widetilde{X}^1A'(000)$ band has been observed for HCF and HSiF at sub-Doppler resolution using the intermodulated fluorescence (IMF) technique. The hyperfine structure due to the ^{19}F nuclear spin/overall rotation interaction has been resolved for HCF, yielding the following coupling constants: C_{aa}''=4.19 (14) and C_{aa}'=−7.71 (20) MHz with one standard error in parentheses for the $\widetilde{X}$ and $\widetilde{A}$ states, respectively. In contrast, no hyperfine structure has been observed for HSiF. The Zeeman effect has also been examined for both species by IMF, and the following rotational g-factors have been derived: $g_{aa}''=-5.69\ (37)\times10^{-3}$ and $g_{aa}'=(5\sim10)\times10^{-3}$ for $\widetilde{X}$ and $\widetilde{A}$ of HCF, respectively, and $g_{aa}''=-1.47\ (9)\times10^{-3}$ and $g_{aa}'=1.57\ (11)\times10^{-3}$ for $\widetilde{X}$ and $\widetilde{A}$ of HSiF, respectively, all in the unit of Bohr magneton with one standard error in parentheses. The two types of molecular constants thus determined have been discussed in terms of electronic Coriolis interaction between the $\widetilde{X}$ and $\widetilde{A}$ states in each of the two molecules.

II-A-10 Infrared Diode Laser Study of the Hydrogen Bifluoride Anion: FHF^- and FDF^-

Kentarou KAWAGUCHI and Eizi HIROTA

[*J. Chem. Phys.*, **84**, 2953 (1986)]

The ν_3 vibration-rotation transition of the hydrogen bifluoride anion in the $\widetilde{X}^1\Sigma_g^+$ state has been detected for the first time by infrared diode laser spectroscopy using the magnetic field modulation technique. The anion was generated by a hollow cathode discharge in a mixure of H_2 and a fluorine-containing molecule such as CF_4, C_2F_4, and CHF_3. The carbon compound was indispensable to produce the anion. Identification of the species was based on the spectral pattern showing intensity alternation, the magnitude of the rotational constant (B''=0.334 181 cm^{-1}), and the ion drift velocity sign determined by the velocity modulation method. The observed ν_3 frequencies of FHF^- (1848.699 cm^{-1}) and FDF^- (1397.236 cm^{-1}) are much different from the reported values in the solid phase. By contrast, the ν_1 and ν_2 frequencies estimated from the centrifugal distortion constant and the perturbation of Coriolis interaction between the $\nu_1+\nu_2$ and ν_3 states are in good agreement with solid state measurements.

II-A-11 The Vibrational Assignment for the $A^2\Pi$-$X^2\Sigma^+$ Band System of the SiN Radical: The 0-0 Bands of ^{29}SiN and ^{30}SiN

Chikashi YAMADA, Satoshi YAMAMOTO *(Nagoya Univ.)*, **Shuji SAITO** *(Nagoya Univ. and IMS)*, **and Eizi HIROTA**

The vibrational assignment for the A-X system of the SiN radical was reexamined by observing the spectra at the 5 μm region of ^{29}SiN and ^{30}SiN in natural abundance. The original assignment of Mulliken for the A state was found to be correct, rather than the one currently accepted, i.e. the 5 μm spectrum was assigned to the 0-0 band of the A-X system. The term value of the A state was thus modified to T_e(A)=2032.4 (1) cm^{-1} and the equilibrium internuclear distance in the A state was recalculated to be 1.641 878 8 (48) Å, with one standard deviation in parentheses. The vibrational and isotopic variations observed for the Λ-type doubling and the spin-orbit interaction constants of the A state and for the spin-rotation interaction constants in the X state were explained by treating the electronic matrix elements of the spin-orbit interaction and of the orbital angular momentum between the A/X, B/A, and D/X states as parameters.

II-A-12 The Diode Laser Spectrum of the NO_3 Radical: A New Assignment for the 1490 cm^{-1} Band

Kentarou KAWAGUCHI, Takashi ISHIWATA *(Tokyo Inst. Tech.)*, **Ikuzo TANAKA** *(Tokyo Inst. Tech.)*, **and E. HIROTA**

We have previously observed a band of the NO_3 radical around 1490 cm^{-1} and have assigned it to the ν_3 N-O degenerate stretching band in the $^2A_2'$ ground electronic state.[1] However, we noticed that there were

some anomalies which were difficult to explain: (1) the observed first-order Coriolis coupling constant ζ=0.19 did not agree with a value ζ=0.7 calculated from a force field, (2) the observed ε_{cc} spin-rotation interaction constant was much larger than the values expected for both the v=0 and v_3=1 states, and (3) the observed centrifugal distortion constants agreed poorly with the calculated values and, furthermore, higher order terms were needed in explaining the observed spectrum.

We have reexamined the assignment by calculating combination differences from the observed data which were made more extensive than those reported earlier.[1] The revised assignment gave ground-state molecular parameters including centrifugal distortion constants in good agreement with the calculated values. For the upper state, a spin-orbit interaction constant of $a\xi d$=0.17 cm^{-1} was found indispensable, whereas the ε_{cc} spin-rotation parameter could not be determined for both the upper and lower states when the spin-orbit interaction was taken into account in the upper state. The observed spectrum has, therefore, been assigned to an electronic transition from the $^2A_2'$ ground state to an excited electronic state of $^2E''$ or $^2E'$ symmetry, rather than to the ν_3 band in the ground electronic state, as assumed in Ref.1).

Reference

1) T. Ishiwata, I. Tanaka, K. Kawaguchi, and E. Hirota, *J. Chem. Phys.*, **82**, 2196 (1985).

II-A-13 Excimer Laser Photolysis of Acetylene at 193 nm: Detection of the ν_3 Band of the CCH Radical by Time-Resolved Infrared Diode Laser Spectroscopy

Hideto KANAMORI and Eizi HIROTA

Curl et al.[1] have succeeded in observing the $\tilde{A}$-$\tilde{X}$ system of the CCH radical and a few accompanying vibrational bands within the $\tilde{X}$ state which borrow intensity from the $\tilde{A}$-$\tilde{X}$ transition, in the region from 3600 to 4200 cm^{-1}, but no other infrared spectra of CCH have been observed in the gas phase. It has been known that acetylene yields the CCH radical, when it is photodecomposed at 193 nm. Therefore, infrared diode laser kinetic spectroscopy was applied to this system, in order to observe vibrational bands of the CCH radical. We have observed a number of absorption lines in the region between 1750 and 1860 cm^{-1}, but have found it difficult to assign the ν_3 (C-C stretching) band, because the excess energy of the photolysis distributed CCH molecules over highly excited vibrational states. In fact, addition of methane or hydrogen relaxed CCH to the ground vibrational state and allowed us to observe the ν_3 fundamental band. Table I lists molecular parameters of CCH in the v_3=1 state. It is to be noted that the spin-rotation interaction constant is changed as much as 30% on ν_3 excitation. The present value of the band origin agrees with the matrix result of Jacox.[2] We have also observed a hot band from the ν_2 bending excited state, which is split into two components by ℓ-type doubling. The lower-state parameters agree well with those of Curl et al.,[1] but the upper-state constants do not coincide with our result on the ν_2+ν_3 band (see II-A-21). The upper state is probably a state with the bending mode excited by odd quanta.

References

1) R.F. Curl, P.G. Carrick, and A.J. Merer, *J. Chem. Phys.*, **82**, 3479 (1985): **83**, 4278 (1985).
2) M.E. Jacox, *Chem. Phys.*, **7**, 424 (1975).

Table I. Molecular Constants of the CCH Radical in the $\tilde{X}^2\Sigma^+$ Ground Electronic State (cm^{-1})[a]

Constant	v_3=1	v=0[b]
B	1.438 506 8 (48)	1.456 824 95 (18)
D	3.685 (8) × 10^{-6}	3.509 (10) × 10^{-6}
γ	−2.835 2 (4) × 10^{-3}	−2.091 4 (5) × 10^{-3}
ν_0	1840.570 2 (4)	

a. Values in parentheses denote standard deviation and apply to the last digits of the constants.
b. Taken from K.V.L.N. Sastry, P. Helminger, A. Charo, E. Herbst, and F.C. DeLucia, *Astrophys. J.*, **251**, L119 (1981).

II-A-14 Hyperfine Coupling Constants of NCO in $\tilde{A}^2\Sigma^+$ by Sub-Doppler Spectroscopy

Tetsuo SUZUKI, Shuji SAITO, and Eizi HIROTA

[*J. Mol. Spectrosc.*, in press]

Molecular constants including ^{14}N hyperfine coupling constants of the NCO radical in the $\tilde{A}^2\Sigma^+$(000) state have been determined precisely by using the microwave-optical double resonance (MODR) and intermodulated fluorescence (IMF) techniques, where the $\tilde{A}^2\Sigma^+$ (000)-$\tilde{X}^2\Pi$ (000) band was pumped by a dye

laser. The results are B=12 056.559 (41), D=0.0045 (16), γ=22.06 (17), b=430.4 (12), c=80.3 (28), and eQq=2.6 (36), all in MHz with one standard error in parentheses. It was found that, because the $\tilde{A}^2\Sigma^+$ state closely approximates a coupling case ($b_{\beta S}$), MODR did not provide any precise value for the Fermi contact term, but this constant was determined accurately by combining the MODR spectrum with the IMF spectrum.

II-A-15 The Microwave Spectrum of CD_2CDO and the Molecular Structure of the Vinoxy Radical

Yasuki ENDO and Eizi HIROTA

The microwave spectrum of CH_2CHO has been reported previously[1] and has been employed to unravel the mechanism of the O+ethylene reaction, as described in II-A-6. In order to derive information on the molecular structure, the fully deuterated species of the vinoxy radical was investigated by submillimeter-wave spectroscopy. The observed spectrum will be of some use for further studies of the O+ethylene reaction.

The CD_2CDO radical was generated by the reaction of fully deuterated acetaldehyde with the microwave discharge products of CF_4. The rotational transitions of N=17←16 up to 22←21 were observed and measured. Some lines were found to be perturbed by the off diagonal term of the spin-rotation interaction. The least-squares analysis of the observed spectrum yielded the rotational and spin-rotation interaction constants which are listed in Table I. By combining the data on the normal species, three structural parameters were calculated, which are referred to as Set I in Table II, where the parameters involving hydrogens were constrained to *ab initio* values.[2] Set II, which was obtained by increasing all C-H bonds by 0.01 Å, seems to be more reasonable than Set I.

References

1) Y. Endo, S. Saito, and E. Hirota, *J. Chem. Phys.*, **83**, 2026 (1985).
2) M. Dupuis, J.J. Wendoloski, and W.A. Lester, Jr., *J. Chem. Phys.*, **76**, 488 (1982).

Table I. Rotational and spin-rotation interaction constants of CD_2CDO (in MHz)[a]

A	43 228.726 (170)	ε_{aa}	−579.43 (108)
B	10 064.720 1 (70)	ε_{bb}	−61.080 (60)
C	8 155.979 5 (65)	ε_{cc}	−0.531 (49)
		$\lvert\varepsilon_{ab}+\varepsilon_{ba}\rvert/2$	−74.423 (58)

a. Values in parentheses denote 2.5 standard deviations and apply to the last digits of the constants.

Table II. Molecular structure of the vinoxy radical

Parameter	Set I[a]	Set II[b]	ab initio calc.[c]
C-C/Å	1.420	1.408	1.405
C-O/Å	1.256	1.261	1.275
CCO/°	121.8	122.4	122.9

a. With C-H and CCH fixed to the values reported in Ref.2.
b. With the same assumptions as for Set I, except for C-H increased by 0.01 Å.
c. Ref.2.

II-A-16 Magnetic Field Modulated Infrared Laser Spectroscopy of the Chloronium ClH_2^+ Ion ν_2 Band

Kentarou KAWAGUCHI and Eizi HIROTA

The chloronium ion (ClH_2^+) has been detected in the gas phase by infrared diode laser spectroscopy with magnetic field modulation. The ion was generated by a hollow-cathode discharge in an H_2, He, and HCl mixture. One hundred and forty eight lines were observed between 1040 cm^{-1} and 1330 cm^{-1}, of which 99 and 25 were assigned to the ν_2 fundamental bands of $^{35}ClH_2^+$ and $^{37}ClH_2^+$, respectively. The observed spectra were analyzed by using Watson's A-reduced Hamiltonian to determine the band origins [$\nu_2(^{35}ClH_2^+)$ = 1184.1256 (2) cm^{-1}, $\nu_2(^{37}ClH_2^+)$ = 1183.2165 (13) cm^{-1}] and the rotational and centrifugal distortion constants. The r_0 structure was calculated for $^{35}ClH_2^+$ to be r_0 (H−Cl) = 1.3135 (87) Å and θ_0 (HClH) = 94.3 (12)° with standard errors in parentheses.

II-A-17 Optical-Optical Double Resonance Study of HCF: Vibration-Rotation Energy Levels in the $\tilde{X}^1A'$ State

Tetsuo SUZUKI and Eizi HIROTA

In order to investigate highly excited vibrational states and metastable states which are difficult of access from the ground state by a single photon process, we have developed an optical-optical double resonance method. This method is identical to the so-called PUMP-DUMP technique, except that we employ high-resolution cw lasers achieving higher resolution than that with ordinary pulsed lasers. We have applied the method to the HCF molecule.

A dye laser (SP 380A) pumps HCF to a single rotational level of the $\tilde{A}^1A''$ (000), and the fluorescence is induced from this rovibronic level to a rotational level in the ground state manifold by using the second dye laser (CR 599-21). The line width of the observed signal is about 0.002 cm^{-1}, which is determined mainly by the frequency jitter of the first dye laser. Because the wave numbers of both lasers are measured in reference to the I_2 spectrum, the accuracy of the observed line position is not better than 0.003 cm^{-1}. The signal-to-noise ratio of the observed spectrum is determined by the intensity fluctuation of the fluorescence excited by the first dye laser. Four vibrational levels, ν_2, $2\nu_2$, ν_1 and $\nu_2+\nu_3$, have been observed by this method; the numbers of the observed lines are 145, 143, 65, and 8, respectively. The last two states were found to be Coriolis coupled. Molecular constants derived from the observed spectrum are shown in Table I.

Table I. Molecular Constants of the HCF Molecule in the $\tilde{X}^1A'$ State[a]

Constant	(000)[b]	(010)	(020)	(100)
A	466 558 (11)	477 712 (12)	485 370 (10)	456 442 (26)
B	36 664.5(10)	36 674.2(30)	36 683.5(35)	36 654.9(33)
C	33 866.9(10)	33 706.8(31)	33 566.1(25)	33 771.3(27)
Δ_J	0.116(5)	0.1291(38)	0.1327(27)	0.0924(69)
Δ_{JK}	2.37(7)	1.82(10)	1.949(60)	10.16(22)
Δ_K	72.7(19)	91.26(67)	80.38(53)	42.8(14)
δ_J	0.00968(28)	0.0113(32)	0.0109(22)	−0.0116(71)
δ_{JK}	1.58(15)	1.8(13)	2.2(11)	[1.58][c]
ν_0/cm^{-1}		1403.2045(13)	2812.4844(10)	2643.0393(26)
(011): $B+C$ 69 670.7 (41), G 9 527 (102)				
$\nu_0(100)-\nu_0(011)/cm^{-1}$ 74.723 6 (53)				

a. In MHz, unless otherwise noted. Values in parentheses denote one standard deviation and apply to the last digits of the constants.
b. M. Kakimoto, S. Saito, and E. Hirota, *J. Mol. Spectrosc.*, **88**, 300 (1981).
c. Fixed.

II-A-18 Infrared Diode Laser Spectroscopy of the ν_2 Band of the SH_3^+ Ion

Takayoshi AMANO *(NRC and IMS)*, **Kentarou KAWAGUCHI, and Eizi HIROTA**

The protonated hydrogen sulfide ion is an interesting species, like the H_3O^+ ion which has been investigated in detail by infrared and microwave spectroscopy. Nakanaga and Amano[1] have recently succeeded in observing the ν_3 band of SH_3^+ using a difference-frequency laser system at the National Research Council in Ottawa. It is interesting to explore the inversion motion in this ion. The ν_3 band does not exhibit any indication of inversion splitting. The ν_2 band is much more suitable for the study of the inversion.

The SH_3^+ ion was generated by the discharge in a mixture of hydrogen sulfide and hydrogen. Magnetic-field modulation was employed to selectively detect the spectral lines of the ion. A number of lines were observed in the 10 μm region, and a least-squares analysis gave molecular constants shown in Table I, where the ground-state parameters were constrained to those derived from the ν_3 band.[1] The observed spectrum showed the effect of weak Coriolis interaction with the ν_4 state, as indicated by the anomalous values of centrifugal distortion constants in the $\nu_2=1$ state.

Reference

1) T. Nakanaga and T. Amano, to be published.

Table I. Molecular constants of the SH_3^+ Ion (cm^{-1})[a]

Constant	v_2=1	Ground[b]
ν_0	1 033.314 35 (88)	
B	4.725 63 (11)	4.894 750
C	4.244 613 (75)[c]	[4.223 9][d]
D_J	−0.000 050 2 (43)	0.000 156 12
D_{JK}	0.000 211 0 (72)	−0.000 214 38
D_K	−0.000 056 0 (43)	0.000 154 54
$H_J\times10^7$	2.9 (5)	0.7
$H_{JK}\times10^7$	4.7 (10)	−2.5
$H_{KJ}\times10^7$	1.5 (7)	5.1

a. Values in parentheses denote standard deviation and apply to the last digits of the constants.
b. Fixed to the values derived from the ν_3 band of Ref.1).
c. Only the difference C_2-C_0 was determined.
d. Assumed.

II-A-19 Detection of HBO by Discharge Modulated Infrared Diode Laser Spectroscopy

Yoshiyuki KAWASHIMA *(Ikutoku Tech. Univ.)*, **Kentarou KAWAGUCHI, and Eizi HIROTA**

[*Chem. Phys. Lett.*, in press]

The IR spectrum of a transient species HBO was observed in the gas phase using a discharge modulation method. The HBO molecule is formed in an ac discharge plasma of a B_2H_6/O_2 or B_2H_6/NO mixture. Figure 1 shows the R(7) transition of the ν_3 band of $H^{11}BO$. The ν_3 band origin and the rotational constants of $H^{11}BO$ were determined to be ν_0 = 1825.5610 (13), B_0 = 1.30839 (12), and B_3 = 1.29973 (10) cm^{-1}, with three standard deviations in parentheses.

II-A-20 Infrared Diode Laser Spectroscopy of the BH_3 ν_2 Band

Kentarou KAWAGUCHI, James E. BUTLER *(NRL and IMS)*, **Chikashi YAMADA, Hideto KANAMORI, Tatsuya MINOWA, Simon H. BAUER** *(Cornell Univ. and IMS)*, **and Eizi HIROTA**

Many spectroscopic attempts have been made to detect the BH_3 molecule in the gas phase, but so far no one has succeeded in observing its spectrum in any wavelength region. According to a discussion of Walsh, BH_3 is expected to be planar. We have attempted to observe the ν_2 out-of-plane bending band by infrared diode laser kinetic spectroscopy, where BH_3 was generated by photodecomposing either B_2H_6 or BH_3CO at 193 nm. Although we observed a number of lines of about 300 μs duration around 1100 cm^{-1}, we could not make any definite assignment for them, primarily because of overlap with strong lines of the precursors. We have recently introduced discharge modulation in infrared diode laser spectroscopy. This method was found to be more suitable than excimer laser photolysis, for observing BH_3 spectra, because diborane molecules are decomposed to a greater extent. The $^qQ(J, K=J)$ series with J=1 to 6 were identified, yielding $B'-B''=-0.2036$, $C'-C''-D_J' + D_J'' = 0.0265$, and $-2D_J' + 2D_J'' - D_{JK}' + D_{JK}'' = 0.002$ cm^{-1}. It was, however, found that other branches were difficult to assign, presumably because the ν_2 state is perturbed by the Coriolis interaction with the ν_4 state.

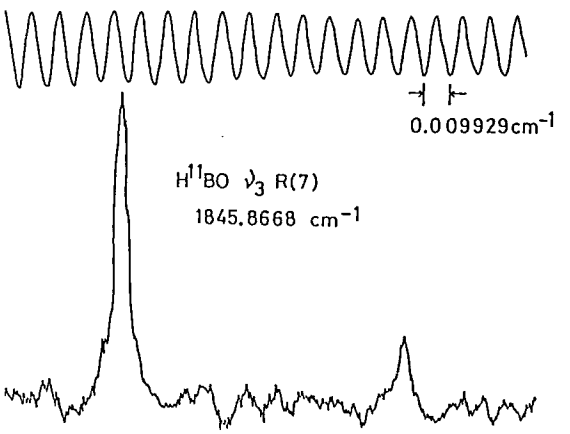

Figure 1. R(7) transition of the ν_3 band of $H^{11}BO$ observed by the discharge modulation method. A weak signal observed is not assigned. The upper trace shows fringes of a vacuum-spaced etalon. The time constant of the lock-in amplifier was 1 s.

II-A-21 Infrared Diode Laser Sectroscopy of the CCH $\nu_2+\nu_3$ Band

Kentarou KAWAGUCHI, Takayoshi AMANO *(NRC and IMS)*, **and Eizi HIROTA**

During a course of searching for C_3H_2 or $C_3H_3^+$ around 2120 cm^{-1}, we unexpectedly observed a series of doublets which were likely to be due to a Π-Σ transition. The sample employed was a mixture of H_2, C_2H_2, and CO, and a discharge modulation technique was applied. The spacing between successive members of the series suggested that these lines were due to the CCH radical. In fact, the observed spectrum was well

fitted to a pattern calculated by fixing lower-state molecular constants to the values which Saykally et al.[1] derived for the ground vibronic state of CCH. Table I lists the upper-state parameters determined by the least-squares analysis. The change of the B constant, i.e. the α value, which was determined to be 0.02254 cm^{-1}, agrees well with the sum of α_2[2] and α_3[3], namely 0.02379 cm^{-1}, suggesting this band to be assigned to $\nu_2 + \nu_3$. Then the ν_2 frequency was calculated to be 249 cm^{-1}, which is much lower than the value 389 cm^{-1} estimated from the ℓ-type doubling constant.[2]

References

1) R.J. Saykally, L. Veseth, and K.M. Evenson, *J. Chem. Phys.*, **80**, 2247 (1984).
2) R.F. Curl, P.G. Carrick, and A.J. Merer, *J. Chem. Phys.*, **82**, 3479 (1985): **83**, 4278 (1985).
3) II-A-13

Table I. Molecular Constants of the CCH Radical (cm^{-1})[a]

Constant	$\nu_2+\nu_3$	Ground[b]
B	1.434 278 (21)	1.456 819 9
A	−1.020 1 (48)	
γ	−0.016 91 (79)	−0.002 091 9
$D\times10^5$	0.700 6 (95)	0.351 7
q_3	0.016 868 (13)	
$q_{3N}\times10^5$	−0.266 9 (94)	
ν_0	2 089.389 8 (9)	

a. Values in parentheses denote standard deviation and apply to the last digits of the constants.
b. Ref.1). Fixed.

II-A-22 The Microwave Spectrum of the HBO Molecule

Yoshiyuki KAWASHIMA *(Ikutoku Tech. Univ.)*, **Yasuki ENDO, and Eizi HIROTA**

The recent success of detecting the HBO molecule by infrared diode laser spectroscopy (II-A-19) prompted us to observe its pure rotational spectrum by microwave spectroscopy. As in the infrared study, the HBO molecule was generated by the discharge in a mixture of diborane and oxygen.

The J=1←0, 2←1, and 5←4 transitions were observed for the ^{11}B species, whereas for the ^{10}B species the measurement was made on the J=2←1, 4←3, and 5←4 transitions. To our surprise, the vibrational satellites were observed for the excited states, ν_2, $2\nu_2$, ν_3, and ν_1, for both isotopic species. This result suggests that the effective vibrational temperature of HBO in the cell is much higher than room temperature. Table I summarizes the rotational constants, the vibration-rotation constants, and the ℓ-type doubling constant, which were derived from the observed spectrum. It is interesting to note that all these constants behave quite parallel to those of HCN. The electric nuclear guadrupole coupling constant was determined to be −3.816 MHz for ^{11}B. The equilibrium internuclear distances were calculated from the B_e constants of Table I to be r_e (H−B) = 1.1680 Å and r_e (B=O) = 1.2004 Å.

Table I. Rotational, vibration-rotation, and ℓ-type doubling constants of HBO (in MHz)

Constant	$H^{11}BO$	$H^{10}BO$
B_0	39 224.247	40 575.402
α_1	269.755	299.509
α_2	−89.846	−101.650
α_3	259.235	268.716
q_2	181.925	192.318
B_e	39 398.897	40 757.864

II-A-23 Third-Order Anharmonic Potential Constants and Equilibrium Structures of the Formyl and Hydroperoxyl Radicals

Eizi HIROTA

[*J. Mol. Struct.*, in press]

Observed vibration-rotation constants for HCO/DCO and HO_2/DO_2 are combined with vibrational frequencies and ground-state rotational constants in order to derive harmonic as well as third-order anharmonic potential constants, and also equilibrium structure parameters for the formyl and hydroperoxyl radicals. The "diagonal" terms of the third-order anharmonic constants thus obtained for the stretching modes are discussed in terms of a diatomic-molecule model.

II-A-24 A Simultaneous Determination of Third-Order Vibrational Anharmonicity Constants and Equilibrium Structure: Molecular Structure of Non-linear HXY-Type Molecules

Eizi HIROTA

[*J. Chem. Soc. Jpn.* (in Japanese), in press]

In order to eliminate ambiguities in spectroscopically determined molecular structure caused by intramolecular vibrations, a method has been developed which analyzes ground-state rotational constants and vibration-rotation constants of a sufficient number of isotopes simultaneously by the least-squares method using equilibrium structure parameters and third-order anharmonicity constants as adjustable parameters. The method has been applied to HNO/DNO and HOCl/DOCl, for both of which not all vibration-rotation constants have been determined, preventing the equilibrium structure from being determined through a conventional procedure of calculating equilibrium rotational constants. The equilibrium structures thus obtained are r_e (H−N) = 1.0628 (25) Å, r_e (N−O) = 1.2058 (27) Å, and θ_e (HNO) = 109.09 (24)° for HNO and r_e (H−O) = 0.9654 (35)Å, r_e (O−Cl) = 1.6891 (29)Å, and θ_e (HOCl) = 103.21 (60)° for HOCl, with three standard deviations in parentheses. The analysis has also yielded some of the third-order anharmonicity constants, which are indispensable in analyzing vibrational changes of molecular constants and also in discussing the dynamical behavior of molecules. The "diagonal" third-order constants which are determined are F_{111} = −25.31 (22) aJÅ^{-3}, F_{222} = −77 (12) aJÅ^{-3}, and F_{333} = −1.05 (15) aJrad^{-3} for HNO and F_{111} = −42.5 (10.4) aJÅ^{-3}, F_{222} = −21.8 (8.4) aJÅ^{-3}, and F_{333} = −0.42 (1.14)aJrad^{-3} for HOCl, where the internal coordinates are numbered such that 1 for δr (H-X), 2 for δr (X-Y), and 3 for $\delta\theta$ (HXY), and the values in parentheses denote three standard deviations. It has also been shown that the method can be applied to molecules in an excited electronic state, using HNO in the $\tilde{A}^1A''$ state as an example. The result is by no means satisfactory; the precision of the derived constants is not high. This is mainly ascribed to perturbations in the excited state, and the present analysis may provide us with chances of examining the interactions affecting the excited state. The method developed in the present paper will be applicable to a few other simple molecules such as bent XYZ-type molecules without involving any hydrogen/deuterium atoms and planar C_{2v} H_2XY-type molecules.

II-A-25 Excimer Laser Photolysis of Acetylene at 193 nm: Generation and Annihilation of Photoproducts

Hideto KANAMORI and Eizi HIROTA

The photochemistry of acetylene has been attracting much attention and has been investigated several times. However, most of these studies relied on product analysis, leaving reaction intermediates unknown. We have applied infrared laser kinetic spectroscopy which we have recently developed,[1] to this problem; we monitored the CCH radical, the diacetylene molecule, and other transient species.

The sample was acetylene of 0.03 to 0.6 Torr diluted with a buffer gas of 0 to 4 Torr and was continuously pumped through a 2-m long multiple reflection cell. We have observed three types of photodecomposition products, which were discriminated one another by the time profiles of their spectra, as shown in Figure 1. The first molecule (1) is diacetylene, the second species (2) is the CCH radical, and the third one (3) has not been identified. From the dependences of the spectral intensities of these molecules on the amounts of the buffer gas and acetylene, it is concluded that the decomposition of acetylene proceeds through a very reactive unknown species, i.e., the third species, which is probably either CCH or acetylene in (a) highly excited state (s), and results finally in diacetylene. If an appropriate buffer gas such as CH_4 or H_2 is used, CCH is relaxed to the ground vibronic state before diacetylene is formed.

Reference

1) H. Kanamori, J.E. Butler, K. Kawaguchi, C. Yamada, and E. Hirota, *J. Mol. Spectrosc.*, **113**, 262 (1985).

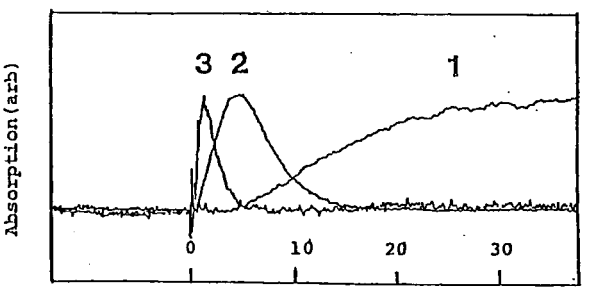

Figure 1. Time profile of absorption spectra of three molecular species generated by the 193 nm photolysis of acetylene: (1) R(29) of the $\nu_6+\nu_8$ band of diacetylene, (2) R(2) of the ν_3 band of CCH, and (3) a line of an unidentified species.

II-B Development of New Instruments and New Experimental Methods for High Resolution Spectroscopy

The scope of a research is limited by the techniques and the capabilities of instruments available to a researcher. This is particularly true for spectroscopic investigations of simple molecules, free radicals, and ions, which are main research themes this Department is interested in. The high precision with which we determine molecular paramaters often unravels new features of molecular structure which have previously escaped experimental observation. The diversity of molecular systems which we can detect and analyze is often limited by the sensitivity of the spectrometer employed. It is thus imperative for us to steadily improve our research facilities and to develop equipments of radically new conceptual design. The rewards of these efforts will include not only the detailed knowledge of the molecules under investigation, but also contributions to related fields. Various technical problems need to be solved to attain these goals. In this respect the collaboration of the Equipment Development Center is indispensable. New instruments developed in this program promise to open new research area in the field of molecular science.

II-B-1 Millimeter- and Submillimeter-Wave Kinetic Spectroscopy of Reaction Intermediates

Yasuki ENDO, Hideto KANAMORI, and Eizi HIROTA

A spectroscopic method has been developed to study chemical reaction processes through *in situ* observation of the time profile of molecular absorptions in the mm- and submm-wave regions. Figure 1 shows a block diagram of the system, and two absorption cells are illustrated in Figure 2: (a) one for mercury sensitized reactions and (b) the other for excimer laser photolysis reactions. The method has been applied to oxidation reactions of unsaturated hydrocarbons initiated by mercury photosensitization, in particular the O+acetylene reaction. It has also been combined with the excimer laser photolysis to examine photodecomposition processes of SO_2, CS_2, and Cl_2SO, where nascent distributions of photofragments such as SO and CS were measured. Advantages and disadvantages of the method have been discussed in some detail.

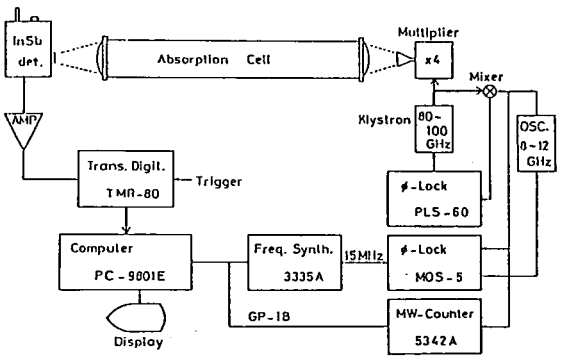

Figure 1. Block diagram of the system.

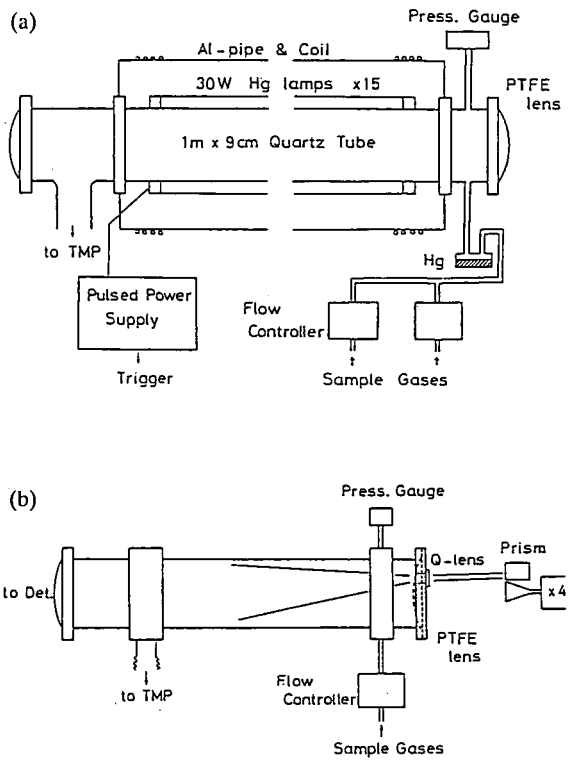

Figure 2. Absorption cell used for mercury sensitized reactions, (b) Absorption cell used for excimer laser photolysis experiments.

II–C High Resolution Spectroscopy of Molecules of Fundamental Importance

The need for high quality spectroscopic data has recently been increasing, especially for molecules of fundamental importance. Perhaps such spectroscopic data have been accumulated in the past because of interest in precise molecular structure determination. However, research activities in other related fields such as reaction kinetics, environmental sciences, plasma chemistry and physics, astronomy, and semiconductor technology have recently been advanced such that precise spectroscopic data are indispensable as a means of monitoring molecules. Spectroscopic data which are available at present are not necessarily good enough and must often be replaced by new data that meet necessary requirements. Such spectroscopic data on chemically stable molecules of fundamental importance will be presented in this section.

II-C-1 The Microwave Spectra of Deuterated Silanes, Germanes, and Stannanes

Keiichi OHNO *(Hiroshima Univ.)*, **Hiroatsu MATSUURA** *(Hiroshima Univ.)*, **Yasuki ENDO, and Eizi HIROTA**

[*J. Mol. Spectrosc.*, **118**, 1 (1986)]

A previous measurement of the rotational spectra of SiH_3D, SiH_2D_2, and $SiHD_3$ has been extended in frequency region to determine rotational constants and quartic centrifugal distortion constants. Similar observations have been performed on GeH_3D, GeH_2D_2, and $GeHD_3$, consisting of five, three, and three Ge isotopes, respectively, and also on SnH_3D, SnH_2D_2, and $SnHD_3$ with seven, three, and three Sn isotopes, respectively. The observed rotational constants were analyzed to estimate the equilibrium internuclear distance for the three molecules: r_e (Si–H) = 1.4734 (10) Å, r_e (Ge–H) = 1.5158 (48) Å, and r_e (Sn–H) = 1.6935 (84) Å.

II-C-2 The Microwave Spectrum of Cyclopropane-1, 1-d_2

Man Chai CHANG *(Sun Cheon Natl. Univ. and IMS)*, **Yasuki ENDO, and Eizi HIROTA**

Cyclopropane has been known as a molecule which involves a largely strained ring, and much attention has been paid to the electronic structure of its C-C bond. Although numerous infrared, Raman, and electron diffraction investigations have already been performed on this molecule, a microwave study on partially deuterated species will provide more detailed information on its molecular structure. In the present study, we observed and analyzed the microwave spectrum of the 1, 1-d_2 species.

A commercially available sample of cyclopropane-1, 1-d_2 was used after purifying with a gas chromatograph. The absorption cell was maintained at about −20°C. In the region from 320 to 410 GHz, 64 a-type transitions of J = 11←10 up to J = 17←16 were observed and assigned. The spectrum clearly showed the effect of spin statistics i.e. the presence of a C_2 axis; the weights for K_a = even and odd lines were 78 and 66, respectively. Table I lists molecular constants obtained by analyzing the observed spectrum. When the effect of intramolecular vibrations was neglected, the following structure parameters were derived from the observed rotational constants: r_0(C–C) = 1.514 725 Å, r_0(C–H) = 1.078 647 Å, and θ_0(HCH) = 115.453°, which, when r(C–H)−r(C–D) = 0.003 Å was assumed, were modified to 1.513 78 Å, 1.082 6 Å, and 115.31°.

Table I. Molecular Constants of Cyclopropane-1, 1-d_2 in the Ground Vibronic State (MHz)[a]

A	18 835.662 (18)
B	16 370.270 3 (70)
C	11 409.228 5 (67)
Δ_J	0.011 246 (12)
Δ_{JK}	0.005 087 (35)
Δ_K	0.007 06 (12)
δ_J	0.003 028 0 (79)
δ_K	0.005 561 (27)

a. Values in parentheses denote three standard deviations and apply to the last digits of the constants.

II-C-3 Stark Modulation Infrared Diode Laser Spectroscopy of the $\nu_6+\nu_8$ Band of Diacetylene

Keiji MATSUMURA *(Seinan Gakuin Univ.)*, **Kentarou KAWAGUCHI, Eizi HIROTA, and Takehiko TANAKA** *(Kyushu Univ.)*

The infrared diode laser spectrum of the $\nu_6+\nu_8$ band of diacetylene (HC≡CC≡CH), i.e. a combination band of a symmetric $\pi_g(\nu_6)$ and an antisymmetric $\pi_u(\nu_8)$ C≡C-H bending vibration, was recorded by the Stark and source modulation techniques. The analysis of the Stark modulation spectrum allowed us to locate the $2\nu_6$ (Σ_g^+) and $2\nu_8$ (Σ_g^+) vibrational states, which are inaccessible by infrared transitions from the ground state. It is also shown that the Stark modulation spectrum can be used to confirm the rotational assignment of the $\nu_6+\nu_8$ band.

II-C-4 Diode Laser Spectrum of the ν_8 Band of CH_3SH

Kuniaki NAKAGAWA *(Toyama Univ.)*, **Takeshi KOJIMA** *(Toyama Univ.)*, **and Eizi HIROTA**

[*Bull. Chem. Soc. Jpn.*, in press)]

The Stark effect was used to assign four series of the transitions in the heavily perturbed spectrum of methanethiol in the 14 μm region: $K=0$ and two $K=1$ series of A torsional symmetry and $K=0$ series of E symmetry. Effective parameters were determined for each series. The $K=0$ levels of A symmetry in the ν_8 state were found to be perturbed by a Fermi-type resonance.

II-C-5 The Microwave Spectrum of Cubane-d

Eizi HIROTA, Yasuki ENDO, E.W. DELLA *(Flinders Univ.)*, **and P.E. PIGOU** *(Flinders Univ.)*

Cubane was synthesized for the first time in 1964,[1] and its structure has been investigated by X-ray diffraction,[2] infrared spectroscopy,[3] and electron diffraction.[4] However, as shown in Figure 1, there are some discrepanices among the results of these studies. We started the present investigation to provide a more reliable information on the structure of cubane. To begin with, we observed the microwave spectrum of cubane-d. This species is a symmetric-top molecule, and the transitions with $J=14\leftarrow13$ up to $J=26\leftarrow25$ were identified. These transitions did not show any K splittings, but some high-K lines exhibited asymmetrical line shapes, indicating the D_{JK} constant to be negative. These findings are in agreement with the D_{JK} value of −0.000 032 MHz calculated by Robiette.[5] The least-squares analysis of the observed spectrum yielded B_0=3220.720 08 (85) and D_{J0}=0.000 180 99 (93) MHz with three standard errors in parentheses. The latter value agrees with Robiette's calculated value, 0.000 184 MHz. The B_0 constant was used as it is, to derive a relation between the r(C−C) and r(C−H) distances shown by a solid line in Figure 1.

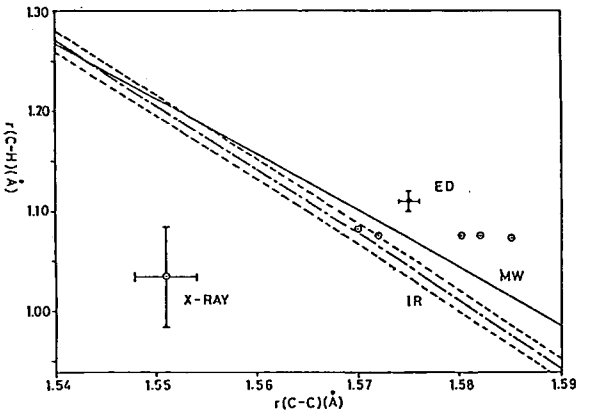

Figure 1. Relation between the r(C−C) and r(C−H) distances of cubane. X-ray, IR, and ED denote the results reported in Refs. 2), 3), and 4), respectively, while MW represents the present result. Circles with a dot at the center indicate the distances calculated by *ab initio* MO methods.

References

1) P.E. Eaton and T.W. Cole, Jr., *J. Am. Chem. Soc.*, **86**, 962 (1964).
2) E.B. Fleischer, *J. Am. Chem. Soc.*, **86**, 3889 (1964).
3) A.S. Pine, A.G. Maki, A.G. Robiette, B.J. Krohn, J.K.G. Watson, and Th. Urbanek, *J. Am. Chem. Soc.*, **106**, 891 (1984).
4) A. Almeningen, T. Jonvik, H.D. Martin, and T. Urbanek, *J. Mol. Struct.*, **128**, 239 (1985).
5) A.G. Robiette private communication.

II–D Raman Spectroscopy and Its Application

Raman scattering reveals the vibrational spectrum of a molecule which is sensitive to a molecular structure and bond strength. We apply this technique to study the following three projects; 1) Structure-function relationship of biological molecules, 2) Structure of short-lived molecules, 3) Solution structure. The first project utilizes resonance enhancement of Raman intensity, which enables us to observe selectively the vibrational spectra of chromophores of a large molecule with a small amount of dilute solution. Various kinds of heme proteins, flavoproteins, retinoid proteins, and pyridoxal proteins and their model compounds are investigated. Currently we focus our attention to elucidate the mechanisms of biological activation of oxygen and of the proton- and electron-transfers by proteins. So far we have used visible lasers to see the spectra of chromophores, but we are extending the excitation wavelength to the UV region to enhance selectively the Raman bands of aromatic amino acid residues of proteins. The second project aims to determine resonance Raman spectra of transient states, that is, reaction intermediates and excited molecules, by using two-color delayed pulses and optical multichannel detection system. An artificial cardiovascular device involving the enzyme reproduction system was constructed to obtain transient Raman spectra of enzymic reactions. The third project intends to evaluate a relative size of solute-solvent and solvent-solvent interactions for a binary mixtures of liquids and to elucidate a structure of local assembly of molecules. For this purpose a system to measure difference Raman spectrum was constructed.

II-D-1 Resonance Raman Characterization of Iron-Chlorin Complexes in Various Spin-, Oxidation-, and Ligation-States. I: Comparative Study with Corresponding Iron-Porphyrin Complexes

Y. OZAKI *(Jikei Univ.)*, **K. IRIYAMA** *(Jikei Univ.)*, **H. OGOSHI** *(Tech. Univ. of Nagaoka)*, **T. OCHIAI** *(Tech. Univ. of Nagaoka)*, **and T. KITAGAWA**

[*J. Phys. Chem.*, **90**, 6105 (1986)]

Resonance Raman (RR) spectra of octaethylchlorinato-iron [Fe(OEC)] complexes in various spin-, oxidation-, and ligation-states have been measured and compared with those of the analogous complexes of octaethylporphyrinato-iron [Fe(OEP)] in an attempt to gain new insight into chlorin chemistry. Regarding the methine-bridge stretching modes, the ν_{19} frequencies were different between the two kinds of complexes while the ν_{10} and ν_3 frequencies were close between them. For the $C_\beta C_\beta$ stretching modes, the frequency separation between the ν_2 and ν_{11} modes became markedly larger for the Fe(OEC) complexes. When these frequencies were plotted against the center-to-pyrrole nitrogen distance, both the Fe(OEC) and Fe(OEP) complexes gave straight lines, and their inclinations were similar between the OEC and OEP complexes except for ν_{19} band. Ferrous low-spin complexes deviated from the straight lines but the deviations were appreciably smaller for the OEC complexes. Frequencies of the ν_4 mode were lower by 2–6 cm^{-1} for Fe^{III}(OEC) complexes and higher by 1–5 cm^{-1} for Fe^{II}(OEC) complexes compared with those of the corresponding Fe(OEP) derivatives. As a result, downward shifts of the ν_4 mode upon reduction of the iron ion, which have been attributed to the increased π-back donation from the d_π(Fe) to the Π^* (macrocycle) orbitals, are considerably smaller for the OEC complexes. Frequencies of the ν_{10}, ν_{11}, and ν_4 modes of ferrous low-spin complexes decreased linearly with the increase of pK_a of axial ligands, but the linear correlations were much less steep with the Fe^{II}(OEC) complexes than with Fe^{II}(OEP) ones. These observations for the ferrous complexes suggested that the π-back donation is less significant for the Fe^{II}(OEC) complexes than for the Fe^{II}(OEP) ones.

II-D-2 Resonance Raman Characterization of Iron-Chlorin Complexes in Various Spin-, Oxidation-, and Ligation-States. II: Low-Frequency Skeletal Vibrations and Fe-Ligand Stretching Modes

Y. OZAKI *(Jikei Univ.)*, **K. IRIYAMA** *(Jikei Univ.)*, **H. OGOSHI** *(Tech. Univ. of Nagaoka)*, **T. OCHIAI** *(Tech. Univ. of Nagaoka)*, **and T. KITAGAWA**

[*J. Phys. Chem.*, **90**, 6113 (1986)]

The low frequency region of resonance Raman (RR) spectra of octaethylchlorinato-iron [Fe(OEC)] in

various spin-, oxidation-, and ligation-states and octaethylchlorinato-copper [Cu(OEC)] has been explored and compared with that of the analogous complexes of octaethylporphyrin (OEP). The Fe-axial ligand (L) stretching frequencies of Fe(OEC) derivatives are in general very close to those of the corresponding Fe(OEP) derivatives. The RR bands due to internal modes of pyridine (Py) have been identified at almost the same frequencies between Fe^{II}-(OEC)$(Py)_2$ and $Fe^{II}(OEP)(Py)_2$. These facts indicate the nature of the Fe-L bonds remains unaltered upon saturation of one of four $C_\beta C_\beta$ bonds. Excitation profiles of the bound-pyridine modes of $Fe^{II}(OEC)(Py)_2$ imply that $d_\pi(Fe)$-$\Pi^*(Py)$ charge transfer band is located near 500 nm. With regard to the vibrations of the macrocycle, the ν_{16}, $2\nu_{35}$ and ν_8 frequencies of chlorin derivatives are always lower than those of porphyrin derivatives while the ν_7 frequency exhibits the opposite trend. The ν_7 and ν_{16} RR bands can be used as markers of a chlorin skeleton.

II-D-3 Resonance Raman Spectra of Red-Shifted Retinal Schiff's Base

Toshiharu SUGIHARA *(Gifu Univ.)* **and Teizo KITAGAWA**

[*Bull. Chem. Soc. Jpn.*, **59**, 2929 (1986)]

We have found that the visible absorption maximum (λ_{max}) of retinal Schiff's base in fluoro alcohols is considerably red-shifted. The C=N stretching Raman line exhibits a frequency shift in deuterated fluoro alcohols, indicating that the Schiff's base is protonated. Frequencies of the in-phase C=C stretching Raman lines ($\nu_{C=C}$) changed linearly with λ_{max}, and the $\nu_{C=C}$ vs. λ_{max} correlation coincides with that observed for retinoid proteins.

II-D-4 Characterization of Low Frequency Resonance Raman Bands of Metallo-protoporphyrin IX: Observation of Isotope Shifts and Normal Coordinate Treatments.

H. LEE, M. ABE *(Shoin Women's Univ.)*, **R.K. PANDEY** *(Univ. of California)*, **H.-K. LEUNG** *(Univ. of California)*, **K.M. SMITH** *(Univ. of California)*, **and T. KITAGAWA**

[*J. Mol. Struct.*, **146**, 329 (1986)]

Resonance Raman spectra are observed for six specifically deuterated derivatives of protoporphyrinato-Ni(II) [Ni(PP)] in CH_2Cl_2, CCl_4 and benzene solutions with the 406.7, 441.6 and 514.5 nm excitation lines. Normal coordinate calculations are carried out for appropriate model porphyrins and on the basis of the calculated deuteration shifts the observed Raman bands of Ni(PP) are assigned. The assignments of Raman bands previously established for symmetric octaethylporphyrinato-Ni(II) [Ni(OEP)] are generally applicable to the high frequency skeletal modes of Ni(PP), although the vinyl CH_2 rocking mode is considerbly mixed with the porphyrin modes near 1000-1200 cm^{-1}. For the modes below 450 cm^{-1}, asymmetric disposition of the peripheral groups makes the corresponding modes of the four pyrrole rings non-equivalent and it appears that each pyrrole ring has specific intensity and frequencies in the Raman spectra.

II-D-5 Tautomeric Equilibrium of Salycylidene Schiff Base; UV-Visible Absorption and Raman Spectroscopic Studies

Ho-Hi LEE and Teizo KITAGAWA

[*Bull. Chem. Soc. Jpn.*, **59**, 2897 (1986)]

The solvent effect and temperature dependence on the Raman and absorption spectra demonstrated the existence of a tautomeric equilibrium for the title compound between the enol form and the protonated Schiff base form in methanol; the latter form is more stable by ca. 850 cal/mol than the former. Characteristic Raman bands for the two tautomers have been identified.

II-D-6 Resonance Raman Study on Catalytic Intermediates of Cytochrome *c* Oxidase

Teizo KITAGAWA and Takashi OGURA

[Nonlinear Raman Spectroscopy in press]

Resonance Raman (RR) Spectra of redox- and reaction-intermediates of cytochrome *c* oxidase was investigated. Aerobic laser irradiation to this enzyme produced a photo-steady state for catalytic reduction of

oxygen and Raman scattering from it probed the RR spectra of cytochrome a^{2+} and cytochrome $a_3{}^{3+}$ separately upon excitations at 441.6 and 406.7 nm, respectively. Measurements with variable-speed spinning cell allowed to deduce the rate constant of electron transfer from cytochrome a^{2+} to cytochrome $a_3{}^{3+}$ to be 0.5 s^{-1} at most. A mixed flow transient Raman apparatus was constructed and the RR spectrum of an oxygenated intermediate having the Fe^{2+} heme in cytochrome *a* and the $Fe^{2+}-O_2$ or Fe^{4+} = O heme in cytochrome a_3 was observed.

II-D-7 The Behavior of Ethanol in Various Binary Solutions: Difference Raman Spectroscopy of the C-H Stretching Vibrations.

K. KAMOGAWA, S. KAMINAKA, and T. KITAGAWA

[*J. Phys. Chem.* in press]

Frequency shifts of the C-H stretching modes of ethanol upon mixing with various liquids were observed as a function of the concentration, and their shift-behaviors were analyzed by using the homogeneous ($\Delta\nu_{AA}$) and heterogeneous ($\Delta\nu_{AB}$) interaction factors proposed previously. The values of $\Delta\nu_{AB}$ at $\chi\cong1.0$ (χ: mole fraction of ethanol) became smaller as the polarizability of the perturbing species became larger. This suggested that the dispersion force plays an essential role in determining the frequency shifts of the C-H stretching modes upon mixing. The $\Delta\nu_{AA}$-vs-χ curve of the C_2H_5OH/H_2O solution exhibited noticeable similarity to the corresponding curve of the partial molar volume of ethanol as anticipated from the previous study on the CH_3CN/H_2O and $(CH_3)_2CO/H_2O$ solutions. This study provides a spectroscopic evidence for the presence of the discrete composition segments in the binary solutions.

II-D-8 Resonance Raman Characterization of Highly Reduced Iron Porphyrin

J. TERAOKA *(Osaka City Univ.)*, **S. HASHIMOTO, H. SUGIMOTO** *(Osaka City Univ.)*, **M. MORI** *(Osaka City Univ.)*, **and T. KITAGAWA**

[*J. Am. Chem. Soc.* in press]

Resonance Raman, EPR, and visible absorption spectra were observed for highly reduced iron octaethylporphyrin complexes, $[Fe(OEP)]^{n-}$, which were obtained in tetrahydrofuran (THF) by the sodium-mirror contact reduction technique. Raman and EPR spectra were measured with the same preparation as was used in the study of visible absortption spectrum which showed clear isosbestic points in each stage of the oxidoreduction: $Fe^{III}(OEP)Cl \leftrightarrow Fe^{II}(OEP)(THF) \leftrightarrow [Fe(OEP)]^{-} \leftrightarrow [Fe(OEP)]^{2-}$. Raman lines of $[Fe(OEP)]^{-}$ and $[Fe(OEP)]^{2-}$ were qualitatively assigned on the basis of the frequency shifts observed for ^{15}N substitution and meso-deuteration. $[Fe(OEP)]^{-}$ which exhibited EPR signals at $g_{\perp} = 2.26$ and $g_{\parallel} = 1.93$ at 77 K, gave the ν_4 line at the same frequency as the Fe^{II} complex but the ν_{10} line at much lower frequency, and the overall spectral pattern of $[Fe(OEP)]^{-}$ in THF was distinctly different from that of $Fe^{II}(OEP)$ in THF which gave a RR spectrum of the five coordinate high spin type. The RR spectrum of $[Fe(OEP)]^{-}$ in THF was altered between 77 K and 300 K. This is in agreement with the spin transition reported between 77 and 200 K. $[Fe(OEP)]^{2-}$, which was EPR silent, gave the ν_4 line at a considerably lower frequency but the ν_{10} and other C_aC_m stretching modes at frequencies similar to those of the $Fe^{II}(OEP)$-THF complex. Frequencies of the modes involving the C_bC_b stretching character like ν_2 and ν_{11} were distinctly lower for $[Fe(OEP)]^{2-}$, suggesting the formation of a porphyrin π-anion radical.

II-D-9 Ligand-aided Photoreduction of Iron-Porphyrin Complexes Probed by Resonance Raman Spectroscopy

Y. OZAKI *(Jikei Univ.)*, **K. IRIYAMA** *(Jikei Univ.)*, **H. OGOSHI** *(Technological Univ. of Nagaoka)*, **and T. KITAGAWA**

[*J. Am. Chem. Soc.* in press]

Photoreduction has been observed for the first time for an iron porphyrin with a biologically-relevant axial ligand by using resonance Raman (RR) spectroscopy; for $Fe^{III}(OEP)$ (2-MeIm) (OEP: octaethlyporphyrin, 2-MeIm: 2-methylimidazole). The photoreduction is wavelength-dependent and is more efficient upon irradiation in blue than in green as was so for

hemeproteins thus far investigated. Similar photoreduction was observed for Fe^{III}(OEP) (1,2-Me_2Im) (1,2-Me_2Im: 1,2-dimethylimidazole) but not for Fe(OEP)L_2 (L = imidazole and 1-methylimidazole) and Fe^{III}(OEP)X (X = F, Cl, Br, I, and ClO_4). The coincidence of the RR spectrum of the photoreduced species with that of the ferrous porphyrin rules out a possibility of the ring reduction to a porphyrin anion radical or chlorin. The dependence of the photoreduction on the concentration of 2-MeIm suggested that the ligand free Fe^{II}(OEP) is a likely intermediate and thus that the light-induced charge-transfer from the axial ligand to the iron ion is the primary process of the photoreduction.

II-D-10 Oxygen Exchange between the Fe(IV)=O Heme and Bulk Water for the A_2 Isozyme of Horseradish Peroxidase

Shinji HASHIMOTO, Ryo NAKAJIMA *(Hokkaido Univ.)*, **Isao YAMAZAKI** *(Hokkaido Univ.)*, **Yoshitaka TATSUNO** *(Osaka Univ.)*, **and Teizo KITAGAWA**

[FEBS Lett. **208**, 305 (1986)]

Resonance Raman spectra were observed for compound II of horseradish peroxidase A_2, and the Fe(IV)=O stretching Raman line was identified at 775 cm^{-1}. This Raman line shifted to 741 cm^{-1} upon a change of solvent from $H_2{}^{16}O$ to $H_2{}^{18}O$, indicating occurrence of the oxygen exchange between the Fe(IV)=O heme and bulk water. The oxygen exchange took place only at the acidic side of the heme-linked ionization with pK_a=6.9.

II-D-11 The Properties of Chemically Modified Ni(II)-Fe(II) Hybrid Hemoglobins: Ni(II) Protoporphyrin IX as a Model for a Permanent Deoxy-Heme

Naoya SHIBAYAMA *(Osaka Univ.)*, **Hideki MORIMOTO** *(Osaka Univ.)*, **and Teizo KITAGAWA**

[*J. Mol. Biol.* in press]

Chemical modifications, NES-Cys(β93), des-Arg (α141), and both modifications on the same molecule, were applied on Ni-Fe hybrid hemoglobins, and the effect of modifications on individual subunit was investigated separately by measuring oxygen equilibrium curves, the Fe(II)-N_ε (His F8) stretching Raman lines, and light absorption spectra. The oxygen equilibrium properties indicated that modified Ni-Fe hybrid hemoglobins remain as good models for the corresponding deoxy ferrous hemoglobins, although K_1, the dissociation equilibrium constant for the first oxygen to ligate to hemoglobin, was decreased by chemical modifications. Resonance Raman spectra of deoxy α_2(Fe)β_2(Ni) and light absorption spectra of deoxy α_2(Ni)β_2(Fe) revealed that the state of α-hemes in both hybrid hemoglobins showed a transition from a deoxy-like state to an oxy-like state by these chemical modifications when K_1 was about 3 mmHg. On the other hand, the state of β hemes in hybrid hemoglobins was little affected, when K_1 was larger than 1 mmHg. Modified α_2(Fe)β_2(Ni) gave Hill coefficient well deviated from unity with the maximum of 1.4 when K_1 was about 4 mmHg. The two state model [Monod, J., Wyman, J. and Changeux, J.P. (1965) J. Mol. Biol. 12, 365-385] predicted that the K_1 value at the maximum Hill coefficient should be much larger than this value. Upon oxygen binding to unmodified α_2(Ni)β_2(Fe), oxygen equilibrium data suggested to structural change, while the spectral data showed a structural change around Ni(II) protoporphyrin IX in the α subunits. Similar situation was encountered in modified α_2(Ni)β_2(Fe), although K_1 was decreased resulting from the structural changes induced by the modifications.

II-E Structure of Noncrystalline Materials by EXAFS

It is very important to know the structure of supported catalyst in order to understand the roles of catalyst in catalytic reactions. EXAFS is best suited for the purpose because the local structure around the selected elements can be determined irrespective of the phase. Very tiny metals or metal clusters in the supported catalyst, which TEM and XRD fail to observe, can be studied. Especially, the structural changes at every stage of catalyst preparation procedures can be probed by EXAFS, making it easier to make a comparison of the catalysts prepared by different

procedures. In addition, the structure under the reacting conditions can be studied by the use of an in situ cell, since EXAFS measurements can be done with the presence of the reacting gas.

In the past year, our efforts was mainly concentrated on the determination of the structures of several supported mono- and bimetallic catalysts. Structural changes at the several stages of the preparation procedure and under the presence of reacting gases have been investigated. Studies on the local structure around the metal in aqueous solutions and in glassy materials have also been continued as joint studies program.

Improvements in the experimental conditions in the past year have made it possible to extend the EXAFS measurement to various elements ranging from Ti to Ag. The control of the current of x-ray generator has made it possible to keep the x-ray intensity distribution constant, making the measurement more accurate (see Special Research Project). A possibility of Raman spectroscopy by x-ray excitation has been continuously pursued.

The followings are the abstracts of the manuscripts submitted to several journals.

II-E-1 Catalyst Structure Studied by A Laboratory EXAFS Facility; Ru/Al_2O_3

Yasuo UDAGAWA, Kazuyuki TOHJI, Zheng-Zhong LIN*, Toshio OKUHARA*, and Makoto MISONO*
*(*The University of Tokyo)*

[*J. de Physique.*, in press]

A laboratory EXAFS spectrometer is described which features the utilization of higher order reflections from curved dispersing crystal. With this spectrometer a sufficient performance for structural analysis is obtained in the high energy region up to about 25 keV. It was appllied to structurally characterize two kinds of Ru/Al_2O_3 catalysts prepared from $RuCl_3$ and $Ru_3(CO)_{12}$, by the Ru K EXAFS, combined with H_2 adsorption and EM observations. It was found that Ru metal particles of different sizes were formed depending on the starting material and the preparation procedure. In the catalyst obtained from $Ru_3(CO)_{12}$, small metal particles, possibly consist of about 20 atoms, are formed. They are small enough to show a contraction of the nearest neighbor distance by 0.06 A.

II-E-2 A Development of EXAFS and XANES Measurements in the Laboratory – An Application to Silica Supported Cu-Rh Bimetallic Catalyst

Kazuyuki TOHJI, Yasuo UDAGAWA, Mutsumi HARADA*, and Akifumi UENO** *(*Graduate Student from Toyohashi Univ. of Technology, **Toyohashi Univ. of Technology)*

[Nippon Kagaku Kaishi, **1986**, 1553]

An improvement of an EXAFS facility was attempted by the use of higher order reflections from dispersing crystals. A resolution good enough to observe XANES structure has been obtained in the lower energy region (5-10 keV), and EXAFS measurements have been extended to cover up to about 26 keV, including K absorption edges of Ru, Rh, Pd, and Ag, which are important in catalysis. Some examples of the performances of this spectrometer is presented.

By making use of the spectrometer, local structures around Cu and Rh atoms in $Cu\text{-}Rh/SiO_2$ catalysts have been studied by the EXAFS of Cu and Rh and also by the XANES of Cu. Catalysts prepared by two kinds of preparation procedures, the impregnation method and the alkoxide method, have been examined. In the catalyst prepared by both the method, Rh atoms are in the metallic environment and are surrounded by other Rh atoms but Cu atoms are not. Cu atoms are concluded to have both Cu and Rh neighbors and are concentrated on the surface. The tendency is more pronounced in the catalyst prepared by the alkoxide method, indicating the differences in the metal particle size of both the catalysts prepared by the different method.

II-E-3 Present Aspects of X-ray Raman Scattering

Kazuyuki TOHJI and Yasuo UDAGAWA

[*Bunko Kenkyu* **35**, 72 (1986)]

A two crystal spectrometer for x-ray Raman scattering measurement has been constructed. In short, it consists of a Johansson cut and bent crystal to pick out Cu $K_{\alpha 1}$ line as an excitation source, and a flat crystal

spectrometer to analyze scattered photon. A combination of a position sensitive proportional counter (PSPC) and a multichannel analyzer has been employed to detect scattered photons.

In Figure 1 shown is an inelastic scattering spectrum obtained for graphite. Rayleigh (elastic), Compton, and Raman scatterings are indicated in the figure. The energy difference between the excitation light and the edge of the Raman scattering is about 280 eV. Although very weak,the spectrum is always reproducible and agrees well with the one previously reported by Suzuki.[1] A possibility of local structure determination by the analysis of this x-ray Raman scattering is discussed.

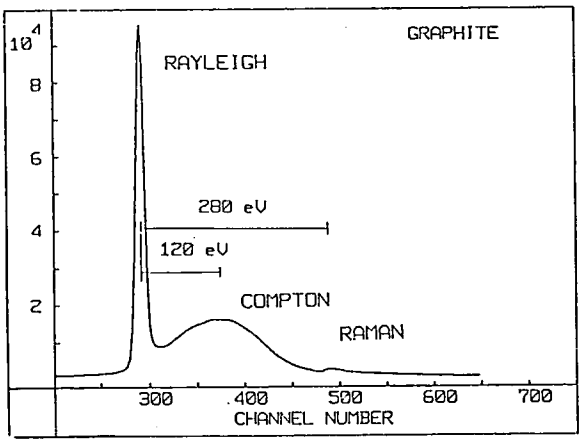

Figure 1. Inelastic scattering spectrum from graphite.

Reference

1) T. Suzuki, *J. Phys. Soc. Jpn.*, **22**, 1139 (1967).

II-E-4 Preparation and Characterization of Binary Oxide-Powder Composed of TiO_2 and ZrO_2

Yutaka HIRASHIMA, Hideyasu TSUIKI, Akifumi UENO *(Toyohashi Univ. of Technology)*, **Kazuyuki TOHJI, and Yasuo UDAGAWA**

[*J. Catal.* **102**, 249 (1986)]

Binary oxide powder was prepared by simultaneous hydrolytic decomposition of Ti and Zr alkoxides, and compared with that prepared by physical mixing. High dispersion of Ti and Zr ions in the former was proved by means of EPMA and AES. Although no ZrO_2 crystal formation was observed by XRD, EXAFS results show that the local structure around Zr ions is very similar to that of ZrO_2 crystal when the calcination temperature is low. At high calcination temperature Zr-O distance as well as the coordination number around Zr atoms decreases, indicating a reconstruction of the metal-O-metal network. Above 650°C both EXAFS and XRD data clearly show the formation of $ZrTiO_4$ particles, while $ZrTiO_4$ formation was observed in the physically mixed oxide at the calcination temperature higher than 1200°C. Catalytic performance of this binary oxide powder is discussed on the basis of its catalytic activity for the reverse shift reaction.

II-E-5 Preperation of Fine Fe-Ni Alloy Particles Dispersed in Silica

Mutsumi HARADA *(Graduate Student from Toyohashi Univ. of Technology)*, **Kazutaka ONO, Hideyasu TSUIKI, Akifumi UENO** *(Toyohashi Univ. of Technology)*, **Takanori MIZUSHIMA, and Yasuo UDAGAWA**

[*Chem. Lett.* **1986**, 1569]

Fine Fe-Ni bimetallic clusters dispersed in silica were prepared by hydrolysis of a mixed solutiuon of ethyl silicate and iron and nickel nitrates dissolved in ethylene glycol. It was found that the fine alloy particles with fcc structure is formed over all the concentration ratio studied; from 1:3 to 3:1 in atomic ratio. X-ray diffraction as well as electron microscope study indicates that the size of alloy prepared by the method employed here is well controlled, the average size being about 160 A.

II-E-6 Synthesis and Characterization of Bis (2,4,6-tri-t-butylphenyl)-germanium

Kunio MOCHIDA, Akira FUJII, Noriko TSUCHIYA *(Gakushuuin Univ.)*, **Kazuyuki TOHJI, and Yasuo UDAGAWA**

[submitted to *Organometallics*]

The title compounds was synthesized from germanium (II) iodide and the corresponding aryl lithium, and characterized directly by EXAFS.

RESEARCH ACTIVITIES III
Department of Electronic Structure

III-A UV and VUV Photochemistries of Olefins, Alkylbenzenes, and Organic Germanium, Titanium, and Tin Compounds

Irradiation of molecules with UV or VUV light often induces photodissociation. Besides direct and pre-photodissociation, we have been investigating another type of photodissociation, which consecutively involves excitation of electronically excited state, efficient internal conversion to the ground state, and dissociation. The ground electronic state thus produced has a very high vibrational energy, in other words, the corresponding vibrational temperature is thouthands Kelvin. Since the internal energy of this state is determined by photon energy and unique, we have directly obtained the specific rate constants of unimolecular dissociation. We show that the dissociation rate constants of olefines can be predicted on the basis of RRKM theory. Deuterium isotope effect on the rate constants of alkylbenzenes suggests that intramolecular vibrational redistribution is complete before the dissociation reaction. We have studied photochemistries of alkyl compounds containing Si, Ge, and Sn atoms.

III-A-1 Comparison of Photo-Dissociation Rate Constants of Olefins with RRKM Theory

Nobuaki NAKASHIMA and Keitaro YOSHIHARA

The primary intermediate of olefin photochemistries in the gas phase is hot molecule (S_0**: highly excited vibrational states in the ground electronic state).[1] The same mechanism is operative in the photo-isomerization of benzene and dissociation of alkylbenzenes. For the first time, the specific dissociation rate constants (k_d) are measured from S_0** of more than 50 molecules.[2]

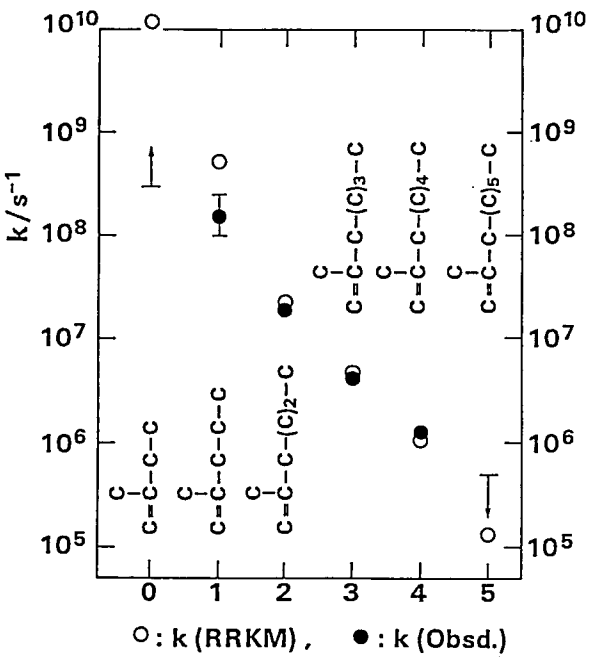

Figure 1. Comparison of dissociation rate constants (open circles) from S_0** and calculated ones (closed circles) on the basis of RRKM theory. 2-methyl-1-olefins are irradiated with an ArF laser (193 nm). Rate constants of olefns in the both sides were too great or too small to be measured.

The rate constants are measured on irradiation with the ArF laser (193 nm) light by observing the rise time of allylic radicals for olefins under collision free conditions. The k_d depends on the size of parent molecules. For example, 2-methyl-1-hexene dissociates with $1.9 \times 10^7 s^{-1}$ while 2-methyl-1-octene with $1.3 \times 10^6 s^{-1}$. These reaction rate constants can be explained in terms of RRKM theory of thermal reactions as shown in Figure 1.

References

1) N. Nakashima, N. Shimo, N. Ikeda, and K. Yoshihara, *J. Chem. Phys.*, **81**, 3738 (1984).

2) N. Nakashima, N, Shimo, N, Ikeda and K. Yoshihara, *XIIth Int. Conf. on Photochemistry*, Tokyo, 1985, Abstract pp451-454.

III-A-2 Deuterium Isotope Effects on Photodecomposition of Alkylbenzenes

Yoshizumi KAJII *(Tokyo Inst. of Tech.)*, **Kinichi OBI** *(Tokyo Inst. of Tech.)*, **Ikuzo TANAKA** *(Tokyo Inst. of*

Tech.), **Noriaki IKEDA** *(Kyoto Inst. Tech.)*, **Nobuaki NAKASHIMA, and Keitaro YOSHIHARA**

Deuterium isotope effects on photodecomposition of alkylbenzenes (toluene,[1] ethylbenzene, and butylbenzene) have been studied by ArF laser flash photolysis. Formation rate constants of hot benzyl radical have been measured under collision free conditions. It has been found that the formation rate constant of hot benzyl radicals decreases in accordance with the extent of deuterium substitution and that they seem to have no selectivity on the position of deuterium substitution. These findings indicate that, in addition to benzene ring, alkyl groups play a role in intramolecular vibrational redistribution (IVR), in other words, IVR is complete before dissociation. Figure 1 shows some examples of formation of hot benzyl radicals upon irradiation of ethylbenzene d_0 (a) and d_{10} (b).

References

1) N. Ikeda, N. Nakashima, and K. Yoshihara, *J. Chem. Phys.*, **82**, 5285 (1985).

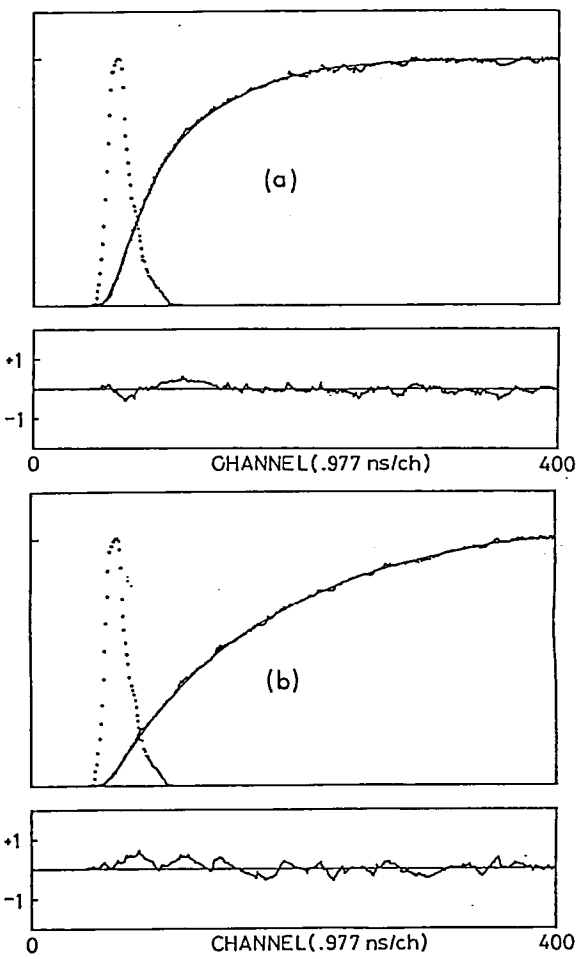

Figure 1. Rise curve of formation of benzyl radicals upon irradiation of ethylbenzene d_0 (a) and d_{10} (b) with the ArF laser light (193 nm).

III-A-3 Laser Photodissociation of Organic Germanium and Tin Compounds

Nobuo SHIMO *(Cen. Res. Lab. Idemitsu Kosan)*, **Nobuaki NAKASHIMA, and Keitaro YOSHIHARA**

Organic germanium compounds ($(CH_3)_4Ge$, $(CH_3)_4GeGe(CH_3)_4$, $(CH_3)_3GeCl$, CH_3GeCl_3) and organic tin compounds ($(CH_3)_4Sn$, $(CH_3)_4SnSn(CH_3)_4$, and $(CH_3)_3SnCl$) have been photolyzed with an ArF excimer laser in the gas phase. On irradiation of $(CH_3)_4Ge$, $(CH_3)_4GeGe(CH_3)_4$, and $(CH_3)_3GeCl$, trimethyl germyl radical (λ_{max} = 253 nm with ε = 5900 $M^{-1}cm^{-1}$) has been obtained, as shown in Figure 1, for the first time. The bimolecular recombination rate constant is 2.5×10^{-11} molecule^{-1}s^{-1}. The spectrum and the rate constant are similar to those of trimethylsilyl radical.[1] For the case of tin compounds, one of the peaks in the transient absorbption spectra was tentatively assigned to dimethylstannylene ($(CH_3)_2Sn$).

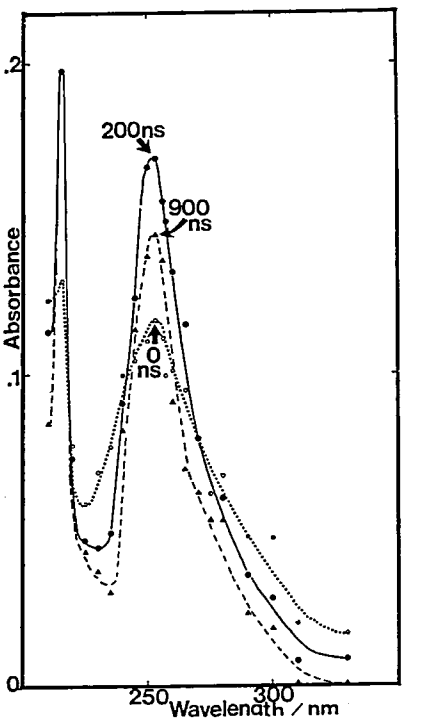

Figure 1. Time resolved transient absorption spectra of tetramethylgerman (5 Torr) with ArF laser irradiation.

Reference

1) N. Shimo, N. Nakashima, and K. Yoshihara, *Chem. Phys. Lett.*, **125**, 303 (1986).

III-B Dynamical Behavior of Excited Dye Molecules Adsorbed on Organic Single Crystals: A Novel System for Study of Electron Transfer

The system of dye molecules adsorbed on a single crystal allows unique oppotunities for separate measurements of energy and electron transfer. A few years ago we studied two-dimentional energy transfer among adsorbed dye molecules on naphthalene and phenanthrene single crystals. Uninfluenced by energy transfer at a coverage of about 0.01, electron transfer has been studied with anthracene, pyrene, and other single crystals for which the free energy of electron transfer reaction, ΔG_0, is negative. In this chapter, we firstly describe in two sections the properties of adsorbed dyes, i.e., observation of dimer fluorescence and site-dependent fluorescence; and secondly, the electron transfer characteristics, in particular, the quantum mechanical analysis of electron transfer rate of the present system.

III-B-1 Fluorescence Decays and Spectral Properties of Rhodamine B in Submono-, Mono-, and Multilayer Systems

Klaus KEMNITZ, Naoto TAMAI *(Instrument Center),* **Iwao YAMAZAKI** *(Instrument Center),* **Nobuaki NAKASHIMA, and Keitaro YOSHIHARA**

[*J. Phys. Chem.*, **90**, 5094 (1986)]

Absorption and fluorescence properties of rhodamine B in submono-, mono-, and multilayer systems adsorbed on fused quartz plates have been studied in detail at 295 and 77 K. The results were compared with a system of dye on single crystal of naphthalene and phenanthrene.[1] Existence of fluorescent and non-fluorescent dimers of rhodamine B at 295 K and structural changes of the aggregate geometry at low temperatures have been postulated. Some of the fluorescence decays as functions of observed wavelengths and temperature are shown in Figure 1. Rates of nonradiative decay and photoinduced electron transfer of dimers adsorbed on organic crystals and their possible role in hole-injection are discussed.

Reference

1) K. Kemnitz, T. Murao, I. Yamazaki, N. Nakashima, and K. Yoshihara, *Chem. Phys. Lett.*, **101**, 337 (1983).

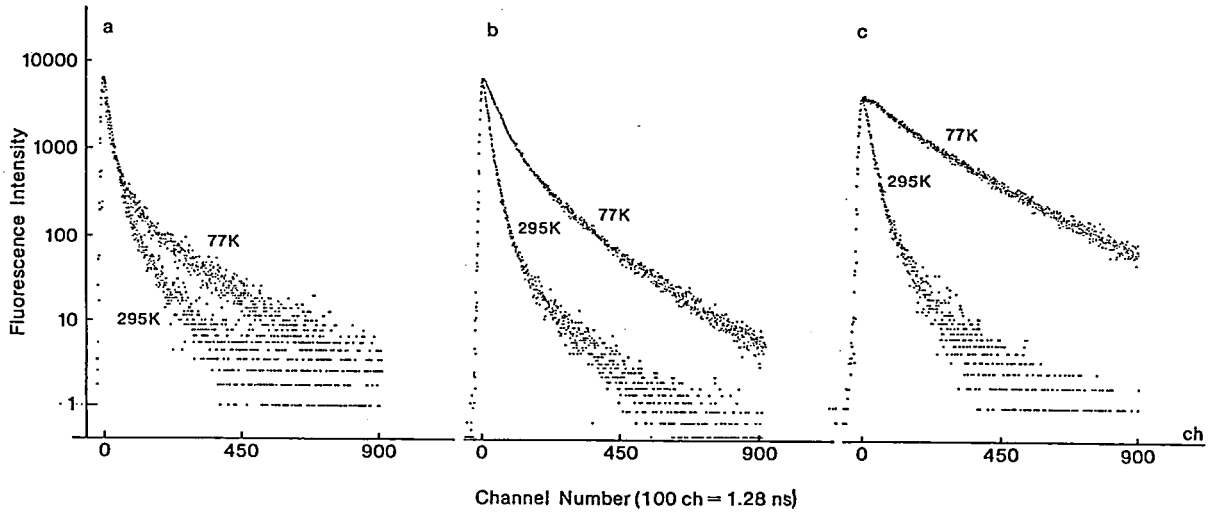

Figure 1. Dependence of the fluorescence decays on the observation wavelength of a rhodamine B monolayer adsorbed on glass at 295 and 77 K: 573 nm (a), 590 nm (b) and 620 nm (c). λ_{ex} = 550 nm, 100 ch = 1.28 ns. Note that there is no rise observed at 620 nm.

III-B-2 Site-Dependent Fluorescence Lifetimes of Isolated Dye Molecules Adsorped on Organic Single Crystals and Other Substrates

Klaus KEMNITZ, Naoto TAMAI *(Instrument Center)*, **Iwao YAMAZAKI** *(Instrument Center)*, **Nobuaki NAKASHIMA, and Keitaro YOSHIHARA**

[*J. Phys, Chem.*, in press]

Fluorescence dynamics of dye molecules monomerically adsorbed on single crystals of naphthalene and phenanthrne, fused quartz plates, Teflon, CaF_2, and polyester have been observed on the subnanosecond timescale. All of the observed decays are nonexponential. Measurements with organic single crystals of different surface quality revealed, some of the examples being shown in Figure 1, that distorted adsorption sites are responsible for reduced fluorescence lifetimes. By comparing the fluorescence properties of three xanthene dyes with different rigidity, rhodamine B, rhodamine 101, and pyronine B, the reduced lifetimes at distorted sites was postulated to be due to enhanced internal conversion. The rhodamine B molecule can be used as a convenient probe for the investigation of surface structure and its adsorption site the distribution, as it was applied, for the first time, to the study of the phase transition of single crystals. Addition of thin layer of water on the substrate/dye system considerably reduces the fast fluorescence component. A possible mechanism for the water effect is discussed.

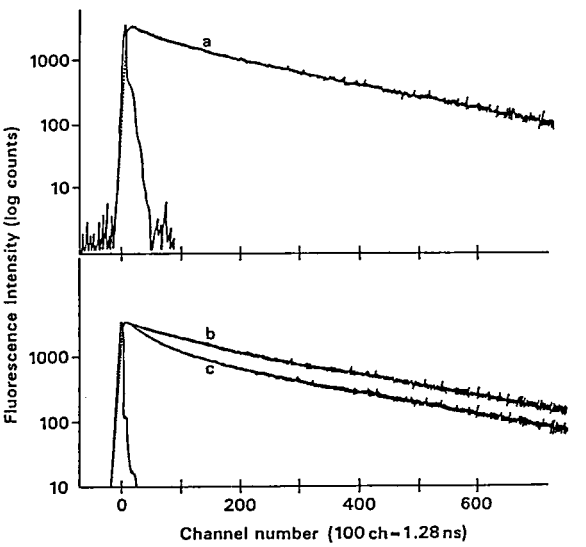

Figure 1. Effect of crystal quality on the decay kinetics: Rhodamine B adsorbed on naphthalene (a) and pyronine B on phenanthrene (b) and (c), coverage = 0.04. (a) flawless crystal: 0.17 ns (22%), 1.17 ns (27%), and 3.10 ns (51%), (b) flawless crystal: 0.20 ns (26%), 1.12 ns (17%), and 3.80 ns (57%) (c) specimen covered with dislocations: 0.19 ns (40%), 1.14 ns (32%), and 3.30 ns (28%).

III-B-3 Energy and Electron Transfer of Adsorbed Dyes on Molecular Single Crystals and Other Substrates

Klaus KEMNITZ, Nobuaki NAKASHIMA, and Keitaro YOSHIHARA

[*Ultrafast Phenomena V*, A. Siegman and G. Fleming Ed., Springer, (1986), in press]

Energy and electron transfer frequently occur in the same system. Therefore it is of considerable interest to investigate a system, where both phenomena can be observed independently from one another. The system of dye molecules adsorbed on organic crystals is ideally suited to serve either as inert or chemically interacting (electron transfer) substrates, depending on the choise of substrates and dyes, as shown in Figure 1. In order to study electron transfer through the crystal surface, it is

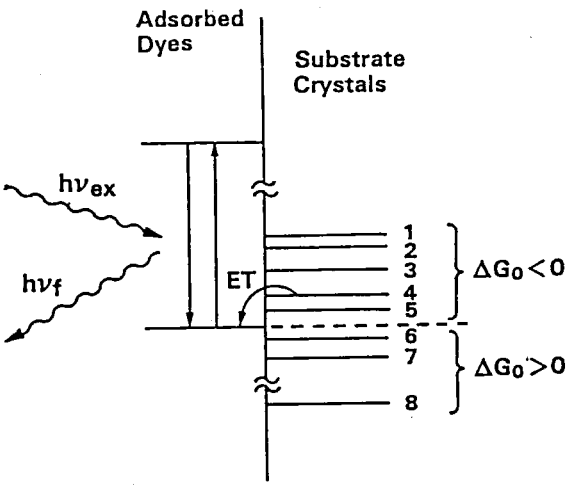

Figure 1. Energy diagram of adsorbed dye-substrate system. The substrate materials used are 1. perylene, 2. phenazine, 3. benzoperylene, 4. anthracene, 5. pyrene, 6. phenanthrene, 7. naphthalene, and 8. quartz plate. The dyes used are rhodamine B, rhodamine 101, and pyronine B. ΔG_0 is the free energy change for electron transfer between adsorbed dye and substrate.

necessary to know the competitive contribution of energy transfer on the surface to the overall fluorescence decay. On organic crystals, the competitive processes are electron transfer from the crystal to the excited dye and energy transfer from excited dye monomer to other monomers[1] or to dye aggregates like dimers.[2,3,4] We chose to study dry solvent-free systems which show no solvent-solute interaction, allowing the measurement of the temperature dependence and of vibronic interactions on electron transfer due to the small reorganization energy.

References

1) F. Willing, A. Blumen, and G. Zumofen, *Chem, Phys. Lett.*, **108**, 222 (1984).
2) N. Nakashima, K. Yoshihara, and F. Willig, *J. Chem. Phys.*, **73**, 3553 (1980).
3) K. Kemnitz, T. Murao, I. Yamazaki, N. Nakashima, and K. Yoshihara, *Chem. Phys. Lett.*, **101**, 337 (1983).
4) K. Kemnitz, N. Tamai, I. Yamazaki, N. Nakashima, and K. Yoshihara, *J. Phys. Chem.*, (1986), in press.

III-B-4 An Analysis of Electron Transfer Rate Constants from Single Crystal Substrates to Adsorbed Dye on the Basis of Quantum Mechanical Theory

Nobuaki NAKASHIMA, Klaus KEMNITZ, and Keitaro YOSHIHARA

Electron donors are organic crystals and the acceptor is the lowest excited singlet state of an adsorbed dye, rhodamine B. When the free energy change is negative for electron transfer reaction, fluorescence of rhodamine B will be quenched by electron injection. We measured fluorescence decay curves for 5 systems.[1] The electron transfer rate constants have been derived from the major component in a multi-exponential fit.

In Figure 1, circles are observed electron transfer rates and the solid line is a curve simulated on the basis of a quantum mechanical electron transfer theory, using a modified model of Jortner's theory (Sarai's version)[2]. The Marcus' inverted region is observed for the first time for the adsorbed system. One important finding is the small exchange matrix element. It is probably caused by adsorption configuration. Anthracene and dye are not in sandwich configuration, but have a large angle.

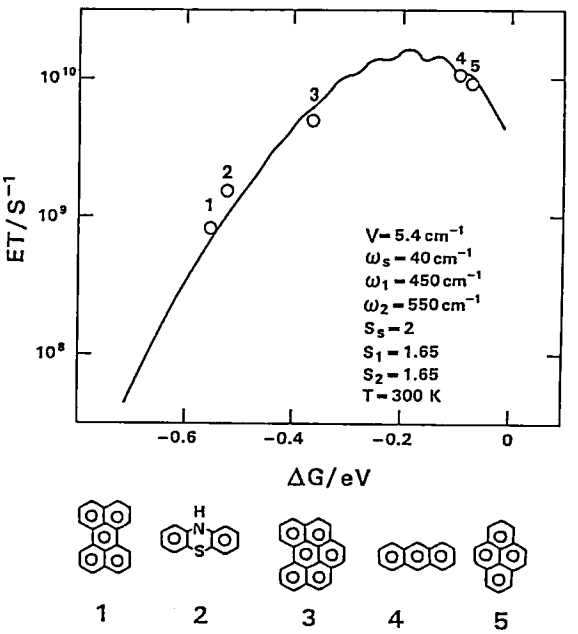

Figure 1. Analysis of electron transfer rate constants for adsorbed systems. Rhodamine B is adsorbed on organic single crystals shown at the bottom. Circles(o) are observed rates and the solid line is a curve simulated on the basis of a quantum mechanical electron transfer theory.

References

1) K. Kemnitz et at., *Conference on Molecular Structure* Japan, 1984, Nagoya.
2) A. Sarai, *Chem. Phys. Lett.*, **63**, 360 (1979).

III-C Alternative Methods for Studying Molecular Dynamics on Picosecond and Femtosecond Timescale

The advances in picosecond light generation and detection system technologies have fostered significant advances in understanding of chemical reaction dynamics. However, there are some ultrafast processes beyond the resolution of current systems, and other processes that can be investigated more conveniently without recourse to state-of-art picosecond technology. Two alternative techniques are described: one uses the molecular vibrational frequency as a femtosecond timescale clock in order to study photofragmentation and isomerization dynamics; and the other uses

excitation from S_1 to S_n state to shorten S_1 state lifetime to picosecond timescale thereby imposing timing on the resolved fluorescence spctrum from S_1 state.

III-C-1 Emission Spectroscopy of Dissociating and Isomerizing Molecules

Hrvoje PETEK and Keitaro YOSHIHARA

Recently it has been demonstrated by Imre and coworkers[1] that it is possible to observe weak emission from a molecule excited to an unbound electronic state during the half-vibrational period that it takes the molecule to dissociate. The large geometry change during the dissociation process results in emission to high vibrational levels of the ground state for those vibrational modes that have the best overlap with upper state dissociation coordinate. In this manner it is possible to follow the evolution of nuclear geometry on the femtosecond time scale. The frequency and intensity information in the emission spectrum allows the determination of the upper and lower state potential surfaces along the reaction coordinate.

A molecular beam apparatus has been constructed for the purpose of observing emission from dissociating and isomerizing molecules, and harmonics of a YAG laser have been used to measure emission spectra of CH_3I (4ω), HI (4ω), and Raman spectra of C_2H_4. A VUV laser excitaition source based on YAG harmonic generation and anti-Stokes Raman shifting is under construction.

Reference

1) D. Imre, J.L. Kinsey, A. Sinha, and J. Krenos, *J. Phys. Chem.*, **88**, 3956, (1984).

III-C-2 Photochemical Timing Investigation of Picosecond Timescale IVR in t-Stilbene

Hrvoje PETEK and Keitaro YOSHIHARA

Photochemical timing, a new technique for picosecond-gated spectroscopy, is used to study intramolecular vibrational relaxation (IVR) in t-stilbene. Upon excitation of t-stilbene to a state near the 1200 cm^{-1} barrier to isomerization in S_1 state, the initially excited zero-order state that carries the oscillator strength of the transition and is coupled to a bath of dark states, undergoes rapid dephasing. The resolved fluorescence spectrum shows sharp structure due to the initially excited zero-order state and broad background produced by its time evolution; if the excited state can be quenched on the time scale of IVR, the ratio of sharp-to-broad fluorescence can be increased. Therefore if the quenching rate is known, the IVR rate can be measured.

In this experiment, the second harmonic of a Nd: YAG laser pumped dye laser excites t-stilbene 1048 cm^{-1} above the S_1 origin. The intense fundamental (20-30 mJ) of the same laser excites t-stilbene from the prepared state to non-fluorescing S_4 state thereby quenching the S_1 fluorescence. The six fold reduction of intensity of quenched from unquenched spectra (Figure 1) corresponds to lifetime reduction from 2.7 ns natural lifetime to 450 ps effective lifetime. The quenched spectrum shows clear increase in sharp-to-broad fluorescence ratio. For lower energy states, quenching by a factor of 300 has been observed corresponding to a lifetime of less than 10 ps.

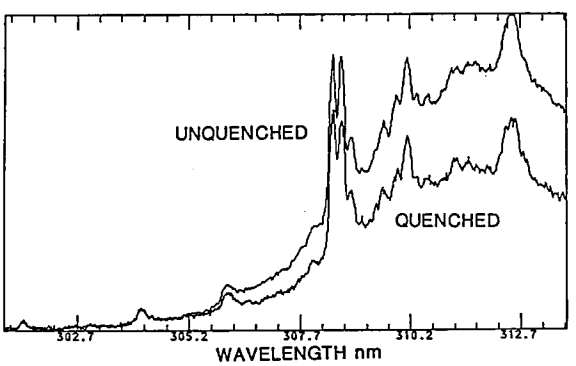

Figure 1. Typical unquenched and quenched fluorescence spectra. The intensities are adjusted to emphasize the decrease in broad fluorescence intensity.

III-D Dynamic Behavior of Excited States

Optical excitation of molecules to electronic excited states causes a variety of dynamical behavior, depending upon the nature of electronic structures and environments, such as energy transfer, proton transfer, chemical reaction, radiationless transition, ionization, and others. Most of these processes fall into the nanosecond and picosecond timescale. Firstly, we describe a mechanism of intramolecular proton transfer in both ground and excited states of 3-hydroxyflavon and the related compounds. Secondly, we discuss on an effect of NaCl on the excited-state proton dissociation reaction of naphthols and thirdly, intramolecular hydrogen transfer in the o-tolyl radical in the gas phase. Finally, we dicuss on the triplet lifetime of dichlorobenzene in the gas phase.

III-D-1 Mechanism of Intramolecular Excited State Proton Transfer and Relaxation Processes in the Ground and Excited States of 3-Hydroxyflavone and the Related Compounds

Michiya ITOH *(Kanazawa Univ.)*, **Yoshihisa FUJIWARA** *(Kanazawa Univ.)*, **Minoru SUMITANI, and Keitaro YOSHIHARA**

Two components of fluorescence rise due to the photo-tautomer generated in the excited-state proton transfer were observed in 3-methylpentane solutions of 3-hydroxyflavone (3-HF) and its derivatives, while only a fast rise observed in 3-hydroxychromone (3-HC) which lacks a 2-phenyl group. The shorter rise times are independent of temperature and substituent at the para position in the 2-phenyl group of 3-HF, whereas the longer rise times are dependent on each of them. As a result, the former and latter were ascribed to excited-state proton transfer in the Franck-Condon state (probably a twisted form of phenyl group to γ-pyrone ring) and to that in the vibrationally and/or torsionally relaxed excited state (a coplanar form of phenyl group to pyrone ring), respectively, as shown in Figure 1. The transient absorption of these compounds exhibits absorption bands at 430-530 nm with lifetimes of 7-30 μs at room temperature, which were attributable to the ground-state tautomers of these compounds. The two-step laser excitations (TSLE) of these transient absorption bands show TSLE fluorescence spectra being identical with the steady-state fluorescence spectra. Further, variable delay plots of TSLE fluorescence intensity afford lifetimes of the ground state tautomers.

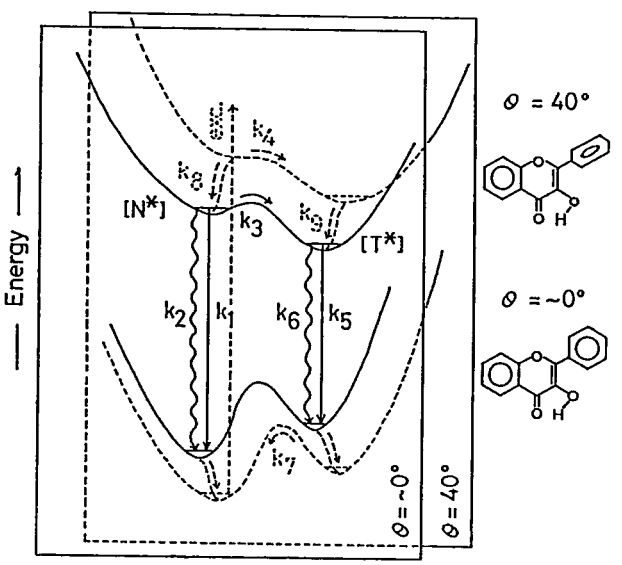

Figure 1. Schematic dual-coordinate potential energy diagram for the ground- and excited-states. The angle (θ) illustrates an angle which γ-pyrone and phenyl planes in flavonols make about C_2-C_1, bonding to each other.

III-D-2 NaCl Effect on the Excited-State Proton Dissociation Reaction of Naphthols: Water Structure in the Presence of NaCl

Haruo SHIZUKA *(Gunma Univ.)*, **Toshiaki OGIWARA** *(Gunma Univ.)*, **Akiko NARITA** *(Gunma Univ.)*, **Minoru SUMITANI, and Keitaro YOSHIHARA**

The NaCl effect on the proton dissociation reaction in the excited singlet state of naphthols in water at 300K has been studied by means of nanosecond and picosecond spectroscopy with fluorimetry. The proton dissociation rate constant k_1 decreased with an increase of NaCl according to the equation: $k_1 = k_0[(H_2O)_4](1-\alpha[NaCl])$, where k_0 denotes the second-order rate constant for the proton transfer from excited naphthols to water clusters $(H_2O)_4$ and α is a constant value. This means that the decrease in the k_1 value is caused by

NaCl-induced destruction of water clusters resulting in production of the hydrated ions $(Na^+)_{hyd}$ and $(Cl^-)_{hyd}$. The average hydration number of Na^+ and Cl^- in water is obtained to be 4.4 and 6.6, respectively. The kinetic H-D isotope effect on k_1 in the presence of NaCl was also examined. Some of the examples of the fluorescence rise-curves of naphtholate ions are shown in Figure 1.

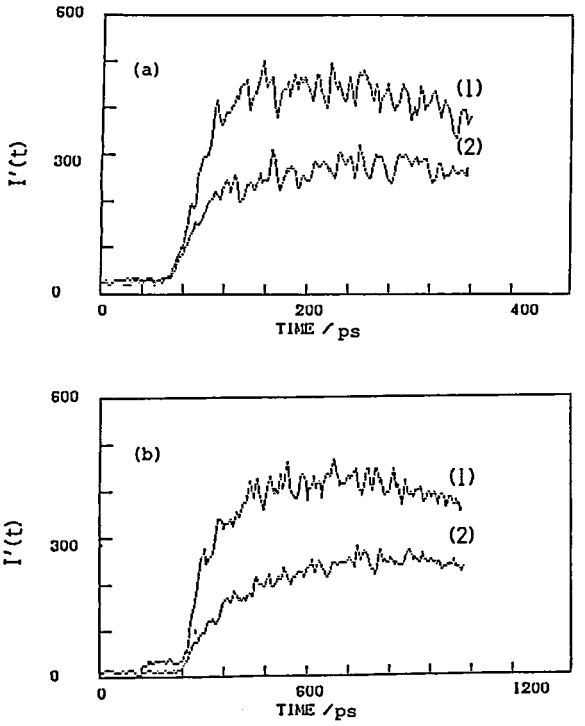

Figure 1. The builtup curves of the fluorescence intensities of 1-naphtholate ion at 480 nm obtained by picosecond experiment: (a) the 1ROH/H_2O (1ROH = 1-naphthol) system with (2) and without 3M NaCl (1): (b) the 1ROH/D_2O system with (2) and without 3M NaCl (1).

III-D-3 Intramolecular Hydrogen Transfer in the o-Tolyl Radical Studied by Time-Resolved Absorption Measurements

Teijiro ICHIMURA *(Tokyo Inst. of Tech.),* **Yuji MORI** *(Tokyo Inst. of Tech.),* **Minoru SUMITANI, and Keitaro YOSHIHARA**

[*J. Chem. Phys.*, **84**, 1943 (1986)]

The benzyl radical is well known reaction intermediate and was first detected in the gas phase with a flash photolysis technique by Porter and Wright.[1] Recently we measured the photodecomposition rate of benzyl chloride under collision free conditions[2] by monitoring the time-resolved absorption of benzyl radicals formed in the 266 nm picosecond laser photolysis. In this paper we describe the rise time of the benzyl radical absorption following a 266 nm photolysis of o-chlorotoluene. A typical result is illustrated in Figure 1, which gives an absorption rise of the benzyl radical. The rate constant of rearrangement of o-tolyl radical to benzyl radical by intramolecular hydrogen transfer was obtained to be 1.5×10^8 s^{-1} as the lowest limit if we assume unit efficiency for the rearrangement.

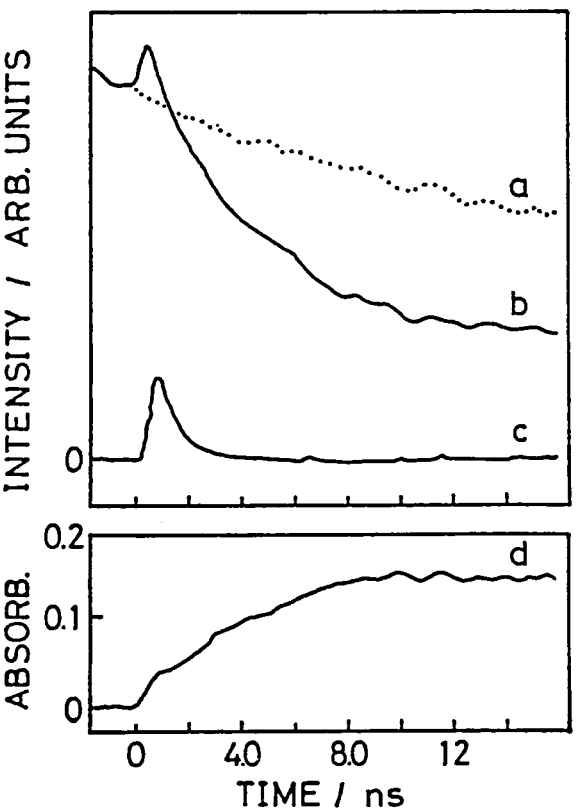

Figure 1. Time-resolved absorption for the excitation of o-chlorotoluene with a picosecond 266 nm laser pulse; time evolution of (a) the probe light intensity at 305 nm (I_0), (b) the probe light intensity at 305 nm (I_b) when o-ochlorotoluene vapor (1 Torr) was irradiated by the laser pulse, (c) the fluorescence intensity (I_f) of o-chlorotoluene vapor excited by the laser pulse and observed at 305 nm, and the absorption of the benzyl radical $\log_{10}[I_0/(I_b - I_f)]$.

References

1) G. Porter and F.J. Wright, *Spectrochim. Acta,* **12**, 299 (1958).
2) T. Ichimura, Y. Mori, M. Sumitani, and K. Yoshihara, *J. Chem. Phys.*, **80**, 962 (1984).

III-D-4 Triplet Lifetime of Dichlorobenzene in the Vapour Phase Studied by Time-Resolved and Stationary Observations of Photosensitized Phosphorescence

Teijiro ICHIMURA *(Tokyo Inst. of Tech.)*, **Katsunori NAHARA** *(Tokyo Inst. of Tech.)*, **Yuji MORI** *(Tokyo Insti. of Tech.)*, **Minoru SUMITANI, and Keitaro YOSHIHARA**

[*J. Photochem.*, **33**, 2986 (1986)]

Time-resoleved and stationary observations of biacetyl phosphorescence sensitized by dichlorobenzene vapour have led to the determination of the rate constant k_{nr} for nonradiative decay and the rate constant k_{ET} for energy transfer to biacetyl from the lowest triplet states of dichlorobenzenes in the vapour phase. The values of k_{nr} for p-dichlorobenzene, m-dichlorobenzene, and o-dichlorobenzene are 1.4×10^5 s^{-1}, 1.1×10^5 s^{-1}, and 1.5×10^5 s^{-1}, respectively. The values of k_{ET} obtained are 3.2×10^{10} $M^{-1}s^{-1}$, 2.1×10^{10} $M^{-1}s^{-1}$, and 7.6×10^{10} $M^{-1}s^{-1}$, respectively, for p-dichlorobenzene, m-dichlorobenzene, and o-dichlorobenzene. The values of k_{nr} and k_{ET} for dichlorobenzenes are similar to those for chlorotoluenes, and they are rather insensitive to the introduction of the second chlorine atom substituent but are slightly dependent upon its position.

III-E Solar Energy Conversion by Using Photocatalytic Effects of Semiconductors and Dyes ——Decomposition of Water and Application to Organic Synthesis——

Essential roles are played by semiconductors and dyes in the photocatalytic effects to which a particular attention has been paid in connection to the direct conversion of solar energy to chemical energy. One of the most important application is the water splitting reaction. Photocatalytic reactions of water with various organic compounds are also interesting not only from the view point of hydrogen production but also from that of the application to organic synthesis. In order to elucidate the mechanism of these photocatalytic reactions, we need detailed knowledges on the electronic structures of adsorbed molecules, the fundamental processes of photoinduced electron transfer at the semiconductor-liquid interface and catalysis on the surface. Work on he following topics is in progress with the purpose of clarifying the photocatalytic effects of semiconductors and dyes from the view point of solar energy conversion.

III-E-1. Visible-Light Induced Water Splitting on New Semiconductor Electrodes Made by Photolithography

Masahiro HIRAMOTO, Kazuhito HASHIMOTO, and Tadayoshi SAKATA

[*Chem. Lett.*, 899 (1986)]

The photocorrosion of small bandgap semiconductors has been a difficult barrier to the stable and efficient decomposition of water with visible light. In order to solve this problem, mosaic coating composed of thick metal films and a transparent silicon oxide film was applied to the surface of the small bandgap semiconducting electrodes such as Si electrodes with a p-n junction or an MIS (Metal-Insulator-Semiconductor) junction, *n*-CdS/*p*-CdTe heterojunction electrodes by making use of a photolithography technique. These electrodes are stable and evolve oxygen efficiently with visible light in concentrated alkaline solutions.

For *n*-Si with an MIS structure, the microstructured electrode (shown in Figure 1) exhibited the best efficiency for oxygen evolution. The photocurrent density of this electrode was 2 to 5 times larger than that of the same MIS electrode having large metal islands (2 mm × 2 mm). This result might be explained by the following effect. A number of fine metal islands on the microstructure electrode could collect any photogenerated holes (in the case of an *n*-type semicon-

ductor) more efficiently than for an electrode with a small number of large metal islands. Moreover, in some case, the microstructure electrode is expected to work more efficiently than solid solar cells, because a large number of metal islands, through which current flows, are isolated from each other.

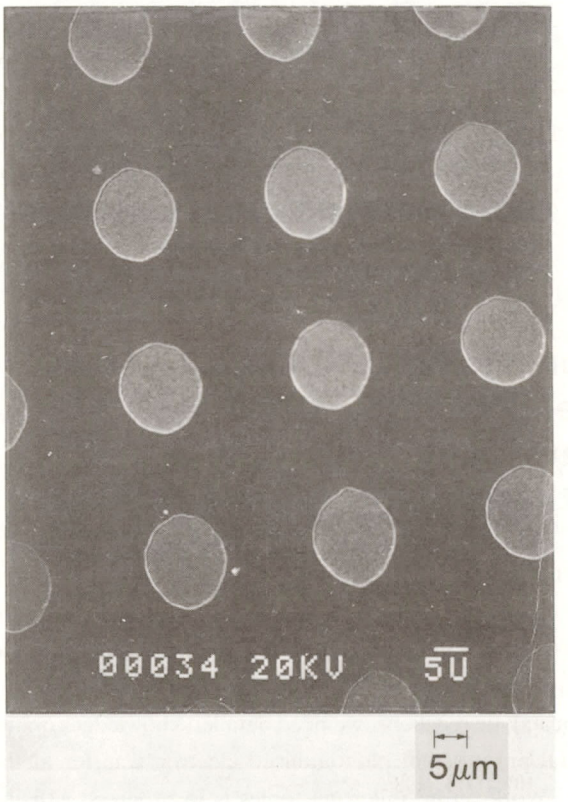

Figure 1. A SEM picture of the MIS-Si electrode surface produced by a microscopic photolithography technique. Shiny circles are metal parts which have an area of 13% of the whole surface. The rest of the surface is covered with SiO_2.

III-E-2 pn-Heterojunction Electrode

Tadayoshi SAKATA, Masahiro HIRAMOTO, and Kazuhito HASHIMOTO

Photoelectrode reactions with a semiconductor electrode can be regarded as the reactions by minority carriers of the semiconductor. The same reactions can be carried out not only by photo-exciting semiconductor electrodes but also by injecting the minority carriers through a semiconductor pn-junction held in dark. Pursuing this idea we investigated the electochemistry of several kinds of semiconductor electrodes with a pn-junction held in dark.

When a p-Si was used as an anode, an anodic current stopped flowing in 2 minuites due to the corrosion of the electrode. However, for n-Fe_2O_3/p-Si (the p-Si was covered with a thin film of 3000A n-Fe_2O_3), an anodic current flow was stable and no deterioration of the electrode was observed. A fairly large anodic current began to flow at 1.5 V vs SCE and bubbles of oxygen were evolved vigorously from the surface of the iron oxide, indicating that holes are injected from the p-Si to n-Fe_2O_3. Fig. 1 shows the current voltage curve of n-Fe_2O_3/p-Si (the surface of the n-Fe_2O_3 is in contact with the electrolyte solution). This result suggests that the pn-junction electrode can do the same work with the semiconductor photoelectrode. These pn junction electrodes can be applied to the study of electroded reactions of minority carriers of semiconductors held in dark. Especially this method may be advantageous to those semiconductors that show a poor photosensitivity. This electrode would also be interesting from the view point of application to organic synthesis making use of electrocatalytic effect of semiconductor surface and also to electrochemical devices.

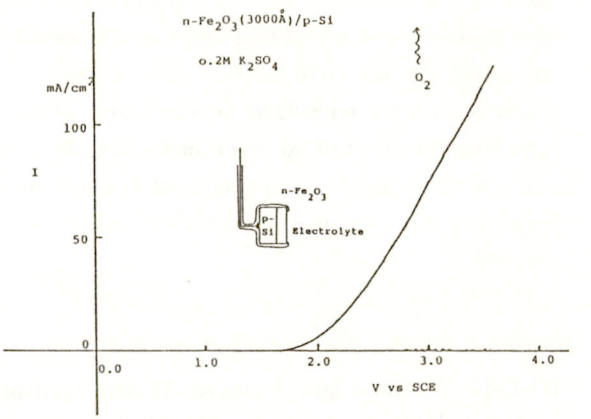

Figure 1. A current voltage curve of n-Fe_2O_3/p-Si

III-E-3 Organic Silicon Films Prepared by Plasma CVD

Nariaki HIROSHIGE *(Saga Univ.)*, **Tadayoshi SAKATA, Masahiro HIRAMOTO, Kazuhito HASHIMOTO, Hiroshi OGAWA** *(Saga Univ.)* **and Akira YOSHIDA** *(Toyohashi Inst. of Tech.)*

Various nonstoichiometric materials have been produced by plasma CVD. Amorphous SiC:H, used for solar cell, is one of them and usually prepared from a

mixed gas of SiH_4 and CH_4. As an extension, we have prepared various "organic-silicon" films from mixed gases of SiH_4 and various organic compounds such as alcohols, benzene and aniline.

Uniform films were formed on various substrates. The color of the films depended on the kind of organic compounds and the flow ratio. Among them, films prepared from benzene and alcohols showed rather strong photoluminescence. Table 1 shows several properties of the films prepared from SiH_4 and ethanol. The films are classified into three groups by the flow ratio of silane and ethanol(r). Even with decreasing the flow ratio below $r < 0.1$, the atomic ratio of Si, C, and O keeps a constant value, 1:1:2. However, with decreasing r, a 2110 cm^{-1} band (Si-H stretching) in the infrared spectra disappeared, indicating the decrease of hydrogen content. Simultaneously, the band gap and the intensity of photoluminescence were increased as shown in table 1. Interestingly, the atomic ratio of oxygen to carbon in the films prepared from alcohols alone is below 3%, suggesting that water is formed and removed during plasma reactions of alcohols.

Table 1. Properties of the films prepared from silane and ethanol by plasma-CVD method.

	flow rate ratio	atomic ratio Si:C:O	emission peak (ev)	optical bandgap (ev)
A	1	2:1:2	1.61	1.1
B	0.1	1:1:2	1.85	1.05
C	0.01	1:1:2	3.26	4.55

III-E-4 Effect of Semiconductor on Photocatalytic Reaction on α-Hydroxy Carboxylic Acids

Hisashi HARADA *(Meisei Univ.)*, **Tadayoshi SAKATA and Toyotoshi UEDA** *(Meisei Univ.)*

Specificity of a semiconductor for a given reaction is an important method of controlling that reaction. We have reported the effect of semiconductor on photocatalytic[1] and photoanodic[2] reactions of lactic acid.

Here we report the dependence of photocatalytic reactions of other α-hydroxy carboxylic acids, i.e. glycol acid and 2-hydroxy-3-metyl butyric acid, on the kind of semiconductor. From the results shown in Table 1, the reaction dependence on semiconductor is summarized in the following reaction equations. In the case of glycol acid,

for Pt/TiO_2:

$$H_2C(OH)COOH \rightarrow H_2 + CO_2 + HCHO$$
$$H_2C(OH)COOH \rightarrow H_2 + HCOCOOH. \quad \text{------- (1)}$$

for Pt/CdS:

$$H_2C(OH)COOH \rightarrow H_2 + HCOCOOH$$

And in the case of 2-hydroxy-3-methyl butyric acid,

for Pt/TiO_2:

$$(CH_3)_2CHCH(OH)COOH \rightarrow H_2 + CO_2 + (CH_3)_2CHCHO$$
$$(CH_3)_2CHCH(OH)COOH \rightarrow CO_2 + (CH_3)_2CHCH_2OH$$
$$(CH_3)_2CHCH(OH)COOH \rightarrow H_2 + (CH_3)_2CHCOCOOH. \quad \text{-------(2)}$$

for Pt/CdS:

$$(CH_3)_2CHCH(OH)COOH \rightarrow H_2 + (CH_3)_2CHCOCOOH.$$

In the case of CdS photocatalyst, carbon dioxide is hardly produced and hydroxy acids are oxidized only into the corresponding keto acids, while decarboxylation takes place besides dehydrogenation in the case of TiO_2 photocatalyst. Electrochemical experiments with various electrode material suggested that this clear difference comes not only from the different location of the valence bands but also from the different adsorption properties of the reactants on the semiconductor surfaces.

References

1) H. Harada, T. Sakata and T. Ueda, *J. Am. Chem. Soc.*, **107**, 1773 (1985).
2) H. Harada, T. Sakata and T. Ueda, *The sixth international conference on photochemical conversion and storage of solar energy*, C-37 (1986).

Table 1. Photocatalytic reaction products from α-hydroxy carboxylic acid.

	Glycol acid*a		2-hydroxy-3-metyl butyric acid*b	
Product/μmol	Pt/TiO_2	Pt/CdS	PT/TiO_2	PT/CdS
H_2	157	588	210	480
CO_2	114	5.1	330	3
HCHO	47	–		
HCOCOOH	36	494		
$(CH_3)_2CHCHO$			75	–
$(CH_3)_2CHCH_2OH$			45	–
$(CH_3)_2CHCOCOOH$			34	384

*a Irradiated with 1-kW Xe lamp (under 500-W operation) for 5h.
*b Irradiated with 1-kW Xe lamp (under 500-W operation) for 4h.

III-E-5 Photocatalytic Organic Reactions on Cadmium Sulfide Particles; Effect of Heat-Treatment and Metal Deposition

Bu Yong LEE *(Gyeongsan Univ., Korea),* **Masahiro HIRAMOTO, Kazuhito HASHIMOTO, and Tadayoshi SAKATA**

The control of photocatalytic organic reactions is one of the important problems. Concerning this problem, we report here the effect of heat-treatment and metal deposition on the photocatalytic activity of CdS as photocatalyst. In the decomposition of lactic acid (reaction 1) and alanine synthesis from lactic acid and ammonia (reaction 2), the catalytic activity depends strongly on the heat-treatment of CdS particles.

Reaction (1)

$$CH_3CH(OH)COOH \longrightarrow CH_3COCOOH + H_2$$

Reaction (2)

$$CH_3CH(OH)COOH + NH_3 \longrightarrow CH_3CH(NH_2)COOH + H_2O$$

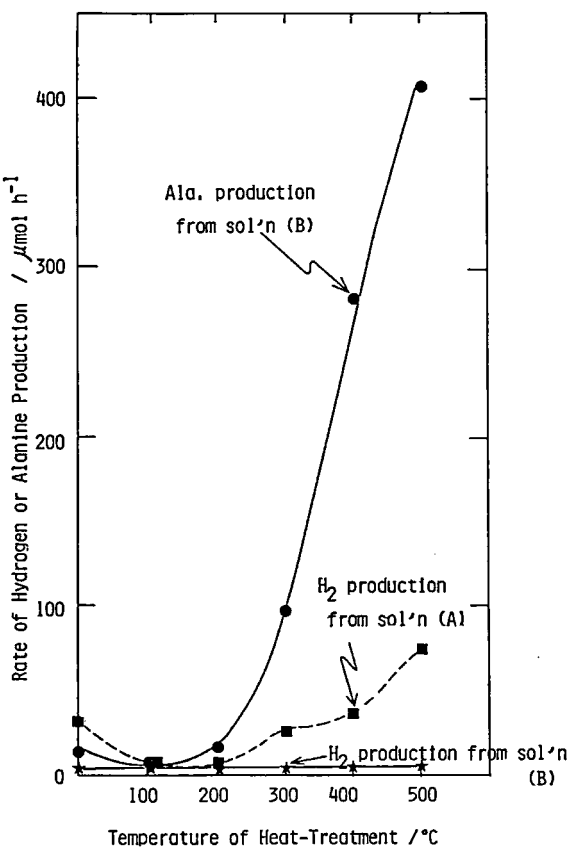

Figure 1. Effect of the heat-treatment on the rate of hydrogen and lactic acid production on bare CdS photocatalysts (Mitsuwa). Reaction conditions, CdS: 0.2 g, light source 500 W Xe lamp, Solution: (A) water 40 ml, lactic acid 10 ml, (B) 10 ml NH_3 was added to the solution (A).

Figure 1 shows the effect of heat-treatment (He atmosphere, 1h) on the rate of hydrogen and lactic acid production on bare CdS particles (Mitsuwa, amorphous). In the presence of NH_3, alanine is selectively produced (reaction (1) is suppressed) in the case of the samples heated above 300°C. Moreover, the production rate increases drastically with increasing the temperature of the heat-treatment. Improvement of the catalytic activity seems to depend on the crystal structure and on the concentration of the surface defects of CdS particles.

Pt deposition on CdS particles (Mitsuwa) has no effect for alanine production, while it improves the hydrogen evolution. On the other hand, Ni and Co deposition improves the alanine production.

III-E-6 Electron Transfer and Photoluminescence Dynamics of CdS Particles Deposited on Porous Vycor Glass

Masahiro HIRAMOTO, Kazuhito HASHIMOTO, and Tadayoshi SAKATA

Photoinduced electron transfer between semiconductor and redox species in an electrolyte is one of the elementary processes in electrochemical cells, photocatalysis, and photography. Luminescence measurements represent a powerful tool for studying this fast process, since the luminescence lifetime reflects the electron-transfer rate. Here we report on the effects of various redox species in aqueous solutions regarding the photoluminescence spectra and the decay of CdS particles deposited on porous Vycor glass (CdS/PVG), and discuss the mechanism.

CdS/PVG shows a strong red emission with a peak around 800 nm (Figure 1A). Figure 1B and C show the effects of electron donor (S^{2-}) and acceptor (S_n^{2-}) on this red emission in an equeous solution. Many electron acceptors such as S_n^{2-}, Fe^{3+}, methyl viologen, and benzoquinone effectively quench red emission, even if their concentrations are very low. On the other hand, most electron donors such as S^{2-}, Fe^{2+}, hydroquinone, SO_3^{2-}, and lactic acid do not quench the red emission, although they are easily photooxidized by holes at the valence band of CdS. Luminescence decay measurements revealed that the quenching was static for any type acceptor. These results can be well explained by the SA center (Self-Activated center) model in which

the emission center is a Cd vacancy associated with a halogen atom. In this model, any decrease in the initial intensity of the luminescence decay directly reflects the electron-transfer rate between the CdS and the acceptor.

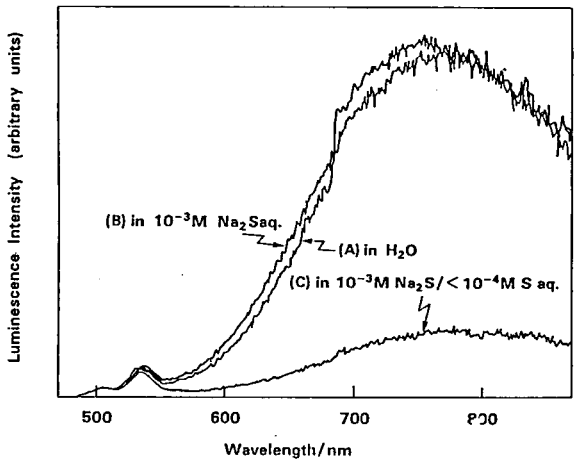

Figure 1. The photoluminescence spectra of CdS/PVG in pure water (A), in a 10^{-3}M Na_2S aqueous solution (B), and in a 10^{-3}M $Na_2S/<10^{-4}$M S aqueous solution (C). The excitation wavelength is 453 nm.

III-E-7 Photoluminescence of TiO_2 Powder and Its Relation with Photocatalytic Reactions

Kazuhito HASHIMOTO, Masahiro HIRAMOTO, and Tadayoshi SAKATA

When TiO_2 powder was irradiated in vacuo, a broad emission with a peak position of ca. 500 nm was observed. The excitation spectrum consists of a very strong band which rises sharply near 380 nm corresponding to a band-gap excitation and a weak band aroung 400-500 nm which might originate from impurity levels. Neither a heat treatment of TiO_2 nor the introduction of various gases to the system did not affect the emission observed by the impurity states excitation. On the other hand, the emission intensity observed by a band-gap excitation decreased drastically by the heat treatment. After introducing a water vapor to this system and evacuating it, the intensity recovered. Moreover, this emission was drastically affected by the introduction of various gases as summarized in Table 1. Oxygen serving as a good electron acceptor of photoexcited TiO_2 strongly quenched the emission, and the gases of (3)-(6) which serve as donors also quenched it. However, methanol and ethanol which are good donors rather increased the intensity of the emission. This emission was not observed with TiO_2 singel crystal. These results indicate that the emission originates in a surface phenomenon. The emission decayed non-exponentially and its decay profile depended on the excitation intensity. By the introduction of the gases, the initial intensity of the decay curve did not change but the decay rate changed corresponding the variation in intensity. In order to explain these experimental results, we propose a model that the emission originates in the recombination of a relaxed hole existing near the surface the hydrogen atom adsorbed on the surface or a surface trapped electron which is stabilized by the surface OH of TiO_2.

Table 1. Intensity of photoluminescence from TiO_2 under various gases.
(*) 10 Torr, (**) saturated vapor pressure at room temperature.
Excitation 330 nm, Observation 500 nm

gas		relative intensity
(1)	in vacuo	1.0
(2)	oxygen(*)	0.05
(3)	water(**)	0.2
(4)	hydrogen peroxide(**)	0.2
(5)	acetic acid(**)	0.8
(6)	triethylamine(**)	0.5
(7)	methanol(**)	1.5
(8)	ethanol(**)	1.5
(9)	benzene(**)	1.0

III-E-8 Electron Transfer from Adsorbed Ruthenium (II) Complexes to Semiconductors in Vacuo: Temperature and Energy Gap Dependence

Kazuhito HASHIMOTO, Masahiro HIRAMOTO, and Tadayoshi SAKATA

By comparing the luminescence decays of a Ru(II) complex adsorbed on a semiconductor to that adsorbed on an insulator, the electron transfer rate can be obtained. We measured the luminescence decays of $Ru(bpy)_3^{2+}$ and $Ru(bpz)_3^{2+}$ adsorbed on TiO_2 (rutile, anatase) and SiO_2 at a various temperature from 300 K to 4 K. The luminescence decays on a semiconductor could be expressed by the sum of four exponentials, and the electron transfer rate of each component at each temperature could be determined. In Fig. 1 is shown the case of $Ru(bpz)_3^{2+}/TiO_2$(anatase). The rate

of each component decreased by lowering the temperature, and it became almost constant below about 100 K. Each component has a quite different absolute value of the electron transfer rate but the tendency of the temperature dependence is almost the same each other. The activation energy estimated from the relatively high temperature region was 0.04 eV for all components in this case. These results indicate that the difference of the rate of each component is determined by the overap of the electronic wavefunctions of the complex and the semiconductor, and the activation energy term of the electron transfer rate is same among these four components. We also measured the luminescence decays of $Ru(bpy)_3^{2+}$ and $Ru(bpz)_3^{2+}$ adsorbed on various semiconductors. The electron transfer rates were obtained as a function of the energy gap; the energy difference between the oxidation energy of excited Ru(II) complex and the energy of conduction band edge of semiconductor.

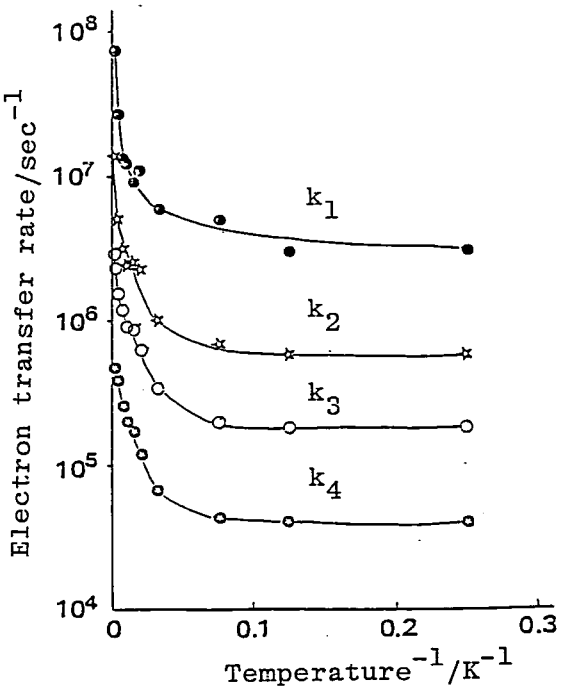

Figure 1. Temperature dependence of the electron transfer rate from excited $Ru(bpz)_3^{2+}$ to TiO_2(anatase).
Decay curves were analyzed with four exponentials, k_1-k_4 correspond to the electron transfer rates of those four components.

III-E-9 Time-resolved Measurements of Luminescence of Ru(II) Complexes Chemically or Physically Immobilized on Semiconductor or Insulator Particles in Various Solvents

Kazuhito HASHIMOTO, Masahiro HIRAMOTO, Tadayoshi SAKATA, Hiroji MURAKI *(Tokyo Inst. of Tech)*, **Hirofumi TAKEMURA** *(Tokyo Inst. of Tech.)*, **and Masamichi FUJIHIRA** *(Tokyo Inst. of Tech.)*

Dynamic properties of the photo-excited ruthenium (II) complexes, chemically bound to powdered TiO_2 and SiO_2 in several solvents, and physically adsorbed on powdered TiO_2, SnO_2, SiO_2, and Al_3O_3 in water were investigated by measuring luminescence decays and time-resolved spectra. Most of the decays for the complexes adsorbed on powdered semiconductors in solvents could be fit by the sum of two exponentials with lifetimes τ_f(fast) and τ_s(slow). τ_f is mainly determined by the electron transfer process from the photo-excited complexes to semiconductor, whereas τ_s might be determined by the original radiative and nonradiative processes of adsorbed molecules. These results were compared to those obtained from the measurements done in vacuo, which suggests that the interaction of adsorbed ruthenium (II) complexes with semiconductor surface becomes weak in those solvents and the electron transfer rate constants become much smaller in solvents than in vacuo. The dependence of the electron transfer rates on the kinds of solvents and pH of water were also studied. Those rates do not depend on solvents so much, but the quantum yields of the electron transfer strongly depend as shown in Table 1. Moreover, the rate and the quantum yield of the electron transfer to TiO_2 in water do not change in the pH region of 1 to 7, but become small by increasing the pH to alkaline region.

Table I. Rate constants and quantum yields of the electron transfer from immobilized $Ru(bpy)_3^{2+}$ to TiO_2 in deaerated solvents.
*) No fast component was observed.

	1-amide-TiO_2		1-ester-TiO_2	
THF	$3.6\times10^6 sec^{-1}$	0.41	$2.6\times10^6 sec^{-1}$	0.54
DMF	2.5×10^6	0.30	3.3×10^6	0.48
CH_2Cl_2	1.9×10^6	0.36	3.5×10^6	0.34
CH_3CN	3.6×10^6	0.17	3.2×10^6	0.40
CH_3OH	2.2×10^6	0.21	3.7×10^6	0.57
H_2O	2.2×10^6	0.29	–*)	

III-F Dynamical Processes in Electronically and/or Vibrationally Excited Molecules

III-F-1 Overtone Spectroscopy of Acetyl Compounds. Inequivalent CH Oscillators and Substituent Effects of the Carbonyl Group

Ryoichi NAKAGAKI and Ichiro HANAZAKI

[*Chem. Phys. Lett.*, **128**, 432 (1986)]

CH stretching overtone spectra of acetyl compounds are measured in the liquid phase. A doublet structure is commonly observed in the overtone spectra of acetyl CH stretching vibrations and is attributed to the sterically inequivalent orientations of methyl CH bonds. The present interpretation is in accordance with the theoretical calculations.[1] The substitutent effects exerted by carbonyl group are obtained from the analysis of the spectral changes in the methyl and ring CH stretching overtones induced by the following transformations: $X\text{-}CH_3 \rightarrow X\text{-}COCH_3$ (where X is an aromatic or heterocyclic ring) and $H_2C = C(CH_3)Y \rightarrow O = C(CH_3)Y$.

Reference

1) I. Hanazaki, M. Baba, and U. Nagashima, *J. Phys. Chem.*, **89**, 5637 (1985).

III-F-2 Pyroluminescence and Photoluminescence of Uranyl Nitrate Hexahydrate

Hari Datt BIST *(IIT Kanpur, India and IMS)*, **Teruhiko NISHIYA, Masaaki BABA, and Ichiro HANAZAKI**

The pyroluminescence (PyL) spectrum of uranyl nitrate hexahydrate (UNH), $UO_2(NO_3)_2 \cdot 6H_2O$, observed between 100-135 K on slow cooling and warming of its crystals has been recorded for the first time by means of an intensified diode array detector. The PyL emission was observed as very brilliant spark-like flashes for transparent UNH crystals in an evacuated sample tube. A careful comparison of the PyL and photoluminescence (PL) spectra has established that both spectra originate from the first excited electronic state ($^3\Pi_u$) of the uranyl ion, although the PyL spectrum shows a characteristic blue shift with respect to the corresponding PL spectrum. The pyroelectric (PyE) voltage was also observed as an irregular pulses during cooling and warming processes across two faces of the crystal and found to be coincident with the PyL pulse. It is noteworthy that the sign of the PyE voltage was reversed between cooling and warming. It is suggested that the internal strain in a crystal formed by a temperature change causes the transient pulses of both PyL and PyE. Possibility of a second order phase transition to cause such stress is suggested on the basis of the temperature dependence of the PL spectra. The mechanism of excitation of PyL emission is discussed in detail. Possibilities of the excitation of PyL by a discharge between charged microcrack surfaces and/or by the stress-enhanced intermolecular charge-transfer state formation are suggested.

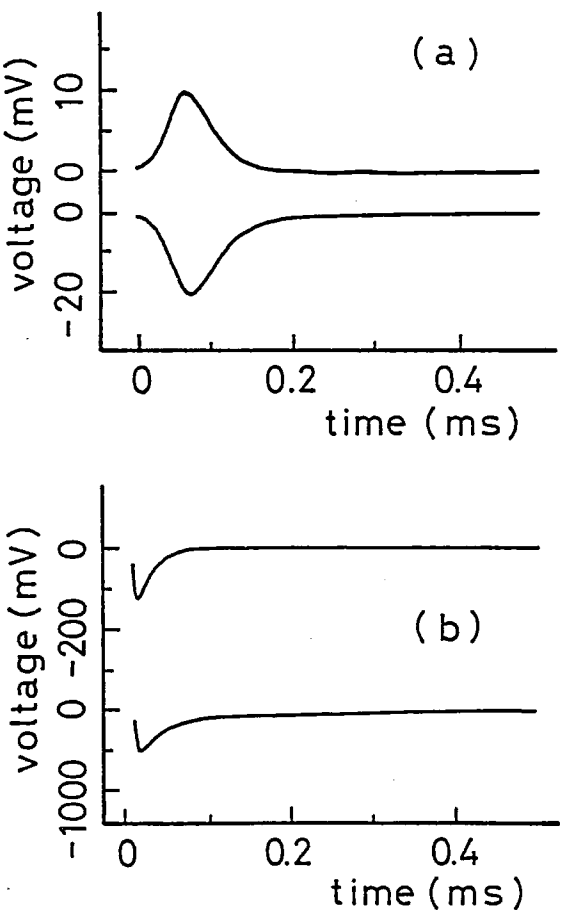

Figure 1. Pyroelectric voltage, V_{PyE}, (top) and pyroluminescence voltage, V_{PyL}, (bottom) recorded simultaneously from a single crystal of uranyl nitrate hexahydrate during (a) cooling and (b) warming processes in the temperature range 135-100 K.

III-F-3 Intermolecular Dynamics and Exciplex Formation of the 1-Cyanonaphthalene/ triethylamine van der Waals Complex

Hiroyuki SAIGUSA *(Kanazawa Univ.)*, **Michiya ITOH** *(Kanazawa Univ.)*, **Masaaki BABA, and Ichiro HANAZAKI**

Dynamic of the exciplex formation upon optical excitation of the 1-cyanonaphthalene/triethylamine van der Waals (vdW) complex excitation has been examined under collision free conditions. Mode-specificity has been found in the excitation of a combination band between intra- and intermolecular vibrational modes in the S_1 state of the vdW complex to promote the exciplex formation reaction. The specificity is lost at higher excess energies since randomization of energy among intermolecular modes is more extensive than the reaction rate. The fluorescence decays of the S_1 and exciplex states have been measured as a function of excess vibrational energy above the S_1 origin. The lifetime of the S_1 state at the excess energy where the mode-specific reaction is observed is different from that of the exciplex fluorescence. As the excess energy increases, the decay rate of the S_1 state shows increase due to the exciplex formation while the exciplex fluorescence rate remains constant. The observed decay rates and mode specificity have been shown to be nicely explained by a simple kinetic model illustrated in the Figure 1.

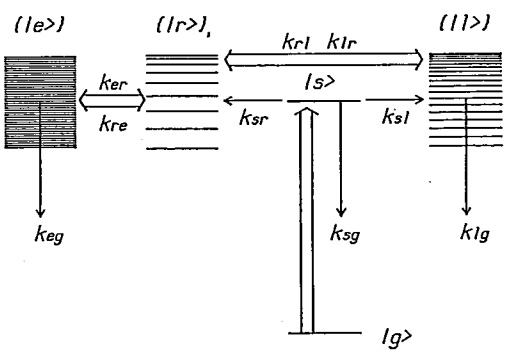

Figure 1. A schematic respresentation of the excitation/ decay processes in the CNN/TEA complex, |s> = initially excited state (either intramolecular mode |m>, intermolecular mode |a>, or combination |m + a>); {|r>} = reactive intermolecular vibrational states; {|1>} = nonreactive intermolecular vibrational states; {|e>} = exciplex states; |g> = ground state. The model allows for irreversibility of IVR into the {|1>} and {|r>}.

III-F-4 Fluorescence Studies of the Intramolecularly Hydrogen-bonded Molecules; o-Hydroxyacetophenone, Salicylamide and Related Molecules

Teruhiko NISHIYA, Seigo YAMAUCHI *(Kyoto Univ.)*, **Noboru HIROTA** *(Kyoto Univ.)*, **Masaaki BABA, and Ichiro HANAZAKI**

Structures and dynamic processes in the excited states of intramolecularly hydrogen-bonded molecules have attracted much attention in recent years in view of the possibilities of making a four-level proton transfer laser and an information storage device at a molecular level.

We have investigated the nature of the ground and excited states of o-hydroxyacetophenone (OHAP), salicylamide (SAM), methyl salicylate (MS) and 7-hydroxy-1-indanone (7HIN) by means of high-resolution fluorescence spectroscopy. The fluorescence emission and excitation spectra were obtained in durene mixed crystals at 4.2 K, as shown in Figure 1, and in supersonic helium jets. In the cases of OHAP and SAM, sharp but very weak 0-0 bands were observed both in the emission and excitation spectra followed by the vibronic bands with increased intensities. The vibronic structures are consistent with the tautomerization in the excited state from the keto to the enol form. The potential energy change with respect to the tautomerization reaction coordinate in each molecule is qualitatively explained on the basis of the observed spectra. A particularly drastic change is observed in the case of 7HIN in which the O-H...O distance is expected to be larger.

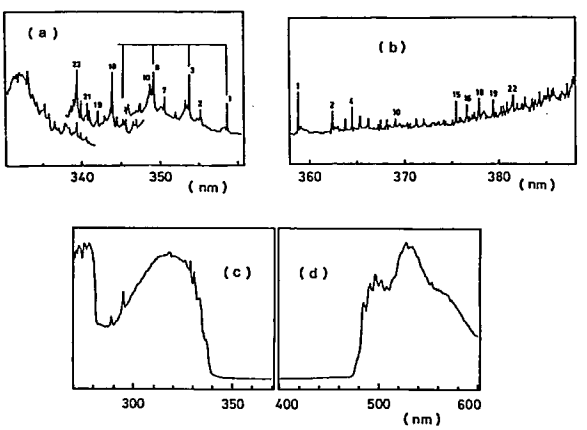

Figure 1. Fluorescence (a) excitation and (b) emission spectra of SAM in a durene mixed crystal at 4.2 K, and fluorescence (c) excitation and (d) emission spectra of 7HIN in a durene mixed crystal at 4.2 K.

III-F-5 Electronic Spectra of Hydrogen-Bonded Indazole in Supersonic Free Jets

Masayo TERAZIMA *(Tokai Women's Junior College)*, **Noboru HIROTA** *(Kyoto Univ.)*, **Masaaki BABA, and Ichiro HANAZAKI**

It has been known that indazole forms hydrogen-bonded complexes in some carboxylic acid solutions, which are consequent upon the proton transfer in the S_1 (π, π^*) state. In this case, the indazole and carboxylic acid molecules probably form a double hydrogen-bonded link (Figure 1(a)) which gives rise to a double proton transfer (or switching).

We observed the fluorescence excitation and emission spectra of indazole complexes with HCOOH, CH_3COOH, H_2O, C_2H_5OH in supersonic jets. However, their spectral features were similar to that of free indazole molecule, with no evidence for the proton transfer. The frequencies and intensities of some prominent vibronic bands were almost the same. It indicates that the stable conformation in the excited state is not so much different from that in the ground state. Further complexes containing some deuterated compounds such as indazole-d_1, D_2O, and DCOOH showed small deterium shifts of $8 \sim 12\ cm^{-1}$. This small shift indicates that the force constants in the ground and excited states are very similar to each other.

The most plausible explanation for these observations would be that only a single hydrogen bonding (presumably, N(1)-H...O) is formed in the isolated system even for the carboxylic acid complexes (Figure 1(b)). The double proton switching can never occur in this case. This model could account for the spectral similarity observed for all the complex studied here, and also for the relatively small difference between the ground and excited state potential curves.

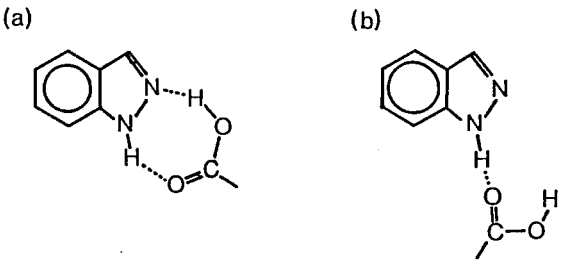

III-G Molecular Beam Studies of Hydrated Clusters and Strongly Bound Molecular Associates

Molecular liquids will be described as assemblies of molecular clusters with various sizes and short lifetimes. Sudden isolation of a liquid drop in vacuum causes adiabatic expansion which fragments the assemblies into clusters and free molecules by dissociating the weaker intermolecular bonds between clusters. This expansion also cools the temperature of the isolated clusters. Excess energy remaining in a cluster causes evaporation of weakly bound molecule(s). These processes convert the internal energies of clusters into kinetic energies of dissociated molecule(s) and clusters mostly. These cooling processes make the thermal fragmentation of clusters inactive and stable cluster beams are formed finally. Details of the apparatus was described in *Chem. Phys. Lett.*, **122**, 599, (1985).

For the analysis of cluster composition, a quadrupole mass spectrometer was used coupled with an electron impact or a VUV photon impact ionizer. Ionization of a molecule in a cluster provides an excess energy inducing ion-molecule reaction between the ionized molecule and a neighbor molecules or it dissociates weak intermolecular bond(s) near the ion. Mass spectra of the cluster beams are usually composed of fragmented clusters, although their patterns always reflect the size distribution of the cluster beams. Experimental analyses of fragmentation mechanisms are reported in the next section.

III-G-1 Average Size Ratio of Aqueous Clusters of Some Simple Solute Molecules

Nobuyuki NISHI and Kazunori YAMAMOTO

Aqueous solutions of C_2H_5OH, $C_2H_5NH_2$, CH_3NH_2, HCOOH, CH_3COOH, and ethylene glycol($HOCH_2CH_2OH$) were converted to cluster beams of $X(H_2O)_n$ and $(H_2O)_m$. Electron beams with 40 eV kinetic energy were irradiated to ionize clusters, which also cleave some intermolecular bond(s) of clusters. Assuming similar fragmentation patterns for

the clusters with large hydration numbers ($7 \leq n, m \leq 20$), the average size ratio S_a of hydrated clusters $X(H_2O)_m$ to pure water clusters $(H_2O)_n$ (in the same solution) is defined based on the intensity distribution of the mass spectrum. After the calibration of the mass dependence of the q-pole transmission and the correction of the solute concentration dependence of the hydration size, the ion intensities are fitted with a function of $I(n) = A \exp(-R_a n)$, where n is a hydration number and R_a is a constant representing a size distribution of ionized clusters. Good fitness to this function was seen for the hydration numbers larger than 6. Table 1 gives the obtained average size ratios of hydrated solute clusters relative to pure water clusters, $S_a = (R_a/R_w)^{-1}$. In aqueous solution, C_2H_5OH and CH_3NH_2 form smaller cluster units compared with pure water clusters, while HCOOH produces much stronger aqueous mixed clusters. Ethylene glycol was found to form large hydrated clusters as expected.

Table 1. Average size ratios of hydrated clusters $X(H_2O)_m$ to water clusters $(H_2O)_n$ defined by $S_a = (R_l/R_w)^{-*}$ [X] represents molar ratio of X.

Solute Molec. X	Range of n** investigated	[X] = 0.05	[X] = 0.01
C_2H_5OH	4-17	0.68 ± 0.03	0.68 ± 0.04
CH_3NH_2	4-19	0.71 ± 0.03	0.73 ± 0.03
$C_2H_5NH_2$	4-17	1.00 ± 0.10	0.93 ± 0.10
CH_3COOH	4-17	1.05 ± 0.10	0.71 ± 0.10
HCOOH	4-17	1.38 ± 0.07	1.01 ± 0.07
$HOCH_2CH_2OH$	8-17	1.70 ± 0.10	1.40 ± 0.10

* R_w was obtained for $(H_2O)_n$ with n = 6 − 20 in each measurement.

** Range of cluster ions of which intensities fit to the exponential distribution function (see text).

III-G-2 Isolation of Solvent-free Solute Complexes as Molecular Beams by Collisional Desolvation

Kazunori YAMAMOTO and Nobuyuki NISHI

Before the skimming of the clusters at the liquid droplet expansion region, the clusters were desolvated by the collision with Ar gas leaving strongly bound solute complexes which were introduced into a high vacuum region through two skimmers in tandem. This technique has a great advantage for the formation of molecular beams of nonvolatile molecules or molecular complexes since it is not necessary to heat the sample so much. Figure 1 shows the mass spectra of the cluster beam generated from an aqueous solution of HCOOH and CH_3NH_2 with molar ratios of $[HCOOH]/[H_2O] = [CH_3NH_2]/[H_2O] = 0.1$, where $H^+(HCOOH)_m(CH_3NH_2)_n$ is expressed by "m-n-0". Most of the strong ions are protonated indicating that the observed cluster ions were produced through intracluster ion-molecule reactions of primary ions with a neighbor molecule which abstract a proton from the primary ions. In low-energy electron impact ionization, prominent are the mixed cluster ions with one more amine molecule such as $H^+HCOOH(CH_3NH_2)_2$ and $H^+(HCOOH)_3(CH_3NH_2)_4$ as well as one-to-one clusters $H^+(HCOOH\text{-}CH_3NH_2)_{1,2}$. Intensities of $H^+(CH_3NH_2)_2$ and $H^+HCOOH(CH_3NH_2)_3$ were highly dependent on electron energies indicating that these ions are the fragments of mixed clusters with amine-amine bond(s). Concentration change and ionization energy dependence experiments suggested the presence of the following fragmentation processes.

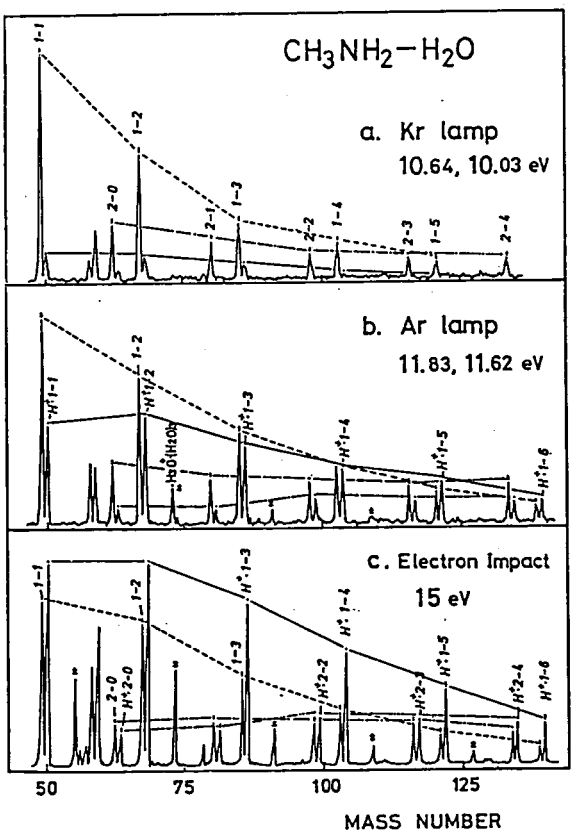

Figure 1. Photoionization and electron impact mass spectra of the cluster beams of $(HCOOH)_m(CH_3NH_2)_n$ solute complexes generated from a ternary solution with a molar ratio of $[HCOOH]/[H_2O] = [CH_3NH_2]/[H_2O] = 0.1$. Weakly bound water molecules were peeled off by the collision with Ar gas. "k-1-m" denotes a cluster ion, $H^+(HCOOH)_k(CH_3NH_2)_l(H_2O)_m$. The signals indicated by arrows are non-protonated ions.

$$[(HCOOH)_m(CH_3NH_2)_n]^+ \rightarrow HCOO + H^+(HCOOH)_{m-1-a}(CH_3NH_2)_{n-a} + (HCOOH\text{-}CH_3NH_2)_a,\ (a = 0, 1).$$

Photoionization at 10.64 and 10.03 eV enhanced the intensities of $H^+HCOOH(CH_3NH_2)_2$, $H^+(HCOOH)_2(CH_3NH_2)_2$, and $H^+(HCOOH)_3(CH_3NH_2)_2$. The parent complexes which exist dominantly in the beam are most probably $(HCOOH)_m(CH_3NH_2)_m$ (m = 1 ~ 4) and $(HCOOH)_2(CH_3NH_2)_n$(n = 1, 3).

III-G-3 Ab initio Calculation of Stabilization Energies of Acid-Base Binary Clusters: $(HCOOH)_m(NH_3)_n$ (m, n = 0, 1, or 2)

Kazunori YAMAMOTO, Umpei NAGASHIMA *(Computer Center),* **and Nobuyuki NISHI**

Molecular beams generated by expanding the aqueous solution of ammonium formate revealed that various acid-base complexes $(HCOOH)_m(NH_3)_n$ exist in aqueous solutions as hydrated forms. Dehydration procedure isolated the nucleous complexes in molecular beams. Particularly, the presence of $(HCOOH)_m(NH_3)_n$ (m, n =1 or 2, m ≠ n) units in an equimolar aqueous solution has been confirmed. In order to explain these observations, the stabilization energies have been caluculated by the SCF gradient method with the STO-3G basis set. Full optimization has been performed at SCF level. All the clusters, except $(NH_3)_2$, have planar cyclic structures with the symmetry C_s. The results are listed in Table 1. The obtained stabilization energies change considerably depending on hydrogen-bonding. For example, the ammonia rich cluster $(HCOOH)_1(NH_3)_2$, which may be regarded as a composit of $(NH_3)_2$ and HCOOH, has a large stabilization energy of −21.1 kcal/mol compared with the respective stabilization energies of −3.8 kcal/mol ($(NH_3)_2$) and −10.8 kcal/mol ($(HCOOH)_1(NH_3)_1$). The stabilization energies per hydrogen-bond are −3.8, −5.4, and −7.0 kcal/mol for $(NH_3)_2$, $(HCOOH)_1(NH_3)_2$, and $(HCOOH)_1(NH_3)_2$, respectively. The acid-base alternative cyclic tetramer, $(HCOOH)_2(NH_3)_2$, has four hydrogen bonds and its energy is −32.3 kcal/mol (which gives a value of −8.1 kcal/mol as an energy per bond). The results suggest the following general tendency for the acid-base binary clusters. The stabilization energy per hydrogen bond goes on increasing as the number of molecules in mixed clusters increases. The table also indicates that the presence of the acid-acid bond enhances the stabilization energy of complexes compared to the regular acid-base bond.

Table 1. Stabilization Energies $(HCOOH)_m(NH_3)_n$ in kcal/mol

n (Number of NH_3)	m(Number of HCOOH) 0	1	2
0	–	0.0	−15.2
1	0.0	−10.8	−23.3
2	−3.8	−21.1	−32.3* −34.1**

* alternative cyclic $(HCOOH)_2(NH_3)_2$

** ┌HCOOH-HCOOH-NH_3-NH_3┐

III-G-4 Ab initio Calculation of Structures of Acid-Base Binary Clusters: $(HCOOH)_m(CH_3NH_2)_n$, (m, n = 1 or 2)

Kazunori YAMAMOTO, Umpei NAGASHIMA *(Computer Center),* **and Nobuyuki NISHI**

Equilibrium structures of the HCOOH·CH_3NH_2 complex and the cyclic $(HCOOH)_1$

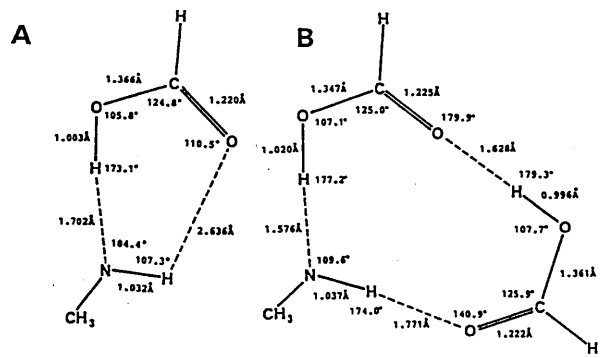

Figure 1. Optimized geometries of cyclic HCOOH·CH_3NH_2 (form A) and cyclic trimer $(HCOOH)_2(CH_3NH_2)_1$(form B) with the STO-3G basis set. Stabilization energies are −10.6 kcal/mol (for form A) and −22.5 kcal/mol (for form B).

$(CH_3NH_2)_2$ and $(HCOOH)_2$ CH_3NH_2 clusters were determined by the ab initio calculations at SCF revel. Full optimization was carried out with the STO-3G basis set. For $HCOOH{\cdot}CH_3NH_2$ complex, cyclic and linear structures were calculated and the stabilization energies of −10.7 and −10.1 kcal/mol were obtained for the respective conformations. In the cyclic structure, formation of the hydrogen-bond, –NH···O = C<, was found to make little contribution (−0.6 kcal/mol) to the stabilization energy of the complex and its bond length was calculated to be 2.64Å. The cyclic trimer of $(HCOOH)_1(CH_3NH_2)_2$ has three hydrogen-bonds, –OH...NH_2–, –NH...NH_2–, and –NH...O = C<. The –OH...NH_2– bond is 0.11Å shorter than that in the cyclic $HCOOH{\cdot}CH_3NH_2$ complex (R = 1.7Å). Similarly, cyclic $(HCOOH)_2(CH_3NH_2)_1$ trimer has an –OH···NH_2– bond of 1.58Å, which is 0.12Å shorter than that in the dimer. It is remarkable that the four constituent atmos of the hydrogen-bond, –OH···O = C<, in the cyclic $(HCOOH)_2(CH_3NH_2)_1$ trimer stand in a line, that is quite different from the usual hydrogen-bond angle of a carboxyl group.

III-H Fragmentation Mechanisms of Hydrogen-bonded Molecular Clusters on Photoionization

Molecular clusters are generally formed through interactions compared with chemical bondings in molecules. Intramolecular vibrations are believed to be activated subsequently to electronic excitation of a constituent molecule. In hydrogen-bonding clusters with water molecules, the dissociation energy of an H_2O-H_2O bond is ca. 5 kcal/mol. According to RRK theory, the lifetime of an $X(H_2O)_4$ cluster is estimated to be 10^{-9}-10^{-10} sec for an excess energy of 1 eV (ca. 23 kcal/mol). Although the lifetime becomes longer with increasing cluster size, clusters containing less than 10 molecules are destined to fragment within 1μs for an excess energy larger than 1 eV. The near-threshold ionization of a solute-solvent binary cluster, one can specify the fragmentation pathways by the selective ionization of solute molecules. In the solute-solvent binary clusters studied here, near-threshold photons can ionize either one of the lone-pair (LP) electrons of an 'acid' molecule (hydrogen donor) or one of the hydrogen-bonding pair (HBP) electrons of a solute 'base' molecule as follows:

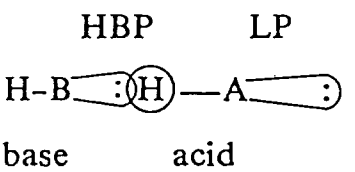

III-H-1 Switching of Fragmentation Channel in $[(CH_3NH_2)_m$-$(H_2O)_n]^+$

Nobuyuki NISHI, Kazunori YAMAMOTO, Hisanori SHINOHARA, Umpei NAGASHIMA *(Computer Center),* **and Nobuaki WASHIDA** *(Nat. Inst. for Environmental Studies)*

[*Faraday Discuss. Chem. Soc.*, in press]

Methylamine hydrated clusters, $(CH_3NH_2)_m(H_2O)_n$ were generated by the liquid-jet expansion of aqueous solutions. Photoionization of the hydrated clusters with a Kr lamp (10.64 and 10.03 eV) produced mostly non-protonated ions, as shown in Figure 1, while Ar lamp ionization (11.83 and 11.62 eV) produced protonated ions with comparable intensities to those of the non-protonated ones with the same number of water molecules (Figure 1-b). These photoionization spectra are compared with the electron impact ionization spectrum in Figure 1-c. Methylamine is strongly associated with three water molecules. Further water association will be performed through these water molecules. Near-threshold ionization of this cluster with three water molecules removes an electron participating in the strong hydrogen bond, –H_2N--HOH, so that this bond will be immediately dissociated:

$$-(H_2O-H)_2-\underset{\underset{CH_3}{|}}{N}-HOH \rightarrow -(H_2O-H)_2-\overset{\overset{CH_3}{|}}{N^+}...HOH$$

$$\rightarrow -(H_2O-H)_2-\overset{\overset{CH_3}{|}}{N^+} + H_2O$$

An increase in the excess energy may dissociate other water molecule(s), but the hydrogen atoms of these water molecules are not abstracted by the methylamine cation, since those hydrogen atoms are not directly connected with methylamine. The hydrogen affinity of $CH_3NH_2^+$(111.6 kcal/mol) is not so large as those of H_2O(140 kcal/mol) and NH_3(127 kcal/mol). Therefore, insofar as a hydrogen-bonding lone-pair electron of methylamine is ionized, the proton-transfer reaction cannot be induced. Direct ionization of a water non-bonding electron, however, may immediately lead to the transfer of a positive charge to methylamine through a proton-transfer reaction.

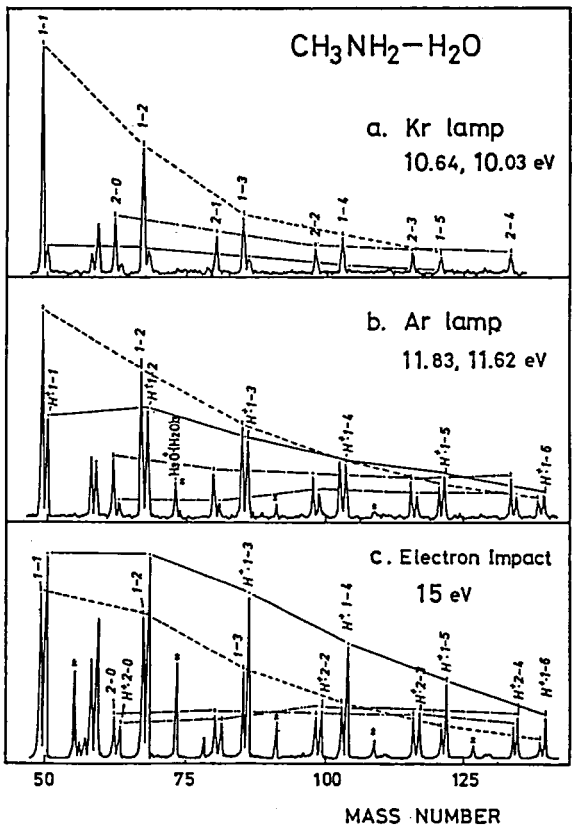

Figure 1. Ionization-energy dependence of the mass spectra of $(CH_3NH_2)_n$ $(H_2O)_m$ cluster beams generated by expanding the liquid jet of a methylamine-water solution (1:3.2 molar ratio); (a) Kr lamp ionization (10.64 and 10.03 eV), (b) Ar lamp ionization (11.83 and 11.62 eV) and (c) electron impact ionization at 15 eV. The protonated water clusters, $H^+(H_2O)_n$, are indicated by asterisk.

III-H-2 Photofragmentation of (Methylformamide)$_m$ $(H_2O)_n$

Nobuyuki NISHI, Kazunori YAMAMOTO, Hisanori SHINOHARA, Umpei NAGASHIMA *(Computer Center),* **and Nobuaki WASHIDA** *(Nat. Inst. Environmental Studies)*

[*Faraday Discuss. Chem. Soc.*, in press]

Figure 1 shows the photoionization mass spectra of MFA hydrated clusters generated from aqueous solution with different solute-solvent molar ratics of 1:10

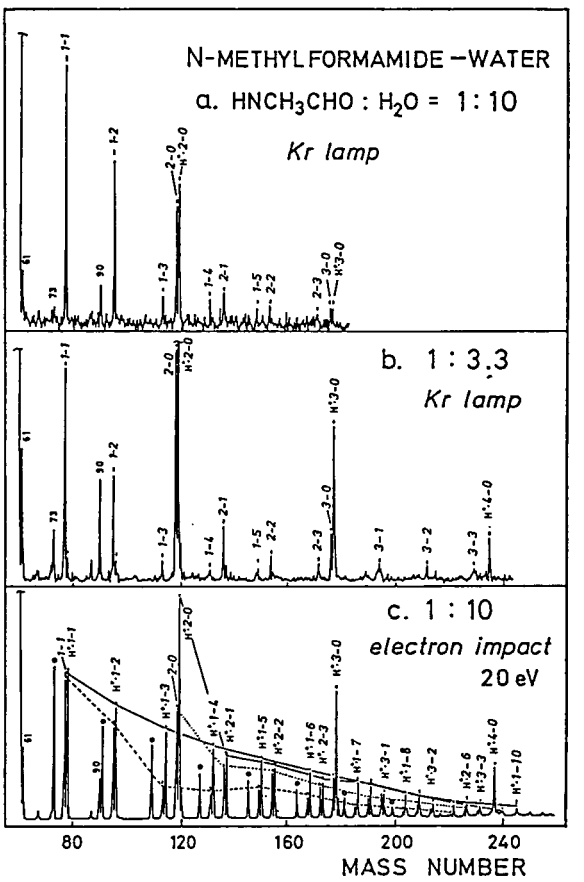

Figure 1. Photoionization (10.64 and 10.06 eV) and electron impact (20 eV) mass spectra of N-methylformamide (MFA)-water cluster beams generated by expanding the liquid jet of the solutions with MFA: H_2O ratios of 1:10 (a and c) and 1:3.3 (b). The protonated MFA dimer signal at mass number 119 in (b) is saturated. The intensity ratio, $H^+(MFA)_2/(MFA)_2^+$, is 3.3. The broken line and the dotted line in (c) connect the water sequences of $[MFA(H_2O)_n]^+$ and $[(MFA)_2\text{-}(H_2O)_n]^+$ ions, respectively. The solid lines connect the water sequences of the protonated ions, $H^+(MFA)(H_2O)_n$ and $H^+(MFA)_2(H_2O)_n$. The peaks indicated by circles are $H^+(H_2O)_n$ clusters. Molecular composition of the binary cluster $(MFA)_l(H_2O)_k$ are indicated by l-k. The protonated ion is expressed by H^+l-k. At mass 61 and 90, signals of the reaction products were seen whose intensities increased proportionally to that of the non-protonated MFA dimer ion.

and 1:3.3, respectively, by Kr lamp irradiation(10.64 and 10.03 eV). The spectrum of the water-rich cluster beam only shows strong peaks for MFA^+H_2O, $MFA^+(H_2O)_2$, $(MFA)_2^+$ and $H^+(MFA)_2$. An increase in the molar fraction of MFA by a factor of three enhanced the intensities of $H^+(MFA)_2$, $H^+(MFA)_3$ and $H^+(MFA)_4$ and caused $H^+MFA(H_2O)_n$ clusters to appear. At a higher MFA ratio, the protonated ion intensities increased. This fact indicates that the proton originated from the ionization of an MFA-MFA pair followed by the intracluster ion-molecule reaction:

$$-(-NHCH_3CHO-NH^+CH_3CHO-)- \rightarrow -(-NHCH_3CHO-H^+-NCH_3CHO-)-$$
$$\rightarrow -HNCH_3CHOH^+ + NCH_3CHO-$$

The intensity of $H^+(HNCH_3CHO)_2^+(= H^+(MFA)_2)$ is 3.3 times as strong as that of $(MFA)_2^+$. In the spectrum of the water-rich cluster beam the protonated dimer showed an intensity comparable to the non-protonated dimer. Namely, the ratio of $H^+(HNCH_3CHO)_2/(HNCH_3CHO)_2^+$, decreased to 1/3, almost exactly corresponding to the solute dilution ratio. Thus the origin of the non-protonated MFA dimer ion is attributed to $(HNCH_3CHO)_2(H_2O)_n$.

III-I Formation and Properties of Molecular Clusters in Supersonic Nozzle Beams

III-I-1 Photoionization of Water Clusters at 11.83 eV: Observation of Unprotonated Cluster Ions $(H_2O)_n^+$ $(2 \leqq n \leqq 10)$

Hisanori SHINOHARA, Nobuyuki NISHI, and Nobuaki WASHIDA *(Nat. Inst. for Environmental Studies)*

[*J. Chem. Phys.*, **84**, 5561 (1986)]

Unprotonated cluster ions $(H_2O)_n^+(2 \leqq n \leqq 10)$ and $(Ar)_m(H_2O)_n^+(1 \leqq m \leqq 3; 2 \leqq n \leqq 7)$ are detected in the mass spectra, for the first time, in addition to normally observed protonated ions $(H_2O)_{n-1}H^+$ when supersonic cluster beams of water-argon mixtures ($P \gtrsim 2$ atm) are photoionized with the vacuum-UV resonance lines at 11.83 and 11.62 eV. The protonated water cluster ions $(H_2O)_{n-1}H^+$ are produced by ionization of neutral water clusters $(H_2O)_n$ followed by intracluster proton-transfer reactions, whereas the unprotonated cluster ions $(H_2O)_n^+$ are generated via the photoionization of water-argon binary clusters: $(Ar)_m(H_2O)_n + h\nu \rightarrow (H_2O)_n^+ + mAr + e^-$. The excess energies on ionization can be randomized within the $[(Ar)_m(H_2O)_n^+]^*_{vip}$ clusters ("intracluster excess energy dissipation") and finally converted to the decompositions of argon atoms, giving rise to the stable $(H_2O)_n^+$ and various $(Ar)_k(H_2O)_n^+$ ions. The $(H_2O)_n^+$ ions have the distinct potential energy minima along the proton transfer reaction coordinates.

III-I-2 The Electronically Excited States $\tilde{A}$ of Ammonia Clusters as Revealed by Two-Photon-Ionization Mass Spectroscopy

Hisanori SHINOHARA, Kenji SATO *(Department of Molecular Assembly)*, **Yohji ACHIBA** *(Department of Molecular Assembly)*, **Nobuyuki NISHI, and Katsumi KIMURA** *(Department of Molecular Assembly)*

[*Chem. Phys. Lett.*, in press]

The two-photon-ionization (TPI) via the $\tilde{A}$ state of ammonia clusters has been investigated in a pulsed jet to get information about the excited state characters of the hydrogen-bonded clusters.[1,2] One of the most salient features of the TPI spectra is that the $(NH_3)_nH^+$ ion intensity decreases more rapidly with increasing n at longer excitation wavelengths, suggesting the absorption profiles of the $\tilde{A}$ state of the ammonia clusters are dependent on the cluster size.

A distinct evidence for the resonance-enhancements at the $\tilde{A}$ states of the ammonia clusters is found in Figure 1, where three semilogarithmic plots of ion intensity vs. one-photon excitation wavelength are presented for the NH_4^+, $(NH_3)_2^+$, and $(NH_3)_2H^+$ ions. The onset of the formation of these cluster ions has an apparent wavelength threshold just below 217 nm; this can be ascribed to the fact *the present two-photon-ionization of the ammonia clusters is the one which resonantly-enhanced at the $\tilde{A}$ states.*

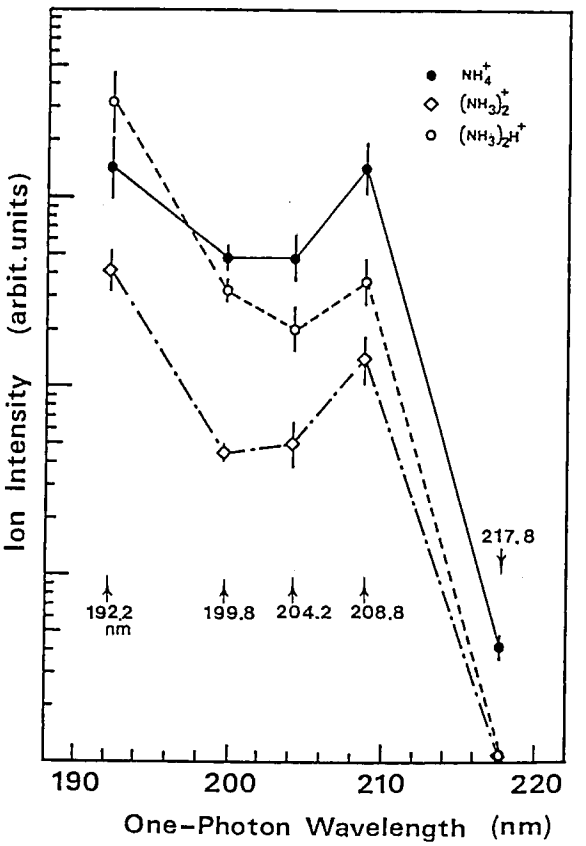

Figure 1. Semilogarithmic plots of ion intensity vs. excitation laser wavelength for the NH_4^+, $(NH_3)_2^+$, and $(NH_3)_2H^+$ cluster ions. The observations are made at 192.2, 199.8, 204.2, 208.8 and 217.8 nm. The ordinate is calibrated with respect to the laser intensity. Error bars are shown.

References

1) H. SHINOHARA and N. NISHI, *Chem. Phys. Lett.*, **87**, 561 (1982).
2) H. SHINOHARA, *J. Chem. Phys.*, **79**, 1732 (1983).

III-I-3 Ionization of NO_2 Clusters in a Supersonic Nozzle Beam: Appearance of the Odd-Number Cluster Ions of NO_2

Nobuaki WASHIDA *(Nat. Inst. for Environmental Studies)*, **Hisanori SHINOHARA, Umpei NAGASHIMA** *(Computer Center)*, **and Nobuyuki NISHI**

[*Chem. Pys. Lett.*, **121**, 223 (1985)]

Cluster ions $(NO_2)_n^+$, n = 2 − 13, were detected mass spectrometrically in a supersonic nozzle beam by both photon- and electron-impact ionization. The odd-number cluster ions $(NO_2)_{2m+1}^+$ appeared dominantly over the even-number cluster ions $(NO_2)_{2m}^+$. The results are consistently explained by the dissociative ionization of the $(sym\text{-}N_2O_4)_n$ clusters and ionization (involving intra-cluster charge transfer) of the $(sym\text{-}N_2O_4)_nNO_2$ clusters produced via supersonic expansion of NO_2: $(sym\text{-}N_2O_4) + h\nu \rightarrow (sym\text{-}N_2O_4)_{n-1}NO_2^+ + NO_2 + e^-$ and $(sym\text{-}N_2O_4)_nNO_2 + h\nu \rightarrow (sym\text{-}N_2O_4)_nNO_2^+ + e^-$.

III-J Photofragmentation Dynamics and Photochemistry of Gaseous Molecules

III-J-1 Photochemistry of Acetylene at 193 nm: Two Pathways for Diacetylene Formation

Kanekazu SEKI, Nobuaki NAKASHIMA, Nobuyuki NISHI, and Minoru KINOSHITA *(Inst. for Solid State Phys, Univ. of Tokyo)*

[*J. Chem. Phys.*, **85**, 274 (1986)]

Nonosecond time-resolved absorption spectra of diacetylene were observed in the 193 nm excitation of acetylene to the $\tilde{A}\ ^1A_u(v'_3 = 10)$ state. The formation of diacetylene was confirmed by comparing it with the spectrum of pure diacetylene. Time behavior of the diacetylene spectrum showed that there are two pathways for diacetylene formation. The results obtained from this study are summarized in Figure 1. The excited molecule dissociates into a hydrogen atom and a C_2H radical in the singlet manifold (A) and it is expected to isomerize to a triplet vinylidene radical through an excited triplet state of acetylene (B). The ratio of diacetylene produced by process (B) to that by process (A), [(B)/(A)], is obtained to be 1.5-1.2 in the acetylene pressure range of 30 to 600 Torr from the intensity ratio of the fast and slow components in the C_4H_2 transient absorption. Dissociation processes (A) and the following C_2H reaction (C) are rapid processes and finish within the 20 ns laser pulse time scale. The sequencial process of reactions (B) and (D) occurs

relatively slowly within 2 μs. The two pathways for the fast and the slow diacetylene formation could be characterized as "singlet pathway" and "triplet pathway", respectively.

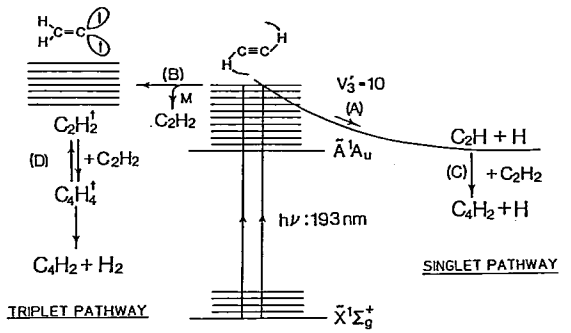

Figure 1. Proposed photochemical pathways for the formation of diacetylene on the Ã state excitation of acetylene.

III-J-2 Fast Photodecomposition of Chlorobenzene and m-Chlorotoluene in Molecular Beams at 193 nm

Teijiro ICHIMURA *(Tokyo Inst. of Tech.)*, **Yuji MORI** *(Tokyo Inst. of Tech.)*, **Hisanori SHINOHARA, and Nobuyuki NISHI**

[*Chem. Phys. Lett.*, **122**, 51 (1985)]

Molecular beams of C_6H_5Cl and m-$ClC_6H_4CH_3$ were photodissociated at 193 nm. It appeared that the time-of-flight spectra of chlorobenzene and m-chlorotoluene consist of two components: the fast and narrow distribution and the slow and broad one. The peak value of E_T for the narrow distribution of chlorobenzene is approximately 34 kcal/mol and that for the broad one is ca. 9 kcal/mol. The high translational energy peak is attributed to the dissociation through an excitation to a repulsive state and/or the fast predissociation competing with the intramolecular vibrational relaxation or internal conversion from the initially excited state. Since the slow components have stronger intensity than fast ones, the slow dissociation process must be a major process in the photolysis of chlorobenzene and m-chlorotoluene. The energy distribution of this component, however, cannot be represented by a statistical distribution function suggesting that the dissociation process should be faster than complete thermalization. Accordingly the most probable exit state to give the slow photofragments may be the highly vibrationally excited triplet state generated through a fast intersystem crossing from the initial optically excited singlet state.

III-J-3 Photodissociation Channels for Pentafluorochlorobenzene Excited at 193 nm in Molecular Beams

Teijiro ICHIMURA *(Tokyo Inst. of Tech.)*, **Yuji MORI** *(Tokyo Inst. of Tech.)*, **Hisanori SHINOHARA, and Nobuyuki NISHI**

[Chem. Phys. Lett., **125**, 263 (1986)]

Translational energy distribution of the photofragments produced by the photodissociation of pentafluorochlorobenzene at 193 nm was measured and revealed to be composed of two components. Dominant one fits to a statistical distribution function with a average translational energy of 6.5 kcal/mol and the other one showed non-statistical distribution which is represented by a Gaussian function with a mean energy of 15 kcal/mol. The state which produces the low energy distribution must have a long lifetime to distribute the electronic excitation energy over the various vibrational modes of the molecule. The most probable exit state must be a vibrationally excited ground electronic state. The formation of the hot molecule is thought to be a common process in the 193 nm photolysis of benzene derivatives. But the transition to the dissociative state from the hot vibrational states is enhanced by fluorination. Thus the dissociated pentafluorophenyl radical is vibrationally excited but translationally rather cooled. Appearance of the high energy component is attributed to the highly vibrationally excited triplet state generated through fast intersystem crossing from the optically pumped excited singlet state. Table 1 summarized the result obtained and it also shows the reanalized data of chlorobenzene.

Table 1. Average partitioning of available energy and probability of dissociation channels in the photolysis of chlorobenzene and pentafluorochlorobenzene at 193 nm

Parent molecule	D_0(C-Cl) (kcal/mol)	E_{avl}[c] (kcal/mol)	E_T[d] (kcal/mol)	Most probable exit state	Probability
C_6H_5Cl[a]	97	52	5.0	$S_0^* \leftarrow S_3(\pi^*,\pi)$	0.39
			16	$T^* \leftarrow 3_3(\pi^*,\pi)$	0.34
			30	$S(\sigma^*,n)$	0.27
C_6F_5-Cl	97b)	52	6.5	$S_0^* \leftarrow S_2(\pi^*,\pi)$	0.86
			15	$T^* \leftarrow S_2(\pi^*,\pi)$	0.14

a) The result of a previous work (III-J-2) is reanalyzed by the assumption that the dissociation involves three dissociation processes in analogy to *p*-dichlorobenzene.
b) Dissociation energy of pentafluorochlorobenzene is assumed to be the same with that of chlorobenzene.
c) $E_{avl} = h\nu - D_0 + 2RT$.
d) Average translational energy.

III-K Effects of External Magnetic Field upon Chemical Reactions

Magnetic field effects upon chemical reactions provide us with (1) useful methods for studying reaction mechanism and (2) technique for controlling reaction rates, product yields, and concentration of a certain isotope. In recent years, the magnetic field effects upon photochemical reactions in the solution phase have been extensively studied by several methods, *e.g.* steady state and laser photolysis. Among other things, the photoreactions of aromatic carbonyls in micellar media and of bifunctional molecules in homogeneous solutions are investigated in some detail. In addition, we have also examined the magnetic field effects on afterglow activated by a microwave discharge and the mechanism of magnetic quenching of CS_2 fluorescence in the gaseous state.

III-K-1 Magnetic Field Effects on the Photoinduced Electron Transfer Reaction of 1-Acetonaphthone and Diphenylamine in Micellar Solution

Yoshifumi TANIMOTO *(Kanazawa Univ.)*, **Masanari TAKAYAMA** *(Kanazawa Univ.)*, **Michiya ITOH** *(Kanazawa Univ.)*, **Ryoichi NAKAGAKI, and Saburo NAGAKURA**

[*Chem. Phys. Lett.*, in press]

Megnetic field effects on the photoinduced electron transfer reaction between 1-acetonaphthone (1-AN) and diphenylamine (DPA) in SDS micellar solution have been studied by nanosecond laser photolysis. When 1-AN is excited, a rapid intersystem crossing populates the lowest triplet state of the electron acceptor, and then the charge separation takes place in the triplet manifold. The time profile of transient absorption due to DPA cation radical shows anomalous external magnetic field effects, which can be explained by considering the participation of inter- and intramicellar processes.

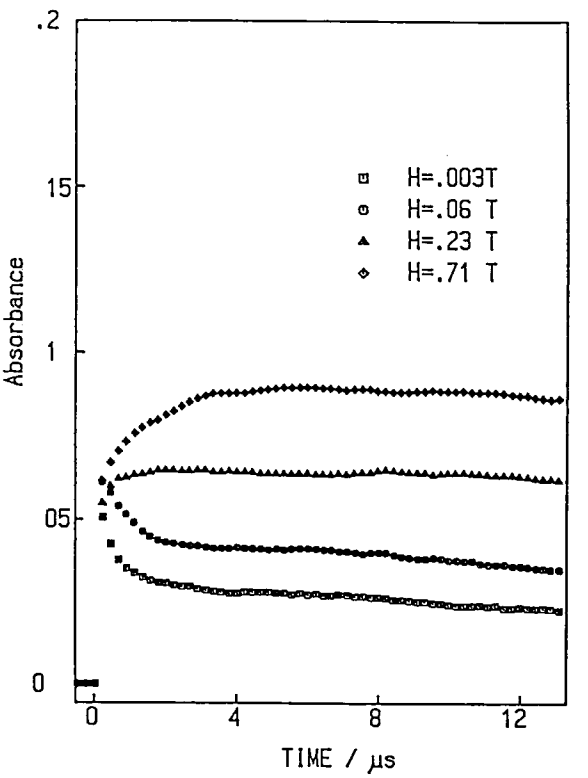

Figure 1. Magnetic field effect upon the transient signal of DPA cation radical at 680 nm (1-AN 4×10^{-4}mol/l, DPA 3×10^{-3}mol/l, and SDS 0.4mol/l).

III-K-2 Magnetic Field Effect upon Radical Reactions Initiated by Photo-induced Electron Transfer. Photosensitized Isomerization of *trans*-3,3-Dimethyl-1-(2-naphthyl)-1-butene (DMNB)

Hirochika SAKURAGI *(Univ. of Tsukuba and IMS)*, **Ryoichi NAKAGAKI, Takahisa OGUCHI** *(Univ. of Tsukuba)*, **Katsumi TOKUMARU** *(Univ. of Tsukuba)*, **and Saburo NAGAKURA**

Photochemistry of DMNB in the presence of electron acceptors has been studied by means of steady state and laser photolysis. The photochemical primary process is an electron transfer from the fluorescent state of DMNB to acceptor, 1,4-dicyanobenzene (DCB). The reaction involves a singlet radical pair consisting of DMNB cation and DCB anion, which were identified by comparing the transient absorption spectra obtained by nanosecond photolysis with the authentic spectra for these ion radicals.

It has been revealed that the disappearance yield of *trans*-DMNB decreases on application of external magnetic fields by using steady state photolysis. The mechanism of photoisomerization is summarized in Figure 1. The precursor of *cis*-DMNB is the excited triplet state of the *trans*-isomer, and therefore the decreased yield of *trans-cis* isomerization corresponds to the decrease in *trans*-DMNB triplet. Since the precursor of *trans*-DMNB triplet is the triplet radical ion pair, the intersystem crossing between the singlet and triplet radical pairs plays an important role in photoisomerization. It was found that the hyperfine interaction is of dominant importance in the present case.

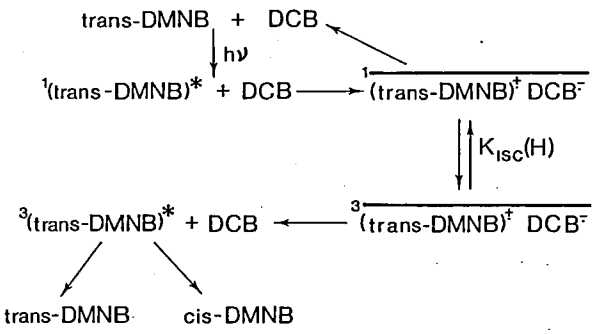

Figure 1. Reaction mechanism of *trans* → *cis* icomerization for DMNB(2-$C_{10}H_7CH=CH^tBu$) in the presence of an electron acceptor (DCB).

III-K-3 Photochemistry of Bichromophoric Chain Molecules Containing Electron Donor and Acceptor Moieties. III[1] Photoinduced Redox Reaction Involving Intramolecular Oxygen Transfer

Mitsuo HIRAMATSU *(Hamamatsu Photonics K.K.)*, **Ryoichi NAKAGAKI, Yoshifumi TANIMOTO** *(Kanazawa Univ.)*, **and Saburo NAGAKURA**

A chain molecule containing *p*-nitrophenoxy and triphenylphosphine moieties undergoes an intramolecular photoredox reaction (see Figure 1):

$$p\text{-}O_2N\text{-}C_6H_4O\text{-}(CH_2)_{12}\text{-}p\text{-}OC_6H_4P(C_6H_5)_2 \xrightarrow{h\nu} p\text{-}ON\text{-}C_6H_4O\text{-}(CH_2)_{12}\text{-}p\text{-}OC_6H_4P(O)(C_6H_5)_2.$$

The product yield decreases in the presence of an external magnetic field (0.64 T). The reaction mechanism of this intramolecular oxygen transfer appears to be remotely related to that for N-[ω-(*p*-nitrophenoxy)-alkyl]anilines, because the latter accompanies a bond cleavage between the anilino nitrogen and the methylene carbon. The observation of the magnetic field effect suggests an intermediacy of the biradical consisting of the donor cation and the acceptor anion.

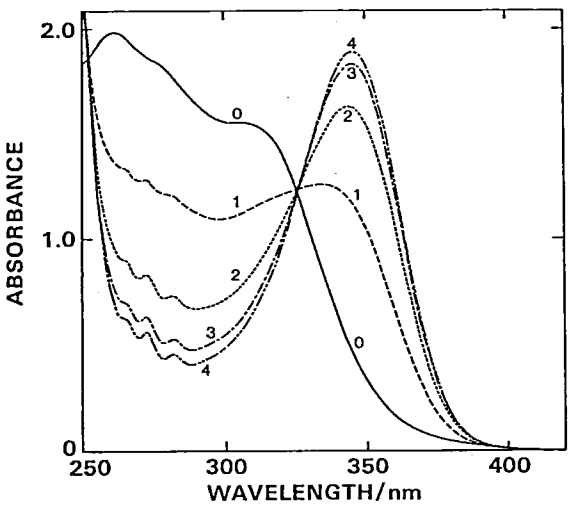

Figure 1. Development of photoredox reaction as revealed by UV-absorption spectroscopy. The number refers to the period of irradiation in minute. The absorption band peaking around 350 nm is due to *p*-nitrosophenoxy chromophore, and the band with vibrational structures around 270 nm is assigned to the triphenylphosphine oxide moiety.

Reference

1) Part II of this series, R. Nakagaki, M. Hiramatsu, Y.

Tanimoto, K. Mutai, and S. Nagakura, *IMS Ann. Rev.*, **70**, (1985).

III-K-4 Photochemistry of Bichromophoric Chain Molecules Containing Electron Donor and Acceptor Moieties. IV
Photocyclization and Photodecomposition Reactions of N-[ω-(*m*-Nitrophenoxy)alkyl]anilines

Kiyoshi MUTAI *(Univ. of Tokyo)*, **Ryoichi NAKAGAKI, and Saburo NAGAKURA**

The photochemistry of bichromophoric species containing *m*-nitrophenoxy and anilino moieties depends on the chain length n. When n = 12, unsubstituted aniline is released by a photo-induced decomposition, while a photochemical ring closure reaction is observed for the molecule with two methylene groups. The photodecomposition reaction yield depends on the applied magnetic field strength. The photochemical behavior of *m*-nitrophenoxy homologues is more or less related to that observed for the para-substituted series[1], and therefore, it may be concluded that
(1) the charge-separated biradical D^+-$(CH_2)_n$-A^- is involved as a reaction intermediate and
(2) the charge-separation occurs in the triplet manifold of the electron acceptor moiety.

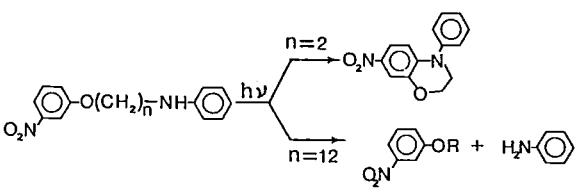

Figure 1. Photochemical cyclization and decomposition reactions of *m*-nitrophenoxy homologues.

Reference

1) R. Nakagaki, M. Hiramatsu, K. Mutai, and S. Nagakura, *Chem. Phys. Lett.*, **121**, 262, (1985).

III-K-5 Photochemistry of Bichromophoric Chain Molecules Containing Electron Donor and Acceptor Moieties. V
External Magnetic Field Effects upon Photodecomposition of N-[12-(4-Nitro-1-naphthoxy)-dodecyl]aniline(NNDA)

Ryoichi NAKAGAKI, Kiyoshi MUTAI *(Univ. of Tokyo)*, **Mitsuo HIRAMATSU** *(Hamamatsu Photonics K.K.)*, **and Saburo NAGAKURA**

Photodecomposition of NNDA yields 4-nitrosonaphthoxy and 4-nitronaphthoxy derivatives (Product 1 and Product 2). The relative yield [Product 1]/[Product 2] is critically dependent on the magnetic field strength. Product 1 is major one in the absence of the field, while Product 2 becomes major one on application of an external magnetic field (0.64 T). This clearly shows that the magnetic field effect has some potentiality for selecting reaction pathway. Under the present experimental condition (H = 0.64 T), the hyperfine coupling mechanism is more important than the Zeeman mechanism. By analogy with the photoreaction observed for the corresponding *p*-nitrophenoxy homologue[1], the photochemical primary process is concluded to be an electron transfer from the donor moiety to the excited acceptor moiety. The observed results are consistent with the assumption that the initially prepared precursor biradical has triplet spin multiplicity and that Product 1 and Product 2 are escape and cage products, respectively.

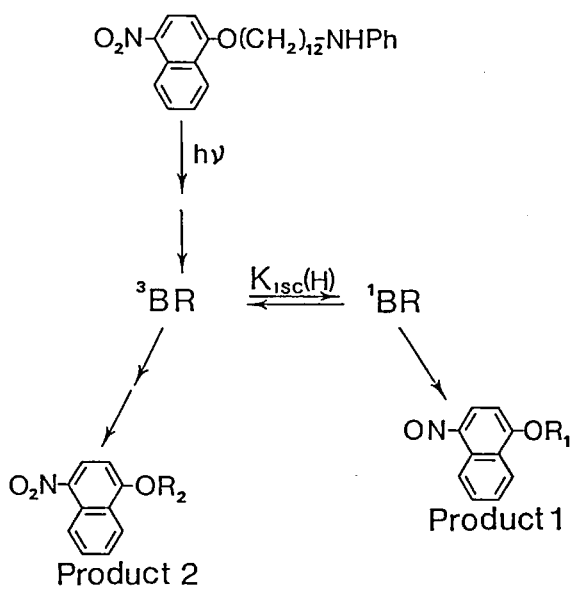

Figure 1. Reaction mechanism of photodecomposition for NNDA. ^{3}BR and ^{1}BR denote the charge-separated biradicals in the triplet and the singlet states, respectively. The third photoproduct aniline is not illustrated in the figure, because its formation yield exhibits no magnetic field effects. Absorption spectra of Product 1 and Product 2 show that the side chain R_1 or R_2 cannot contain an anilino chromophore. Aniline is released from the formation processes of both Product 1 and Product 2.

Reference

1) R. Nakagaki, M. Hiramatsu, K. Mutai, and S. Nagakura, *Chem. Phys. Lett.*, **121**, 262 (1985).

III-K-6 Magnetic Field Effect on the Fluorescence of Intramolecular Electron-Donor-Acceptor Systems

Yoshifumi TANIMOTO *(Kanazawa Univ.)*, **Natsuo OKADA** *(Kanazawa Univ.)*, **Michiya ITOH** *(Kanazawa Univ.)*, **Kaoru IWAI** *(Nara Women's Univ.)*, **Kayoko SUGIOKA** *(Nara Women's Univ.)*, **Fukuo TAKEMURA** *(Nara Women's Univ.)*, **Ryoichi NAKAGAKI, and Saburo NAGAKURA**

The intramolecular exciplex fluorescence of α-(4-dimethylaminophenyl)-ω-(9-phenanthryl)alkanes (DMA-n-Phen, n = 3-10) has been studied in the presence and absence of external magnetic fields. The fluorescence of intramolecular exciplex is observed in the region of 450-550 nm as well as that of phenanthryl moiety (350-400 nm). The magnetic field effects on the fluorescence intensity monitored at 540 nm is shown in Figure 1, where the relative intensity I_H/I_0 is recorded as a function of applied field strength. Long-chain species exhibit remarkable magnetic field effects. The present system involves a radical pair consisting of DMA cation and Phen anion radicals. The observed phenomena can be interpreted in terms of the radical pair theory considering the singlet-triplet mixing due to the hyperfine coupling.

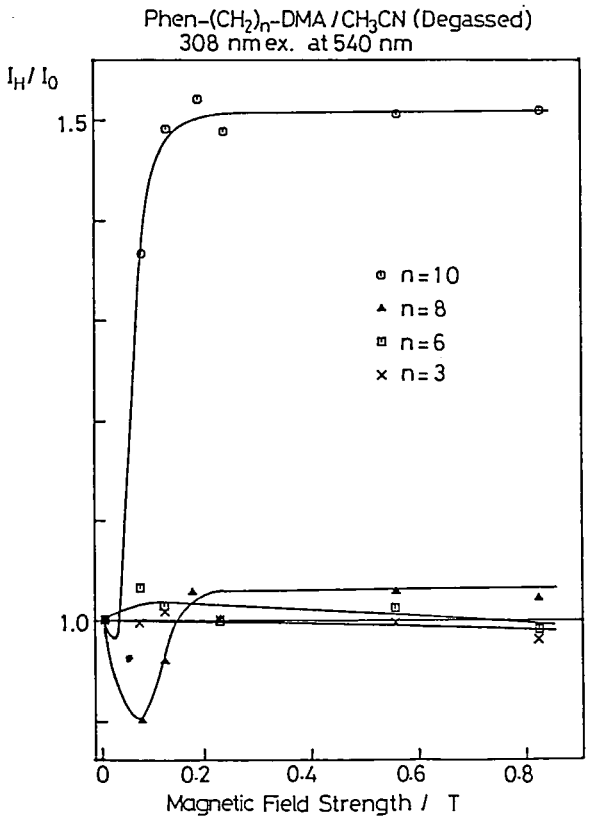

Figure 1. Relative fluorescence intensity I_H/I_0 *vs.* field strength H, where I_H and I_0 represent the intensity in the presence and absence of magnetic fields, respectively. Excitation wavelength = 308 nm, and monitoring wavelength = 540 nm. Spectra were measured for degassed solutions in acetonitrile.

III-K-7 External Magnetic Field Effect on CS_2 Banded Emission. Laser Excitation in the Wavelength Region of Nitrogen Laser

Takashi IMAMURA, Saburo NAGAKURA, Haruo ABE *(Inst. of Phys. and Chem. Res. and IMS)*, **Yoshio FUKUDA** *(Inst. of Phys. and Chem. Res. and IMS)*, **and Hisaharu HAYASHI** *(Inst. of Phys. and Chem. Res. and IMS)*

External magnetic field effects on the banded

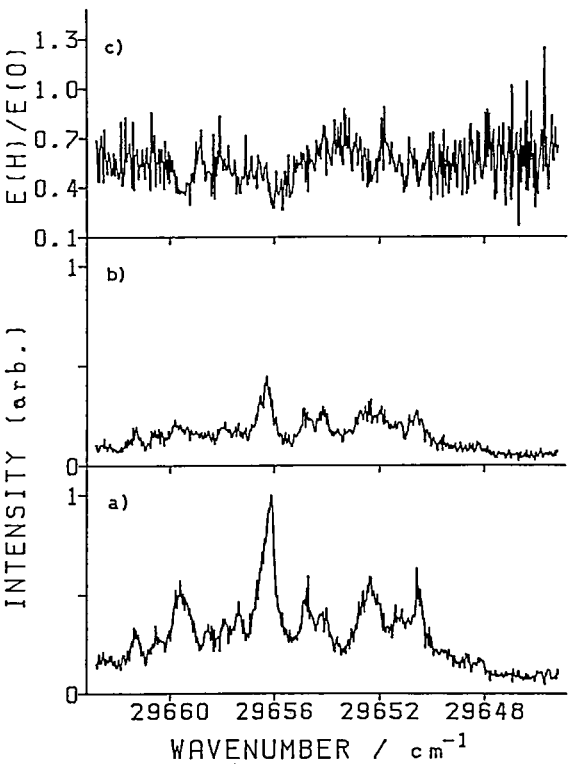

Figure 1. Excitation spectra in the t + 3 band region observed (a) at H = 0 G and (b) at H = 8.3 kG. CS_2 pressure was 61 mTorr. Emission was monitored at 26346 cm^{-1}. (c) The relative intensities of excitation spectra, $E(H)/E(0)$, are calculated for H = 8.3 kG.

emission of gaseous CS_2 were measured at room temperature by the excitation near the nitrogen laser wavelengths. The magnetic field effects observed below 8.3 kG have the following characteristics: 1) a magnetic field affects only the emission intensity without changing its lifetime, 2) the integrated intensity of the excitation spectrum of the banded emission is reduced by a magnetic field, 3) magnetic field effects can be observed even under a supersonic jet condition, and 4) the magnetically induced decrease in the integrated intensity of the excitation spectrum is independent of the Zeeman broadening in the absorption spectrum. These experimental results suggest that a magnetic field affects intramolecular processes. The possible mechanisms for the novel magnetic field effect on the CS_2 banded emission are discussed.

III-K-8 External Magnetic Field Effects on the Emission Intensities of the OH(A-X) and CH(A-X) Bands in Low Pressure C_2H_2/O_2 and C_3H_8/O_2 Flames

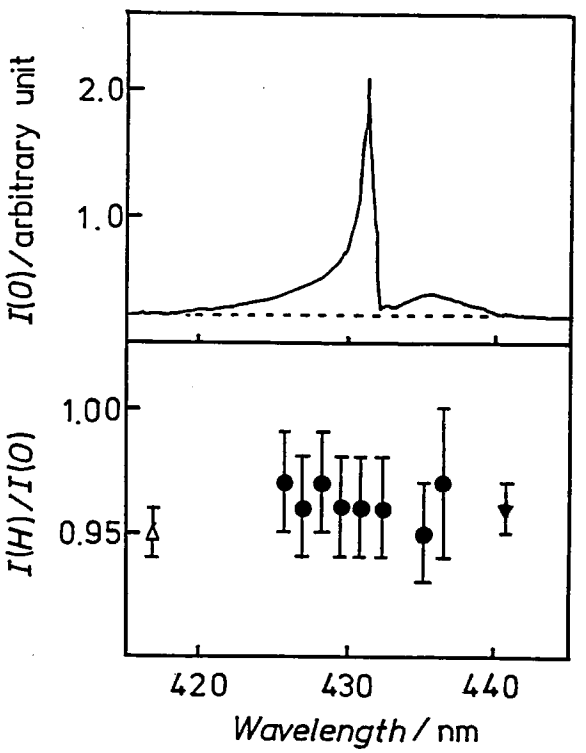

Figure 1. Wavelength dependence of $I(H)/I(0)$ of the CH(A-X) (•) and H_2CO^* emission (△,▼) observed at 1.8 T with the C_2H_2/O_2 flame. $I(H)/I(0)$ of the CH(A-X) emission was obtained by subtracting the H_2CO^* emission as indicated by a broken line. Resolution is 0.8 nm.
Pressures of O_2, C_2H_2 are 30 and 3 Pa, respectively.

Yoshio FUKUDA *(Inst. of Phys. and Chem. Res. and IMS)*, **Haruo ABE** *(Inst. of Phys. and Chem. Res. and IMS)*, **Hisaharu HAYASHI** *(Inst. of Phys. and Chem. Res. and IMS)*, **Takashi IMAMURA, and Saburo NAGAKURA**

[*Chem. Lett.*, 777 (1986)]

Magnetic field effects on emission intensities of the CH(A-X) and OH(A-X) emission were studied with low pressure C_2H_2/O_2 and C_3H_8/O_2 flames produced by a microwave discharge of O_2. When a magnetic field of 1.8 T was applied, the intensity of the CH(A-X) emission was reduced to 95% of that at zero field.

III-K-9 Dynamics of Cs_2 Excited by a Synchronously Pumped Mode-Locked Dye Laser and the Effects of Magnetic Field

Hajime KATO *(Kobe Univ.)*, **Kazushige YOKOYAMA** *(Kobe Univ.)*, **Masaaki BABA** *(Kobe Univ.)*, **Naoto TAMAI** *(Instrument Center)*, **Iwao YAMAZAKI** *(Instrument Center)*, **and Saburo NAGAKURA**

When the Cs_2 molecule was excited by a dye-laser line of 15841 cm^{-1}, the fluorescence from the energy-transferred states as well as the resonance fluorescence from the optically excited levels, which were assigned to C $^1\Pi_u$ and d $^3\Pi_u$, were observed. We measured the picosecond time-resolved fluorescence intensities by changing the vapor pressure and the temperature. The decay curves were analysed by a least-squares curve fitting, and the lifetimes in the collisionless limit and the collision cross sections were determined. By comparing the rates of the rise and the decay of fluorescence intensities, the kinetic pathways of the collisional energy transfer were estimated. When an external magnetic field was applied, the intensity of the fluorescence d $^3\Pi_U$ - X $^1\Sigma_g^+$ was found to decrease appreciably. The effect of magnetic field on the time-resolved fluorescence intensity was measured and analysed. A new interaction due to the magnetic field occurs between the d $^3\Pi_u$ and c $^3\Sigma_u^+$ states. The observed results are ascribed to the magnetic predissociation similar to the one already found in the iodine molecule.

RESEARCH ACTIVITIES IV
Department of Molecular Assemblies

IV–A Photoelectron Spectroscopy of Organic Solids in Vacuum Ultraviolet Region

Photoelectron spectroscopical (UPS) study of organic solids and polymers has been carried out. UPS of solid iodine, a typical electron acceptor, was observed. The construction of UVSOR-UPS apparatus has been completed.

IV-A-1 Valence Bands of Oriented Finite Linear Chain Molecular Solids as Model Compounds of Polyethylene Studied by Angle-Resolved Photoemission

Kazuhiko SEKI *(HASYLAB at DESY, FRG and IMS)*, **Nobuo UENO** *(HASYLAB at DESY and Chiba Univ.)*, **Ulf O. KARLSSON** *(HASYLAB at DESY and Linköping Univ., Sweden)*, **R. ENGELHARDT** *(Univ. Hamburg, FRG)* **and Ernst-E. KOCH** *(Fritz-Haber Inst. der MPG, FRG)*

[*Chem. Phys.*, **105**, 247 (1986)]

Angle-resolved photoemission spectra were measured using synchrotron radiation of two kinds of oriented model compounds of polyethylene with their molecular axes perpendicular to the substrate surface, *i.e.* evaporated films of hexatriacontane $CH_3(CH_2)_{34}CH_3$ and Langmuir-Blodgett films of Cd arachidate $(CH_3(CH_2)_{17}COO)_2Cd$. Both films show similar photoelectron energy distribution curves determined by the long-alkyl chain. The intramolecular energy-band dispersion of polyethylene was determined from the photon-energy dependence of the normal-emission spectra. This is the first direct observation of an energy-band dispersion in organic solids. The upper bands formed by C 2*p* and H 1*s* electrons extend from 8.8 to 15.5 eV below the vacuum level, ant the deeper-lying bands originating from C 2*s* electrons lie from 17.5 eV to 24.7 eV. The band structure obtained is compared to results from XPS and ESR studies. Furthermore, the experimentally determined band structure is discussed in detail in view of thoretical calculations from polyethylene. *Ab initio* and extended Hückel calculations give a good description of the experimental results, as shown in Figure 1.

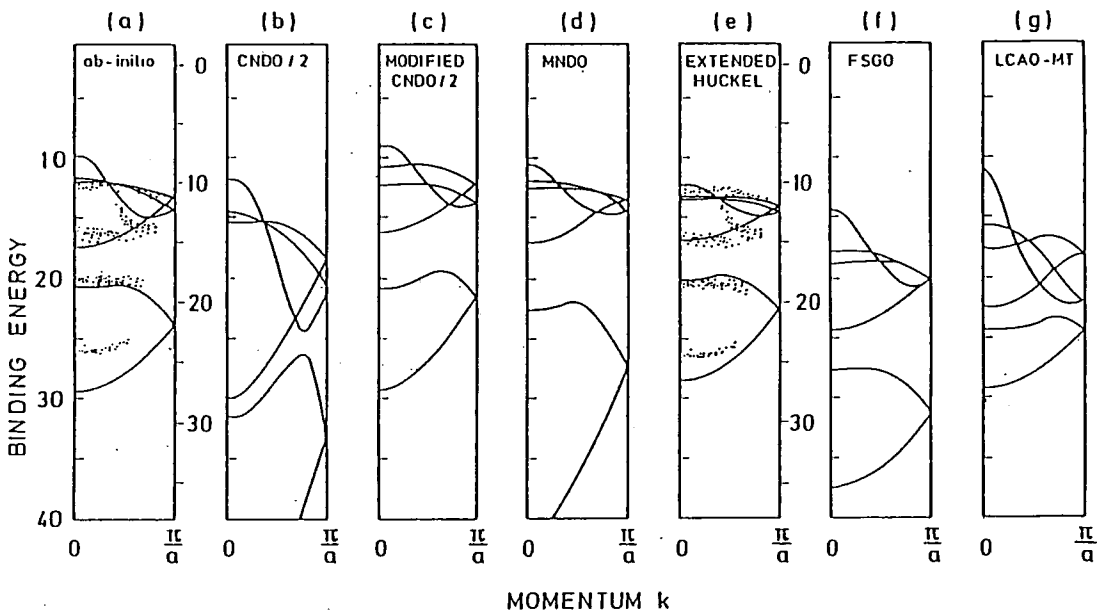

Figure 1. Comparison of the experimentally observed $E=E(k)$ relation [points in (a) and (e), this work] with theoretical calculations.

IV-A-2 Ultraviolet Photoelectron Spectroscopy of Solid Iodine

Hiromichi YAMAMOTO *(Nagoya Univ. and IMS)*, **Kazuhiko SEKI, Takehiko MORI, and Hiroo INOKUCHI**

[*J. Chem. Phys.*, in press]

The ultraviolet photoelectoron spectra of solid iodine have been measured. The observed spectral features show a large deviation from a one-to-one correspondence with the gas phase spectrum[1] as shown in Figures 1 (a) and (b). These results are examined by an extended Hückel band calculation, which indicates that this deviation is caused by the effect of a strong intermolecular interaction on the electronic structure, namely the formation of broad bands (0.7 to 2.0 eV).

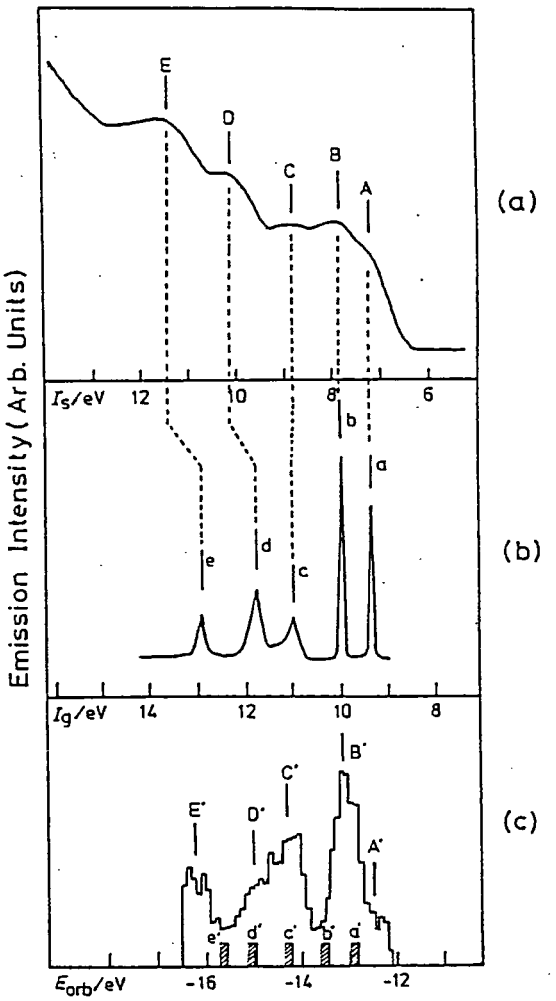

Figure 1. HeI UPS spectrum of solid iodine (a), HeI UPS spectrum of iodine vapor (b), and calculated density of occupied states (c). The hatched bars in (c) indicate the energy levels of a molecule estimated from a calculation for a molecule and the experimentally observed spin-orbit splittings.

The characters of the observed spectral features are assigned by the calculated density of states shown in Figure 1(c). The energy gap is estimated to be 1.6 eV from the observed energy difference between the Fermi level and the top of valence bands (5.52 eV and 6.34 eV relative to the vacuum level, respectively), by assuming that iodine is an intrinsic semiconductor. The large decrease of ionization threshold energy (2.92 eV) from the gas to the solid state is also discussed.

Reference

1) K. Kimura, S. Katsumata, Y. Achiba, T. Yamazaki, and S. Iwata, Handbook of HeI Photoelectron Spectra of Fundamental Organic Molecules, Japan Scientific Societies Press, Tokyo, 1981.

IV-A-3 Valence Electronic Structures of Tetrakis(alkylthio)tetrathiafulvalenes (TTC_n-TTFs)

Kazuhiko SEKI, Tong B. TANG *(IMS and Univ. Cambridge, UK)*, **Takehiko MORI, Peiji Wu** *(IMS and Inst. Chem., Academia Sinica, China)*, **Gunzi SAITO** *(Univ. Tokyo)*, **and Hiroo INOKUCHI**

[*J. Chem. Soc. Faraday Trans. 2*, **82**, 1067 (1986)]

Tetrakis(alkylthio)tetrathiafulvalenes which have the general molecular structure in Figure 1, constitute a new class of organic semiconductors offering unusually high conductivities, and ultraviolet photoelectron spectroscopic experiments were performed to investigate the valence electronic structures of these molecular solids. The results have been analysed with help from extended-Hückel molecular orbital calculations. In this series of compounds, the central tetrathiotetrathiafulvalene moiety is nonplaner, but it was shown that the degree of departure from planarity

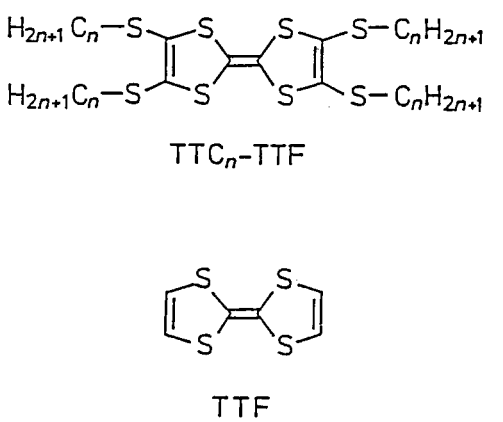

Figure 1. Molecular structures of TTC_n-TTFs and tetrathiafulvalene (TTF).

affects little the electronic structure. On the other hand, members of the series with many (>8) carbon atoms in each alkyl chain possess extraordinarily low photoionization thresholds (4.6_5 eV at minimum). For such solids large polarisation energies were deduced, implying relatively strong intermolecular interaction. Organic semiconductors where, between adjacent molecules, the close packing of their side chains enhance the interaction of their conjugated parts, are candidates for which high conductivity is desired.

IV-A-4 Ultraviolet Photoelectron Spectroscopsy of Poly(*p*-phenylene Sulfide) (PPS)

Satoshi ASADA *(IMS and Toyota Motor Co.)*, **Kazuhiko SEKI, and Hiroo INOKUCHI**

[*Chem. Phys. Lett.*, **130**, 155 (1986)]

Ultraviolet photoelectron spectra were measured for films of poly(*p*-phenylene sulfide) prepared by vacuum evaporation. The threshold ionization potential was determined to be 6.0±0.1 eV. The peaks in photoelectron spectra were assigned by comparison with theoretical calculations, and the π-bandwidth of PPS and related compounds were discussed.

References

1) J. Riga, J. P. Boutique, J. J. Pireaux and J. J. Verbist, *Proc. ACS Int. symp. Physico-Chemical Aspects of Polymer Surfaces* (New York) (1981) p.45.
2) J. L. Brédas, R. R. Chance, R. Silbey, G. Nicolas and Ph. Durand, *J. Chem. Phys.*, **77**, 371 (1982).

IV-A-5 UV Photoelecton Spectroscopy of Conducting Polymers and Their Model Compounds

Kazuhiko SEKI, Satoshi ASADA *(IMS and Toyota Motor Co.)*, **Takehiko MORI, Hiroo INOKUCHI, Ichiki MURASE** *(Research Association for Basic Polymer Technology)*, **Ulf O. KARLSSON** *(Linköping Univ.)*, **R. ENGELHARDT** *(Univ. Hamburg)*, **and Ernst-E. KOCH** *(Fritz-Haber Inst. der MPG, FRG)*

[*Syn. Metals*, in press]

UV photoelectron spectra were measured of *p*-phenyls (as model compounds of poly(*p*-phenylene)), poly(*p*-phenylene sulfide), poly(*p*-phenylene vinylene), beta-carotene (as a model compound of polyacetylene), and poly(dimethylsilane). Accurate values of ionization threshold and width of the uppermost valence band were determined as shown in Table 1 (which also includes the data of other polymers and the calculated results by VEH mehtod[1]), and they are discussed in relation to acceptor doping and electrical conduction.

Table I. Ionization thresholds (I_s^{th}) and the widths of the uppermost band (W) by UPS and VEH calculations (in eV)

Compound	observed		VEH	
	I_s^{th}	W	I_s^{th}	W
Poly(*p*-phenylene) (PPP)	5.65	2.0	5.6	1.8
Poly (*p*-phenylene vinylene) (PPV)	5.5	1.9	5.1	2.8
Poly (*p*-phenyle sulfide) (PPS)	6.0	1.4	6.3	1.2
Poly (*p*-xylylene) (PPX)	6.9	0	—	—
Polystyrene (PS)	6.95	—	5.9[a]	1.01
trans-Polyacetylene (PA)	5.24	5-6	4.7	6.5
beta-Carotene	5.4		—	—
Poly(dimethylsilane) (PDMS)	5.9	2.0	—	—
Polyethylene (PE)	8.5	4.0[b]		
Poly(vinyl carbazole) (PVK)	5.85	—	—	—
Polypropylene (PP)	8.5	—	—	—
Poly(vinyl chloride) (PVC)	8.8	—	—	—
1,2-Polybutadiene (1,2-PB)	7.5	—	—	—

[a] calculated energy was read from the reported $E=E(k)$ diagram

[b] total band width of two overlapping pairs of bands.

Reference

1) J. L. Brédas and G. B. Street, *J. Chem. Phys.*, **82**, 3284 (1984) and references therein.

IV-A-6 Electronic Structures of Polysilane and Poly(Dimethylsilane) Studied by Band Calculation, XPS, and UPS

Kazuhiko SEKI, Takehiko MORI, Hiroo INOKUCHI, and Kentaro MURANO *(Natl. Inst. Environmental Studies)*

The valence electronic structures of polysilane $(SiH_2)_n$ and poly(dimethylsilane) (PDMS) $(Si(CH_3)_2)_n$ were studied in comparison with polyethylene $(CH_2)_n$. Band calculations were performed for both compounds, and PDMS was also experimentally studied by X-ray photoelectron spectroscopy and UV photoelectron spectroscopy (UPS). The films of PDMS could be prepared by vacuum evaporation and such films enabled UPS measurements without sample charging.

The calculated band structures and the observed spectral features were assigned and discussed through a comparison with theoretical and experimental results for oligomers and polyethylene. In Figure 1, the XPS and UPS results are compared with the calculated density of states. Such an analysis has demonstrated how the electronic structures of these compounds are correlated through factors such as (i) change of chain length, (ii) methylation, and (iii) the substitution of Si by C. PDMS has a small ionization energy (5.9 eV) almost as low as that of poly-*p*-phenylene (5.6 eV). Such a small value comes from the combined contribution from the small electronegativity of silicon, σ-conjugation, and the inductive effect of methyl groups. The small ionization energy and the large σ-delocalization explains the reported high conductivity of PDMS and its derivatives upon acceptor doping.

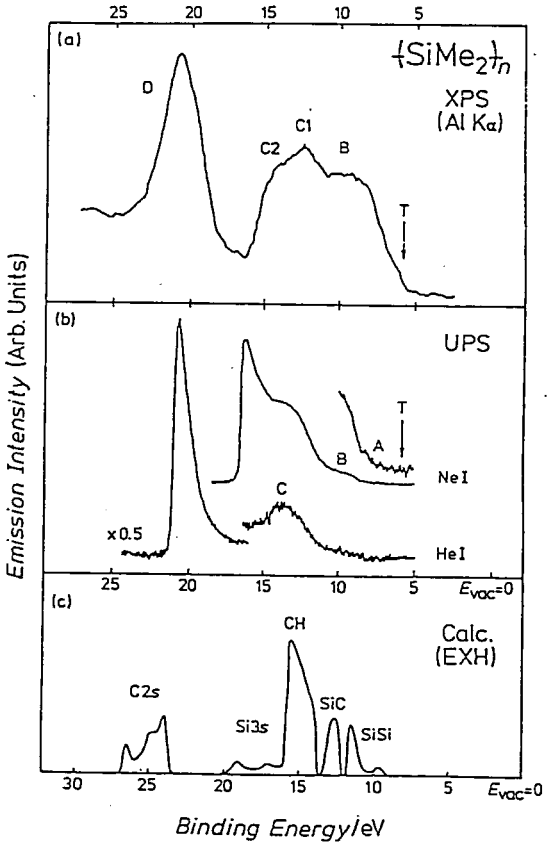

Figure 1. X-ray (a) and ultraviolet (b) photoelectron spectra of polydimethysilane solid compared with (c) the density of states deduced from extended Hückel calculation.

IV-A-7 Low-energy Electron Transmission and Secondary Electron Emission Experiments on Crystalline and Molten Long chain Alkanes

Nobuo UENO*, Kazuyuki SUGITA*, Kazuhiko SEKI, and Hiroo INOKUCHI *(*Chiba Univ.)*

[*Phys. Rev. B*, in press]

This paper describes the results of low-energy electron transmission and secondary electron emission experiments on thin films of long chain alkanes deposited on metal substrates. The spectral changes due to crystal-melt phase transition were in situ measured in both experiments. As an example, the effects of melting on the electron transmission spectra are shown in Figure 1. The ground state energy V_0 of the quasi-free electron in crystalline state was determined to be 0.5±0.1 eV. The value of V_0 for molten state was found to be negative. Further, an evidence is demonstrated for the crystalline state that there is a direct correspondence between the transmission maxima and the high-density-of-states parts in the conduction bands.

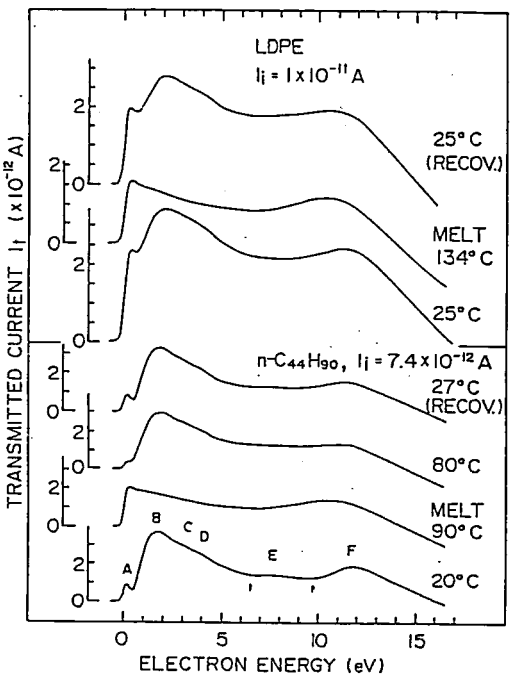

Figure 1. Low-energy electron transmission spectra for crystalline and molten staes of n-$C_{44}H_{90}$ and low-density polyethylene (LDPE). Recovered spectra by recrystallization after first melting are shown in the upper parts.

IV-A-8 Ultraviolet Photoelectron Spectroscopic Study of Perfluorinated Carboxylic Acid Monomolecular Films Prepared by Vacuum Deposition

Munehisa MITSUYA *(IMS and Hitachi Ltd.)*, **Kazuhiko SEKI, and Hiroo INOKUCHI**

Ultraviolet photoelectron spectra were measured for monomolecular films of perfluorinated carboxylic acids prepared by vacuum-deposition. Their threshold ionization potentials were determined to be 8.5 eV with their work functions being larger than those for other organic compounds. Figure 1 shows the effect of carbon number on the spectra. Escape depth of photoelectrons through the perfluorocarbon chain was evaluated to be 2.3 nm. These results are interpreted in relation to the large electronegativity of constituent fluorine atoms.

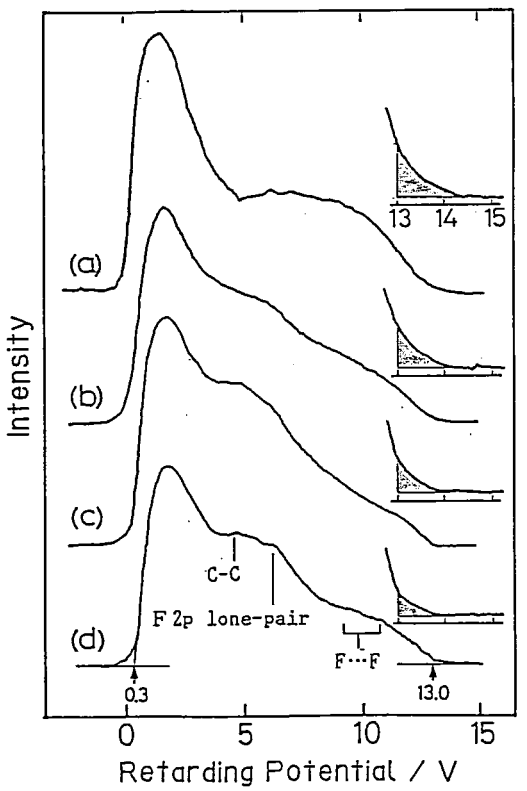

figure 1. Photoelectron spectra on the retarding potential scale, (a) Indium oxide substrate and deposited films of (b) $CF_3(CF_2)_6COOH$, (c) $CF_3(CH_2)_8COOH$, and (d) $CF_3(CH_2)_9COOH$. Incident photon energy is 21.2 eV. The hatched part is ascribed to the electron emission from the substrate.

IV-A-9 Photoemission from an Amorphous Pentacene Film

Naoki SATO *(Kumamoto Univ.)*, **Kazuhiko SEKI, Hiroo INOKUCHI and Yoshiya HARADA** *(Univ. Tokyo)*

[*Chem. Phys.*, **109**, 157 (1986)]

An amorphous pentacene film was vapor-deposited on the clean surface of a substrate at room temperature in a high vacuum. Ultraviolet photoelectron spectra of the film (Figure 1 (b)) were compared with those of a highly crystalline film deposited on a substrate at 353 K (Figure 1(a)). A larger threshold ionization potential of the amorphous film (5.15 eV) than that of the highly crystalline one (4.85 eV) was ascribed to a looser molecular packing.

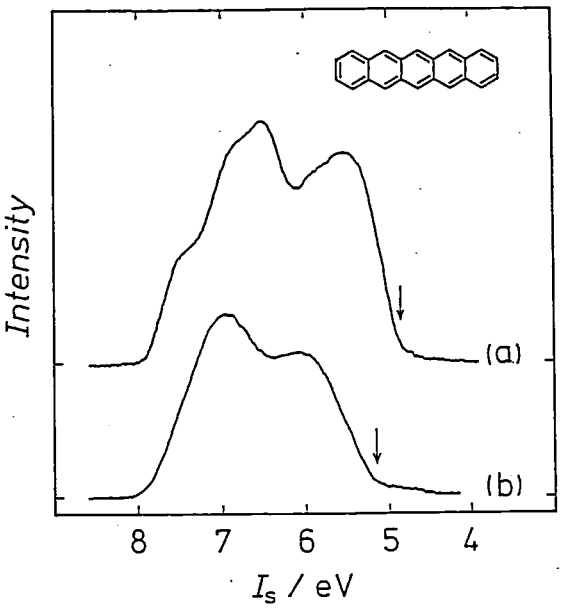

Figure 1. UP spectra of pentacene films, vapor-deposited on a clean substrate (a) at 353 K and at room temperature, measured using $h\nu$=7.75 eV light. The abscissa is the ionization potential in the solid state. The arrows indicate the thresholds determined from examining UP spectra of each film as a function of incident photon energy.

IV-A-10 UV Photoelectron Spectroscopy of Organic Molecular Materials

Hiroo INOKUCHI, Kazuhiko SEKI *(IMS and Hiroshima Univ.)*, **and Naoki SATO** *(Kumamoto Univ.)*

[*Physica. Scripta*, in press]

An overview is given on the recent progress in UPS studies of organic molecular materials, with taking the subjects chiefly from the results obtained in the authors laboratory. The materials contain molecular solids with and without strong intermolecular interactions, molecular complexes and polymers.

IV–B Electrical Conduction of Organic Solids

A series of uncapped alkyl-substituted tetrathiafluvalenes, novel type organic semiconductor, has been studied.

IV-B-1 A Novel Type of Organic Semiconductors. Molecular Fastener.

Hiroo INOKUCHI, Gunzi SAITO *(Univ. Tokyo)*, **Peiji WU, Kazuhiko SEKI, Tong Bor TANG, Takehiko MORI, Kenichi IMAEDA, Toshiaki ENOKI, Yoshiki HIGUCHI,* Koji INAKA,* and Noritake YASUOKA*** *(*Osaka Univ. and Himeji Inst. Tech.)*

[Chem. Lett. 1263 (1986)]

The electrical conductivity of alkylthio-substituted tetrathiafulvalene(TTC_n-TTF) single crystal has been measured in a vacuum of 10^{-4} Pa with the two probe method. The room temperature dark conductivity of TTC_{10}-TTF reaches 10^{-5} S cm^{-1}, a value that is extraordinarily high compared with those of other organic semiconductors constructed with a single component. The cause of this high conductivity is that the central tetrathiafulvalene skeleton has been fastened strongly with the four long alkyl chains.

IV–C Characterization of Cytochrome c_3 and Hydrogenase

AC conductivity and charge mobility of cytochrome c_3 have been measured. Recently, we succeeded to make single crystals of hydrogenase, molecualr weight 89,000, to analyse its molecular structure.

IV–D Physics and Chemistry of Graphite and its Intercalation Compounds

Graphite-alkali metal intercalation compounds absorb hydrogen chemisorptively, leading to the occlusion of hydrogen in intercalate layers. The introduction of hydrogen gives effects on the electronic and lattice properties of the compounds due to the strong electron affinity of hydrogen and the occupation of the sites by hydrogen species in the intercalate layers.

We investigate the properties of the alkali metal-hydrogen-graphite ternary intercalation compounds by means of specific heat, positron annihilation and superconductivity. (See also VII-J).

IV-D-1 Positron Annihilation in a Hydrogen-physisorbed Graphite-Ceasium Intercalation Compound.

Mizuka SANO *(Kumamoto Univ.)*, **Ikuzo KANAZAWA** *(Tokyo Gakugei Univ.)*, **Hideoki MURAKAMI** *(Tokyo Gakugei Univ.)*, **Yoshiharu SAKURAI** *(Tokyo Gakugei Univ.)*, **Toshiaki ENOKI and Hiroo INOKUCHI**

[Chem. Phys. Letters **122**, 143 (1985)]

The annihilation spectrum for CsC_{24} obtained from the Doppler broadening of 511 keV γ-radiation consists fo a narrow band superimposed on a broad band, as shown in Figure 1. Upon hydrogen physisorption at 77K, the spectral height decreased. These facts are explained in terms of an interlayer state, the electrons of which are blocked to interact with positrons through the hydrogen physisorption.

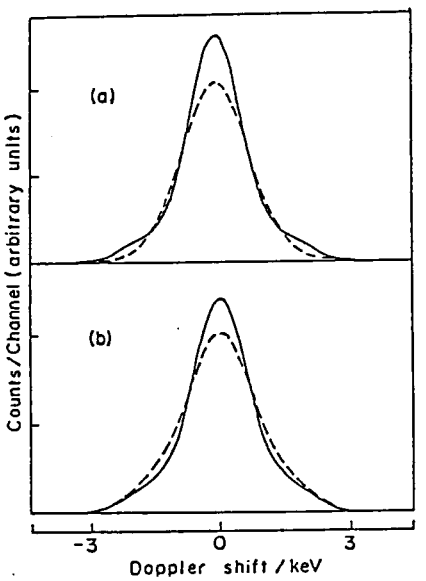

Figure 1. The deconvoluted positron-annihilatio spectra for (a) CsC_{24} at 300K, $\gamma \perp c$ (solid line) and $\gamma \parallel c$ (broken line), and (b) CsC_{24} at 77K, $\gamma \perp c$, in vacuo (solid line) and in the presence of hydrogen gas (broken line).

IV-D-2 Positron Annihilation in Graphite-Alkali Metal-Hydrogen Ternary Systems

Ikuzo KANAZAWA*, Mizuka SANO *(Kumamoto Univ.)*, **Toshiaki ENOKI, Hideoki MURAKAMI*, Yoshiharu SAKURAI* and Hiroo INOKUCHI** *(*Tokyo Gakugei Univ.)*

[Synth. Metals **12**, 225 (1985)]

Chemisorption and physisorption of hydrogen into the graphite-alkali metal intercalation compounds, KC_8 and CsC_{24}, were studied by means of positron annihilation. The changes of the annihilation spectra obtained from the Doppler-broadening, upon hydrogen-introduction to the compounds, were explained in terms of changes in the positron-electron-annihilation probability in the intercalate layers of graphite.

IV-D-3 Superconductivity in the First Stage Rubidium Graphite Intercalation Compound C_8Rb

Mototada KOBAYASHI, Toshiaki ENOKI, Hiroo INOKUCHI, Mizuka SANO *(Kumamoto Univ.)*, **Akihiko SUMIYAMA*, Yasukage ODA* and Hiroshi NAGANO*** *(*Univ. of Tokyo)*

[Synth. Metals **12**, 341 (1985)]

The superconductivity in C_8Rb has been observed in AC magnetic susceptibility and magnetization measurements with the magnetic field applied perpendicularly and parallel to the c-plane. The transition temperature T_c is found to be 26 mK. The superconducting properties are discussed in comparison with those of C_8K. Figure 1 shows the temperature dependence of the critical fields. The superconductivity in C_8Rb is found to have more 3D character than that in C_8K. The difference in T_c between C_8Rb and C_8K is mainly due to the difference in the electron-phonon coupling constant between them.

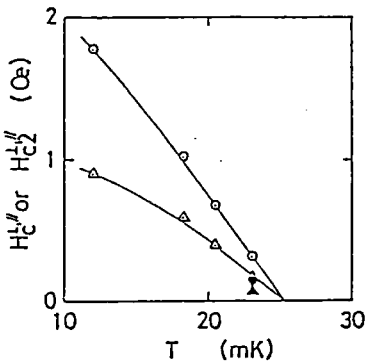

Figure 1. Temperature dependence of $H_c^{\perp}$, $H_c^{\parallel}$, $H_{c2}^{\perp}$ and $H_{c2}^{\parallel}$. The symbols ⊙ and △ denote $H_c^{\parallel}$ and $H_{c2}^{\parallel}$, respectively, and symbols ● and ▲ $H_c^{\perp}$, and $H_{c2}^{\perp}$, respectively.

IV–E Organic Metals

In an attempt to develop a novel organic superconductor and to explore the related phenomena, we prepared several new organic charge-transfer complexes, and studied their crystal structures, transport properties, and electronic structures. The complexes studied include iodine complex of TTM-TTF (tetraikis(methylthio)tetrathiafulvalene), TCNQ (tetracyanoquinodimethane) complexes of TTM-TTF and BEDT-TTF (bis(ethylenedithio) tetrathiafulvalene), and $AuBr_2^-$- and ClO_4^--complexes of BEDT-TTF (Figure).

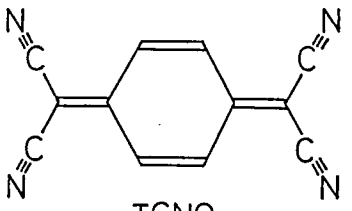

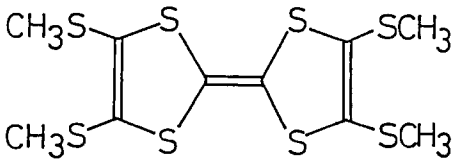

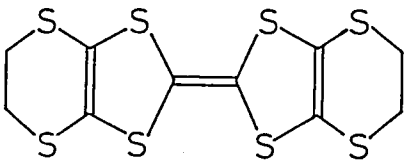

IV-E-1 Crystal Structure and Physical Properties of (TTM-TTF)$I_{2.47}$

Peiji WU *(IMS and Inst. Chem., Academia Sinica, China)*, **Takehiko MORI, Toshiaki ENOKI, Kenichi IMAEDA, Gunzi SAITO** *(Univ. Tokyo)*, **and Hiroo INOKUCHI**

[*Bull. Chem. Soc. Jpn.*, **59**, 127 (1986)]

The X-ray crystal structure analysis of a novel organic conductor (TTM-TTF)$I_{2.47}$ shows that the donors with an almost flat structure are stacked face-to-face to form columns (Figure 1). The iodine lattice composed of I_3^- columns is incommensurate with the donor lattice. The measurements of resistivity, thermoelectric power, and ESR show a metal-insulator transition around 100 K. This transition is attributed to the Peierls type of phase transition. The quasi-one-dimensional electronic structure is supported by the arrangement of the donor molecules in the crystal and the calculated anisotropy of the transfer integrals.

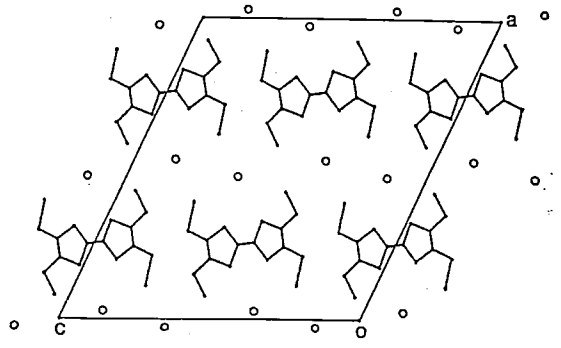

Figure 1. Crystal structure of (TTM-TTF)$I_{2.47}$

IV-E-2 Crystal Structures of TTM-TTF Complexes

Takehiko MORI, Peiji WU *(IMS and Inst. Chem., Academia Chinica, China)*, **Kenichi IMAEDA, Toshiaki ENOKI, Hiroo INOKUCHI, and Gunzi SAITO** *(Univ. Tokyo)*

[*Synth. Metals*, in press]

Crystal structures and physical properties of TTM-TTF complexes are reported. The donor TTM-TTF forms 2:1 and 1:1 complexes with TCNQ. These complexes are composed of alternating stacks in anomalous stacking sequences, DDADDA and DDAADDAA, respectively.

IV-E-3 Crystal and Band Structures of an Organic Conductor β″-(BEDT-TTF)$_2$AuBr$_2$

Takehiko MORI, Fumiko SAKAI*, Gunzi SAITO* and Hiroo INOKUCHI *(*Univ. Tokyo)*

[*Chem. Lett.*, **1986**, 1037]

An organic conductor β″-(BEDT-TTF)$_2$AuBr$_2$ is prepared and its crystal structure is determined. The structural change from superconductive β-(BEDT-TTF)$_2$X (X=I_3, IBr_2, AuI_2, etc.) and β′-(BEDT-

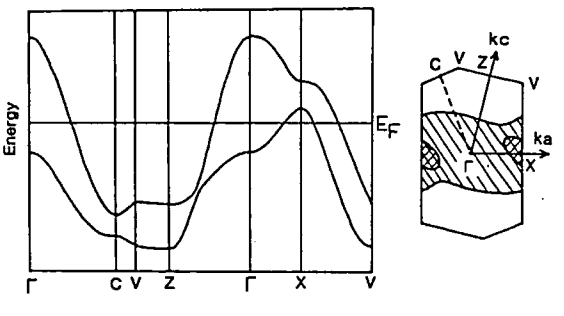

Figure 1. Energy band structure and Fermi surface of β″-(BEDT-TTF)$_2$AuBr$_2$. The shaded regions indicate hole-like parts.

$TTF)_2X$ (X=IBrCl and ICl_2) to the present β"-phase is discussed. A band structure calculation indicates that its intermolecular interaction is largest along the transverse molecular array (Figure 1).

IV-E-4 Crystal Structure and Electrical Properties of an Organic conductor δ-(BEDT-TTF)$_2$AuBr$_2$

Takehiko MORI, Fumiko SAKAI*, Gunzi SAITO*, and Hiroo INOKUCHI *(Univ. Tokyo)*

[*Chem. Lett.*, **1986**, 1589]

The crystal structure of a novel organic conductor δ-(BEDT-TTF)$_2$AuBr$_2$ is determined by X-ray analysis. This complex is essentially isostructural with δ-(BEDT-TTF)$_2$AuI$_2$ and one-dimensional along the adjacent stacks. Along this direction a two-fold superlattice is present at room temperature. The resistivity and the thermoelectric power exhibit anomalies above 320 K (Figure 1).

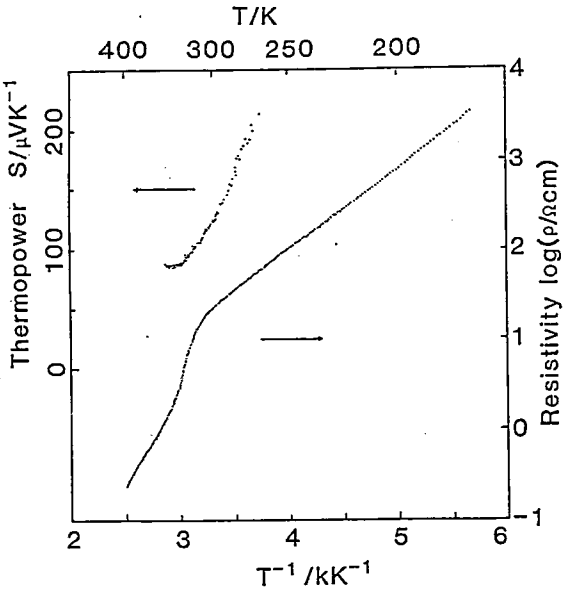

Figure 1. Electrical resistivity and thermoelectric power of δ-(BEDT-TTF)$_2$AuBr$_2$

IV-E-5 Structural and Electrical Properties of (BEDT-TTF) (TCNQ)

Takehiko MORI, and Hiroo INOKUCHI

[*Solid State Commun.*, **59**, 335 (1986)]

An organic complex (BEDT-TTF) (TCNQ) crystallizes in two different phases: the monoclinic phase and the triclinic phase. In the triclinic phase the TCNQ molecules are stacked face to face, whereas the BEDT-TTF molecules are arranged side by side along the TCNQ stacks (Figure 1). This complex undergoes a metal-semiconductor transition around 330 K. The measuremet of anisotropic thermoelectric power shows that the electron conduction on the TCNQ column is superior to the hole conduction on the BEDT-TTF only along the stacking direction of TCNQ and only above the phase transition.This result is consistent with the tight-binding band structure calculation.

In the monoclinic phase, the donors and the acceptors form alternating stacks.

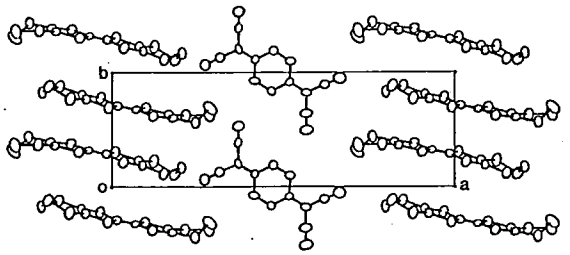

Figure 1. Crystal Structure of the triclinic (BEDT-TTF) (TCNQ), projection along the c axis.

IV-E-6 ESR Studies of Organic Conductors with Bis(ethylenedithio)tetrathiafulavalene, (BEDT-TTF)$_2$ClO$_4$(C$_2$H$_3$Cl$_3$)$_{0.5}$ and (BEDT-TTF)$_3$(ClO$_4$)$_2$, and Their Two-dimensionality.

Toshiaki ENOKI, Kenichi IMAEDA, Mototada KOBAYASHI, Hiroo INOKUCHI and Gunzi SAITO *(Univ. of Tokyo)*

[*Phys. Rev.* **B33**, 1553 (1986)]

The magnetic properties of two (BEDT-TTF)-ClO$_4$ radical salts, (BEDT-TTF)$_2$ClO$_4$(C$_2$H$_3$Cl$_3$)$_{0.5}$ and (BEDT-TTF)$_3$(ClO$_4$)$_2$, have been investigated by means of ESR measurement. For the former (2:1:0.5) phase crystal, as shown in Figure 1, the susceptibility shows a nesting transition at 20K, which is affected by the degree of the incompleteness in the ordering of the C$_2$H$_3$Cl$_3$ molecules below 200K. The large linewidth suggests two-dimensionality, consistent with the low T_c of the nesting instability and the small anisotropy in the resistivity in the ac plane. In the case of the latter (3:2)

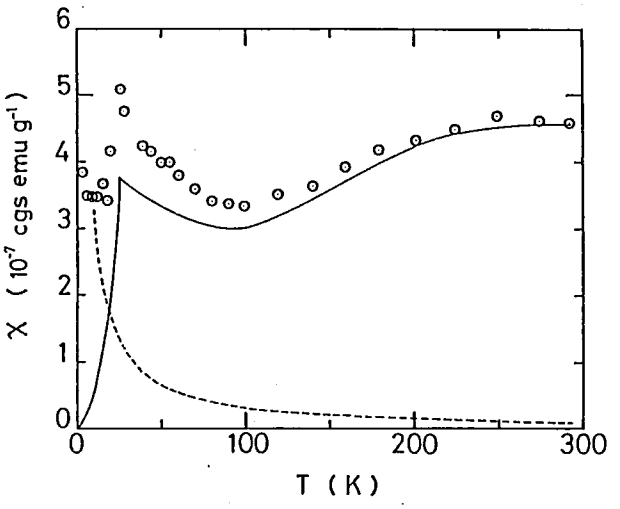

phase crystal, the susceptibility shows a metal-insulator transition at 150K. Below T_c, and insulating state with a spin singlet is stabilized after the displacement of the BEDT-TTF molecules in one-dimensional chain through the Peierls instability. The large linewidth also suggests two-dimensionality.

Figure 1. Temperature dependence of the ESR intensity of the (2:1:0.5) phase for a slow cooling. The solid line is obtained after the subtraction of the Curie tail at low temperatures. The Curie susceptibility is shown by the dash line.

IV-F Studies of Ion-Molecule Reactions by a Threshold Electron-Secondary Ion Coincidence (TESICO) Technique

The knowledge of the microscopic reaction cross sections for evolution of a system in a single reactant quantum state (translational, rotational, vibrational, and electronic) to a single product quantum state is essential for a complete understanding of a chemical reaction. Ion-Molecule reactions are particularly suited for studying such microscopic cross sections since ions can readily be prepared in various internal states in the initial ionization processes, such as photoionization, and the emitted photoelectrons provide information on the distribution among these states.

In this project, we study state-selected ion-molecule reactions by the use of a photoionization technique which utilizes the threshold photoelectron-secondary ion coincidence. The technique allows direct determination of (i, v), i.e. the reaction cross section as a function of the internal and collisional energies of reactants. The selection of electronic, vibratinal, rotatinal, and fine-structure states are possible by this technique.

IV-F-1 Reinvestigation of the State Selected Ion-Molecule Reactions $O_2^+(v)+CH_4$

Kenichiro TANAKA, Tatsuhisa KATO, and Inosuke KOYANO

[*J. Chem. Phys.*, **84**, 750(1986)]

Vibrational state selected reaction cross sections have been determined for v=0−3 of the O_2^+ ion, for each of the three product channels of the reaction $O_2^+(v)+CH_4$, viz.

$$O_2^+(v)+CH_4 \rightarrow CH_3O_2^+ + H \quad (1)$$
$$\rightarrow CH_3^+ + HO_2 \quad (2)$$
$$\rightarrow CH_4^+ + O_2, \quad (3)$$

using the TESICO technique.[1] Figure 1 summarizes the experimental results. At a fixed collision energy of 0.27 eV, it has been found that the cross section of exoergic channel (1) increases most prominently with increasing vibrational quantum number v in the range v=0−2, but decreases sharply in going from v=2 to v=3. The cross sections of endoergic channels (2) and (3) also increase with increasing v but their rates of increase are much smaller than that of channel (1) in the range v=0−2. When v is increased to 3, however, charge transfer channel (3) is enhanced dramatically and the CH_4^+ ion becomes the most abundant product ion. The cross section of channel (2) also increases more sharply in going from v=2 to v=3 than in the range v=0−2, but the CH_3^+ ion still remains the least abundant of the three product ions.

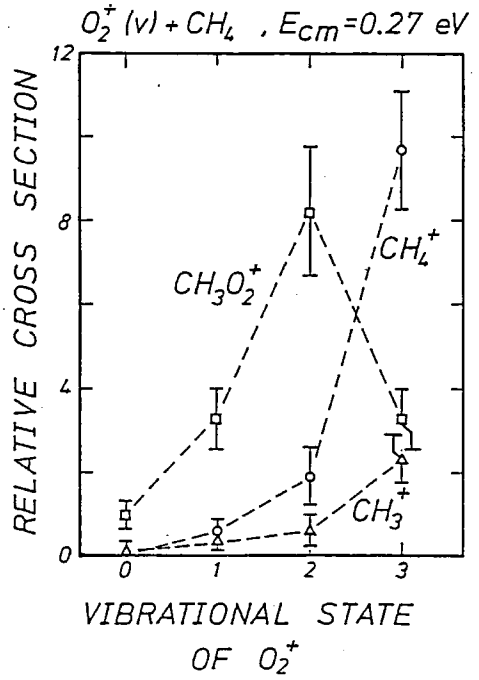

Figure 1. State selected cross sections for reactions (1)-(3).

Reference

1) I. Koyano and K. Tanaka, *J. Chem. Phys.*, **72**, 4858 (1980).

IV-F-2 Vibrational State Dependence of the Charge Transfer and Rearrangement Cross Sections in the Reaction $H_2^+(HD^+)+N_2$

Shinzo SUZUKI and Inosuke KOYANO

In a previous study,[1] we found that the cross section for the charge transfer channel of the reaction $D_2^+ + N_2$ oscillates as a function of the vibrational quantum number v of the D_2^+ ion, whereas that for the rearrangement channel (producing N_2D^+) is almost independent of v. In order to examine whether this seemingly interesting phenomenon reflects some inportant dynamical aspects of this system or simply is a result of accidental energy resonances and/or favorable Franck-Condon factors between the reactant and product states, we have performed similar state selected studies of the reactions $H_2^+ + N_2$ and $HD^+ + N_2$. Figure 1 shows the result for the $H_2^+ + N_2$ reaction at a center-of-mass collision energy of 2.5 eV. It is seen that, although the charge ransfer cross section exhibits a resonance-like enhancement at v=1 and an indication of another enhancement at v=5, the oscillatory structure does not exist in this system. On the other hand, the cross section for the rearrangement channel is almost independent of v, as in the $D_2^+ + N_2$ reaction. Similar results were obtained at other collision energies studied, as well as in the $HD^+ + N_2$ reaction. A model calculation indicated that all these results are interpreted in terms of the energy defects and Franck-Condon factors between the reactant state and each of the energetically attainable product states.

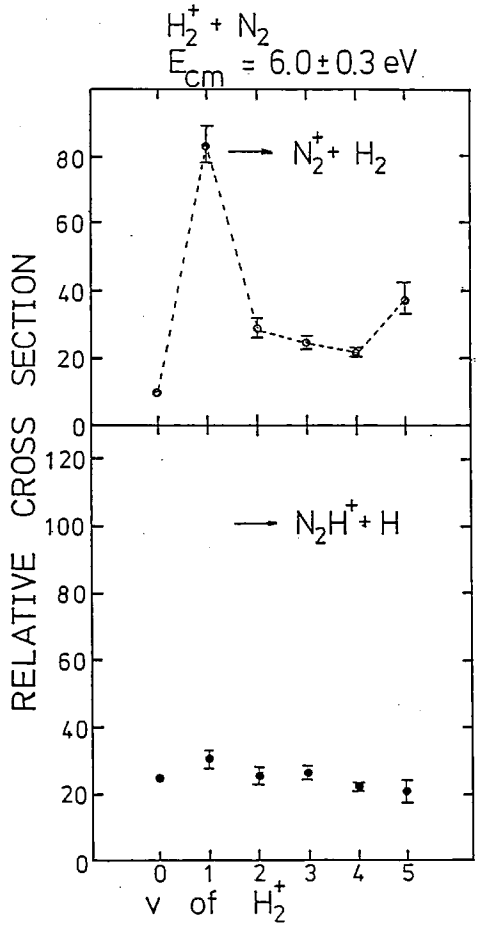

Figure 1. Cross sections for the reactions $H_2^+ + N_2 \rightarrow H_2 + N_2^+$, $N_2H^+ + H$ as a function of the vibrational quantum number of H_2^+

Reference

1) K. Tanaka, T. Kato, and I. Koyano, *IMS Ann. Rev.* 83 (1984).

IV-F-3 Vibrational Energy Dependence of the Microscopic Mechanism Branching in the Reaction $CH_3Cl^+ + CH_3Cl \rightarrow CH_4Cl^+ + CH_2Cl$

Shinzo SUZUKI and Inosuke KOYANO

Ion-molecule reactions of the type $MH^+ + MH \rightarrow MH_2^+ + M$ in general have three possible microscopic reaction mechanisms, i.e., direct proton transfer and hydrogen atom transfer mechanisms, and an intermediate complex formation. In the present study, we succeeded in distinguishing the former two mechanisms in the reaction $CH_3Cl^+ + CH_3Cl \rightarrow CH_4Cl^+ + CH_2Cl$ by means of the TESICO technique[1] and determined the relative cross section for each of them as a function of the vibrational energy of the reactant.

Figure 1 shows TOF coincidence spectra for the reactant (CH_3Cl^+) and product (CH_4Cl^+) ions, which were obtained at the collision energy of 3.6 eV. It can be seen that the TOF spectrum of the product ion consists of two peaks. Based on a comparison between the measured and calculated TOF's of both the parent and product ions, it is concluded that the product peak of the shorter TOF corresponds to the H-atom transfer mechanism and that of the longer TOF corresponds to the H^+ transfer mechanism. The measurements of the internal-energy selected cross sections showed that the H^+ transfer cross section decreases with increasing vibrational energy at low collison energies.

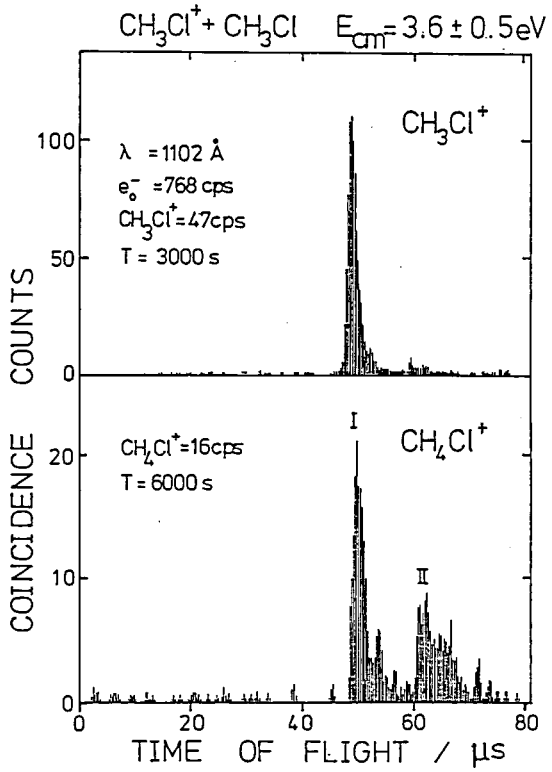

Figure 1. TOF coincidence spectra for the reactant (CH_3Cl^+) and product (CH_4Cl^+) ions at the collision energy of 3.6 eV.

Reference

1) I. Koyano and K. Tanaka, *J. Chem. Phys.* **72**, 4858 (1980).

IV-F-4 Internal Energy Dependence of the Relative Cross Section and Mechanism Branching of the Reaction $CH_4^+(v) + CH_4 \rightarrow CH_5^+ + CH_3$ and its Isotopic Variants

Zdenek Herman *(J. Heyrovsky Inst. of Phys. Chem. and Electrochem.)*, **Kenichiro TANAKA, Tatsuhisa KATO, and Inosuke KOYANO**

[*J. Chem. Phys.* **85**, 5705(1986)]

Total cross sections of the title reaction studied at collison energies 0.6–3 eV by the TESICO method were found to decrease by about 1.6 times as the internal energy of the reactant ion is increased from 0.1 to 1 eV. Branching ratios of collisional mechanisms were derived from isotope labelling studies: with decreasing total initial energy (sum of colision energy and reactant ion internal energy) from 4 to 0.9 eV the fraction of the dominant proton transfer mechanism slightly decreases, the fraction of H-atom transfer is almost constant, and the fraction of intermediate complex formation increases from about 5 to 15%. Signifi-

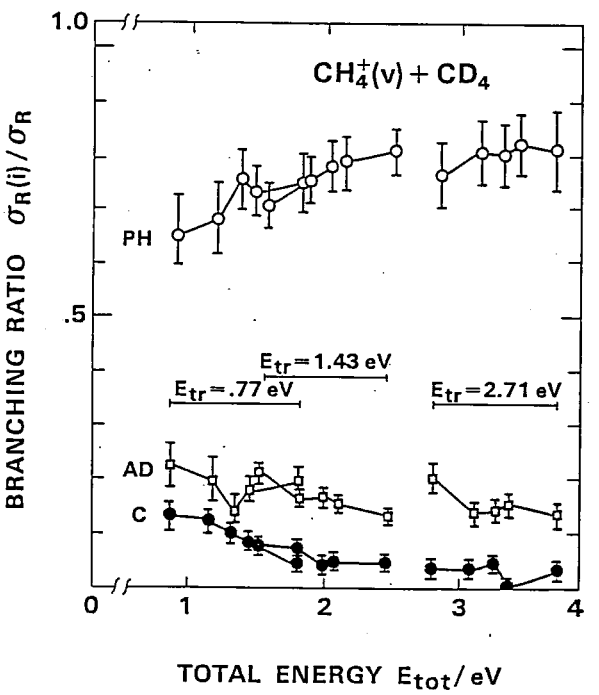

Figure 1. Mechanism branching ratio for the system $CH_4^+(v) + CD_4$ in dependence on the total energy E_{tot}. PH: proton transfer, AD: D-atom transfer, C: intermediate complex formation.

cant isotope effects were observed in the impulsive proton and H-atom transfer mechanisms depending on whether the transferred particle was H or D. The charge transfer channel represents about 10–50% of the chemical reaction channel. Experimental results for the $CH_4^+ + CD_4$ system are shown in Figure 1.

IV-F-5 Vibrational State Dependence of the Cross Sections in the Reaction $C_2D_2^+(v_2)+H_2$

Kenji HONMA *(Univ. of Tokyo)*, **Kenichiro TANAKA, and Inosuke KOYANO**

Vibrational-state selected reaction cross sections have been measured for three product channels of the reaction $C_2D_2^+(v_2)+H_2$, by use of the TESICO technique. The v_2 vibrational states of the $C_2D_2^+$ ion were selected up to v=2 and the collision energies were changed from 0.1 to 2.0 eV. Experimental results are summarized in Figure 1. At low collision energies up to 0.2 eV, considerable enhancement of the cross sections for the channel producing $C_2D_2H^+$ was observed when the vibrational quantum number was increased successively. As the collision energy was increased, the extent of this enhancement diminished gradually and the cross section became almost independent of v at 2.0 eV. The cross section for the H/D exchange channel, on the other hand, was found to decrease with increasing vibrational quantum number at low collision energies. The latter cross section also became independent of v at high collision energies. These results have been explained in terms of the formation of an intermediate complex and the statistical decomposition of this complex to products.

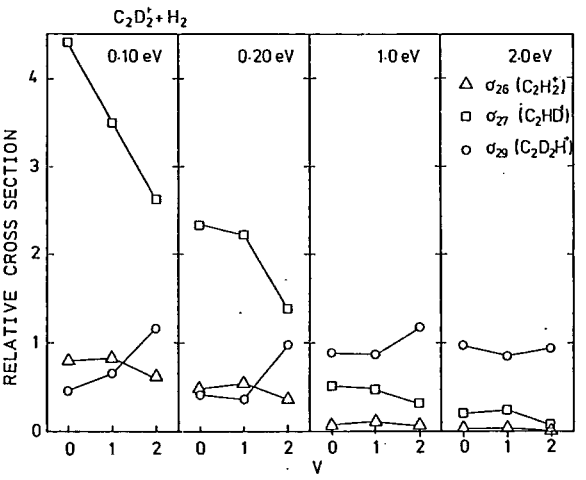

Figure 1. State selected (relative) cross sections for the three product channels (forming $C_2H_2^+$, and $C_2D_2H^+$) of the reaction $C_2D_2^+ + H_2$.

IV–G Photoionization Processes in Small Molecules

Two techniques have generally been used for the study of molecular photoionization processes, i.e., measurements of photoionization efficiency curves (PIEC) and photoelectron spectra (PES). While PIEC yields a wealth of information on the ionization processes and energy levels of ions and neutral molecules, difficulty is often encountered with this technique when autoionization obscures the step structure of the curve. In such a situation, we often resort to PES which provides precise locations of ionic states and transition probabilities of these states. However, ionic states that can be studied by the ordinary (constant wavelength) PES are largely limited to the states which combine with the ground states of the parent molecule with favorable Franck-Condon factors. Another type of photoelectron spectroscopy is the threshold electron spectroscopy (TES) which uses a variable wavelength light source and detects only the zero kinetic energy photoelectrons (threshold electrons). In this method, ionic states which are not favored by direct ionization are often observed through resonance autoionization.

In this project, we study photoionization processes in small molecules by simultaneous measurements of photoionization efficiency curves and threshold electron spectra. Furthermore, we find that the analysis of autoionizing transitions is often possible utilizing charge-transfer processes of the product ions. This technique is also incorporated.

IV-G-1 Threshold Electron Spectra of Some Small Molecules over the Wavelength Range 35–120 nm Using Synchrotron Radiation

Shinzo SUZUKI, Shin-ichi NAGAOKA, and Inosuke KOYANO

[*Z. Physik D*, **4**, 111(1986)]

The TEPSICO-II apparatus at the UVSOR electron storage ring and its primary objectives have been described previously.[1,2] with these objectives in mind, we have studied in the present paper the threshold electron spectra of several small molecules in the wavelength range 35–120 nm. Molecules studied include diatomic molecules H_2, N_2, NO, and O_2 and polyatomic molecules CH_3Cl, CH_3Br, GeH_4, $GeCl_4$, $Sn(CH_3)_4$, and $Pb(CH_3)_4$. The extended wavelength range utilized here yielded new information on the inner-valence and core levels of some molecules. As an example, we show in Figure 1 the spectrum of CH_3Cl in the 40–120 nm range. It is seen that, in addition to the intense valence bands labeled A, B, and C, the fourth band labeled S is excited in this range. Although the corresponding peaks in ethyl and higher alkyl chlorides have been observed in the HeI PES, the band in methyl chloride was observed here for the first time. This should correspond to the removal of an inner valence electron. In molecules containing Ge, Sn, and Pb, many peaks corresponding to the ionization of a (n−1)d core electron, where n is the principal quantum number of the valence shell of these elements, were observed, as well as those corresponding to the inner-valence ionization.

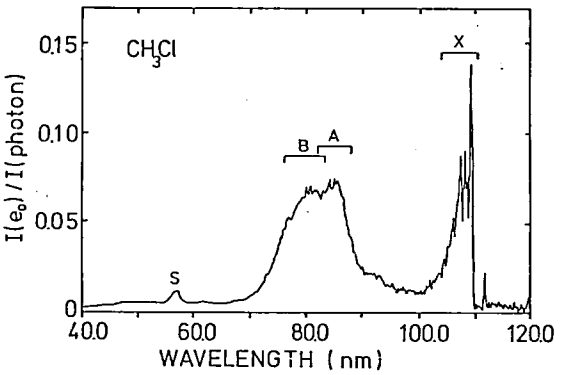

Figure 1. Threshhld electron spectrum of CH_3Cl in the range 40–120 nm.

References

1) I. Koyano, K. Tanaka, T. Kato, S. Suzuki, and E. Ishiguro, *Nucl. Instrum. Meth.*, **A 246**, 507(1986).
2) K. Tanaka, T. Kato, and I. Koyano, *IMS Ann. Rev.*, 85(1984).

IV–H Studies of Unimolecular Decomposition of Complex Molecular Ions

The TESICO technique which we have developed for the study of state selected ion-molecule reactions (see IV-F) is also applicable to the study of unimolecular decomposition of molecular ions. In this technique ions can be prepared with defined amounts of internal energy and their subsequent decomposition investigated. In addition, by comparing the decomposition pattern of the state selected ions with product distribution of appropriate ion-molecule reactions, we can obtain information on the nature of the intermediate collision complex of ion-molecule reactions.

IV-H-1 Unimolecular Decomposition: Fragmentation of n-$C_4H_{10}^+$

Takae TAKEUCHI *(Nara Women's Univ.)*, **Masao YAMAMOTO** *(Nara Women's Univ.)*, **Shinzo SUZUKI, Kenichiro TANAKA and Inosuke KOYANO**

The threshold electron-secondary ion coincidence(TESICO) technique[1] was used to investigate gas-phase unimolecular reactions of excited ions with known internal energy. Figure 1 shows the breakdown curves for molecular and fragment ions of n-butane. The fractional intensities of the observed ions are plotted as a function of the energy absorbed by the parent molecule. From the experimental result, the following scheme can be considered.

n-$C_4H_{10}^{+\cdot}$ → iso-$C_3H_7^+$

n-$C_4H_{10}^{+\cdot}$ → $C_3H_6^{+\cdot}$

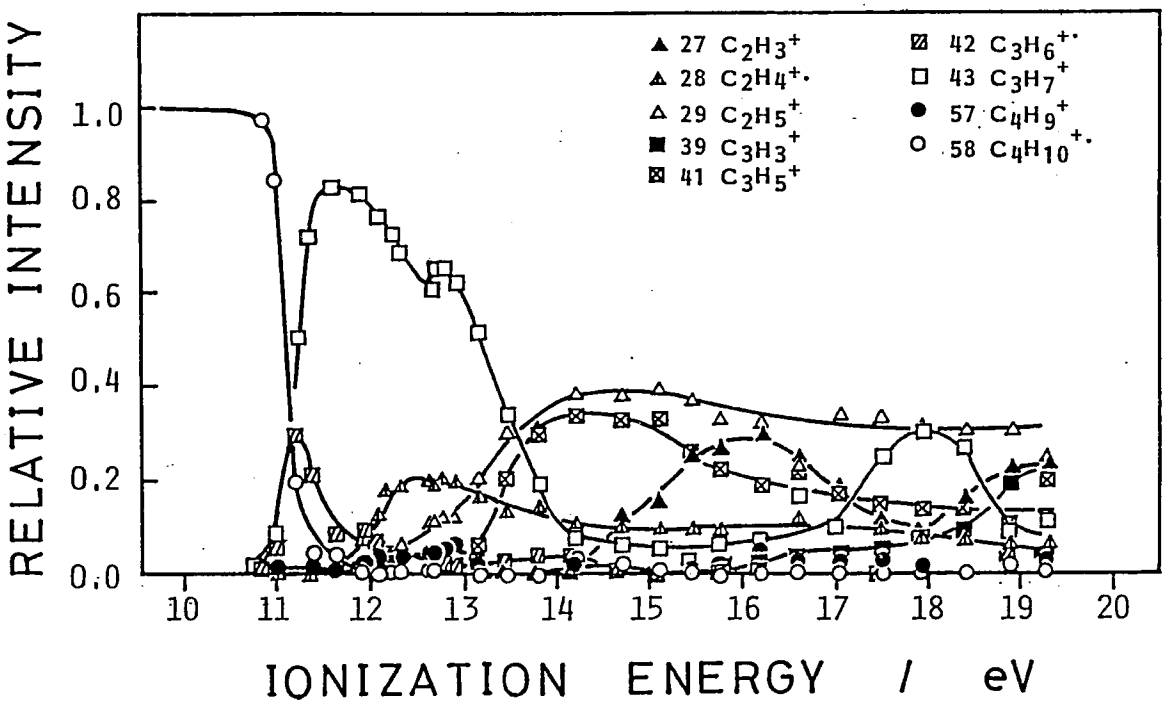

Figure 1. Breakdown curves for molecular and fragment ions from n-butane.

$n\text{-}C_4H_{10}^{+\cdot *} \rightarrow C_2H_5^+ \rightarrow C_2H_3^+$

$n\text{-}C_4H_{10}^{+\cdot *} \rightarrow n\text{-}C_3H_7^+ \rightarrow C_3H_5^+ \rightarrow C_3H_3^+$ (12–17 eV)

$n\text{-}C_4H_{10}^{+\cdot *} \rightarrow n\text{-}C_3H_7^+$

$n\text{-}C_4H_{10}^{+\cdot **} \rightarrow n\text{-}C_3H_7^+$ (>17 eV)

In the breakdown graph of the n-butane ion, the $C_3H_7^+$ and $C_2H_3^+$ ions appear again with substantial fractional abundance (about 30%) after their first intense peaks once declined. In particular, the curve for the $C_3H_7^+$ ion has three peaks. The peaks at 11.5 and 13 eV would probably correspond to the iso-$C_3H_7^+$ and n-$C_3H_7^+$ ion, respectively. An explanation which may account for the reapperance of the $C_3H_7^+$ ion at 18 eV is the occurrence of an isolated (non-interconverting) electronic state of the molecule at this energy.

Reference

1) I. Koyano, K. Tanaka, *J. Chem. Phys.*, **72**, 4858(1980).

IV-H-2 A PIPECO Study of Unimolecular Decomposition of the $C_2H_2D_2^+$ ions produced from three $C_2H_2D_2$ isomers

Kenji HONMA *(Univ. of Tokyo)*, **Kenichiro TANAKA, Shinzo SUZUKI, and Inosuke KOYANO**

Product distributions of unimolecular decomposition of the $C_2H_2D_2^+$ ions have been studied as a function of internal energy of these ions using a threshold electron-photoion coincidence technique. The $C_2H_2D_2^+$ ions were produced by photoionization of the three isomers of $C_2H_2D_2$, i.e., ethylene-1,1-d_2, ethylene-cis-1,2-d_2, and ehtylene-trans-1,2-d_2. No remarkable difference in the product distribution has been observed among the three isomers, indicating that the $C_2H_2D_2^+$ ions from all sources assume a common structure prior to dissociation. Comparison of the results with a QET calculation indicated that the decomposition is statistical and energy and H/D atoms are completely randomized prior to decomposition The results were also compared with the product distributions of the reactions $C_2H_2^+ + D_2$ and $C_2D_2^+ + H_2$ in order to obtain information on the dynamics of these reactions. The result suggested that both reactions proceed via an intermediate complex, at least at low collision energies.

IV–I Investigation of Ionic Fragmentation Following Core Level Ionization in the Vapor Phase Using Synchrotron Radiation

Shallow valence level ionization and subsequent fragmentation of molecules have been studied extensively using various kinds of light source in recent years. However, the investigation of processes following core level excitation have not been so extensive, because, for the purpose of such investigation, the conventional light sources are insufficient both in photon energy and intensity. Synchrotron radiation is expected to provide a powerful means to obtain information about the core level excitation. In contrast to the case of the valence electrons delocalized over the molecule, the core electrons in a molecule are localized near the atom to which they belonged originally. As a result, the photoionization from the core level is expected to produce dissociation pathways quite different from those following photoionization from the valence level.

IV-I-1 Production of Bare Pb^+ Ion Following 5d Core Photoionization of Tetramethyllead as Revealed by a Coincidence Experiment.

Shin-ichi NAGAOKA, Shinzo SUZUKI, Inosuke KOYANO

Volatile compounds with group IV elements are particularly suitable for detailed investigations of ionic fragmentation following core level ionization in the vapor phase, because the rather small binding energies of the (n−1)d core levels allow the studies in the normal incidence region of the vacuum ultraviolet. Accordingly, we have initiated the studies of the core level excitation and subsequent fragmentation in such compounds.

In the present subject, ionic fragmentation following 5d core level ionization of tetramethyllead has been studied using synchrotron radiation. In the wavelength range between 44 and 72 nm, photoionization from the Pb 5d core levels is observed. The amount of Pb^+ ions produced increases above the 5d core edge, while those of other fragments decrease. Figure 1 shows the state selected efficiency of ion production from tetramethyllead as obtained by the threshold electron – photoion coincidence technique. It is shown that the bare Pb^+ ion is predominantly produced following 5d photoionization. It is suggested that the dynamic processes following the core level ionization are quite different from those following valence level ionization.

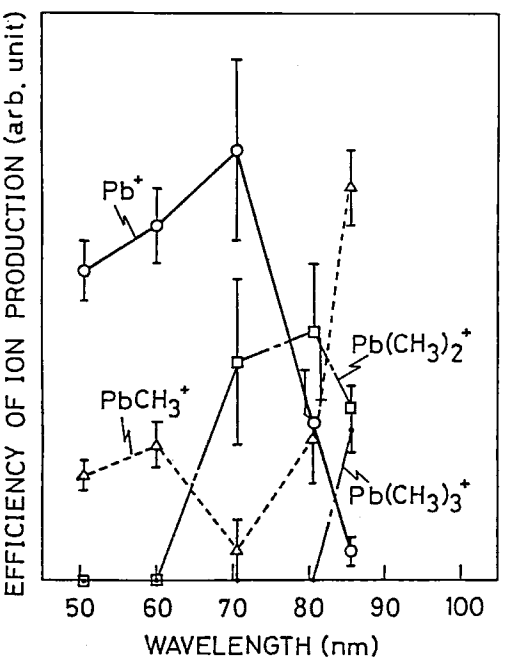

Figure 1. State selected efficiency of ion production for Pb^+ (○), $PbCH_3^+$ (△), $Pb(CH_3)_2^+$ (□), and $Pb(CH_3)_3^+$ (●). The data are normarized by threshold electron intensities.

IV–J Application of Excited-State Photoelectron Spectroscopy to Photophysics and Photochemistry

To study dynamic behavior of excited-state molecules in the gas phase, excited-state photoelectron spectroscopy using resonant multiphoton ionization or two-step ionization has been developed with pulse UV/visible lasers in this Institute since 1980 [IMS Annual Review (1980-85)]. Such laser photoelectron spectroscopy is a powerful tool for studying photochemical and photophysical behaviors of excited states, providing new information about the excited

states which cannot be obtained by other spectroscopic methods. In this project we have further applied our technique to various molecular systems in jets.

IV-J-1 Laser Photoelectron Spectroscopic Determination of Electronic States of Fe Atoms Produced in Multiphoton Dissociation of $Fe(CO)_5$ in the Gas Phase

Yatsuhisa NAGANO, Yohji ACHIBA, and Katsumi KIMURA

[*J. Chem. Phys.*, **84**, 1063 (1986)]

By irradiating a gaseous $Fe(CO)_5$ sample by a visible dye laser, a complicated ion-current spectrum has been obtained, showing many sharp peaks in the laser wavelength region 446–452 nm. From mass spectra observed at these ion-current peaks, it has been indicated that Fe atoms are mainly produced. In order to identify the electronic states of Fe atoms thus produced, photoelectron kinetic-energy spectra were measured at more than thirty ion-current peaks. From the present photoelectron energy analysis, we have been able to identify the electronic states of the Fe atoms up to the fifth electronic term (a $^3P2$). In this paper we demonstrate for the first time that the laser photoelectron spectroscopic technique makes it possible to identify electronic states of atomic species produced by photodissociation.

IV-J-2 UV Multiphoton Dissociation of Volatile Iron Complexes, as revealed by MPI Ion-Current and Photoelectron Spectroscopy

Yatsuhisa NAGANO, Yohji ACHIBA, and Katsumi KIMURA

[*J. Phys. Chem.* **90**, 1288 (1986)]

Gas-phase multiphoton ionization (MPI) ion-current spectra were measured in the laser wavelength region 366.5–370.0 nm for several volatile iron complexes such as (a) ferrocene $Fe(Cp)_2$, (b) iron pentacarbonyl $Fe(CO)_5$, (c) iron triacethylacetonate $Fe(Acac)_2$, and (d) iron trichloride $FeCl_3$. Remarkable differences were found in the ion-current spectra among these complexes as shown in Figure 1 (a–b).

Photoelectron Kinetic-energy spectra were measured at various MPI ion-current peaks to study the origin of these peaks. Several examples of photoelectron spectra are also shown in Figure 1 (e–h). From photoelectron spectra it was found that all these ion-current spectra are due to two- or three-photon ionizations of Fe atoms. It has also been found that $Fe(Cp)_2$ and $Fe(CO)_5$ provide two extreme cases of producing Fe atoms in the multiphoton dissociation. The Fe atoms produced form $Fe(Cp)_2$ are populated mostly in the ground state, whereas those produced from $Fe(CO)_5$ are distributed among various electronic excited states up to 3 eV. In this paper the mechanism of the formation of excited Fe atoms is discussed. It is also concluded that the extent of distribution of excited Fe atoms largely depends on the energy transfer taking place from the molecular electronic excited state to the ligands during fragmentation.

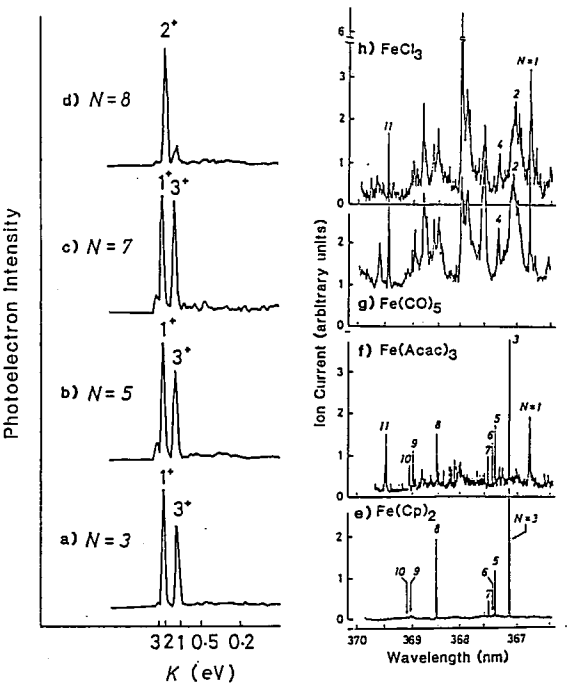

Figure 1. MPI ion-current spectra (a–d) and several typical photoelectron spectra (e–h). The Fe complexes studied are (a) $Fe(Cp)_2$, (b) $Fe(Acac)_3$, (c) $Fe(CO)_5$, and (d) $FeCl_3$. The numbers in the spectra (a–d) indicate the MPI ion-current lines or peaks at which photoelectron spectroscopic measurements were carried out. The photoelectron spectra shown here were obtained at the MPI ion-current lines (N=3, 5, 7, and 8) of $Fe(Cp)_2$. The photoelectron bands corresponding to the ionic states are indicated by 1^+, 2^+, and 3^+.

IV-J-3 Photoelectron Spectroscopic Interpretation on Background Signal Observed in Multiphoton Ionization Ion-Current Spectrum of Iron Pentacarbonyl

Yatsuhisa NAGANO, Yohji ACHIBA, and Katsumi KIMURA

[*J. Phys. Chem.* **90**, 615 (1986)]

Under moderate laser irradiating conditions, a significant background signal has been observed in the multiphton ionization (MPI) ion-current spectra of $Fe(CO)_5$ in the gas phase in the laser wavelength region 360–400 nm. In order to clarify the origin of the ion-current background, photoelectron kinetic-energy measurments have been carried out at three laser wavelengths at which only the ion-current background signal is observed. From an energy analysis of the phtoelectron specra, it has been concluded that the observed background ion-current signal is attributed to two-photon ionizations of Fe atoms populated in various low-lying electronic states. The two-photon ionizations are considered to be non-resonant, since the background signal is quite insensitive to the change in the laser wavelength. The present work provides the first direct evidence for the origin of the background signal in the MPI spectrum of $Fe(CO)_5$. Probably similar situations occur in MPI ion-current spectra of many other transient metal complexes.

IV-J-4 Excited-State Photoelectron Spectra of the One-Photon Forbidden C $^3\Pi_g$ Rydberg State of Molecular Oxygen

Shunji KATSUMATA *(Hokkaido Univ.)*, **Kenji SATO, Yohji ACHIBA, and Katsumi KIMURA**

[*J. Electron Spectrosc.*, in press]

The Rydberg C $^3\Pi_g$ state of molecular oxygen, which is one-photon forbidden from the ground electronic state, has been studied by means of (2+1) MPI ion-current and photoelectron spectroscopic techniques in the laser wavelength region 287-289 nm. The excited-state photoelectron spectra observed here at different rotational levels of the C $^3\Pi_g$ $v'=2$ state of O_2 are shown in Figure 1, indicating marked deviation from the Franck-Condon distribution generally expected in ionization of Rydberg electrons. Namely, in addition to main photoelectron peaks due to $\Delta v=0$ transitions, other vibrational peaks were also observed with considerable intensities. The $v^+=2$ photoelectron peak shows different angular dependence from the other vibrational peaks. The rotational structure in the MPI ion-current spectrum of O_2 has been well interpreted in terms of the rotational constants of the X $^2\Pi_g$ ground electronic state of O_2^+.

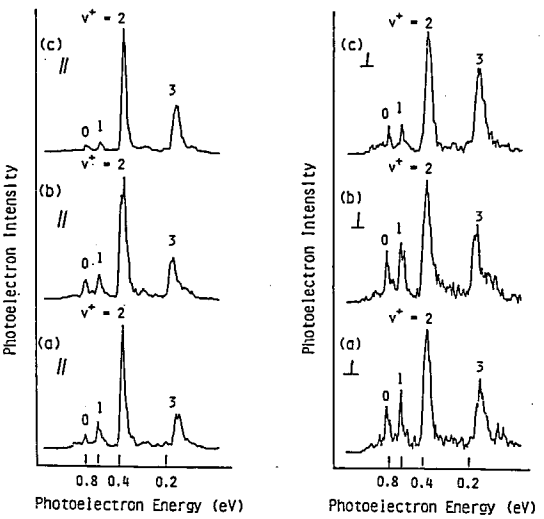

Figure 1. Photoelectron spectra obtained here at three laser wavelengths (a) 288.25 nm, 287.90 nm, and (c) 287.46 nm, measured at the directions parallel and perpendicular to the laser polarization vector.

IV-J-5 Photoelectron Spectroscopic Evidence for Competition of Ionization and Internal Conversion at the S_2 Excited State of Trimethylamine

Hiroyasu SATO,* Masahiro KAWASAKI,* Kenzo TOYA* *(*Mi'e Univ.)*, **Kenji SATO, and Katsumi KIMURA**

When photoionization occurs at a specific excited state in competition with some intramolecular relaxation such as internal conversion and intramolecular vibrational redistribution, photoelectrons can be ejected from relaxed states as well as from the optically prepared excited state under appropriate laser irradiating conditions. The molecule in the initially prepared state is either ionized directly with the rate constant $I\sigma_i$ (I: the laser fluence, σ_i: the ionization cross section), or relax to another state, and then ionized. In such a case, the change in the laser fluence will vary the relative signal intensities associated with these two ionization

processes.

In the present work, laser photoelectron energy measurements in a molecular beam of trimethylamine were carried out at the laser wavelengths 192.1, 208.8, 228.7, and 252.7 nm. The photoelectron spectra thus obtained are shown in Figure 1. It has been found that the photoelectron spectra observed at 192.1 and 208.8 nm can be attributed to two ionization processes competing with each other: One is from the optically prepared S_2 state, and the other from the vibrationallly excited S_1 state ($S_1^{\ddagger}$) produced from the internal conversion $S_2^* \rightsquigarrow S_1^{\ddagger}$.

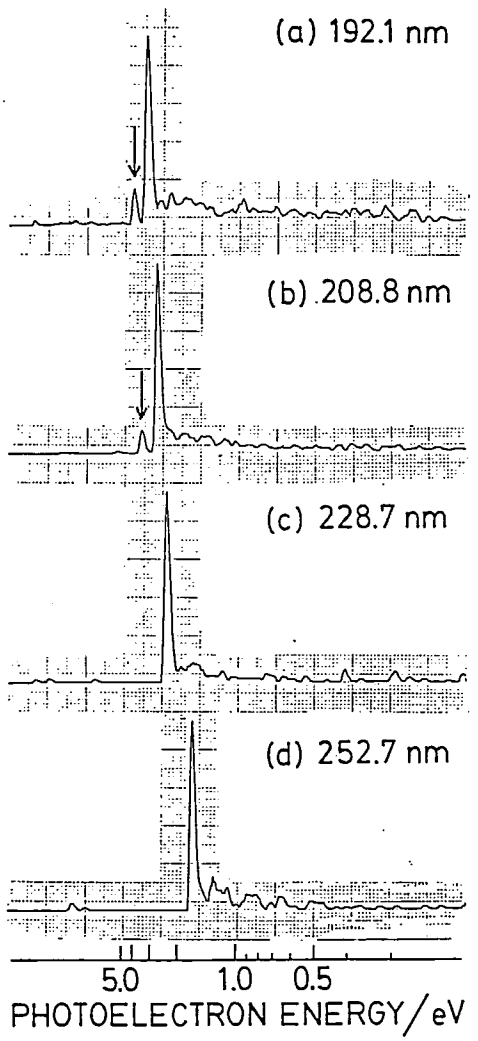

Figure 1. Excited-state photoelectron spectra of timethylamine, obtained with a time-of-flight electron analyzer. The weak peaks indicated by arrows correspond to the ionizations which occur from vibrationally excited S_2 levels, while the main peaks correspond to the ionizations which occur from vibrationally excited S_1 levels produced by the internal conversion $S_2^* \rightsquigarrow S_1^{\ddagger}$.

IV-J-6 Molecular Dynamic Photoelectron Spectroscopy Using Resonant Multiphoton Ionization for Photophysics and Photochemistry

Katsumi KIMURA

[*Int. Rev. Phys. Chem.*, in press]

Photoelectron spectra of resonant multiphoton ionization of gaseous molecules are regarded as 'photoelectron spectra of the resonant intermediate excited states'. Therefore, such a technique using a tunable pulse UV/visible laser makes it possible to observe excited-state photoelectron spectra for various molecules and molecular complexes in the gas phase. Molecular nonradiative elctronic states for which direct observation is difficult by fluorescence spectroscopy can be studied by this technique. With this technique, it is possible to study not only static aspects but also dynamic aspects of various molecular excited states from a photoelectron spectroscopic point of view. In this sense, such photoelectron spectroscopy may be called 'dynamic photoelectron spectroscopy'. This is in striking contrast to UVU photoelectron spectroscopy which is mostly concerned with static aspect of ground-state molecules. Molecular dynamic photoelectron spectroscopy will be prosperous especially for studying dynamic aspect of molecular excited states from photophysical and photochemical points of view. This paper is concerned mainly with advantages of dynamic photoelectron spectroscopy and its applications to molecular processes such as photodissociation, autoionization, and intramolecular relaxation.

IV–K Photodisscociation of a van der Waals Complex and Rotational Rainbow Effect

The excited state of ArNO, which is correlated to the Rydberg A staete of free NO and the ground state Ar, is in sharp contrast to the B, C, and D states of ArNO. From a previous photoelectron work [Annual Review (1984) p.92], it has been indicated that the parent cation is produced with a ns pulse laser by resonant ionization of ArNO throught the excited state, which is correlated to the Rydberg C state of free NO and the ground state of Ar. However, photodissociation is dominant when the complex is excited to the excited state, which is correlated to the Rydberg A state of free NO and the ground state of Ar. In the photodissociation of the ArNO and NeNO complexes, remarkable anomalies are observable in the rotational distribution of the NO A state. The rotational rainbow effect observed in the photodissociation of the van der Waals complexes has been studied in cooperation with Prof. H. Nakamura of this Institute.

IV-K-1 Anomalous Rotational-State Distribution of NO A State in UV Photodissociation of Rare Gas-NO van der Waals Complexes. Rotational Rainbow Effect

Kenji SATO, Yohji ACHIBA, Hiroki NAKAMURA, and Katsumi KIMURA

[*J. Chem. Phys.*, **85**, 1418 (1986)]

Rotational distributions of NO in the Rydberg A state produced in photodissociation of the ArNO and NeNO van der Waals complexes have been found for the first time by using a (1+1) resonant ionization technique in the region 44350–44800 cm^{-1}. Two eminent rotational distribution maxima have been observed at all the UV laser energies studied. Dependences of the distribution maxima on the excess energy and reduced mass have been found to be similar to those reported for the "rotational rainbow" of rotational inelastic scattering. Theoretical formulation is described here for the photodissociation of triatomic molecule. With a half-collision approximation and some assumption on the Franck-Condon factor, it is concluded that the partial cross section is proportional to the rotational transition probability in atom-diatom collision. Furthermore, close-coupling and semi-classical calculations have been carried out with a model potential to reproduce the observed rotational distributions qualitatively. The rotational-rainbow effect of the photodissociation has been strongly supported by these theoretical considerations. The upper limits of the dissociation energies of ArNO and NeNO have also been estimated from the highest accessible rotational levels of the photodissociation products.

IV–L Generation and Detection of Metal Clusters Formed by the Laser Vaporization

IV-L Generation and Detection of Metal Clusters Formed by the Laser Vaporization

Nobuaki WASHIDA *(Nat'l. Inst. Environ. Stud. and IMS)*, **Yohji ACHIBA, Takashi NAGATA*, Tamotsu KONDOW*, Kozo KUCHITSU*** *(Univ. of Tokyo)*, **and Katsumi KIMURA**

The technique of the laser-driven metal vaporization investigated here is basically as described by a few groupes (Smalley et al, Kaldor et al, and Riley et al). Briefly a pulsed supersonic beam of metal clusters is produced by laser (the second harmonic output (15 mJ/pulse) form a Q-switched Nd: YAG laser) vaporization of a target rod (3 mm dia.), located within the throat of pulsed nozzle. The laser is focussed on the side of the rotating target rod and a plasma of metal ions is cooled and recombined by the intense supersonic gas (helium backing pressures of 2–3 atm.) pulses. The cluster-containing carrier gas is then expanded

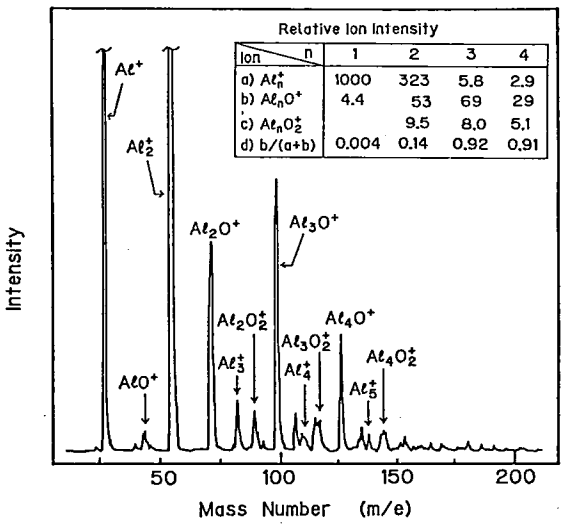

Figure 1. The mass spectrum for small aluminum clusters.

freely into a vacuum chamber and cooled further. This free jet is collimated by a conical skimmer (5 mm dia.) and ionizaed by direct or resonant two-photon laser (ArF excimer laser) photoionization. The ions formed are accelerated and mass separated by a quadrupole or time-of-flight mass spectrometer.

Figure 1 shows the mass spectrum for small aluminum clusters. Signals of Al_n^+, Al_nO^+, and $Al_nO_2^+$ (n=1–4) are observed. The relative ion intensities are also listed in Figure 1. Aluminum oxide may be produced by the reaction of Al_n with O_2 which contained in the helium carrier gas as an impurity. It should be interesting that the signals of Al_nO^+ is stronger than Al_n^+ for larger cluster size n. This suggests that the cross section of the Al_n+O_2 reaction might depend largely on the cluster size n.

IV–M Synchrotron Radiation Researches of Molecules and Molecular Clusters – Photoionization and Photoelectron Spectroscopy

The use of the 750-MeV electron storage ring (UVSOR) of this Institute for photoionization and photoelectron spectroscopy in the gas phase is quite attractive for studying higher electronic states and various ionic states of molecules and molecular clusters (or van der Waals molecules), because of its continuous character of the radiation in the whole VUV region.

IV-M-1 Determination of the C-H Bond Dissociation Energies of Ethylene and Acetylene by Observation of the Threshold Energies of H^+ Formation by Synchrotron Radiation

Haruo SHIROMARU, Yohoji ACHIBA *(Tokyo Metropolitan Univ.)*, **Katsumi KIMURA, and Yuan T. LEE** *(Univ. of Calf.)*

The C-H bond dissociation energies D_0(R-H) of ehtylene (C_2H_4) and acetylene (C_2H_2) are among some of the most important quantities in chemistry which need to be accurately determined. So far, several different values have been reported for the C-H bond dissociation energies of ethylene and acetylene, showing some scatters to a considerable extent.

To determine the C-H bond dissociation energies of ehtylene and acetylene (R-H), we have measured the threshold energies of H^+ formation in the process

$$RH + h\nu \rightarrow R + H^+ + e^-.$$

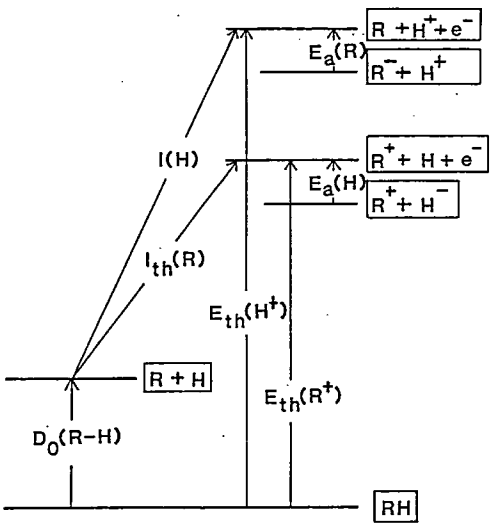

Figure 1. Schematic diagram of the energy levels relevant to evaluation of the C-H bond dissociation energy D_0(R-H), where I_{th} is the threshold ionization potential, I(H) is the ionization potential of H atom, E_{th} is the threshold energy of the ion formation, and E_a is the electron affinity.

using synchrotron radiation in the wavelength region 58–78 nm. The apparatus of the Beam Line BL2B2 of UVSOR was used. Subtracting the ionization potential of hydrogen atom (13.598 eV) from the observed threshold energies, we have deduced values of 5.06±0.05 eV and 5.75±0.05 eV for the C-H bond dissociation energies D_0(R-H) of ethylene and acetylene, respectively. The diagram of the energy levels relevant to evaluation of the C-H bond dissociation energy is schematically shown in Figure 1.

In this work we have carried out the first measurements of $E_{th}(H^+)$ for ethylene and acetylene using synchrotron radiation to deduce D_0(R-H).

IV-M-2 Direct VUV Absorption Measurements of Molecules

Haruo SHIROMARU, Yohji ACHIBA, and Katsumi KIMURA

An experimental setup for measuring a VUV absorption spectrum of a jet-cooled molecule or molecular cluster was made in the apparatus of the Beam Line BL2B2 of UVSOR. A gaseous sample was expanded through a pulsed supersonic nozzle and then introduced through a skimmer into the photon-molecule interaction region. Synchrotron radiation was monochromatized with a 1-m Seya-Namioka monochromator. The synchrotron radiation was crossed with the supersonic beam, and then detected by a photomultiplier operated at the pulsed frequency. Absorption measurements were performed by operating two pulse counters in a microcomputer system: One is synchronized with the open phase of the pulsed nozzle, and the other with the closed phase. The light intensities of I and I_0 were measured by counters A and B, respectively.

A preliminary experimental result obtained by the present system is shown in Figure 1. Molecular nitrogen was use as a test sample for the present purpose. The spectrum shown by an absorbance curve in Figure 1 is attributed to a Rydberg series converging to the third ionic state of molecular nitrogen.

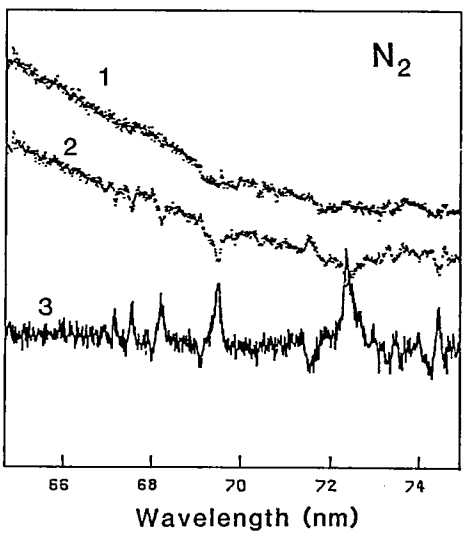

Figure 1. Light intensity curves and an absorbance curve of nitrogen molecule. Curves 1 and 2 indicate the light intensities I_0 and I, respectively, while curve 3 the absorbance curve.

IV-M-3 Photoionization of Methanol Clusters

Nobuaki WASHIDA *(Nat'l. Inst. Environ. Stud. and IMS)*, **Yohji ACHIBA, Haruo SHIROMARU, and Katsumi KIMURA**

Ion molecule reaction of CD_3OH are known to produce ions of $(CD_3OH)H^+$ and $(CD_3OH)D^+$:

$$CD_3OH^+ + CD_3OH \rightarrow (CD_3OH)H^+ + CD_3O \quad (1a)$$

$$\rightarrow (CD_3OH)D^+ + CD_2OH \quad (1b)$$

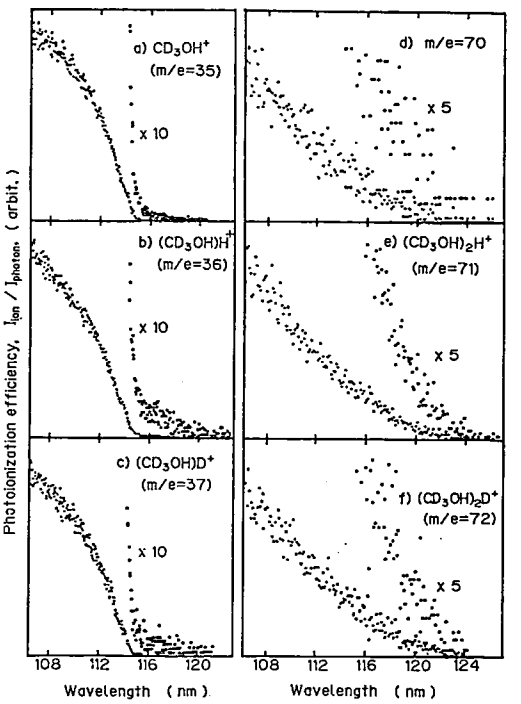

Figure 1. Relative photoionization efficiency curves of ions from CD_3OH cluster: a) CD_3OH^+ from monomer, b) $(CD_3OH)H^+$ from dimer, c) $(CD_3OH)D^+$ from dimer, d) *m/e*=70 from trimer, e) $(CD_3OH)_2H^+$ from trimer, and f) $(CD_3OH)_2D^+$ from trimer.

Intracluster proton transfer reaction of $(CD_3OH)_n^+$ also produces ions of $(CD_3OH)_{n-1}H^+$ and $(CD_3OH)_{n-1}D^+$:

$$(CD_3OH)_n + h\nu \rightarrow (CD_3OH)_n^+ + e^- \rightarrow (CD_3OH)_{n-1}H^+ + CD_3O + e^- \quad (2a)$$

$$\searrow (CD_3OH)_{n-1}D^+ + CD_2OH + e^- \quad (2b)$$

The intensity ratios $(CD_3OH)_{n-1}D^+/(CD_3OH)_{n-1}H^+$ depend on the cluster size n. A question of interest is that the $(CD_3OH)_{n-1}D^+$ is produced from a familiar hydrogen bonded cluster of CD_3OH. For example in the case of the dimer, a neutral precursor of the $(CD_3OH)D^+$ ion is a dimer of type (A) or another type (B).

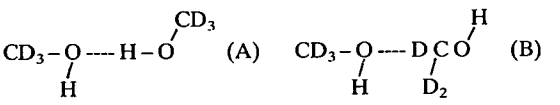

(A) (B)

In order to get an answer, the appearance potentials and ionization efficiency curves of $(CD_3OH)_{n-1}H^+$ and $(CD_3OH)_{n-1}D^+$ (n=2 and 3) were measured by using synchrotron orbital radiation. Results are shown in Figure 1. No significant difference was observed in the photoionization efficiency curves for the $(CD_3OH)_{n-1}H^+$ and $(CD_3OH)_{n-1}D^+$ ions. The results suggest that the precursory dimer of the $(CD_3OH)_{n-1}D^+$ ion is the same as that of the $(CD_3OH)_{n-1}H^+$, probably type A. The H-D exchange may occur in the dimer (A) after ionization.

IV–N Production, Characterization, and Spectroscopic Studies of Molecular Complexes and Clusters

There are several techniques to investigate physics and chemistry of molecular complexes and clusters. One of the most powerful techniques for producing such weakly bound complexes is the supersonic expansion of a high pressure gas through a small nozzle hole, by which one can produce a very large numbers of exotic molecules. However, characterization of such complexes is hard because of its weak bonding character.

In this project we have applied laser induced fluorescence spectroscopy combined with a nanosecond time resolved fluorescence technique to study the dynamics of electronically excited rare gas clusters and solvated molecules of substituted anthracenes produced in a free jet expansion.

IV-N-1 Fluorescence Lifetimes of 9-Methylanthracene in Supersonic Free Jets. A Level Inversion between S_1 and T_2 States upon the Phase Change from Solution to Gas

Fujio TANAKA[+], **Satoshi HIRAYAMA** *(Kyoto Inst. of Tech.)*, **Shigeru YAMASHITA**[+] *(*[+]*Univ. of Osaka Prefecture)*, **and Kosuke SHOBATAKE**

[*Bull. Chem. Soc. Jpn*, **59**, 2011 (1986)]

Fluorescence lifetimes measured for 9-methylanthracene (9MA) in supersonic free jets confirm the occurence of nonradiative decay at the radiationless level of S_1 of free 9MA that has been suggested from the measurement of the fluorescence yield. The nonradiative decay constants in the isolated state and condensed phases at room temperature and liquid nitrogen temperature have been compared from the view points of relative positions $S_1 > T_2$ of S_1 and T_2 levels and the magnitude of the energy gap.

IV-N-2 Fluorescence Decays in Wide Variety of van der Waals Complexes of 9-Cyanoanthracene in Supersonic Free Jets

Satoshi HIRAYAMA[+], **Akiho ADACHI**[+] *(*[+]*Kyoto Inst. Technology)*, **Fujio TANAKA** *(Univ. of Osaka Prefecture)*, **Kosuke SHOBATAKE, and Kyung-Hoon JUNG** *(Korea Advanced Inst. and Tech. and IMS)*

The van der Waals (vdW) complexes of 9-cyanoanthracene (9CNA) with ligands of various types have been formed in supersonic free jets and their dynamics in the electronically excited state have been studied by laser induced fluorescence and nanosecond time-resolved fluorescence spectroscopy. Complexation with H_2O, NH_3 and ethanol did not affect the basic feature of fluorescence decay process of the complexes in either vibrationless or intramolecularly, vibrationally excited states. CS_2 and triethylamine reduce the fluorescence lifetimes of the complexes to less that one half of that of the bare molecule of 9CNA. Furth-

ermore, intramolecular vibrational excitation of 9CNA moiety in these two complexes appears to end up to almost total quenching of the excited states. For C_6H_6 however, rather long fluorescence lifetimes of 36.5 and 48.0 ns have been found for the 1:1 and 1:2 complexes, respectively.

N,N-Dimethylaniline yieled the exciplex emission with the lifetime of 110 ns, which might be formed by direct excitation from the vdW complex in the ground state, since no fine structured vdW bands were observed in the emission excitation spectrum.

The mechanisms of complex formation and the influence of complexation upon the fluorescence lifetime are discussed.

IV–O Molecular Beam Studies of Chemical Reaction Dynamics

In this project we investigate dynamics of (1) the chemical reactions involving reactive species such as N, B, and C atoms, (2) dissociative excitation transfer reactions and excimer formations reactions involving metastable rare gas atoms, and (3) molecule-molecule reactions, using a crossed molecular beams technique. For the production of supersonic beams of reactive species used for the reactions (1) and (2), an arc-heated nozzle beam has been used. For the molecular beam chemiluminescence studies described in the following first three studies, a molecular beam chemistry apparatus -II (MBC-II) with fluorescence detection was used. For the study of molecule-molecule reactions of $F_2+C_6H_6$ a crossed molecular beam apparatus (MBC-I) with a rotatable mass spectrometer detector was used.

IV-O-1 Dissociative Excitation Process of Water by Metastable Rare Gas Atoms: $Rg(^3P_{0,2})+H_2O \rightarrow Rg+OH(A^2\Sigma^+)+H$, (Rg=Ar, Kr)

Kiyohiko TABAYASHI and Kosuke SHOBATAKE

By applying arc-heated metastable rare gas beams to a crossed molecular beam experimets, the title reactions were studied over the relative collision energy range 0.3–1.8 eV. Analyzing the fluorescence from $OH(A^2\Sigma^+–X^2\Pi)$ bands, vibrational and rotatinal state distributions of nascent $OH(A^2\Sigma^+)$ product have been determined. The observed rotational distributions for each vibrational state have been well approximated by a Boltzman distribution with a single temperature. With $Ar^*(^3P_{0,2})$ excitation, both vibrational and rotational distributions were found to show no significant dependence on the collision energy and compare well with those previously observed near thermal energy range. With $Kr^*(^3P_{0,2})$ excitation, however, the state distributions were found to be strongly collision energy dependent, rotational temperature $T_r(v=0)$ increasing 850 to 1750 K and vibrational population ratio $N_{v=1}/N_{v=0}$ from <0.09 to 0.14 with increasing the collision energy from 0.35 to 0.65 eV. The integral cross sections for the formation of nascent OH(A) were also determined by using a time-of-flight (TOF) energy selection method.[1] The collision energy dependence of cross section for the reaction $Ar(^3P_{0,2})+H_2O \rightarrow Ar+OH(A^2\Sigma^+)+H$ was found to be negative, whereas that for the reaction $Kr(^3P_{0,2})+H_2O \rightarrow Kr+OH(A^2\Sigma^+)+H$ exhibited positive dependence in the collision energy range studied (Figure 1).

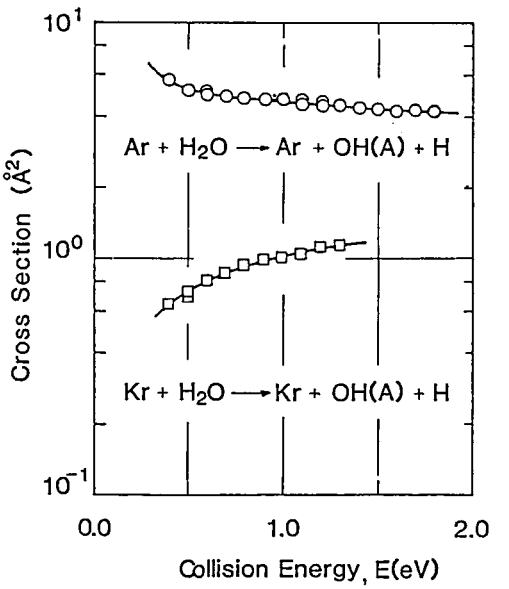

Figure 1. Integral cross section vs collision energy E for the dissociative excitation reaction: $Rg(^3P_{0,2})+H_2O \rightarrow Rg+OH(A^2\Sigma^+)+H$, (Rg=Ar, Kr).

Reference

1) K. Tabayashi and K. Shobatake, *J. Chem. Phys.*, **84**, 4919 (1986).

IV-O-2 Collision Energy Dependence of the Integral Cross Section for the Chemiluminescent Reaction: $N(^2D, ^2P)+CSX \rightarrow NS(B^2\Pi)+CX$, (X= O, S)

Kiyohiko TABAYASHI and Kosuke SHOBATAKE

Previously we observed emission $NS(B^2\Pi-X^2\Pi)$ from the reactions of $N(^2D, ^2P)$ with COS and CS_2 at an average collision energy $\bar{E}$=0.8 eV,[1] and proposed the following processes:

$N(^2D)+COS \rightarrow NS(B^2\Pi)+CO(X^1\Sigma^+)$, $\Delta H=-0.42$ eV (1)

$N(^2P)+CS_2 \rightarrow NS(B^2\Pi)+CS(X^1\Sigma^+)$, $\Delta H=-0.26$ eV (2)

In order to elucidate further details of the reaction mechanisms, we have applied the TOF energy selection technique[2] to the determination of the collision energy dependence of the integral cross section for the $NS(B^2\Pi)$ formation. The relative cross section, determined for both reaction systems using the mixed $N(^2D, ^2P)$ beam, is plotted againt c.m. collision energy E (Figure 1). The integral cross section profile for N^*+COS system, which correspond to the process (1), shows a very small dependence on collision energy whthin our experimental error. On the contrary, the integral cross section for N^*+CS_2 reaction is found to decrease up to around E=1.1 eV, and then to increase gradually in the energy range 1.2–2.0 eV, levelling off at 2.0 eV. This is quite indicative of the contribution of an endoergic process which was not considered before:

$N(^2D)+CS_2 \rightarrow NS(B^2\Pi)+CS$, $\Delta H=1.14$ eV. (3)

Below this threshold, it has also been confirmed that $NS(B^2\Pi)$ is formed by process (2). The present findings enable us to conclude that the $NS(B^2\Pi)$ molecules are produced via both adiabatic and nonadiabatic processes for N^*+CS_2 system.

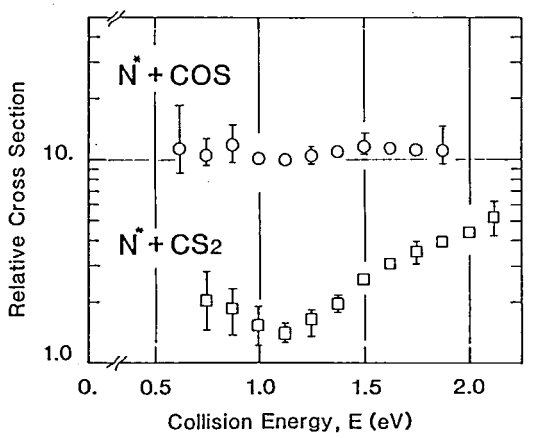

Figure 1. Relative cross section vs. collision energy E for the reaction $N(^2D, ^2P)+CSX \rightarrow NS(B^2\Pi)+CX$, (X=O, S).

References

1) K. Tabayashi and K. Shobatake, *IMS Ann. Rev.*, **1985**, 94.
2) K. Tabayashi and K. Shobatake, *J. Chem. Phys.*, **84**, 4919 (1986).

IV-O-3 Bound-free KrBr B(1/2)–X(1/2) and C(3/2)–A(3/2) Emission Observed in Crossed Molecular Beam Experiments

Marcus J. J. VRAKKING[a], Kiyohiko TABAYASHI, and Kosuke SHOBATAKE

Crossed molecular beam studies of KrBr bound free emission spectra are reported, obtained from reactions of $Kr(^3P_{0,2})$ with Br_2, CBr_4, $CHBr_3$, CH_2Br_2, CH_3Br, HBr and BrCN, using a thermal beam source for low collision energy experiments, and an arc-heated bem source for experiments with collision energies of 2.00–2.64 eV. Our observations include the B(1/2)–X(1/2), C(3/2)–A(3/2), D(1/2)–X(1/2) and B(1/2)–A(1/2) transition. The unexpectedly high intensity of D(1/2)–X(1/2) emission for thermal Br_2 and $CHBr_3$ experiments is assigned to the reaction of $Kr(^3P_0)$ in the beam. The B(1/2)–X(1/2) and C(3/2)–A(3/2) transitions have been analysed using trial-and-error computer simulation. This resulted in the determination of the relative shapes of the potential curves and the dependence of the electronic transition moment on internuclear distance. For thermal beam experiments with CBr_4 and Br_2 vibrational state distributions are assined, which show great similarity with $Xe^*(^3P)$ reactions.

[a] Present address: Physics Department , Eindhofen University of Technology, Eindhofen, The Netherlands.

IV-O-4 Reactive Scattering of F_2 plus C_6H_6 in Crossed Molecular Beams

J. Robb GROVER, Yuan T. LEE *(Univ. of Calif., Berkeley and IMS)*, **and Kosuke SHOBATAKE**

Angular distributions and relative total cross sections were measured for products of the title process at relative collision energies of 14 to 25 kcal/mol. For this work the molecular beam chemistry apparatus MBC-I

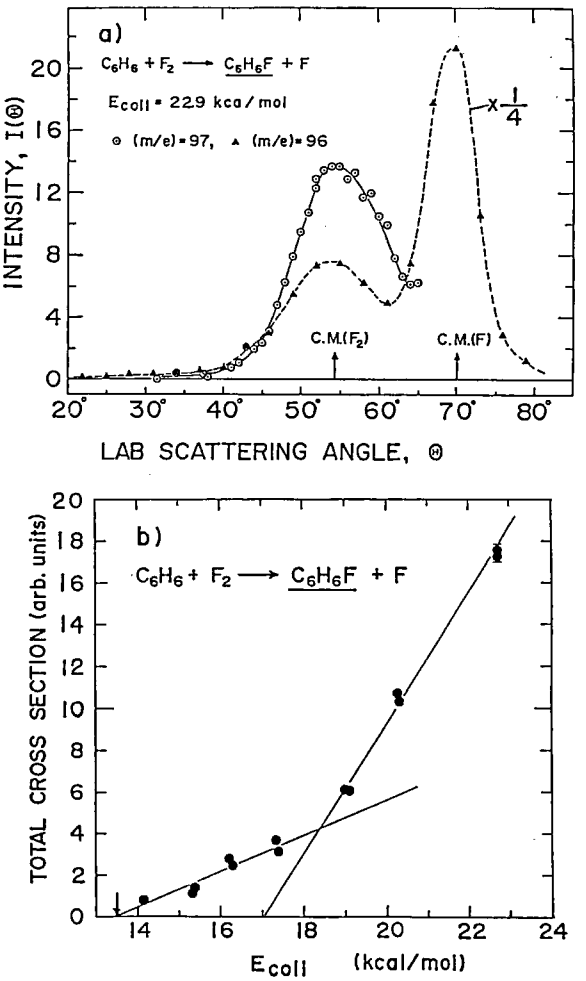

Figure 1. a) Angular distributions of products of the reactions of F_2 with C_6H_6 at a collision energy of 22.9 kal/mol. Circles: M/e=97 which corresponds to $C_6H_6F^+$ ion. Triangles: M/e=96 which corresponds to $C_6H_5F^+$ ion. The peak at 70° is due to a small contamination of atomic fluorine in the molecular fluorine beam, which induces the reaction $C_6H_6+F \rightarrow C_6H_5F+H$. The center-of-mass angles are indicated by arrows for both F_2 and F. b) Dependence on collision energy of the total cross sections for the production of C_6H_6F.

was used, in which seeded nozzle beams of the reagents were allowd to cross, and the angular distributions of the products were measured by means of a rotatable detector. The detector consists of an electron bombardment ionizer, a quadrupole mass spectrometer, and an electron multiplier operated in the ion-counting mode. The most conspicuous product is the "ipso"-fluorocyclohexadienyl radical C_6H_6F at M/e=97, which, as exemplified by Figure 1a, displays a rather narrow peak at the laboratory center-of-mass angle at all collision energies studied. This means that the reaction

$$C_6H_6 + F_2 \rightarrow C_6H_6F + F$$

proceeds preferentially by a statistical (unimolecular decay), or largely statistical, mechanism. Product fluorobenzene, C_6H_5F, M/e=96, is masked by dissociative ionization of C_6H_6F, near the center-of-mass angle but becomes clearly observable at smaller angles to which little or no C_6H_6F is scattered (Figure 1a). This means that the reaction $C_6H_6+F_2 \rightarrow C_6H_5+HF$ occurs, and does so to at least some extent by a direct (nonstatistical) mechanism. The dependence on collision energy of the total cross section for the production of C_6H_6F was measured, Figure 1b, and displays a well-marked onset at 13.6±0.4 kcal/mol.

IV–P Vacuum UV Photochemistry of Molecules in the Gas phase as Studied by Fluorescence Spectroscopy

Photochemistry be vacuum UV (VUV) light has recently become a very active field owing to the rapid progress in and the relatively easy access to the VUV light sources such as synchrotron orbital radiation (SOR) and VUV laser as well as conventional atomic resonance lines. In the present project we seek to obtain more detailed information about 1) photodissociation dynamics of simple molecules 2) production of emitting species from highly excited molecules, applying fluorescence spectroscopy by means of the tunable VUV light from UVSOR.

IV-P-1 Isotope Effect on the Fluorescence Cross Section for Dissociative Excitation Processes. II. CH_3OH and its Deuterated Compounds

Atsunari HIRAYA and Kosuke SHOBATAKE

For a better understanding of the isotope effect on photodissociative excitation processes previously found for CN*(A, B) formed by vacuum UV photolyses of CH_3CN and CD_3CN[1], the isotope effect on the fluorescence cross section of the OH*(OD*) formed by photodissociative excitation of CH_3OH and its deute-

rated compounds have been investigated. Figure 1 shows the absorption and emission cross sections of CH_3OH and CD_3OD. The threshold wavelengths for the formation of OH* and CH_3O* are indicated by arrows in the emission excitation spectrum. Although the CH_3O* can be produced for the excitation wavelength region shorter than 148 nm, the dispersed emission spectrum obtained was dominated by OH* emission band. The emission cross section for CD_3OD is about a factor of two larger than that for CH_3OH in the shorter wavelength region than 134 nm. On the contrary, such an isotope effect is not found for CH_3OH and CH_3OD. Therefore, it was concluded that the deuterium substitution at methyl group enhances the formation of OH* as was already found for CH_3CN and CD_3CN. The isotope effect observed in common for these two different molecules strongly supports our previous model that such an isotope effect on the formation of emitting species is caused by the isotope effect on some competing dissociative channels involving the motion of hydrogen atoms in the methyl group and C-H bond rupture.

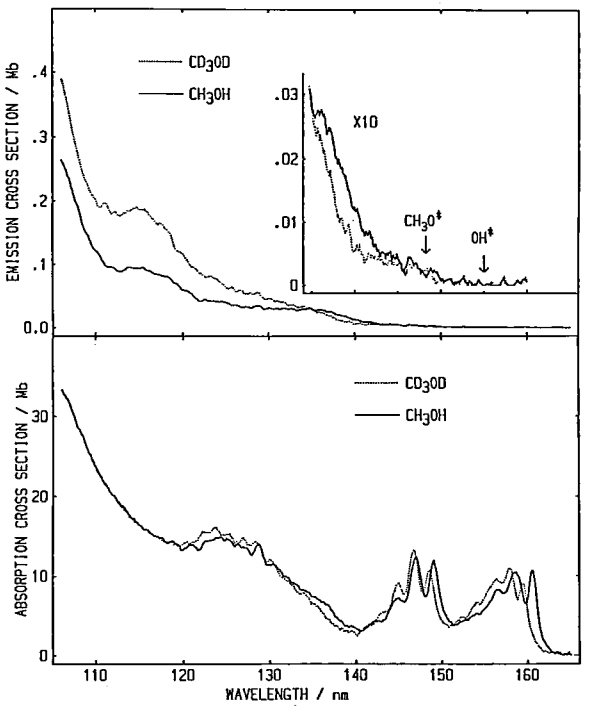

Figure 1. Absorption lower and emission excitation upper spectra of CH_3OH (solid line) and CD_3OD (dotted lien) in the gas phase. The emission cross section was put into the absolute scale by normalizing it to that of H_2O, for which the absolute cross section has been determined by Lee et al. (*J. Chem. Phys.*, **72**, 4334 (1980)).

Reference

1) K. Shobatake et al., *Ann. Rev. IMS* **1984**, p.96.

IV-P-2 Isotope Effect on the Fluorescence Cross Section for Dissociative Excitation Processes. III. $CHCl_3$ and $CDCl_3$

Atsunari HIRAYA, Toshio IBUKI *(Kyoto Univ.)*, **and Kosuke SHOBATAKE**

As a part of a series of our investigations on the isotope effect upon the photodissociative excitation processes, relative emission cross section of excited photofragment(s) formed in vacuum UV photolyses of $CHCl_3$ and $CDCl_3$ were determined. Figure 1(a) shows the emission cross section for $CHCl_3$ and $CDCl_3$ against the excitation wavelength. The absorption spectrum of $CDCl_3$ is almost the same as that of $CHCl_3$ shown in Figure 1(b). The emission cross section for the two isotopic compounds are almost indentical in the wavelength region above 122 nm, while that for $CHCl_3$ is about a factor of 1.5 larger than that for $CDCl_3$ below 120 nm. These isotopic compounds exhibit a deuterium isotope effect opposite to that observed for CH_3CN and CH_3OH for which the deuterium substitution gives rise to the enhancement of fluorescence yield. Although the emitting species for the photodissociation processes for $CHCl_3$ are not clearly known, CHCl* radicals are found to be dominant above 121.6 nm from the lifetime measurements. This finding is in agreement with the

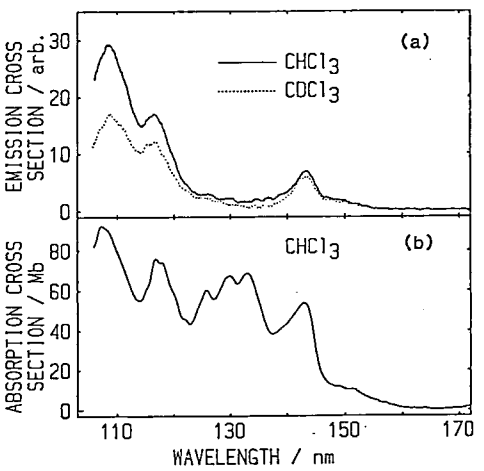

Figure 1. Emission excitation spectra of $CHCl_3$ and $CDCl_3$ (a), and absorption spectrum of $CHCl_3$ (b). Absorption cross section is in absolute scale, while emission cross section is in arbitrary units.

almost identical magnitude of emission cross sections for the two isotopic compounds above 122 nm, because the CHCl* formation process does not involve the C-H rupture for which the dissociation rate is expected to be strongly affected by deuteration. It is strongly suggested from the observed isotope effect that the dominant emitting species below 120 nm is CCl_2* radicals for which C-H rupture is involved in the disssociative excitation processes.

IV-P-3 $CCl_2(\tilde{A}^1B_1)$ Radical Formation in VUV photolyses of CCl_4 and $CBrCl_3$

Tohsio IBUKI[+], Norio TAKAHASHI[+] *([+]Kyoto Univ.)* **Atsunari HIRAYA, and Kosuke SHOBATAKE**

[*J. Chem. Phys.* in press]

In vacuum ultraviolet photolyses of CCl_4 and $CBrCl_3$, a diffuse emission band was observed in the region of 410–750 nm by Ar I resonance and H Lyman-α line irradiation. The band was attributed to a $CCl_2(\tilde{A}^1B_1 \rightarrow \tilde{X}^1A_1)$ transition from measurements of the appearance energies of the emitting species produced from photodissociative excitation of both CCl_4 and $CBrCl_3$, using synchrotron radiation from UVSOR. The fluorescence decay of the $CCl_2(\tilde{A} \rightarrow \tilde{X})$ transition showed a superposition of the two lifetime components of 2.17±0.26 and 4.0±0.12 μsec at pressures from 10 to 140 mTorr. The pressure dependence of the amplitudes for the two lifetimes suggests the occurrence of collision-induced intersystem crossing between the $^1B_1$ and $^3B_1$ states of CCl_2 radicals.

IV-P-4 Photoexcitation and Photofragment Fluorescence Study of Methanethiol in Vacuum Ultraviolet

Ikuo TOKUE *(Niigata Univ.)*, **Atsunari HIRAYA, and Kosuke SHOBATAKE**

Photoabsorption and fluorescence excitation spectra of methanethiol vapor were measured in the 130–200 nm region using synchrotron radiation from UVSOR. Many sharp structures observed in the 130–180 nm region are classified into three Rydberg series. The fluorescence which starts to appear at 175.2±2.0 nm is attributed to the $CH_3S(\tilde{A}^2A_1 \rightarrow \tilde{X}^2E)$ emission. The photodissociation processes are discussed in the light of the $CH_3S(A \rightarrow X)$ fluorescence spectrum observed.

IV-P-5 Absorption and Fluorescence Spectra of CH_3SCN and Related Molecules

Ikuo TOKUE *(Niigata Univ.)*, **Atsunari HIRAYA, and Kosuke SHOBATAKE**

Photoabsorption and fluorescence cross section of CH_3SCN, CH_3NCS, CH_3NCO, and $(CH_3)_2S$ were measured in the 105–210 nm region of exciting photons using synchrotron radiation from UVSOR. The dispersed emission spectra, in the 300–500 nm region, of the excited fragments were also observed. Three Rydberg series are observed in the absorption spectra of these molecules and analyzed, except for CH_3NCS which shows several very intense valence-type transitions. From the dispersed emission spectra, three emitting species, SCN(A), SCN(B), and CN(B) were found for CH_3SCN. At the excitation wavelength of 152.6 nm, emission spectrum is dominated by the SCN(A→X, B→X) bands, while that obtained at 125.6 nm is mainly attributed to the CN(B→X) band. The emitting species for CH_3NCS, CH_3NCO, and $(CH_3)_2S$ are found to be SCN(A, B), NCO(A), and CH_3S(A), repsectively.[1)]

Reference

1) I. Tokue, A. Hiraya and K. Shobatake, *UVSOR activity report*, **13**, 51 (1984/1985).

IV-P-6 Emission from Ion-Pair and Rydberg states of I_2

Robert J. DONOVAN *(Univ. of Edinburgh)*, **B.V. O'Grady** *(Univ. of Tasmania)*, **Atsunari HIRAYA, and Kosuke SHOBATAKE**

[*Chem. Phys. Lett.*, **122**, 612 (1985)]

Absorption and fluorescence excitation spectra of I_2 have been recorded in the region 110–210 nm using synchrotron radiation from UVSOR. The strongest fluorescence is excited in the region 173–200 nm and is associated with the $D(O^+_u)$ ion-pair state and possibly other ion-pair states. Quite intense fluorescence is also excited in the 132–150 nm: most of this is assigned to fluorescence from excited atoms formed by predissocia-

tion of Rydberg states.

IV-P-7 Emission Spectra of I_2 Excited in Rydberg Region

Atsunari HIRAYA, Kosuke SHOBATAKE, and Robert J. DONOVAN *(Univ. of Edinburgh)*

In order to identify the emitting states for the excitation to Rydberg states of I_2, emission spectra have been measured at several excitation wavelengths. The emission spectra obtained by the excitaiton at 150 nm (peak position of the C_7 Rydberg system) and 137 nm (overlapped region of several Rydberg systems) are shown in Figure 1(a) and 1(b). Emission bands at 323 and 340 nm was assigned as the collision induced D→X and D'→A' ion-pair bands, respectively.[1,2] And the 183 and 206 nm bands are the emission bands from excited states of iodine atom. The 270 nm band was assigned as the emission from the F ion-pair state.[3] Because this band observed for the C_7 Rydberg excitation is not affected by sample pressure, it is concluded that the C_7 Rydberg system is strongly mixed with the F ion-pair state. One more interesting feature was found for C_6 Rydberg state. When Xe is added, emission from XeI* excimer become dominant for all Rydberg system except for the C_6 Rydberg state. It is suggested that a very fast dissociation to the ground state atoms takes place from the C_6 Rydberg state.

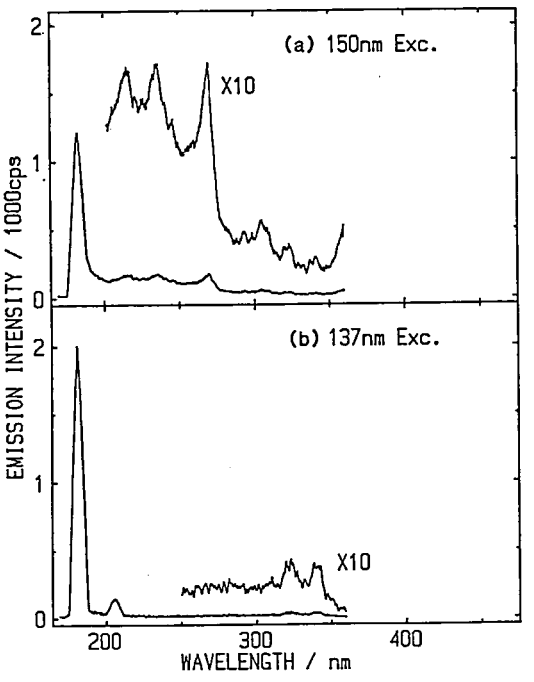

Figure 1. Dispersed emission spectra of I_2 vapor excited at 150 nm (a) and 137 nm (b). Sample gas pressure is 14.7 mtorr.

References

1) R.S. Mulliken, *J. Chem. Phys.*, **55** 288 (1971).
2) K.P. Lawley, M.A. MacDonald, R.J. Donovan and Agust Kvaran, *Chem. Phys. Lett.*, **92**, 322 (1982).
3) H. Hemmati and G.J. Collins, *Chem. Phys. Lett.*, **75**, 488 (1980).

IV-P-8 Fluorescence Lifetime Measurement for Gas Phase Molecules Excited VUV Region by Synchrotron Radiation

Atsunari HIRAYA and Kosuke SHOBATAKE

The synchrotron radiation from UVSOR(IMS) with pulse charactaristics of high repetition rate (90.1 or 5.63 MHz), short duration (ca. 400 ps) and stable intensity in the VUV-UV region is a very useful light source for the studies of dynamics of highly excited states and photodissociative excitation processes. We reports on

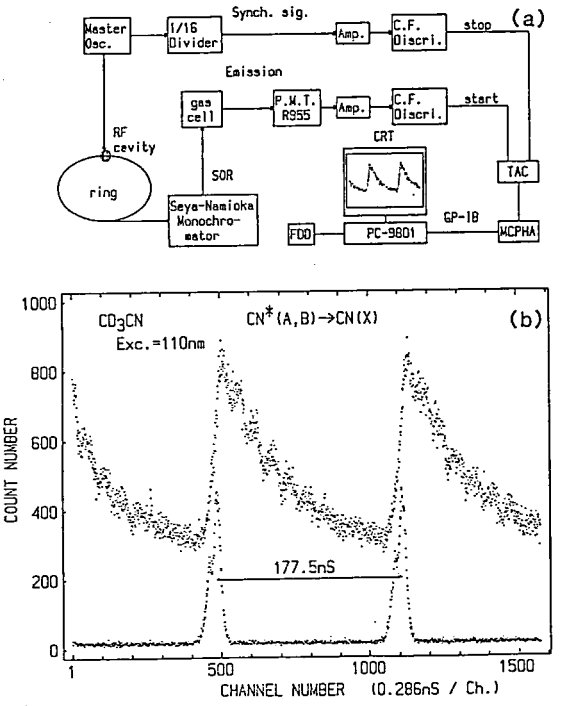

Figure 1. (a) Block diagram for the time-resolved fluorescence measurement system installed in beam line BL2A of UVSOR. TAC, time-to-amplitude converter; MCPHA, multichannel pulse-height analyzer. (b) Decay curve of the emission observed from CD_3CN vapor (50 mtorr) after excitation at 110 nm (upper trace) and the time response for scattering light at 200 nm.

the first successfull installation of a time-resolved fluorescence measurement system in a gas phase fluorescence apparatus on a beam line BL2A. Figure 1(a) shows a block diagram for the time-resolved fluorescence measurement system. As an example of the application of this system to the time-resolved measurements, the time decay of the emission intensity following the excitation of CD_3CN vapor (50 mtorr) at 110 nm and the time response for the scattering light are shown in Figure 1(b). The experiment was performed when the machine was operated in a single bunch operation mode. Although the observed decay curve cannot be expressed exactly by a single exponential function, the lifetime of the short lived emitting species has been estimated to be about 80 ns which is in good agreement with the radiative lifetime (85 ns) of $CN^*(B \rightarrow X)$.[1] The long lifetime component should be due to the $CN^*(A)$ whose radiative lifetime to ground state is 4.2 μs.[1]

Reference

1) T.J. Cook and D.H. Levy, *J. Chem. Phys.*, **57**, 5059 (1972); *ibid.* **57**, 5050 (1972).

IV–Q Optical Properties of Organic Liquids

The study on the liquid state of organic compounds which have relatively strong intermolecular interaction is one of the unexplored interesting problems in the field of molecular assemblies dynamics. In this study, fluorescene spectra, fluorescence life times, and Raman spectra of anthracene and pyrene in the molten state have been observed and compared with those in the solid state at high temperatures.

IV-Q-1 Time Resolved and Temperature Dependent Fluorescence Spectra of Anthracene and Pyrene in the Crystalline and Liuqid States

Rumiko HORIGUCHI *(Toshiba Research & Development Center)*, **Noriko IWASAKI** *(CANON Central Research Lab.)*, **and Yusei MARUYAMA**

[Submitted to *J. Phys. Chem.*]

Excimer states of anthracene have been found not only in the crystalline phase at high temperatures but also in the liquid phase by observing the stationary and the time-resolved fluorescence spectra. Fluorescence decay times in the liquid state are very short, 0.2–0.3 ns, without any emission energy dependence even at the excimer band. On the other hand, there seems to appear a separate component around the excimer band of pyrene liquid of which origin is tentatively assigned to a monomer emission band. The change of Raman spectra profiles of anthracene at the transition from crystal to liquid has been observed and discussed in relation to the disordered and/or ordered structures. Stable molecular-pair configurations are also discussed in terms of atomic-pair potential calculation.

IV–R Black Phosphorus Intercalation Compounds

Black phosphorus is a layered structure semiconductor. It shows interesting pressure-induced structural transitions followed by semiconductor-metal and also normal-to-superconductor transitions. We have tried to prepare novel intercalation compounds of black phosphorus which have presumably metallic character.

IV-R-1 Synthesis and Characterization of Black Phosphorus Intercalation Compounds

Toshifumi NISHII *(Mitsubishi Peterochemical Co. Ltd.)*, **Ichimin SHIROTANI** *(Muroran Inst. of Technology)*, **Tamotsu INABE and Yusei MARUYAMA**

[*Synthetic Metals*, **18**, 559 (1986)]

Black Phosphorus-Iodine intercalation compounds have been synthesized for the first time. Favorable reaction conditions for the synthesis and intercalated structures have been revealed. Temperature dependence of electrical conductivities of black phosphorus

single crystals significantly changes after intercalation and in some cases a metallic phase is realized down to 1.5 K. Moreover, it is noted that the conduction behavior is rather sensitive to the atmosphere in the reaction, namely a trace of moisture.

IV-S Synthesis and Electrical Properties of Organic Conductors

Our research activities are focused on the synthesis and characterization of new type of organic conductors including AzaTCNQ, OCNAQ, phthalocyanine derivatives, and some liuqid crystalline materials.

IV-S-1 New Organic Conductors Based on AzaTCNQ

Hatsumi URAYAMA *(ISSP, Univ. of Tokyo)*, **Gunzi SAITO** *(ISSP, Univ. of Tokyo)*, **Tamotsu INABE, Takehiko MORI, and Yusei MARUYAMA**

[*Synthetic Metals*, in press]

The complexes of AzaTCNQ(4-dicyanomethylenepyridinium dicyanomethylide) with the TTF family have been examined as a new candidate for organic conductors. The TMTSF complex has been found to have high conductivity and the metallic character has been confirmed by thermoelectric power and elecrtron spin resonance measurements. The stoichiometry is 2:1 and the structural study shows that only donor molecules form one-dimensional stack of conduction, while the AzaTCNQ molecular plane is oriented parallel to the donor stack. The orientational disorder of AzaTCNQ is supposed to cause the weak temperature dependence of charge transport.

IV-S-2 Synthesis and Electrical Properties of OCNAQ complexes

Tsutomu MITSUHASHI *(Univ. of Tokyo)*, **Tamotsu INABE, and Yusei MARUYAMA**

The single crystals of OCNAQ complexes have been obtained electrochemically or by slow diffusion methods. The electrical properties are summerized in Table 1. From the IR spectra, which give the ionicity of OCNAQ, the insulating compounds, i.e. phenothiazine-OCNAQ and pyrene-OCNAQ, were found to be a neutral complex. The other conducting complexes show the CN stretching mode at the same position as $Et_4N^+ \cdot OCNAQ^-$. The thermoelectric power of relatively high conducting complexes is small positive value, which means the conduction occurs through the stack of donor molecule. The complexes which show negative thermoelectric power reveal lower conductivity. In these compounds the major route of charge transport is supposed in the OCNAQ stack. It is rather noticeable that they are still conductive in spite of simple salt. This may be due to the effect of small on-site Coulomb repulsion of OCNAQ molecule, which is the main character of OCNAQ. It remains a question why OCNAQ can not exist in partial reduced state in solids like TCNQ. From the structural study of $Et_4N \cdot OCNAQ$ it was found that the OCNAQ molecular plane is not flat due to the steric hindrance between inner CN groups. Such molecular structure is not favorable to form stacking structure with efficient interaction between molecules to stabilize the partial reduced state.

Table 1. Electrical properties of the OCNAQ complexes.

Donor	Resistivity at room temperature (ohm·cm)	Thermoelectric power at room temperature ($\mu V \cdot deg^{-1}$)	Temperature dependence of Charge transport
TTF	1×10^{-1}	+22	metallic above 43K
	1×10^{2}	−150	semiconducting
TTT	3×10^{-2}		metallic above 300K
	1.6×10^{0}	+40	semiconducting
TMTTF	8×10^{2}	−100	semiconducting
phenothiazine			insulator
pyrene			insulator

IV-S-3 Approach to the Synthesis of Electrically Conductive Liquid Crystalline Materials

Kazuchika OHTA *(Shinshu Univ.)*, **Akira TAKAGI** *(Shinshu Univ.)*, **Hiromitsu MUROKI** *(Shinshu Univ.)*, **Iwao YAMAMOTO** *(Shinshu Univ.)*, **Kei MATSUZAKI** *(Shinshu Univ.)*, **Tamotsu INABE, and Yusei MARUYAMA**

Novel discotic liquid crystals have been obtained for bis[1,2-di(p-n-alkoxyphenyl)ethane-1,2-dithione] nickel complexes.[1] Discotic liquid crystals have potential as one-dimensional organic conductors, because they readily form a columnar structure essential to organic conductors. These nickel complexes are the first examples of π-acceptor discotic liquid crystals. The half-wave potentials for the reduction of the nickel complexes determined by cyclic voltametry are −0.06 V for $-OC_9H_{19}$ derivative and −0.07 V for $-OC_{11}H_{23}$ derivative (vs. SCE).

Reference

1) K. Ohta, A. Takagi, H. Muroki, I. Yamamoto, K. Matsuzaki, T. Inabe, and Y. Maruyama, *J. Chem. Soc., Chem. Commun.*, **1986**, 883.

IV−T Synthesis and Characterization of Proton-Transfer/ Charge-Transfer System

Proton-transfer in hydrogen bonding will provide many attractive phenomena if it is coupled to the π-electron system. In such system, there are two kinds of chemical species which can be interconvertible by the proton transfer. Such molecules can be used as memory devices or switching devices. Furthermore, if the π-electron system responds to the proton vibration in the crystalline state, it could create a novel kind of "phonon" which can be coupled with the electronic properties. (see Special Research Projects (2))

IV−U Ultra-Thin Organic Multi-Layers Films Prepared by Molecular Beam Epitaxy Technique

IV-U-1 Ultra-Thin Organic Multi-Layers Films Prepared by Molecular Beam Epitaxy Technique

Yusei MARUYAMA, Hajime HOSHI, and Tomotsu INABE

An ultra-high vacuum evaporation system for organic compounds has been constructed. Ultra-thin TCNQ films are now being prepared under the vacuum of $\sim 10^{-10}$ Torr, and the surface structure observation with an RHEED and/or a SEM is now on the way. The next step for multi-layer film preparation is now in progress.

IV−V Charge Density Waves and Superconductivity in transition metal Oxides and Bronzes and Other Low Dimensional Conductors

As candidates for materials with strong electron phonon coupling, transition metal oxides and bronzes are adopted in order to search new type superconductors. Studies have been carried out mainly from the structural view point. A number of crystals have been prepared and they often exhibit charge density wave (CDW) transition or Peierls transition and superconductivity. Much attention has been paid to the dynamical nature of the lattice systems, the sliding motion of the CDW and the anomalous transport behavior in a superconductor Lithium purple bronze. Competition between superconductivity-CDW has also been observed.

IV-V-1 On the anomalous Transport Properties of $Li_{0.9}Mo_6O_{17}$

Yuji MATSUDA, Masatoshi SATO, Masashige ONODA and Koichi NAKAO* *(*Institute for Solid State Physics)*

[*J. Phys. C*, in press]

In order to study the anomalous resistivity behavior and the superconductivity of $Li_{0.9}Mo_6O_{17}$ reported by Greenblatt et al., crystals of $(Li_{1-x}K_x)_{0.9}Mo_6O_{17}$, $(Li_{1-x}Na_x)_{0.9}Mo_6O_{17}$ and $Li_{0.9}(Mo_{1-x}W_x)_6O_{17}$ have been prepared and their resistivities, magnetic susceptibilities, and low temperature heat capacities have been measured. On the basis of the results of these experiments and the results of the structure determination, the superconducting transition temperature T_c and the origin of the anomalous behavior of the resistivity are discussed. A competition of the CDW in $Na_{0.9}Mo_6O_{17}$ and $K_{0.9}Mo_6O_{17}$ and the superconductivity in $Li_{0.9}Mo_6O_{17}$ are not realized in these mixed compounds, because the stable phase of the electron system changes abruptly with the change of their crystal structures.

IV-V-2 Crystal structure of Lithium Molybdenum Purple Bronze $Li_{0.9}Mo_6O_{17}$

Masashige ONODA, Koshiro TORIUMI, Yuji MATSUDA and Masatoshi SATO

[*J. Solid State Chem.* in press]

The crystal structure of the molybdenum ternary oxide $Li_{0.9}Mo_6O_{17}$ is determined by single crystal X-ray diffraction. The crystal is monoclinic with space group $P2_1/m$ and the lattice constants are a=12.762(2)Å, b=5.523(1)Å, c=9.499(1)Å, β=90.61(1)°, Z=2. Full-matrix least-squares refinement gives the final values of $R(F)$=0.033 and $R_w(F)$=0.066 for 3019 independent reflections. The unit cell contains six crystallographically independent molybdenum sites. One third of the molybdenum atoms are located in the oxygen tetrahedra, while the others are within the oxygen octahedra. The structure is built up of slabs of the MoO_6 octahedra. Each slab consists of three layers of distorted ReO_3-type MoO_6 octahedra sharing corners. The structure is rather different from that of $K_{0.9}Mo_6O_{17}$, although the layered feature is still preserved. The lithium ions are located in the large vacant sites between the slabs. By the application of Zachariasen's bond length-bond strength relation to the observed Mo-O bonds, most of the conduction electrons are found to be located in the Mo(1) and Mo(4) octahedral sites which are associated in pairs to form the –Mo(1)–O(11)–Mo(4)–O(11)– double zigzag chains extending along the b-axis. Therefore the structural properties are considered to lead to the highly anisotropic electronic transport.

IV-V-3 Inelastic Neutron Scattering Study of the Low Dimensional Conductors $(TaSe_4)_2I$ and Mo_8O_{23}

Hideshi FUJISHITA*, Masatoshi SATO, S. M. Shapiro# and Sadao HOSHINO* *(* Institute for Solid State Physics, #Brookhaven National Loboratory)*

[*Proc. Int. Conf. Synthetic Metals*, 1986 Kyoto]

Inelastic neutron scattering was carried out on the low dimensional conductors $(TaSe_4)_2I$ and Mo_8O_{23}. For $(TaSe_4)_2I$, a spoon like anomaly of the dispersion curve of the TA phonon branch was observed around the superlattice point. This result is a direct support of the TA mode condensation at the transition, which was predicted on the basis of x-ray studies and Raman scattering results. Mo_8O_{23} has a structural transition to the incommensurate CDW state at T_{c1}=315K and undergoes a lock in transition at T_{c2}=285K. The present inelastic neutron scattering discloses the existence of a temperature dependent soft mode at the incommensurate superlattice point above T_{c1}. A central peak is observed in the dynamical structure factor and grows as the temperature approaches T_{c1}.

IV-V-4 Superconductivity in $Li_{0.9}Mo_6O_{17}$

Yuji MATSUDA, Masashige ONODA and Masatoshi SATO

[*Proc. 15th Yamada Conf.* 1986 Lake Kawaguchi; *Physica B*]

Further studies on the anomalous behavior of superconductor $Li_{0.9}Mo_6O_{17}$ has been carried out. The one-dimensional-like transport properties predicted by the detailed bond length analysis is confirmed by the

measurement of the anisotropy of the critical magnetic field H_{c2}. Using the physical parameters determined in the revious work, rather detailed analysis of the low temperature behaviors of the resistivity and the magnetoresistance has been carried out and the possibility of the Anderson localization as the origin of the anomalous transport is proposed.

IV-V-5 Charge Density Waves in Mo_nO_{3n-1}

Masashige ONODA, Hideshi FUJISHITA*, Yuji MATSUDA and Masatoshi SATO *(*Institute for Solid State Physics)*

[*Proc. Int. Conf. Synthetic Metals*, 1986 Kyoto]

Single crystals of Mo_nO_{3n-1} (n=8, 9 and 10) have been studied by four circle x-ray diffraction, neutron scattering and other conventional methods. There have been found the superlattice reflection for all the compounds possibly due to the formation of charge density waves (CDW). The anomalous temperature dependence of the resistivities in Mo_8O_{23} and Mo_9O_{26} can be understood by these transitions. The condensed modes in all the compounds have the similar characters. The present system may give an example of superconductivity-CDW competition.

IV-V-6 Direct Evidence of Sliding Motion of CDW in $Rb_{0.3}MoO_3$

Kazushige NOMURA*, Kiyoshi KUME*, Takashi SAMBONGI# and Masatoshi SATO *(*Tokyo Metropolitan Univ.* #Hokkaido Univ)

[*Proc. 15th Yamada Conf.* 1986 Lake Kawaguchi; *Physica B]*

The ^{87}Rb NMR was observed in a single crystals of $Rb_{0.3}MoO_3$ with applying current and the transport measurements were also done at 77K. The narrowing of NMR line supplies the direct evidence for the sliding motion of incommensurate charge density wave (CDW) for a bias current above the threshold. The sliding velocity is estimated to be about 10^{-2} cm/sec for 7 A/cm^{-2} current, around which the motional narrowing occurrs. The fundamental frequency of narrow band noise F increased linearly with the CDW current J_{CDW} with the slope F/J_{CDW}=14 kHz/Acm^{-2}. The density of electrons, which condense to the CDW, is obtained to be 4×10^{27}/cm^3 and 1.5×10^{21}/cm^3 form the NMR and the narrow band noise, respectively. These values are consistent with one expected from the chemical formula.

IV-V-7 Neutron Study of Low frequency Structural Excitations of $K_{0.3}MoO_3$ in the Peierls Insulating State

C. ESCRIBE-FILIPPINI*, J. P. Pouget#, B. HENNION^S and Masatoshi SATO *(*CNRS Grenoble, France, #Univ. Paris Sud, Orsay, France, ^{S}CEN Sacley, France)*

[*Proc. Int. Conf. Synthetic Metals*, 1986 Kyoto]

A cold neutron study of low frequency structural excitations in the incommensurate Peierls insulating phase of the 1 dimensional conductor $K_{0.3}MoO_3$ has been performed. The scattering cross section related to the Peierls transition presents a large frequency distribution extending from very low frequencies (<0.2 THz) to frequencies of about 1.6 THz, with maxima of intensity occurring at frequencies previously observed in optical measurements and attributed to the phase and amplitude modes. The Kohn anomaly has been spatially resolved.

IV-V-8 Dielectric losses of TTF-TCNQ and $K_{0.3}MoO_3$

Hirohsi KUBOTA*, Masami ONUKI*, Taizo MASUMI#, Hiroyuki ANZAI^S and Masatoshi SATO *(*Kumamoto Univ., #Univ. of Tokyo, ^{S}Electrotechnical Laboratory)*

[*Proc. Int. Conf. Synthetic Metals*, 1986 Kyoto]

Measurements on the temperature dependences of the dielectric loss for TTF-TCNQ and $K_{0.3}MoO_3$ have been carried out at various frequencies at temperatures much lower than the Peierls transition temperature by using the blocking electrode method. The observed results are discussed by CDW's domain model under an analogy of the ion-transport in solids, then the values of pinning frequency of CDW's and energy barrier height between domains are obtained. Further, depinning CDW's/or exciting solitons stimulated under electric

fields enough high to reduce energy barrier height of inter-domains are suggested from experimental data.

IV-V-9 Structure Determination of Low Dimensional Conductor Sodium Purple Bronze $Na_{0.9}Mo_6O_{17}$

Masashige ONODA, Yuji MATSUDA and Masatoshi SATO

[*J. Solid State Chem.*, submitted]

Structure determination of the molybdenum purple bronze $Na_{0.9}Mo_6O_{17}$ is carried out by single crystal X-ray diffraction. The crystal is monoclinic with space group A2 and the lattice constants are a=12.983(2)Å, b=5.518(1)Å, c=9.591(2)Å, β=89.94(1)°, Z=2. Full-matrix least-squares refinement gives the final values of $R(F)$=0.028 and $R_W(F)$=0.040 for 1484 independent reflections, in which the occupancy factor of the sodium atom becomes 0.899(12). The present structure is built up of the linkage of the MoO_4 and MoO_6 polyhedra. There are slabs which consist of four layers of distorted MoO_6 octahedra sharing corners. Both the structure and the molybdenum valence distribution estimated from the Mo-O bond lengths are considered to lead to the two-dimensional electronic transport. This structure is compared with those of other members of molybdenum purple bronzes, $K_{0.9}Mo_6O_{17}$ and $Li_{0.9}Mo_6O_{17}$. The difference of the electronic properties among these compounds can be well understood on the basis of their structural characteristics.

IV-V-10 X-ray Four Circle Diffractometer for Use at Low Temperature

Masatoshi SATO, Masashige ONODA, Yuji MATSUDA, Shin-ichi SHAMOTO

X-ray four circle diffractometer with low temperature facility has been built. It is currently working with CS-1003 Displex type refrigerator, although slight problem has to be solved for use of the larger refrigerator. With this diffractometer, studies of materials with strong electron phonon interaction, which often exhibit charge density wave transitions are carried out. Because the informations on the low temperature structures ond on the nature of the transitions can be extracted, it will become, we hope, one of the powerful tools in the search for new type superconductors.

RESEARCH ACTIVITIES V
Department of Applied Molecular Science

V-A High-Spin Organic Molecules

We have been engaged for several years in the molecular design, generation and exploration of physicochemical properties, of high-spin organic molecules. As an extension of our polycarbene series $PhC(m\text{-}C_6H_4C)_{n-1}Ph$, we have prepared two new hexadiazo precursors that are expected to give hexacarbenes in the ground tridecet states. Whereas these polycarbenes have the origin of electron spins in the main framework of the molecules, there is another possibility of designing a series of high-spin systems in which the origin of spins resides on the side chain of a conjugate mainframe, e.g., polyacetylene or polydiacetylene. The spin-spin interaction in the latter systems has now been studied by model compounds. The spin alignment between open-shell molecules continues to be another subject of interest. From the temperature dependence of ESR signal intensities, we have been able to determine the ground state multiplicities and locate the thermally populated states for the isomeric bis(phenylmethylenyl)[2.2]-paracyclophanes, stacking models for two triplet diphenylcarbene molecules. The photolytic processes of some diazo compounds have also been studied in crystals and glassy matrices.

V-A-1 Synthesis of a Linear Hexadiazo Compound, a Precursor to a One-Dimensional Hexacarbene

Hideyuki TUKADA *(Univ. of Tokyo)*, **Tadashi SUGAWARA, and Hiizu IWAMURA**

Hexadiazo compound **1**($X=N_2$) was prepared in six steps (Scheme 1). The hydrogenolysis of the carbonyl groups in *m*-dibromoisophthalophenone for the following organometallic reaction was the key step in this sequence. Hexahydrazone **1**($X=NNH_2$) was prepared under Izuoka's condition.[1] Diazo compound **1**($X=N_2$) was obtained as wine-red polycrystals.

Scheme 1

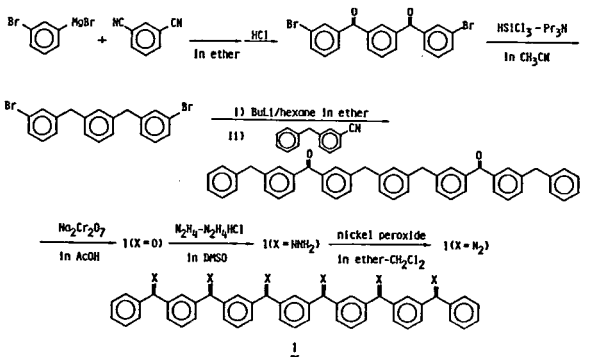

References

1) A. Izuoka and H. Iwamura, to be published elsewhere.

V-A-2 Synthesis of 1,3,5-Benzenetriyltris[α-diazo-{*m*-(α-diazobenzyl)phenyl}methane], a Precursor of a Two-Dimensional Hexacarbene

Toshio FUJIOKA *(Nagoya Univ.)*, **Yasuhiko SAWAKI** *(Nagoya Univ.)*, **and Hiizu IWAMURA**

Hexadiazo compound **1**($X=N_2$) was prepared via a nine-reaction sequence (Scheme 1). The base-catalyzed trimerization of the ethynylketone was a key step. Purification of **1**($X=N_2$) by chromatography on alumina (activity III) with *n*-hexane-CH_2Cl_2 elution at −20 °C gave wine-red microcrystals. Two-dimensional hexacarbene **1**(X= :) in a ground tridecet state is expected to be generated by photolysis at cryogenic temperature.

Scheme 1

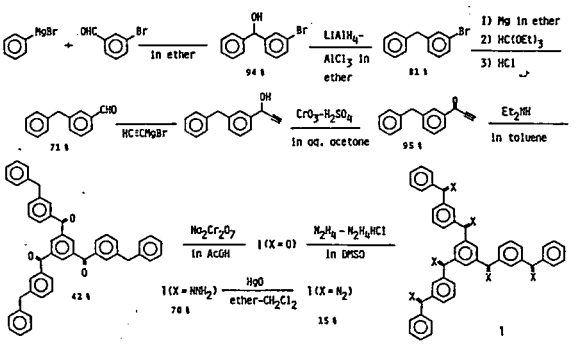

V-A-3 Magnetic Interaction of Two Diphenylcarbene Units Linked with an Ethylenic Double Bond

Shigeru MURATA, Tadashi SUGAWARA, and Hiizu IWAMURA

Two isomeric dicarbenes **1a** and **2a** have been generated by photolysis of the corresponding didiazo precursors **1b** and **2b**, respectively. The ESR spectrum of **1a** at 16 K contained a pair of characteristic signals at ca. 250 mT due to the quintet state. The signal intensity first increased, reached a maximum at 50 K, and then decreased, as we raised the temperature (Figure 1). In contrast, an intense signal at 250 mT due to quintet **2a** followed a linear Curie plot (Figure 1).

It is concluded that the two remote triplet diphenylcarbene moieties interact through a carbon-carbon double bond to form quintet states that are a ground state for **2a** and a thermally populated state for **1a**. The results are in good agreement with the MO theory of Borden and Davidson[1] and the valence-bond theory of Ovchinnikov.[2] The carbon-carbon double bond was now found to be an effective linking group for the construction of organic molecules with higher spin multiplicities.

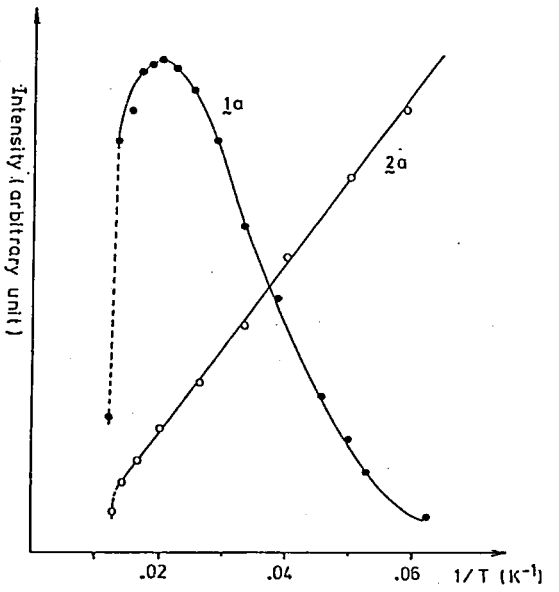

Figure 1. Temperature dependence of the intensities of the ESR signals due to quintet **1a** and **2a**.

References

1) W.T. Borden and E.R. Davidson, *J. Am. Chem. Soc.*, **99**, 4587 (1977).
2) A.A. Ovchinnikov, *Theor. Chim. Acta*, **47**, 297 (1978).

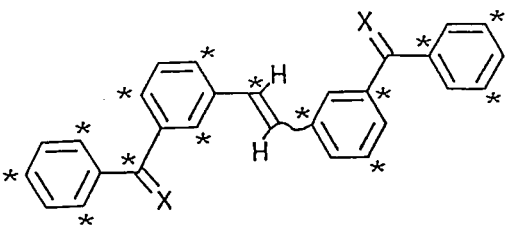

1

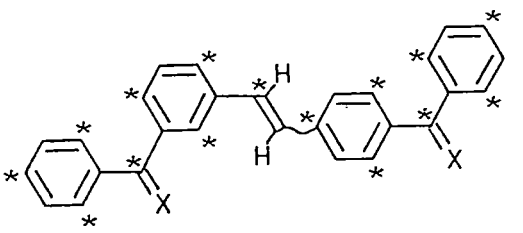

2

a: X = ·· b: X = N_2

V-A-4 The Spin States of Isomeric Bis(phenylmethylenyl)[2.2]paracyclophanes, Geometrically Fixed Models for Two Interacting Triplet Diphenylcarbenes

Akira IZUOKA, Shigeru MURATA, Tadashi SUGAWARA, and Hiizu IWAMURA

In a previous paper,[1] we have shown that pseudoortho-, pseudometa- and pseudopara-bis(phenylmethylenyl)[2.2]paracyclophanes (**1**, **2** and **3**, respectively) have the ground quintet, singlet and quintet states, respectively. The results served as the first experimental test for the McConnell's theory that the interaction between two organic radicals can become effectively ferromagnetic when the spin densities at the interacting sites have opposite sign.[2]

In the case of **1** and **2**, ESR signals due to the triplet states grew in as we raised the temperature higher than ca. 20 K. From the temperature dependence of the signal intensities, we were able to locate the thermally populated triplet states as shown below. In the case of **3**, the dicarbene was too unstable chemically to study the temperature dependence of the ESR fine structures. From the energy gap and the sum of the spin density products at the most strongly interacting sites in **1** and **2**, we were able to determine effective exchange integral J to be -3.5 kcal/mol. The quintet-triplet energy gap in **3** was estimated using this J value.

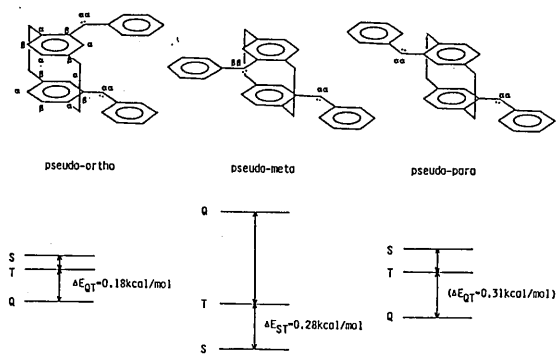

V-A-5 Magnetic Interaction among Diphenylmethylene Molecules Generated in Crystals of Some Diphenyldiazomethanes

Tadashi SUGAWARA, Hideyuki TUKADA *(Univ.of Tokyo)*, **Akira IZUOKA, Shigeru MURATA, and Hiizu IWAMURA**

[*J. Am. Chem. Soc.*, **108**, 4272 (1986)]

When a polycrystalline solid sample of bis(4-methoxyphenyl)diazomethane (**1**) was photolyzed in an ESR cavity at 10 K, quintet signals with $|D|$=0.136 cm^{-1} and $|E|$=0.015 cm^{-1} were most conspicuously detected and ascribed to a pairwise interaction of triplet bis(4-methoxyphenyl)carbene (**2**) formed in the crystal of precursor **1**.[1] The light intensity dependence of the initial rate of formation of the quintet species was studied at 20 K. When the data were analyzed in terms of equation: $k=cI^n$, where k and I stand for the rate constant and the light intensity, respectively, n was found to be 1.65±0.27 or 1.14±0.30 for the incident light of wavelengths 340 or 254 nm, respectively. The results suggest that a one-photon process may be involved in the formation of a pair of **2** in the quintet state by the irradiation at 340 nm and that this process predominates in the 254 nm irradiation. The excess energy left behind on **2** after removal of one nitrogen molecule from **1** in the photoexcited state could be efficiently transferred to the adjacent diazo molecule **1** in the crystal, resulting in the formation of a second molecule of **2** and consequently the quintet carbene pair.

References

1) *IMS Ann. Rev.*, 108 (1986).

V-A-6 Spectroscopic Studies on One-Photonic Decomposition of Polydiazo Compounds $PhCN_2(m\text{-}C_6H_4CN_2)_{n-1}Ph$

Noboru KOGA and Hiizu IWAMURA

The absorption spectra of a series of polydiazo compounds $PhCN_2(m\text{-}C_6H_4CN_2)_{n-1}Ph$ (A) show an interesting cross-conjugation effect. We have studied the photolytic reactions and the photoproducts of A in various kinds of matrix at temperatures lower than 80 K. Whereas the absorption and fluorescence spectra of the products were quite similar to each other, the ESR spectra were entirely different from each other, showing the formation of polycarbenes $Ph\ddot{C}(m\text{-}C_6H_4\ddot{C})_{n-1}Ph$ (B). The fluorescence of the products decayed single exponentially, indicating the presence of only one excited species for each product.

The formation and disappearance of B(n=2) in 2-MTHF and ethanol-d_6 matrices were followed in some detail by ESR and fluorescence spectra. Irradiation through neutral density filters showed that the formation of B(n=2) from A(n=2) is one-photonic. Additionally, the rising curve of the fluorescence intensity under cw irradiation was of a characteristic sigmoid. Biscarbene B (n=2) is concluded to be formed in a one-photon stepwise process. In the disappearing process, the increase of triplet and doublet signal intensities and appearance of a new emission were observed in the ESR and fluorescence spectra, respectively. The latter and the excitation spectrum were very similar to those of diphenylmethyl radicals. Therefore B(n=2) is concluded to disappear stepwise via triplet and doublet species in ethanol-d_6.

V-A-7 An Irreversible Structural Change Observed for Di-(1-naphthyl)methylene in Organic Rigid Glasses

Hideyuki TUKADA *(Univ. of Tokyo)*, **Tadashi SUGAWARA, Shigeru MURATA, and Hiizu IWAMURA**

[*Tetrahedron Lett.*, **27**, 235 (1986)]

When di-(1-naphthyl)diazomethane in glassy 2-MTHF was irradiated with uv light in an ESR cavity at 15 K, a typical set of triplet signals (a) due to di-(1-naphthyl)methylene (**1**) ($|D|$=0.3157 cm^{-1} and $|E|$=0.0109 cm^{-1}) appeared in a few seconds. The

signal intensities obeyed a Curie law in the temperature range 15–50 K. At about 80 K, another set of triplet peaks (b) ($|D|$=0.2609 cm^{-1} and $|E|$=0.0051 cm^{-1}) appeared at the expense of the original peaks (a) which disappeared rapidly at 87 K. The spectral changes were not reversible. Similar annealing effects were observed in other glasssy solid, although at different temperatures. In Fluorolube, the signals a and b were observed simultaneously at 30 K.

There are three near-planar conformations A-C possible for **1** at its birth. Since zero-field splitting parameters are practically determined by the one-center dipole-dipole interaction between the n and π spins, the calculated values fall in the range $|D|$=0.30 – 0.32 cm^{-1} and $|E|$=0.015 – 0.018 cm^{-1} and cannot differentiate between structures A-C. The observed small $|E|$ value of b is incompatible with these structures but consistent with the linearized configuration at the divalent carbon atom in **1**. We assign perpendicular conformation D' as the origin of signals b.

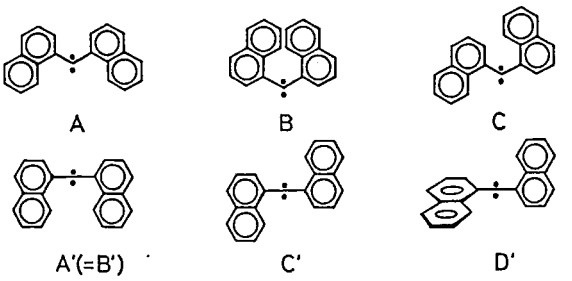

V-B Stereochemical Consequences of the Non-bonded Interactions in Overcrowded Molecules

Disrotatory coupling of the internal rotational degrees of freedom in double rotor molecules has been studied for a series of (9-triptycyl)$_2$X derivatives. These molecules undergo rapid internal rotation (10^9 s^{-1} at room temperature) in a strictly gear-meshed fashion, giving rise to new steroisomerism in the 2,2'- and 3,3'-disubstituted derivatives. The racemic and meso isomers which arise due to different phase relationship between the substituted benzene rings are separated by HPLC. Some rewards of this work for the basic understanding of stereochemistry have now been found.

V-B-1 Synthesis of 9,10-Bis(9-triptycyloxy)triptycenes. Molecular Design of a System with Doubly Correlated Internal Rotation

Noboru KOGA, Yuzo KAWADA *(Ibaraki Univ.)*, **and Hiizu IWAMURA**

[*Tetrahedron*, **42**, 1679 (1986)]

The torsional motions take place in strict disrotation in the bis(9-triptycyl)X derivatives reported previously and the tris(9-triptycyl) derivative in the title.[1] Whereas "disrotatory" motions are the technical expression popular in orbital symmetry-controlled reactions, steric effects can also be responsible for such motions, as our work shows.

As a persuasive demonstration of the strict conservation of orbital symmetry in electrocyclic reactions, **1** and **2** have been taken as examples.[2] They undergo equilibration through intermediacy of **3**. After 51 days at 124°C, each molecule of **3** had faultlessly undergone 2.6×10^6 conrotatory openings, and a disrotatory mistake had yet to appear. In our case, of non-bonded

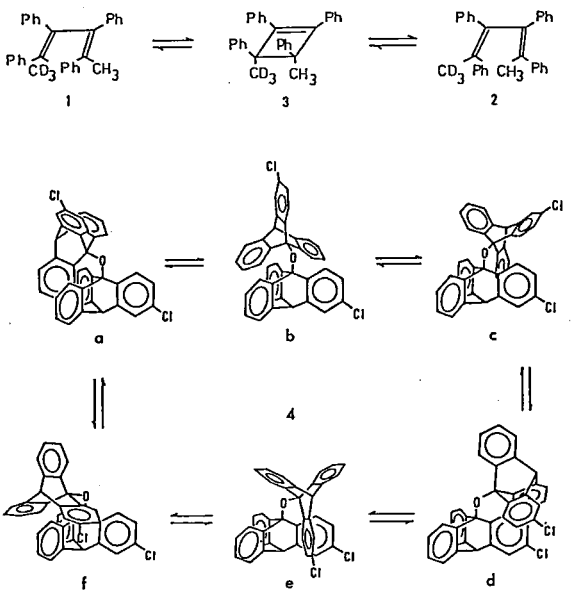

interaction-controlled motions in dichloro ether **4**, each gear undergoes disrotation 3.4×10^{16} times and only one in 50,000 wheels is computed to miss gearing at 124°C in 51 days. The symmetry allowed conrotatory opening

of the cyclobutene ring is estimated to be favored by a minimum of 7.3 kcal/mol over the symmetry forbidden disrotatory opening mode. The disrotatory motion is favored by 30-40 kcal/mol over the other modes in di(9-triptycyl) derivatives. The steric effect can do better job than the orbital symmetry control.

References

1) N. Koga, Y. Kawada, and H. Iwamura, *J. Am. Chem. Soc.*, **105**, 5498 (1983); *IMS Ann. Rev.*, 115 (1983).
2) R.B. Woodward and R. Hoffmann, "The Conservation of Orbital Symmetry", Academic Press, New York, N.Y., p.49, 1970; G.A. Doorakian and H.H. Freedman, *J. Am. Chem. Soc.*, **90**, 5310 (1968). Corrections in *ibid.*, **90**, 6896 (1968).

V-C Oxidation Reaction Mechanisms and New Reactive Intermediates

Whereas thermal and photochemical decomposition of diazo compounds to give triplet carbenes is well-established, little is known about the electrochemical reaction of these compounds. We have succeeded in detecting their cation radicals that decompose with a half-life of ca. 10 s at −33°C. Azides are also good precursors to triplet species, nitrenes. Nitroso oxides formed by oxygenation of the latter were found to transfer oxygen electrophilically. The finding is in striking contrast to the nucleophilic character of carbonyl oxides that are obtained by oxygenation of carbenes. Previously we reported that the cis-trans isomerization of *N*-methyl-4-(β-styryl)pyridinium salts induced by electron transfer from $Ru(bpy)_3^{2+}$ in the photoexcited state became very efficient when the substrate and the sensitizer were adsorbed electrostatically on the surface of anionic micelles. The local concentration effect was now found to be operative at the cationic micellar surface when both the electron donating sensitizer and the substrate are negatively charged.

V-C-1 Cation Radical Species Generated by One-Electron Oxidation of Diazomethanes

Katsuya ISHIGURO,[1] Yasuhiko SAWAKI *(Nagoya Univ.)*, **Akira IZUOKA, Tadashi SUGAWARA, and Hiizu IWAMURA**

Diazomethanes were oxidized in CH_3CN by an anodic electrolysis or with oxidants such as $(p\text{-Br-}C_6H_4)_3N^{+}SbCl_6^{-}$ or $Cu(II)ClO_4$. cis-Stilbene and tetraphenylethylene, C-C coupling products, were obtained from phenyl- and diphenyldiazomethanes (**1** and **2**), respectively.

When the electrolytic oxidation was carried out in CH_2Cl_2 containing 0.1 M $n\text{-}Bu_4NBF_4$ at −70 ~ −90°C, **2** showed an ESR spectrum (at ca. 1.3 V vs Ag/AgCl) consisting of triplet of triplet splittings (Figure 1). The voltage corresponds nicely to the redox potential of **2** obtained by low-temperature cyclic voltammetry. The hfs constants (a_{N-1}=1.72 mT, a_{N-2}=1.01 mT and g=2.0009) are similar to those of phenyldiazenyl radical.[2] Thus the formation of cation radical $Ph_2CN_2^{+}$ and its σ-radical character have been established.

Figure 1. ESR spectrum observed when diphenyldiazomethane (**2**) was electrolytically oxidized at −90°C in CH_2Cl_2.

References

1) IMS Graduate Student from Nagoya University for 1985–1987.
2) T. Suehiro, T. Tashiro, and R. Nakausa, *Chemistry Lett.*, 1339 (1980).

V-C-2 Reactivity of Nitroso Oxides. Oxygen Transfer as an Electrophilic Peroxy Radical

Yasuhiko SAWAKI *(Nagoya Univ.)*, **Shinji ISHIKAWA** *(Nagoya Univ.)*, **and Hiizu IWAMURA**

Reactivity of nitroso oxides, Ar-N-O-O, formed by the photo-oxidation of phenyl azides has been stuided by a trapping and tracer study. Nitrosobenzene was found to be a most reactive substrate. The hydroxylation of benzene and cyclohexene occured in 15–20% yields. Diphenyl sulfides and sulfoxides were oxidized electrophilically by phenylnitroso oxide, the Hammett's ρ-values being −0.98 and −0.64, respectively.

The reactivity order was: Ph-NO>Ph_2S>Ph_2SO>PhH. The results show that nitroso oxides react as electrophilic peroxy radicals. The reactivity is in sharp contrast to that of carbonyl oxides, R_2C-O-O, which are good nucleophiles.

The isomerization of phenylnitroso oxide to nitrobenzene was found to be 65% retention (Eq. 1). Scrambling according to Eq. 2 was substantiated by studying the reaction in the presence of *p*-ClC_6H_4-NO.

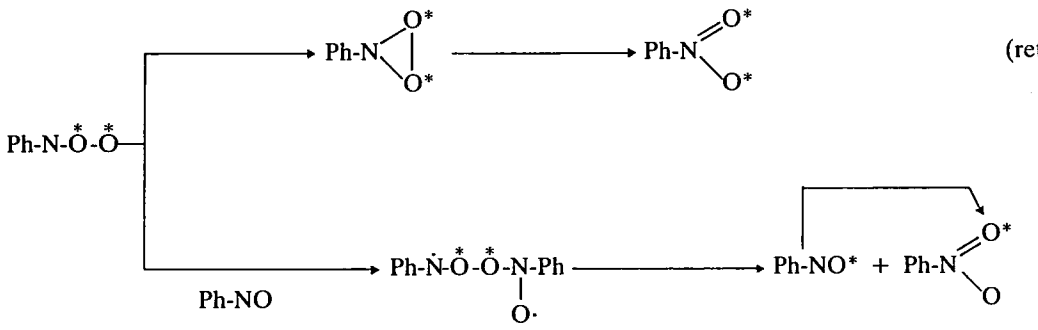

(retention) (1)

(scrambling) (2)

V-C-3 One-Electron Transfer and Radical Chain Reaction on Micellar Surface in the Photosensitized Debromination of 2,3-Dibromo-3-phenylpropionic Acid

Katsuhiko TAKAGI *(Nagoya Univ.)*, **Nobuhisa MIYAKE** *(Nagoya Univ.)*, **Eiichi NAKAMURA** *(Nagoya Univ.)*, **Yasuhiko SAWAKI** *(Nagoya Univ.)*, **and Hiizu IWAMURA**

2,3-Dibromo-3-phenylpropionic acids (**1** and **3**) are photodebrominated in the presence of zinc tetrasodiumtetra(*p*-sulfonatophenyl)porphyrin (ZnTPPS) and triethanolamine (TEOA) to give cinnamic acids (**2**):

$$\underset{\textbf{1}(\text{erythro}),\ \textbf{3}(\text{threo})}{PhCHBrCHBrCO_2X} \xrightarrow{\text{hv/ZnTPPS and TEOA}} \underset{\text{trans-}\textbf{2}}{PhCH{=}CHCO_2X}$$

a: X=Na, b: X=H, c: $X=CH_3$

The reactions have been studied in cationic cetyltrimethylammonium bromide (CTAB) micellar solutions. The dibromides are debrominated via a one-electron reduction by the excited ZnTPPS absorbed on the surface of the micelle followed by a radical chain reaction involving an α-amino radical reductant formed from TEOA as a chain carrier. The debromination proceeds most efficiently when **1** is adsorbed on the micellar surface (see Table 1). The efficiency is controlled both by the electron transfer from ZnTPPS in the excited state to **1** and by the debromination step which is competitive with the back electron transfer. The radical chain debromination on the micellar surface is found to be rather insensitive to the oxygen inhibition.

Table I. Efficiencies for the ZnTPPS-Sensitized Debromination of **1** and **3** under Various Conditions[a]

run	electron acceptor	reductant	system	quatum yields for debromination
1	**1a**	TEOA	[b]	0.28±0.04
2	**1a**	TEOA	O→O[c]	0.10±0.02
3	**1a**	TEOA	S→S	1.47±0.01
4	**3a**	TEOA	S→S	0.002±0.0001
5	**1b**	EDTA	S→I	0.36±0.01

[a]A mixture of 0.12 mM ZnTPPS, 6.7 mM acceptor, 12 mM reductant and 6.7 mM CTAB in water was photolyzed at 426±10 nm. [b]In the absence of CTAB. [c]Symbols I, S and O represent the interior and surface of micelles, and the bulk solution out of micelles, respectively. The arrow indicates the direction of electron transfer.

V-C-4 Photochemistry of *N*-Phenylbenzohydroxamic Acid

Ewa LIPCZYŃSKA-KOCHANY *(Warsaw Technical Univ.)*,[1] **Hiizu IWAMURA, and Jan KOCHANY** *(Inst. Environmental Creation, Warsaw)*

[*Monatsh. Chem.*, in press]

Whereas hydroxamic acids and metal hydroxamates are known to be photostable, the recent discovery of oscillation phenomena in the fluorescence intensity of some aromatic hydroxamic acids[2] suggests that they can be photochemically active when appropriately substituted. *N*-Phenylbenzohydroxamic acid (**1**) has the structural units of benzanilide and phenylhydroxylamine and therefore is expected to be most photolabile.

Irradiation of **1** in a quartz apparatus was carried out in ambient (cyclohexane and methanol) and basic (aqueous methanol, pH>12) media, and the progress of the reaction was followed by HPLC. In a typical run in cyclohexane, **1** disappeared in the quantum yield of 0.067 and gave the products summarized in Scheme 1 (the yields are in parentheses). The formation of benzanilide is accounted for by the initial homolysis of the N-O bond as shown in this Scheme.

A ca. 30 nm bathochromic shift of the absorption maximum of **1** is observed on formation of the anion **1a**. A previous ^{17}O NMR study has shown that the anion of N-substituted derivatives has resonance structures:

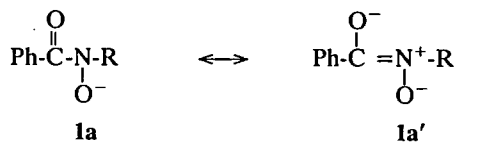

1a **1a′**

Structure **1a′** resembles the nitrone chromophore which is known to undergo photoreactions via oxaziridine intermediates.[3] A similar mechanism could be suggested for the photoreaction of **1** in the basic media.

Scheme 1

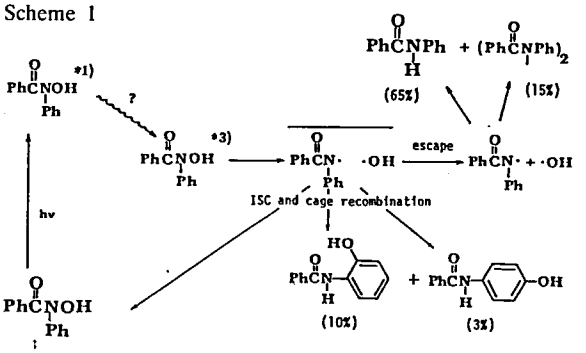

References

1) JSPS Invited Foreign Scholar 1981~1982.
2) E. Lipczyńska-Kochany and H. Iwamura, *Chemistry Lett.*, 1825 (1982).
3) M. Nastasi and J. Streith, "Rearrangements in Ground and Excited States", P. de Mayo, Ed., Academic Press, Vol. 3, p.468, 1980.

V-D One-Dimensional Halogen-Bridged M(II)-M(IV) Mixed-Valence Complexes

Synthesis and characterization of one-dimensional M(II)-M(IV) mixed valence compounds (M=Pt, Pd, Ni) having a linear chain structure is the subject of our continued interest [See *IMS Ann. Rev.*, 119 (1983), *ibid.*, 117 (1984) and *ibid.*, 116 (1985)]. Some structural approaches were carried out for understanding of the M(II)···M(IV) interaction along the chain.

V-D-1 Crystal Structures of Bromo-Bridged One-Dimensional Mixed-Metal Compounds, $[Ni^{II}(en)_2][Pt^{IV}Br(en)_2](ClO_4)_4$ and $[Pd^{II}(en)_2][Pt^{IV}Br(en)_2](ClO_4)_4$

Koshiro TORIUMI, Masahiro YAMASHITA *(Kyushu Univ.)*, **and Ichiro MURASE** *(Kyushu Univ.)*

[*Chem. Lett.*, 1753 (1986)]

In order to compare the structural parameters along the chains of mixed valence compounds having hetero-metal atoms with the corresponding parameters reported for the homo-metal systems, X-ray crystal structure analyses of the title compounds have been made. Crystallographic data are: for $[Ni(en)_2][PtBr_2(en)_2](ClO_4)_4$ **1**, monoclinic, C2/c, a=16.639(2), b=10.930(3), c=16.628(3)Å, β=109.65(1)°,

V=2847.9(10)Å^3, Z=4; for $[Pd(en)_2][PtBr_2(en)_2](ClO_4)_4$ **2**, orthorhombic, Icma, a=13.556(3), b=11.003(3), c=9.664(2)Å, V=1441.5(6)Å^3, Z=2. The sites of Pd^{II} and Pt^{IV} complexes in **2** are disordered and cannot be identified. On the other hand, Ni^{II} and Pt^{IV} atomic sites in **1** are crystallographically identified, and stacked alternately along the chain parallel to the b axis (Figure 1). Stractural parameters along the chain are Pt^{IV}-Br=2.465(1)Å and Ni^{II}···Br=3.000(1)Å in **1**, and Pt^{IV}-Br=2.467(1)Å and Pd^{II}···Br=3.035(1)Å in **2**. The Pd^{II}···Br distance in **2** is significantly longer than that of 2.911(1)Å in $[Pd(en)_2][PdBr_2(en)_2](ClO_4)_4$.[1)]

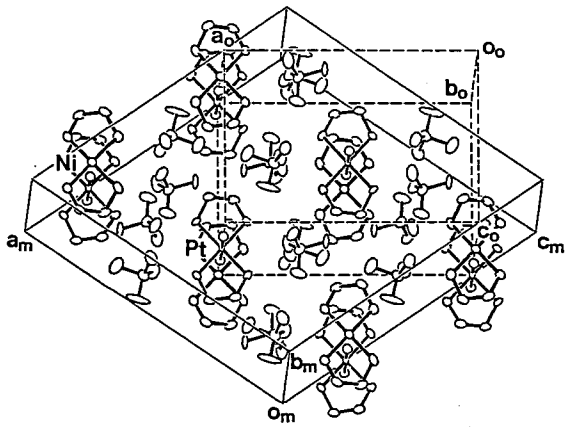

Figure 1. Crystal structure of the monoclinic cell of $[Ni(en)_2][PtBr_2(en)_2](ClO_4)_4$, together with the orthorhombic subcell indicating by broken lines.

Reference

1) M. Yamashita, K. Toriumi and T. Ito, *Acta Cryst.*, **C41**, 876 (1985).

V-D-2 Phase Transitions of the Crystals of Halogen-Bridged M^{II}-M^{IV} Mixed Valence Compounds of $[M(en)_2][MX_2(en)_2](ClO_4)_4$ (M=Pt, Pd; X=Cl, Br)

Koshiro TORIUMI, Masahiro YAMASHITA *(Kyushu Univ.)*, **Ichiro MURASE** *(Kyushu Univ.)*, **and Tasuku ITO** *(Tohoku Univ.)*

Crystals of the one-dimensional Cl and Br bridged Pt^{II}-Pt^{IV} and Pd^{II}-Pd^{IV} mixed valence compounds undergo first-order phase transitions at about −10°C–30°C. Lattice parameters of these compounds become contracted along the linear chains accompanied by the phase transitions (Figure 1). For an understanding of these phenomena, the crystal structures of the low and high temperature phases of $[Pt(en)_2][PtBr_2(en)_2](ClO_4)_4$ have been determined by X-ray diffraction method at room temperature. Crystallographic data are: for the high-temperature form, orthorhombic, Icma, a=13.563(2), b=10.939(3), c=9.664(2)Å, V=1433.9(5)Å^3, Z=2; for the low-temperature form, monoclinic, $P2_1/a$, a=8.544(1), b=10.973(1), c=7.972(1)Å, β=109.39(1)°, V=705.0(2)Å^3, Z=1. Structural parameters along the chains are significantly changed by the phase transitions; Pt^{IV}-Br and Pt^{II}···Br distances are 2.487(1) and 3.006(1)Å for the low-temperature form, and 2.473(1) and 2.997(1)Å for the high-temperature form. A drastic change of the hydrogen bond network accompanied by the phase transition, which play an important role to form the chain structure, was observed and might be a reason for these phenomena.

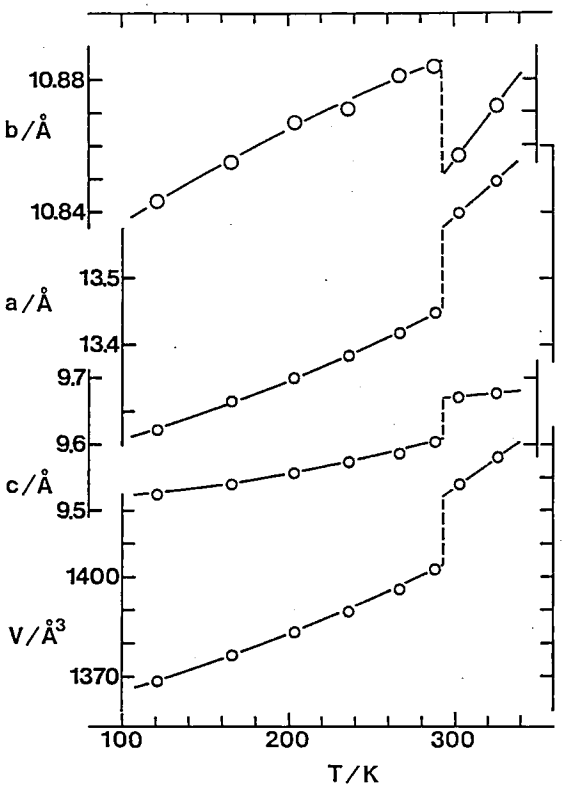

Figure 1. Temperature dependence of the lattice parameters of $[Pt(en)_2][PtCl_2(en)_2](ClO_4)_4$. The chain structure is parallel to the b axis.

V-D-3 The Structure of the Linear Chain Tetraammineplatinum(II) diiodotetraammine-platinum(IV) Hydrogensulfate Dihydrate, $[Pt(NH_3)_4][PtI_2(NH_3)_4](HSO_4)_4 \cdot 2H_2O$

Masako TANAKA *(Kyoto Univ.)*, **Ikuji TSUJIKAWA** *(Kyoto Univ.)*, **Koshiro TORIUMI, and Tasuku ITO** *(Tohoku Univ.)*

[*Acta Cryst.*, **C42**, 1105 (1986)]

In a series of halogen bridged Pt^{II}-Pt^{IV} mixed valence compounds having ammine ligands,[1] the title compound was synthesized and characterized by X-ray structure analysis. Crystallographic data are monoclinic, C2/m, a=18.609(2), b=7.563(1), c=11.862(1)Å, β=126.22(1)°, V=1346.8(6)Å^3, Z=2. As shown in Figure 1, the crystal comprises linear chains, $\cdots Pt^{II}\cdots I\text{-}Pt^{IV}\text{-}I\cdots$, where square planar $[Pt^{II}(NH_3)_4]^{2+}$ and tetragonal $[Pt^{IV}I_2(NH_3)_4]^{2+}$ units are stacked alternately with iodo bridges. The Pt^{IV}-I and $Pt^{II}\cdots$I distances are 2.699(1) and 3.237(1) Å, respectively. There is three dimensional ordering among chains, different from other Wolffram's red salt analogues.

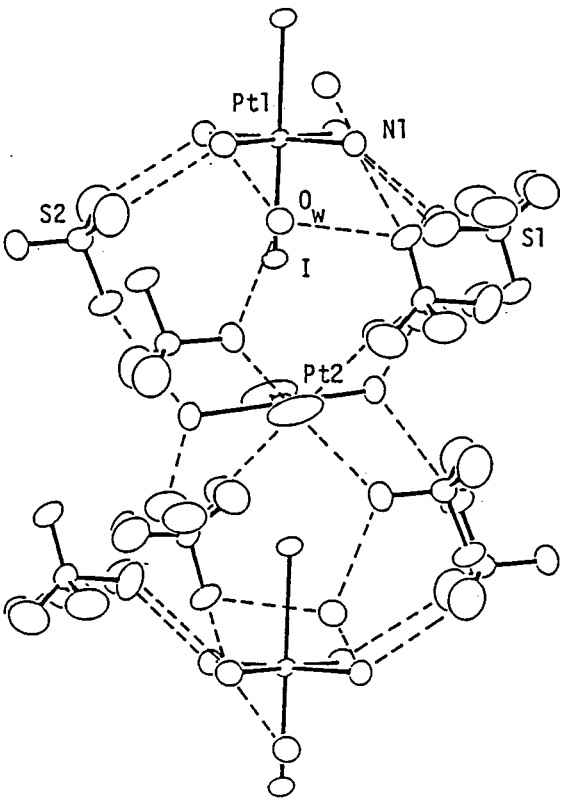

Figure 1. Portion of the infinite chain along the c axis with surrounding HSO_4^- ions and water molecules. The dashed lines correspond to hydrogen bonds.

Reference

1) M. Tanaka, I. Tsujikawa, K. Toriumi and T. Ito, *Acta Cryst.*, **B38**, 2793 (1982).

V-E Organo-Aluminum Complexes of Tetraaza Macrocyclic Ligands

Photoreactivity of metal-alkyl bond is the subject to our continued interest [see, *IMS Ann. Rev. 116 (1985)*]. We extended our work to $Al(C_{22}H_{22}N_4)(C_2H_5)$ system.

V-E-1 Photochemical Behavior of Aluminum-Ethyl Complex with Tetraaza Macrocyclic Ligand, $Al(C_{22}H_{22}N_4)(C_2H_5)$

Hiroki OSHIO, Shozo TERO-KUBOTA *(Tohoku Univ. and IMS)*, **and Tasuku ITO** *(Tohoku Univ.)*

Homolytic photocleavage of aluminum carbon bond in $Al(C_{22}H_{22}N_4)(C_2H_5)$ occurred in benzene in the presence of spin trapping agent 2,4,6-tri-t-butylnitrosobenzene (TBN), yielding spin adducts of $Al(C_{22}H_{22}N_4)$ and ethlyl radicals (Fig. 1A). NMR study of visible light irradiation of the title compound in $CDCl_3$ revealed a photochlorination to $Al(C_{22}H_{22}N_4)Cl$.

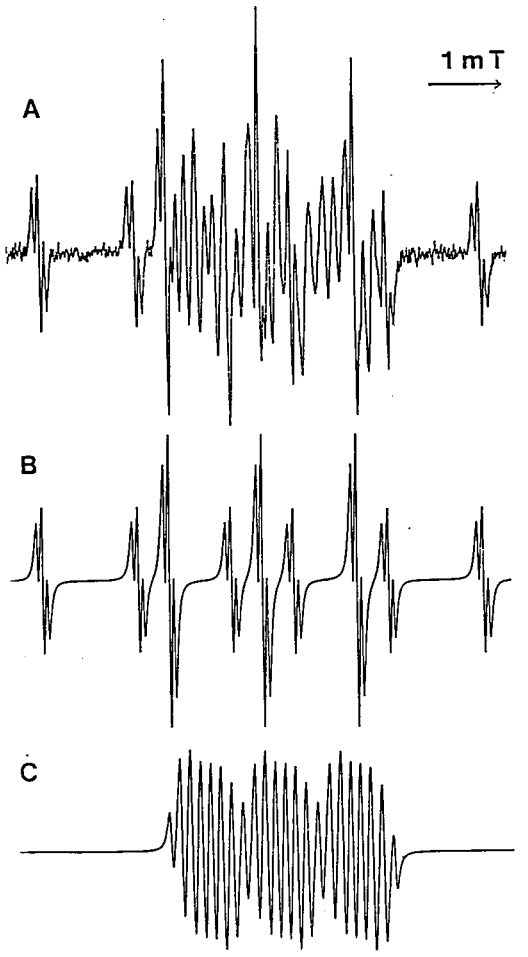

Figure 1. A: EPR spectrum of a benzene solution of $Al(C_{22}H_{22}N_4)(C_2H_5)$ with TBN upon irradiation (λ>450 nm). B and C: EPR simulation spectra of TBN-C_2H_5 and TBN-$Al(C_{22}H_{22}N_4)$, respectively.

V–F Crystallographic Study of Iron(III) Spin-Crossover Complexes

Spin-crossover behavior is well-known in some metal complexes in which a central metal ion has d^4 to d^8 electronic configurations. Recently, some N_4O_2 type ferric complexes were found to show exceptionally rapid spin interconvertion rate (10^{-8} sec) between high-spin ($^6A_{1g}$) and low-spin ($^2T_{2g}$) state in a solid. There are two factors that might be responsible for such rapid spin flipping phenomenon, that is, intermolecular interactions (ex. steric effect between ligands) and intramolecular interactions (ex. vibronic coupling and crystal packing). It is interesting to estimate which factor plays important roles to determine the spin interconversion rate.

V-F-1 Structures of Spin Crossover Ferric Complexes, $[Fe(acpa)_2](PF_6)$ and $[Fe(acen)(3,4\text{-}lut)_2](Bph_4)$

Hiroki OSHIO, Koshiro TORIUMI, Yonezo MAEDA *(Kyushu Univ.)*, **and Yoshimasa TAKASHIMA** *(Kyushu Univ.)*

In this study, crystallographic approach was applied to the spin crossover ferric complexes in order to estimate the effect of intra- and intermolecular interactions upon the spin flipping rate. $[Fe(acpa)_2](PF_6)$ (**1**) and $[Fe(acen)(3,4\text{-lut})_2](Bph_4)$ (**2**) show rapid (1×10^{-7} s) and slow (1×10^{-5} s) spin interconversion, respectively. Figure 1 shows the molecular structures of (**1**) and (**2**) at 120 K. Crystal data are : for (**1**), monoclinic, P2/a, a=13.674(1), b=9.911(1), c=10.325(1)Å, β=110.43(1), V=1311.3(2)Å^3, Z=2 at 290 K; monoclinic, P2/a, a=13.626(2), b=9.847(1), c=10.169(1)Å, β=111.93(1), V=1265.7(3)Å^3, Z=2 at 120 K; for (**2**), monoclinic, $P2_1/a$, a=28.021(3), b=14.313(2), c=11.166(1)A, β=90.68(1), V=4478(1)Å^3, Z=4 at 290

K, monoclinic, $P2_1/a$, a=27.707(4), b=14.085(2), c=10.998(2)Å, β=91.04(1), V=4291(1)Å^3, Z=4, at 120 K. Mean metal ligand bond lengths are : for (**1**), Fe-O=1.939(2)Å, Fe-N=2.117(2)Å at 290 K and Fe-O=1.889(2)Å, Fe-N=1.965(2)Å at 120 K and for (**2**), Fe-O=1.929(3)Å, Fe-N=2.121(3)Å at 290 K and at Fe-O=1.906(2)Å, Fe-N=1.977(2)Å at 120 K. It should be noted that changes of the metal ligand bond length for (**2**) accompanied with the spin interconversion is smaller than that for (**1**). We concluded from this result that the intermolecular rather than intramolecular interaction is the main factor to determine the spin interconversion rate in solid state.

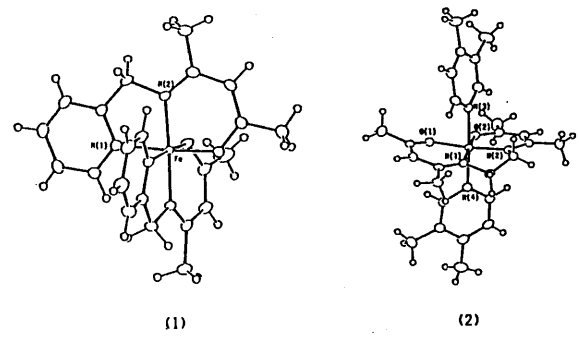

Figure 1. Molecular structures of $[Fe(acpa)_2]^+$ (**1**) and $[Fe(acen)(3,4\text{-lut})_2]^+$ (**2**).

V-G Triple Layered Cyclophanes

Triple layered cyclophanes are important as structural models for terplexes, stacking of donor/acceptor complexes, and other molecular clusters that show interesting physicochemical properties. Several triple layered cyclophanes were newly prepared. Their X-ray crystal structures were analyzed to show the twisted structure of the middle ring. The Ru(0) and Ru(II) complexes were prepared and the redox properties were measured.

V-G-1 The Crystal and Molecular Structure of 12-Bromo[2.2][2.2]triple-layered Paracyclophane.

Yosuke KOIZUMI, Toshihiro TOYODA, Kunio MIKI, Nobutami KASAI *(Osaka Univ.)*, **and Soichi MISUMI** *(Osaka Univ. and IMS)*

[*Bull. Chem. Soc. Jpn.*, **59**, 239 (1986)]

The molecular structure of 12-bromo[2.2][2.2]triple-layered paracylophane has been determined by means of X-ray diffraction. The crystal is orthorhombic, space group Pbcn, a=12.768(1), b=11.515(1), c=13.074(1) Å, Z=4. The structure was solved by the heavy-atom method, and refined anisotropically by the block-diagonal least-squares procedure; R=0.062. The Br-C...C-H axis of the central benzene ring lies on a crystallographic two-fold axis. The outer benzene rings take a boat form, and the central benzene ring is twisted.

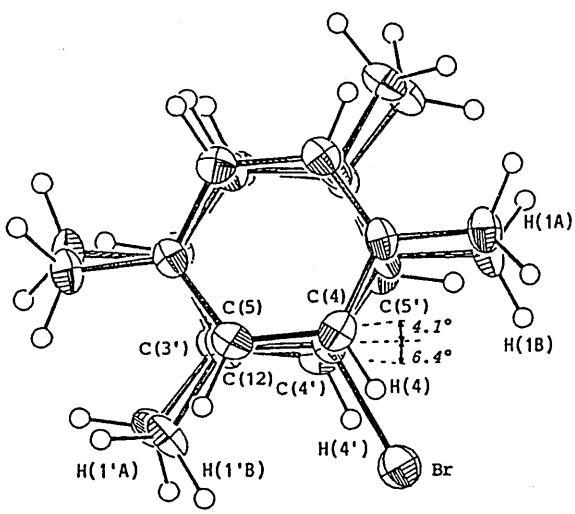

V-G-2 The Crystal and Molecular Structure of Inner Triple-layered Paracyclophanequinone.

Toshihiro TOYODA, Hitoshi TATEMITSU, Yoshiteru SAKATA, Nobutami KASAI *(Osaka Univ.)*, **and Soichi MISUMI** *(Osaka Univ. and IMS)*

[*Bull. Chem. Soc. Jpn.*, **59**, 3994 (1986)]

The molecular structure of inner quinone isomer of two triple-layered paracyclophanequinone has been determined by means of X-ray diffraction. $C_{26}H_{24}O_2$, M 368.5, orthorhombic, space group Pbcn. The structure was solved by the direct method. Anisotropic refinement by the block-diagonal least-squares procedure gave R=0.042 for non-zero reflections. The molecule has a two-fold symmetry. The benzoquinone

moiety is sandwiched by two donor benzene rings, and the two-fold axis passes through the O=C....C=O bonds of the twisted benzoquinone moiety. The outer benzene rings take a boat-form and the central benzoquinone ring is twisted.

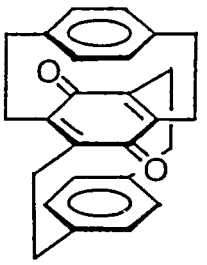

V-G-3 The Synthesis and Electrochemical Behavior of Bis(η^6-hexamethylbenzene)(η^6, η^6-triple-layered[2.2]paracyclophane)diruthenium-(II, II) tetrakis(tetrafluoroborate) and Its Related Mixed-valence Ion.

Hee Chol KANG, Klaus-Dieter PLITZKO *(Univ. Oregon)*, **Hiroyuki HIGUCHI** *(Osaka Univ.)*, **Soichi MISUMI** *(Osaka Univ. and IMS)*, **and Virgil BOEKELHEIDE** *(Univ. Oregon)*

[*J. Organomet. Chem.*, in press]

The synthesis and characterization of (η^6-hexamethylbenzene) (η^6-triple-layered[2.2]paracyclophane)ruthenium(II) bis(tetrafluoroborate), **4**, and bis-(η^6-hexamethylbenzene)(ν^6, η^6-triple-layered[2.2]paracyclophane)diruthenium(II,II) tetrakis(tetrafluoroborate), **6**, together with their corresponding ruthenium(0) derivatives, **5** and **7**, are described. Cyclic voltammetry shows **4** to be reduced by a two-electron, reversible wave, $E_{1/2}$(SCE)=−0.816±0.008 V, and **6** to undergo reduction by two overlapping, reversible two-electron waves, $E^{I}_{1/2}$(SCE)=−0.698±0.005 V and $E^{II}_{1/2}$(SCE)=−0.796±0.005 V. The comproportionation constant, Kc, for the equilibrium between **6**, **7**, and the corresponding $Ru^{II}Ru^{0}$ mixed-valence ion is 2.1×10^{3}. Although this large value of Kc indicates significant interaction between the two ruthenium atoms of the mixed-valence ion, the extent of interaction is appreciably smaller than that found for **2**, the previous example of a mixed-valence ion in this series.

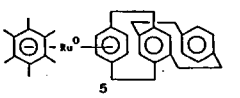

5

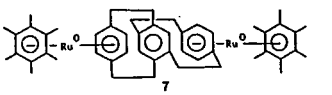

7

RESEARCH ACTIVITIES VI
Coordination Chemistry Laboratories

These laboratories were eatablished in 1984 to facilitate the studies of coordination chemistry in the interdisciplinary region between molecules and a variety of inorganic compounds. Members of staff of Laboratory of Synthetic Coordination Chemistry, who had been transferred from Tohoku University, completed the two years appointment and were newly appointed Adjunct Professor and Adjunct Associate Professor of a new Laboratory of Coordination Bonds to continue research in the new frontiers exploited by themselves in this Institute.

New members of Laboratory of Synthetic Coordination Chemistry were transferred from Kyushu University and Tokyo Institute of Technology and are engaging in the synthesis of novel binuclear transition metal chelate complexes with special reference to spin-spin interaction and also calorimetric studies of complex formation in solution which is otherwise studied with difficulty.

Activity of Laboratory of Complex Catalysis is being extended with a new Research Associate and new Adjunct Members.

VI-A Synthesis, Structure, and Properties of Polynuclear Metal Complexes

Novel type binuclear and polynuclear metal complexes are synthesized by use of organic binucleating ligands. The complexes obtained show interesting physical and chemical properties which could not be observed for mononuclear complexes. Some of them will provide models for substances of biological importance in structure, physical properties, and functions.

VI-A-1 Structures of Novel Type Binuclear Copper(II) Complexes with Octadentate Ligand *N, N', N'', N'''*-Tetrakis (2-aminoethyl)-1, 4, 8, 11-tetraazacyclotetradecane

Masahiro MIKURIYA, Sigeo KIDA, and Ichiro MURASE* *(*Kyushu Univ.)*

The X-ray analyses have revealed that in the cases of complexes, $Cu_2(taec)X(ClO_4)_3$ with X = F, I, N_3, NCO, NO_2, and CH_3CO_2, the coordination modes of taec are all similar to that reported for $Cu_2(taec)Br(ClO_4)_3$.[1] The NCO^-, N_3^-, and NO_2^- ions coordinate to both copper ions in end-on fashion with N, N, and O atoms, respectively (Fig. 1-a). In the case of X = CH_3CO_2, one of the acetate oxygens coordinates to one copper at the axial site, whereas the other one of the acetate oxygens coordinates to the other copper at an equatorial coordination site (Fig. 1-b).

In contrast to the above complexes, the structure of $Cu_2(taec)(NCS)_2(ClO_4)_2 \cdot H_2O$ resembles that of $Cu_2(taec)$-$(ClO_4)_4$ where the axial coordination sites face toward outer sides. The NCS^- ions coordinate to these sites with the nitrogen atoms.

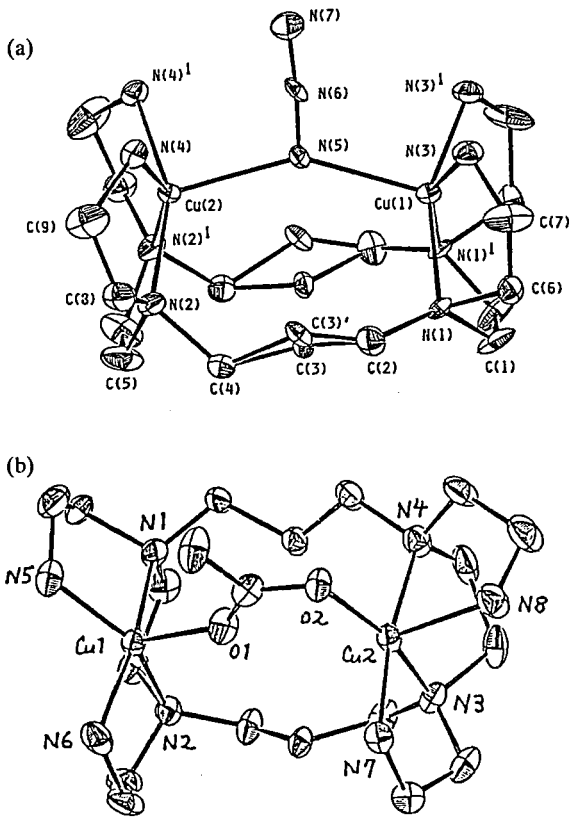

Figure 1. Structures of complex cations, $Cu_2(taec)N_3(ClO_4)_3$ (a), and $Cu_2(taec)(CH_3CO_2)(ClO_4)_3$ (b).

Reference

1) I. Murase, M. Mikuriya, H. Sonoda, Y. Fukuda, and S. Kida, *J. Chem. Soc. Dalton Trans.*, **1986**, 953.

VI-A-2 Structure of Azide-bridged Binuclear Copper (II) Complexes with Octadentate Ligand *N, N', N'', N'''*-Tetrakis (2-aminoethyl)-1, 5, 9, 13-tetra-azacyclohexadecane

Sigeo KIDA, Masahiro MIKURIYA, Ikuhiko UEDA#, and Ichiro MURASE* *(#Yoshitomi Seiyaku, *Kyushu Univ.)*

The title ligand(taeh) containing 16-membered ring has been synthesized. This ligand forms copper(II) complexes with the general formula $Cu_2(taeh)X(ClO_4)_3$ (X = Cl, Br, I, NO_2, N_3) similarly to the taec analogs. X-ray analysis has been performed on $Cu_2(taeh)N_3(ClO_4)_3$. The azide ion bridges the copper ions as in the case of the taec analog, but its coordination mode is entirely different from that of the taec analog in which the azide ion bridges in end-on fasion. In the present complex the azide ion bridges with end-to-end fasion. It is interesting that the expansion of the ring from 14- to 16-membered ring has brought about such a big change in bridging structure.

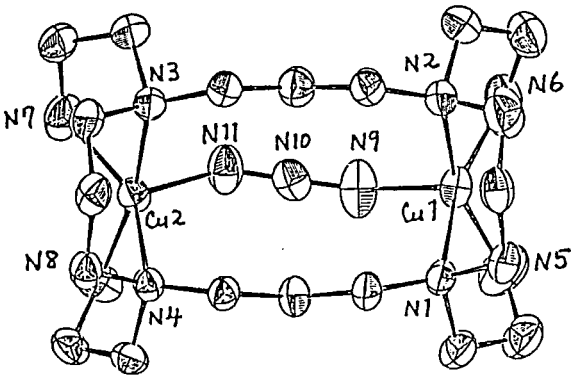

Figure 1. Structure of complex cation $Cu_2(taeh)N_3$.

VI-A-3 Synthesis and Characterization of Binuclear and Trinuclear Mn(II), Fe(II), and Co(II) Complexes with Terdetate Diaminothiols

Makoto HANDA, Sigeo KIDA, and Hisashi ŌKAWA* *(*Kyushu Univ.)*

Linear diaminothiols are expected to act as terdentate ligands forming thiolate-bridged binuclear or polynuclear complexes with various transition metal ions.

In this study the ligands cited in the Table have been synthesized and used for the preparation of metal complexes. The complexes obtained were formulated as two general formulas, i.e., M(L)X and $Mn_3(L)_4X_2$, where L and X represent the terdentate ligand and monovalent anion, respectively. The IR spectra and magnetic susceptibility (300-80 K) are quite consistent with the binuclear and trinuclear structures as illustrated in the Figure.

HL	Ligand
HL^1	H_2N—⁻⁻—NH—⁻⁻—SH
HL^2	H_2N—⁻⁻⁻—NH—⁻⁻—SH
HL^3	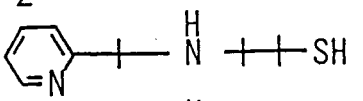
HL^4	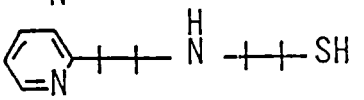

Complex	μ_{eff}/BM(T/K)	μ_{eff}/BM(T/K)
MnL^1Cl	4.88(298)	3.17(93)
MnL^2Cl	5.01(298)	3.54(93)
MnL^3Cl	4.94(298)	3.43(93)
$MnL^4Cl\cdot\frac{1}{4}H_2O$	5.14(298)	3.63(93)
$MnL^4(NO_3)$	5.21(298)	3.68(93)
$Mn_3(L^1)_4(ClO_4)_2$	4.71(298)	3.61(93)
$Mn_3(L^2)_4(ClO_4)_2$	5.16(295)	3.98(94)
$Mn_3(L^2)_4(NO_3)_2$	4.85(298)	3.82(94)
FeL^1Cl	3.58(299)	2.04(87)
FeL^3Cl	4.02(298)	2.20(93)
$FeL^4Cl\cdot\frac{1}{4}H_2O$	4.02(298)	2.37(94)
CoL^3Cl	3.33(298)	1.92(93)
$CoL^4Cl\cdot\frac{1}{4}H_2O$	3.39(298)	1.97(93)
$CoL^4(NO_3)\cdot H_2O$	4.40(295)	3.55(91)

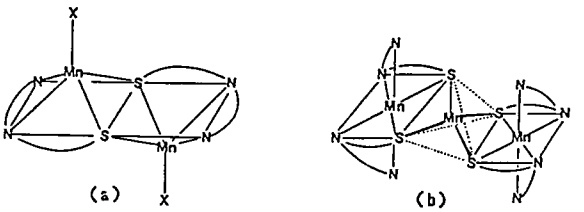

Figure 1. Assumed structure of Mn(L)X (A) and $Mn_3(L)_4X_2$ (b).

VI-B Investigation on Complexes of Transition Metals of High Oxidation State. Preparation and Characterization of Manganese Complexes with N-(2-Hydroxyphenyl)salcylamide and its Derivatives

Masayuki KOIKAWA*, Hisashi ŌKAWA* *(*Kyushu Univ.)*, **and Sigeo KIDA**

Little studies have been reported on high oxidation state transition metal complexes. This may be due to the fact that organic ligands with strong donor group are often oxidized by the high valent metal ion. Thus, we have tried to overcome the difficulty by using chelating ligands which are resistant to xidation despite of strong donating ability. In this strategy we have adopted the title ligands which are abbreviated as H_3hpsa(when R = H) and H_3R-hpsa. The complexes were obtained by mixing $Mn(CH_3\text{-}CO_2)_2\cdot 4H_2O$ with the ligand and KOH in methanol, and stirring overnight in the open atmosphere at room temperature. The complexes were characterized as Mn(IV) complexes by magnetic, ESR, conductometric, and polarographic measurements.

We have obtained violet crystals formulated as $KMn(5\text{-Me-hpsa})_2$ which is likely to be a Mn(V) complex by oxidizing $K_2[Mn(5\text{-Me-hpsa})_2]\ 4.5H_2O$ with $(NH_4)_2Ce(NO_3)_6$ in DMF.

Table 1. Magnetic, conductance, and polarographic data

complex	μ_{eef}	Λ_m	Mn^{IV}/Mn^{III}
$K_2[Mn(hpsa)_2]\cdot 4H_2O$	4.17	158.6	−0.89
$K_2[Mn(5\text{-Me-hpsa})_2]\cdot 4.5H_2O$	3.76	167.0	−0.89
$K_2[Mn(5\text{-Cl-hpsa})_2]\cdot 2H_2O$	3.67	151.1	−0.77
$K_2[mn(5\text{-}NO_2\text{-hpsa})_2]\cdot H_2O$	3.74	153.7	−0.49
$K_2[Mn(4\text{-}NO_2\text{-hpsa})_2\cdot 2H_2O$	4.27	155.1	−0.63

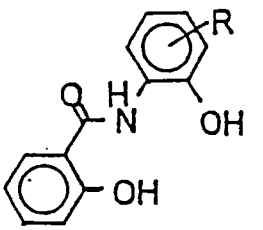

R = H, H_3hpsa, R = 5-CH_3, 5-Cl, 5-NO_2, 4-NO_2, H_3R-hpsa.

VI-C Thermodynamic and Structural Studies of Metal Complexes in Various Solvents

Complexation of Metal ions with ligands (ions or neutral molecules) in solution is significantly influenced by solvent employed. The donor and acceptor properties of solvent play an important role in relation to the

cation-solvent and anion-solvent interactions, respectively. Solvent-solvent interactions in the bulk also affect the complexation of metal ions. Metal complexes thus formed in a solution are solvated within the primary coordination sphere of the metal ion and also solvated through ligands. The coordination structure of these metal complexes changes in the course of complexation. We have studied complexation and structure of bivalent transition metal complexes in aprotic solvents with a special attention to the role of solvent.

VI-C-1 Calorimetric and Spectrophotometric Studies of Copper (II) Chloro Complexes in Dimethyl Sulfoxide

Shin-ichi ISHIGURO, Honoh SUZUKI, Bojana G. JELIAZKOVA*, and Hitoshi OHTAKI** *(*Sofia Univ., Bulgaria and **Tokyo Institute of Technology)*

[*Bull. Chem. Soc. Jpn.*, **59**, 2407 (1986)]

Complexation of Cu(II) with Cl^- ions has been studied by calorimetry and spectrophotometry in DMSO containing 0.2 mol dm^{-3} $(C_2H_5)_4NClO_4$ or 1 mol dm^{-3} $LiClO_4$ as a constant ionic medium at 25°C. Both calorimetric and spectrophotometric data obtained were well explained in terms of formation of $[CuCl_n]^{(2-n)+}$ (n = 1-4) in each solution, and their formation constants, enthalpies and entropies were determined. As well as in *N, N*-dimethylformamide (DMF),[1] positive values of stepwise ΔH_n° and ΔS_n° (n = 1-3) and negative ΔH_4° value were observed in DMSO. However, the ΔS_n° (n = 1, 2 and 4) values in DMSO were appreciably smaller than the corresponding values in DMF. The result was interpreted in terms of stronger intermolecular interactions in the bulk DMSO. The entropies of transfer of $[CuCl_n]^{(2-n)+}$ from DMF to DMSO were significantly positive, the result also suggesting that DMSO is a highly associated solvent. Electronic spectra of individual copper(II) chloro complexes were extracted from the measured spectra. In contrast to the electronic spectra of $[CuCl]_n]^{(2-n)+}$ (n = 0-2), those of $[CuCl_3]^-$ and $[CuCl_4]^{2-}$ were not appreciably different in DMSO and in DMF, indicating that solvation of these complexes are rather weak in both solvents.

Reference

1) S. Ishiguro, B.G. Jeliazkova and H. Ohtaki, *Bull. Chem. Soc. Jpn.*, **58**, 1143 (1985).

VI-C-2 Chloro Complexes of Nickel(II) and Zinc(II) Ions in *N, N*-Dimethylformamide

Shin-ichi ISHIGURO, Kazuhiko OZUTSUMI and Hitoshi OHTAKI* *(*Tokyo Institute of Technology)*

[*Bull. Chem. Soc. Jpn.*, in press]

Calorimetric titration curves obtained by titrating either nickel(II) or zinc(II) perchlorate DMF solution with a $(C_2H_5)_4NCl$ DMF solution were well explained in terms of formation of $[MCl_n]^{(2-n)+}$ (n = 1-4 and M^{2+} = Ni^{2+} or Zn^{2+}), and their formation constants, enthalpies and entropies were determined. Typical calorimetric titration curves are depicted in Figure 1 for the nickel(II) chloride system in DMF. In the nickel(II) chloride system, stepwise ΔH_3° and entropy ΔS_3° values are remarkably large and positive as compared with the ΔH_n° and ΔS_n° (n = 1, 2 and 4) values. Individual electronic spectra of $[NiCl_n]^{(2-n)+}$ (n = 0-2) are significantly different from those of $[NiCl_3]^-$ and $[NiCl_4]^{2-}$ over the range 300-850 nm. These thermodynamic and spectrophotometric results were explained in terms of formation of the octahedral $[NiCl]^+$ complex as well as $[Ni(dmf)_6]^{2+}$ and of formation of the tetrahedral $[NiCl_3]^-$ and $[NiCl_4]^{2-}$ complexes in DMF.

On the other hand, in the zinc(II) chloride system, the ΔS_1° and ΔS_2° values are large and positive but the

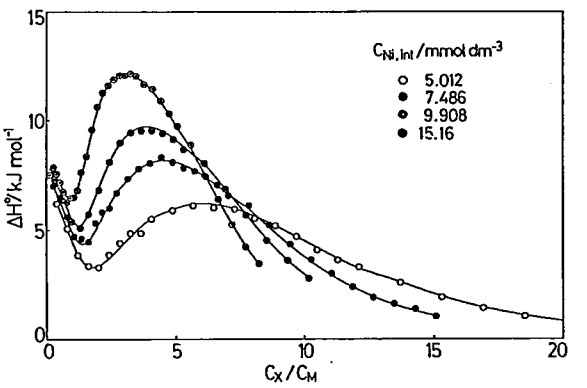

Figure 1. Calorimetric titration curves of nickel(II) chloride DMF solutions containing 0.4 mol dm^{-3} $(C_2H_5)_4NClO_4$ at 25°C. Enthalpies per the addition of a unit mole of Cl^- were plotted against the concentration ratio C_X/C_M in solution at each titration point. The solid lines show the theoretical curves calculated using the formation constants and enthalpies finally obtained by the least-squares refinement.

ΔS_3° and ΔS_4° values are significantly small. The corresponding ΔH_1° and ΔH_2° values are positive but the ΔH_3° and ΔH_4° values are significantly negative. It is thus postulated that the $[ZuCl_n]^{(2-n)+}$ (n = 2 and 3) complexes have the tetrahedral coordination structure as well as the $[ZnCl_4]^{2-}$ complex in DMF.

VI-C-3 An X-Ray Diffraction Study on the Structure of Monochlorocopper(II), Trichloro- and Tetrachlorocuprate(II) Complexes in *N*, *N*-Dimethylformamide

Kazuhiko OZUTSUMI, Shin-ichi ISHIGURO and Hitoshi OHTAKI* *(*Takyo Institute of Technology)*

The structure of the monochlorocopper(II), trichloro- and tetrachlorocuprate(II) complexes in *N*, *N*-dimethylformamide has been determined by X-ray diffraction at 25°C. The radial distribution curve obtained in a solution predominantly involving the monochloro complex was well explained in terms of the distored octahedral six-coordinate structure about the metal ion as represented by $[CuCl(dmf)_5]^+$ similar to $[Cu(dmf)_6]^{2+}$. On the other hand, the distorted tetrahedral four-coordinate structure was proposed for The strucutre of $[CuCl(dmf)_5]^+$, $[CuCl_3(dmf)]^-$ and The strucutre of $[CuCl(dmf)_3]^+$, $[CuCl_3(dmf)]^-$ and $[CuCl_4]^{2-}$ and bond lengths (r/pm) thus obtained are depicted in Figure 1. It is noted that the Cu-dmf bond length within $[CuCl_3(dmf)]^-$ is considerably longer than that at the equatorial position within $[Cu(dmf)_6]^{2+}$ or $[CuCl(dmf)_5]^+$. The structure of the dichloro complex could not be determined in DMF because of a less extensive formation of the complex comapred to that of the other species.

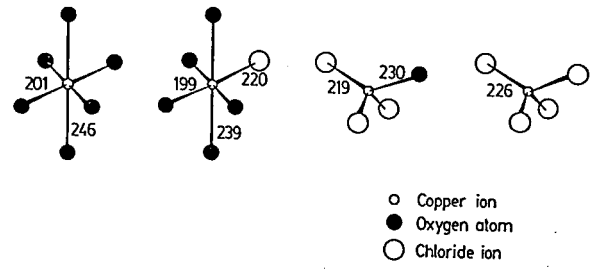

Figure 1. The coordination structure of $[Cu(dmf)_6]^{2+}$, $[CuCl(dmf)_5]^+$, $[CuCl_3(dmf)]^-$ and $[CuCl_4]^{2-}$ in *N*, *N*-dimethylformamide.

VI-D Kinetic Studies of Thermal and Photochemical Decomposition of Binuclear Cobalt Complexes Bridged by Peroxide Ion

This type of complex is an important oxygen carrier and also important intermediate compound for the traditional synthesis of uninuclear cobalt(III) complexes.

VI-D-1 Mechanism of Acid-Catalysed Decomposition of the (Δ, Δ)-(μ-Hydroxo)(μ-persoxo) bis[bis(ethylenediamine)cobalt(III)] ion

Masahiro EBIHARA, Yoichi SASAKI* and Kazuo SAITO *(*Tohoku Univ.)*

[*Inorg. Chem.*, **24**, 3831 (1985)]

The change in absorption spectrum accompanied by the decomposition of this ion to cobalt(II) ions and dioxygen in perchloric acid takes place in two steps. The initial step completes within 5 ms and corresponds to protonation equilibrium with K = *ca.* 10 M^{-1} to give an absorption maximum at 520 nm. The second step is observable at 35°C and k = 0.02 − 0.3 s^{-1} depending on the acid concentration. The decomposition seems to proceed exclusively from the protonated species through the cleavage of hydroxide bridge to give a single bridged binuclear species which subsequently undergoes deoxygenation.

VI-D-2 Photochemical and Thermal Decomposition of (ΔΔ, ΔΔ)-(μ-peroxo)bis[bis(ethylenediamine)covalt(III)] Ions in Basic Solution

Masahiro KIKKAWA, Yoichi SASAKI*, Satoshi KAWATA*, Yoshihiro HATAKEYAMA, Fumio B. UENO and Kazuo SAITO *(*Tohoku Univ.)*

[*Inorg. Chem.*, **24**, 4096 (1985)]

This complex ion does not undergo deoxygenation

in the dark, but does on irradiation with ultraviolet light to reach an equilibrium giving dioxygen and $[Co(en)_2(H_2O)]^{3+}$. The quantum yield is independent of pH at 8.1 to 10.4, and 2.2×10^{-3} and $< 2 \times 10^{-6}$, on irradiation at 366 nm at 5°C and at 515 nm at 25°C, respectively. The O_2 to metal charge transfer excited state is relevant to the deoxygenation. Continuous irradiation leads to subsequent irrevasible decomposition, but such a reaction is much slower in the dark.

VI-E Existence of Selectivity in Electron Transfer Reactions

Such a reaction is very important as an elementary reaction for complex catalysis. Our previous studies are being extended to more complicated systems involving ion triplets as precursor.

VI-E-1 Stereoselectivity Induced by an Optically Active Cationic Cobalt(III) Complex Ion on the Outer-Sphere Redox Reaction between Hexachloroiridate(IV) and Racemic Binuclear Molybdenum(V) Anions in Water

Yoichi SASAKI*, Katsuhiko MEGURO and Kazuo SAITO *(*Tohoku Univ.)*

[*Inorg. Chem.*, **25**, 2277 (1986)]

Redox reaction between $\Delta\Delta$-$(en)_2Co^{III}(\mu\text{-}O_2, NH_2)Co^{III}(en)_2]^{3+}$ and binuclear $[Mo_2O_4$(R or S-pdta)$]^{2-}$ give appreciable selectivity both at the precursor formation and electron transfer stage. Use of non-optically active $[IrCl_6]^{2-}$ in the presence of optically active counter ion Λ-$[Co(en)_3]^{3+}$ exhibits stereoselectivity of the order of less than 1% and the more easily oxidized $Mo_2O_4^{2+}$ species is either S or R isomer depending on the absolute configulation of the cationic Λ- or Δ-cobalt(III) species, respectively.

VI-F ESR Studies on the Thermal and Photochemical Alkyl Elimination Reactions of Hexanuclear Molybdenum Cluster Alkyl Complexes

Taro SAITO *(Osaka Univ. and IMS)* **and Shozo TERO**

The solutions of the molybenum cluster alkyl complexes $[(Mo_6Cl_8)Cl_{4-n}R_n(PR'_3)_2]$ ($n = 2 - 4$) decompose at *ca.* 50°C or upon irradiation with visible light. The ESR spectra of the alkyl radical adducts with nitrosodurene or 2, 4,-6-tri-*t*-butylnitrosobenzene and free benzyl radicals were studied under thermal or phorochemical reaction conditions. The results have shown that the Mo-C bond cleaves homolytically to give transient radicals which can abstract hydrogen either from the solvent or the ligands on the cluster complex but do not couple together. The photolysis was very efficient and upon irradiation with the light ($\lambda > 550$ nm), the Mo-C bond scission took place instantaneously. The tetrabenzyl complex revealed free benzyl radical signals in toluene at −90°C, which persisted as long as the irradiation continued demonstrating the possible homolysis and recombination of the Mo-CH_2Ph bond. The photolysis of the clusters in methyltetrahydrofuran at 77 K indicated the absorptions which could be assigned to the molybdenum cluster species at $g_\perp = 1.96$ and $g_\parallel = 1.89$.

VI-G Solvent Exchange on Metal(II) Ions in Acetic Acid

Solvent exchange processes on metal ions are the fundamental phenomena of metal ions in solution and studies on such processes are very important for elucidating the reaction mechanisms of metal complex formation. Acetic acid (HOAc) is an interesting solvent, which has an amphiprotic character and low dielectric constant. We have

investigated the rate of exchange of acetic acid between the bulk acetic acid and the coordination sphere of divalent cations in acetic acid by the ^{17}O FT-NMR line-broadening technique.

VI-G-1 Oxygen-17 Nuclear Magnetic Resonance Studies on the Acetic Acid Exchange of Manganese(II), Iron(II), Cobalt(II), Nickel(II), and Copper(II) Perchlorates in Acetic Acid

Shigenobu FUNAHASHI *(Nagoya Univ. and IMS)*, **Akiharu HIOKI,* Masao ISHII,* and Motoharu TANAKA*** *(*Nagoya Univ.)*

[*Inorg. Chem.*, **25**, 1360 (1986)]

The exchange between bulk acetic acid molecules and the acetic acid molecules bound to the transition metal cations (Mn(II), Fe(II), Co(II), and Cu(II)) in neat acetic acid and in mixtures involving dichloromethane-d_2 as a diluent has been studied by the oxygen-17 line broadening method. The exchange rate constants at 25 °C and activation parameters were obtained as follows: $k = (1.6 \pm 0.1) \times 10^7\ s^{-1}$, $\Delta H^{\ddagger} = 29 \pm 2$ kJ mol^{-1}, and $\Delta S^{\ddagger} = -10 \pm 7$ J mol^{-1} K^{-1} for $Mn(ClO_4)_2$; $k = (5 \pm 1) \times 10^6\ s^{-1}$, $\Delta H^{\ddagger} = 33 \pm 5$ kJ mol^{-1}, and $\Delta S^{\ddagger} = -8 \pm 20$ J mol^{-1} K^{-1} for $Fe(ClO_4)_2$; $k = (1.3 \pm 0.2) \times 10^6\ s^{-1}$, $\Delta H^{\ddagger} = 37 \pm 3$ kJ mol^{-1}, and $\Delta S^{\ddagger} = -6 \pm 12$ J mol^{-1} K^{-1} for $Co(ClO_4)_2$; $k = (2 \pm 1) \times 10^5\ s^{-1}$, $\Delta H^{\ddagger} = 40 \pm 5$ kJ mol^{-1}, and $\Delta S^{\ddagger} = -10 \pm 20$ J mol^{-1} K^{-1} for $Ni(ClO_4)_2$. The rate constant for $Cu(ClO_4)_2$ is about $1 \times 10^7\ s^{-1}$ at −25°C. The solvent exchange rates in acetic acid increase in the order Ni(II) < Co(II) < Fe(II) < Mn(II) < Cu(II), which is identical with that in the other solvents.

VI-G-2 Kinetic Study of Acetic Acid Exchange on Manganese(II), Cobalt(II), and Copper(II) Acetates in Acetic Acid by Oxygen-17 Nuclear Magnetic Resonance

Shigenobu FUNAHASHI *(Nagoya Univ. and IMS)*, **Akiharu HIOKI,* and Motoharu TANAKA*** *(*Nagoya Univ.)*

[*Inorg. Chem.*, **25**, 2904-2907 (1986)]

The activation parameters for the acetic acid exchange on each acetate salt were independent of the concentration of acetic acid in the acetic acid/dichloromethane-d_2 mixtures. The first-order rate constants at 25°C and the activation parameters are $k = (4.8 \pm 0.9) \times 10^7\ s^{-1}$, $\Delta H^{\ddagger} = 32 \pm 3$ kJ mol^{-1}, and $\Delta S^{\ddagger} = 9 \pm 11$ J mol^{-1} K^{-1} for $Mn(OAc)_2$, $k = (9.9 \pm 3.3) \times 10^6\ s^{-1}$, $\Delta H^{\ddagger} = 37 \pm 3$ kJ mol^{-1}, and $\Delta S^{\ddagger} = 14 \pm 12$ J mol^{-1} K^{-1} for $Co(OAc)_2$, and $k = (2.8 \pm 0.1) \times 10^4\ s^{-1}$, $\Delta H^{\ddagger} = 51 \pm 2$ kJ mol^{-1}, and $\Delta S^{\ddagger} = 12 \pm 6$ J mol^{-1} K^{-1} for $Cu_2(OAc)_4$. These activation parameters were compared with those obtained for the corresponding perchlorates in acetic acid.

VI-H Magnetism and Superconductivity in Rare Earth Rhodium Borides with Cubic Perovskite Structure

Humihiko TAKEI, Toetsu SHISHIDO*, and Hiroyuki TAKEYA*

Up to the present, a large number of oxides, nitrides and carbides with perovskite structure have been reported. However, very few studies on perovskite borides have been performed. In rare earth rhodium boride perovskites $PERh_3B$(RE = rare earth elements and yttrium), RE locates at the corners of perovskite cube, Rh at the face-centered positions and B at the body-centered position. The present report deals with the magnetic properties as well as superconductivity of $RERh_3B$.

Specimens were prepared by argon-arc melting of the mixture of RE ingots, Rh powder and B flakes. All specimens were checked with X-ray powder diffraction technique, and no other phase except cubic perovskite was observed. Single crystals were grown using the flux method from metallic Cu solution(1).

Magnetic susceptibility measurements revealed that the perovskites of Ce, Pr, Nd, Dy, Ho, Er, Tm and Yb exhibited normal paramagnetic behaviors. As shown in Table 1, the normal paramagnetic moments to p_{eff}

corresponds to the Hund's values for free trivallent ions except for $CeRh_3B$. Ferromagnetic orderings were observed for Gd- and Tb-perovskites. VRh_3B showed Pauli-paramagnetism between 300 and 1K, and became superconductive at 0.76K as a typical type II superconductor(2). These results indicate that RE exhibits as a trivallent ion and excess electrons are transferred to Rh and/or B to strengthen the bonds in the octahedral Rh_6B sublattice.

Table 1. Magnetic Properties of $RERh_3B$

RE	Peff*		T_m(K)**	θ_p(K)***
	Exp.	Hund		
Ce	3.88	2.54		0
Pr	3.80	3.58		0
Nd	4.02	3.62		0
Sm		0.84		
Eu		0.00		
Gd	8.04	7.94	12.8	8
Tb	9.92	9.72	14.5	7
Dy	10.8	10.63		0
Ho	10.7	10.60		0
Er	9.83	9.59		0
Tm	7.70	7.54		0
Yb	5.20	4.50		0

* effective paramagnetic moment
** ferromagnetic transition temperature
***extrapolated Curie-Weiss temperature

References

1) H. Takei and T. Shishido, *J. Less-Common Met.*, **97** 223(1984).
2) H. Takei, N. Kobayashi, H. Yamauchi, T. Shishido and T. Fukase, *J. less-Common Met.*, in press.

* The Research Institute for Iron, Steel and Other Metals, Tohoku University

VI-I Time-resolved ESR Study of the Excited Triplet States of Zinc Schiff Base Complexes

Shozo TERO-KUBOTA, Kouto MIGITA *(Yamaguchi Univ.)*, **Hiroki OSHIO, and Jiro HIGUCHI** *(Yokohama National Univ.)*

Time-resolved ESR spectra of the lowest excited triplet states of several Zinc Schiff base complexes were measured in an ethanol-toluene (1:1) glassy matrix at 77 K.

Drawing the transient ESR spectra were detected using a JOEL FE2XG ESR spectrometer modified wide-band preamplifier without magnetic field modulation. The signal was taken into a boxcar integrator at arbitary times after lower pulse. A nitrogen laser (Molectron UV-24) was used as a light source with a repetition rate at 20Hz.

Figure 1 shows the time-resolved EST spectra of Zn (Salphen), Zn (Salen), and Zn (Sal-methyl)$_2$ observed at 1 μs after the light pulse. The triplet ESR spectra ovserved in the present complexes are predominantly attributable to $\pi\pi^*$ of the ligand conjugation system from the value of zero-field splitting parameters. In the quadridentate Schiff base complexes, the electron spin polarization of EEEA/EAA was observed suggesting the initial population to the highest T_X sublevel in the intersystem crossing (ISC) process. On the other hand, bis-bidentate complex shows A0AE/AE0 polarization, where 0 means nearly zero electron spin polarization. This result indicates that the middle T_Y sublevel is mainly populated while the initial population to the lowest T_Z sublevel is not negligible in the ISC process.

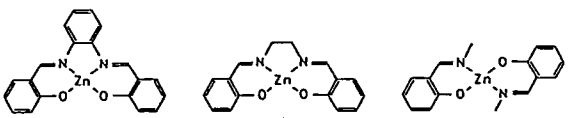

Zn(Salphen) Zn(Salen) Zn(Sal-methyl)$_2$

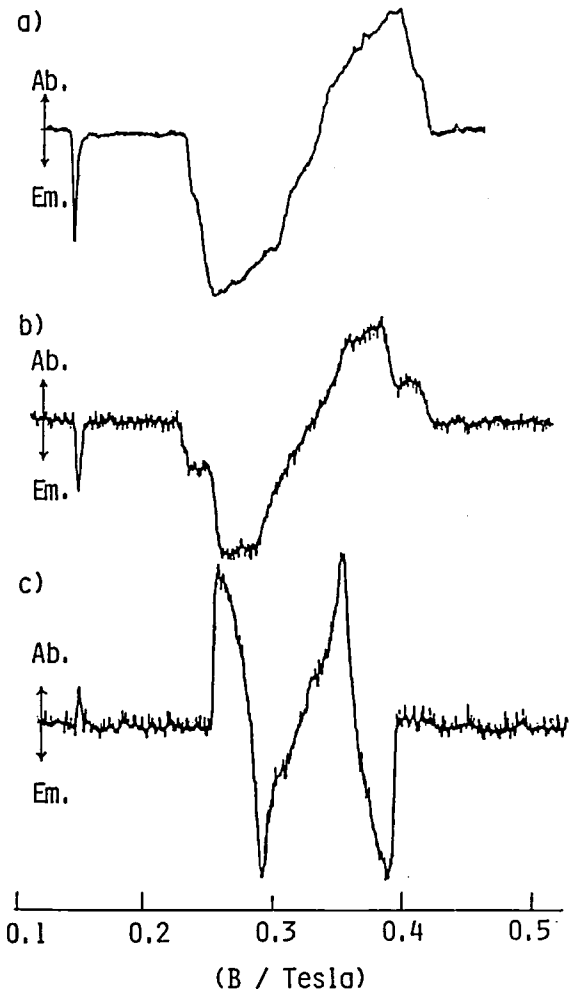

Figure 1. Time-resolved ESR spectra of Zn (Salphen) (a), Zn (Salen) (b), and Zn (Sal-methyl)$_2$ observed in an ethanol-toluene (1:1) glassy matrix at 77 K.

RESEARCH ACTIVITIES VII
Computer Center

VII–A Theoretical Investigatigations of Metalloporphyrins by the Ab Initio SCF MO Method

Metal complexes are interesting polyatomic systems because of their complicated electronic structure and their catalytic functions. Metalloporphyrins are prominently important as an active center of energy conversion processes in biological systems. In this project the electronic structure and the fundamental functions are studied for several complexes by performing *ab initio* MO computations.

VII-A-1 *Ab initio* CASSCF Calculations for Large Molecules

Shigeyoshi YAMAMOTO, Umpei NAGASHIMA, and Hiroshi KASHIWAGI

We developed a new program package "JASON2" for *ab initio* CASSCF (Complete Active Space SCF) calculations with large basis sets. CASSCF is one of the formalisms of MCSCF (Multi-Configuration SCF), proposed by Roos et al.[1] using a density-matrix-formulated super-CI approach. The super-CI method is less laborious than other MCSCF methods in integral transformation which is the most time-consuming step. This fact is advantageous particularly for large molecules. We have performed preliminary calculations on iron-oxo-porphyrin which contains 49 atoms and 236 electrons in C_{2V} symmetry. The total number of CGTOs used is 232. We chose 10 orbitals as the active orbitals in which 12 active electrons can excite in all possible ways. It gives CAS (Complete Active Space) with 5220 configurations. In the actual program, MCSCF iteration goes through three steps i.e. integral transformation, full-CI in CAS and super-CI. The timing data of the calculation is given in table I. All calculations were carried out on a supercomputer HITAC S-810/10 at the IMS Computer Center.

Table I. Timing data of CASSCF calculation of FeP(py)O

Step	scalar S	vector V	ratio S/V
Integral transform	12′33″	3′32″	3.54
CI	8′10″	4′20″	1.89
Super-CI	1′49″	1′11″	1.33
Total	22′33″	9′15″	2.44

CPU-time on S-810/10 for 1 iteration.
S means CPU-time on a scalar processor.

Reference

1) B.O. Roos, P.R. Taylor, and P.E.M. Siegbahn, *Chem. Phys.*, **48**, 157 (1980).

Chemical Materials Center

VII–B Chemistry of New Matallacyclic Compounds

The study on metallacyclic compounds is directly relevant to an understanding of the reaction mechanisms of sysnthetically important catalyses such as olefin oligomerization, cyclocoupling, metathesis, and so on, and may also provide the basis for developments of new efficient catalyst systems. We have been studying synthesis, characterization, and reactions of new metallacyclic compounds.

VII-B-1 Reaction of $(\eta^5\text{-}C_5Me_5)_2\overline{TiOC[=Re(CO)_4Re(CO)_5]CH_2CH_2}$ with *tert*-Butylisocyanide: Molecular Structure of A New Zwitterionic Complex Involving η^2-Imidoyltitanium and Acyldirhenium Carbonyl Moieties

Kazushi MASHIMA, Kouki JYODOI,* Akira OHYOSHI,* and Hidemasa TAKAYA (*: *Kumamoto Univ.*)

[*Organometallics*, in press]

Chemistry of carbene-metal complexes has been the

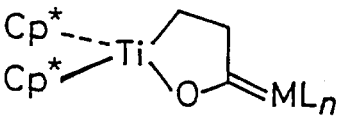

1a, $ML_n = Re_2(CO)_9$
1b, $ML_n = W(CO)_5$

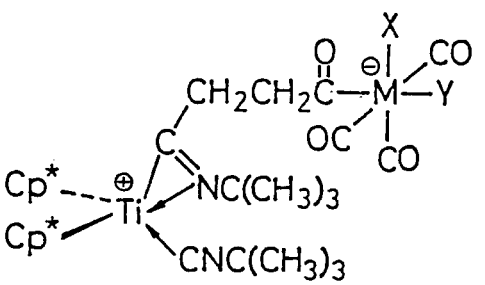

2, M = Re, X = $Re(CO)_5$, Y = CO
3, M = Re, X = CO, Y = $Re(CO)_5$
4, M = W, X = Y = CO

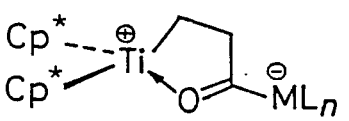

5

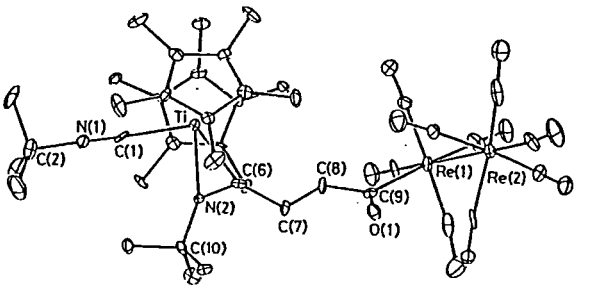

Figure 1. Molecular structure of the complex **2**, with all hydrogens omitted for clarity.

subject of considerable current interest. We have previously reported the synthesis and characterization of new cyclic titanoxycarbene-metal carbonyl complexes (**1**) [Cp* = η^5-C_5Me_5; ML_n = $Re_2(CO)_9$, W $(CO)_5$, *etc.*].[1] We now report the molecular structures of the novel complexes obtained by the reactions of **1** with *tert*-butylisocyanide.

Treatment of an orange-red solution of **1a** in toluene with excess *tert*-butylisocyanide under argon at −35°C and then at room temperature gave, after workup, air-sensitive 1:2 complex **2** in 81% yield. A single-crystal *X*-ray study of **2** has shown that the complex has a novel zwitterionic structure possessing η^2-imidoyltitanium cation and anionic acyldirhenium carbonyl moieties linked by a two-methylene bridge. The controlled experiments show that **2** is produced by a thermal rearrangement of the initially formed complex **3** in which acyl ligand is trans to the Re-Re bond. The tungsten derivative **1b** also gives the corresponding tungsten analogue of **2**. The above results suggest that these reactions will be general for the cyclic titanoxycarbene-metal carboyl complexes of type **1**. Since titanium has strong oxophilic nature, dissociation of oxygen ligand from titanium is rather unusual. This may be a consequence of the unique molecular structure of the starting complex **1** which has a long Ti-O bond and considerably shorter C(3)-O bond length than that of a usual C-O single bond, indicating an important contribution from the dipolar resonance structure **5**.[1]

Reference

1) K. Mashima, K. Jyodoi, A. Ohyoshi, and H. Takaya, *J. Chem. Soc., Chem. Commun.*, 1145 (1986).

VII–C Synthesis of New Chiral Diphosphines and Their Use in Homogeneous Asymmetric Catalysis

The molecular designing and synthesis of new effective chiral ligands are the most important requirements for developing synthetically useful asymmetric catalysis. Our attention has been focussed on the subjects of developments of new effective homogeneous asymmetric catalysis and elucidation of the reaction mechanisms and factors controlling the asymmetric induction.

VII-C-1 Synthesis and Molecular Structure of New BINAP-Ru(II) Dicarboxylate Complexes: Extremely Efficient Catalysts for Asymmetric Hydrogenation

Tetsuo OHTA, Hidemasa TAKAYA, and Ryoji NOYORI *(Nogoya Univ.)*

For the purpose of developing efficient homogeneous asymmetric catalyses utilizing (*R*)- or (*S*)-2,2′-bis(diphenylphosphino)-1,1′-binaphthyl (abbreviated to BINAP),[1),2)] new types of ruthenium complexes, Ru(binap)$(OCOR)_2$ (**1a-e**) have been prepared. The crystal structure of (*S*)-**1b**, determined by *X*-ray crystallography (diffraction data collected at −60 °C, $R = 0.038$, $R_W = 0.044$), is given in Figure 1. The complex has Λ structure, while the BINAP-containing seven-membered chelate ring is fixed in a δ conformation.

These BINAP-Ru complexes serve as extremely efficient catalysts for various homogeneous asymmetric hydrogenations of olefinic substrates such as *N*-acyl-1-alkylidenetetrahydroisoquinolines, allylic alcohols, and α,β-unsaturated carboxylic acids.

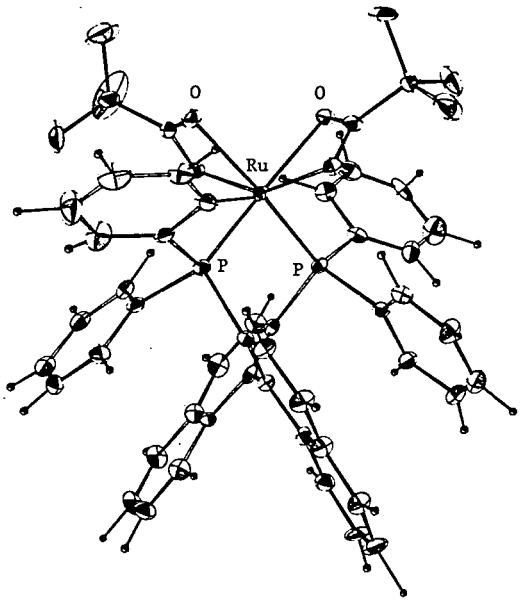

Figure 1. Molecular structure of the complex Ru((S)-binap)$(OCOC(CH_3)_3)_2$ (**1b**). Hydrogen atoms of the *tert*-butyl groups were omitted for simplicity.

References

1) A. Miyashita, A. Yasuda, H. Takaya, K. Toriumi, T. Ito, T. Souchi, and R. Noyori, *J. Am. Chem. Soc.*, **102**, 7932 (1980).
2) H. Takaya, K. Mashima, K. Koyano, M. Yagi, H. Kumobayashi, T. Taketomi, S. Akutagawa, and R. Noyori, *J. Org. Chem.*, **51**, 629 (1986).

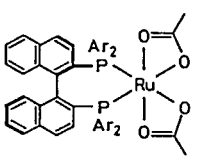

(*R*)−1

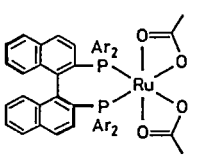

(*S*)−1

a, Ar = C_6H_5 ; R = CH_3
b, Ar = C_6H_5 ; R = $C(CH_3)_3$
c, Ar = C_6H_5 ; R = CF_3
d, Ar = p-$CH_3C_6H_4$; R = CH_3
e, Ar = p-$CH_3C_6H_4$; R = CF_3

VII-C-2 Asymmetric Synthesis of Isoquinoline Alkaloids by Homogeneous Catalysis

Ryoji NOYORI, Masako OHTA, Yi HSIAO, Masato KITAMURA *(Nagoya Univ.)*, **Tetsuo OHTA, and Hidemasa TAKAYA** *(IMS)*

[*J. Am. Chem. Soc.*, **108**, 7117 (1986)]

Extremely efficient asymmetric hydrogenation of *N*-acyl-1-alkylidenetetrahydroisoquinolines catalyzed by new BINAP-based Ru(II) dicarboxylate complexes

has been developed. Homogeneous hydrogenation of the *Z* enamide substrates of type **1** in the presence of a catalytic amount of Ru(*(R)*-binap)$(OCOCH_3)_2$ [*(R)*-**3**] in a mixture of ethanol and dichloromethane under 1 to 4 atm of hydrogen at room temperature leads to the 1-alkyltetrahydroisoquinolines (**2**) having the 1*R* configuration in 95-100% ee. Use of Ru((*S*)-binap)$(OCOCH_3)_2$ catalyst [*(S)*-**3**] affords the 1*S* products. This enantioselective reaction followed by removal and/or modification of the *N*-acyl groups leads easily to tetrahydropapaverine (**4**), laudanosine (**5**), tretoquinol (**6**), and norreticuline (**7**) of high optical purities. The asymmetric hydrogenation of a simple 1-methylene analogue of **1** gives after deacylation salsolidine (**8**). The present catalysis is simple and general, and allows synthesis of both antipodes equally in high enantiomeric excess.

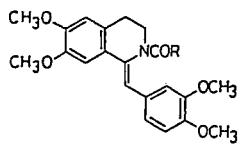

1, R = H, CH_3, C_6H_5, etc.

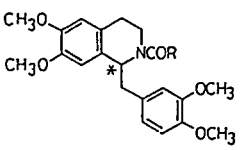

2, R = H, CH_3, C_6H_5, etc.

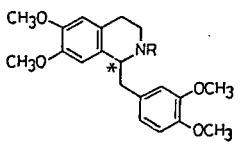

4, R = H
5, R = CH_3

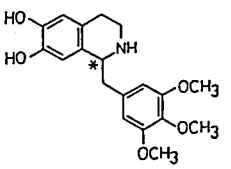

6

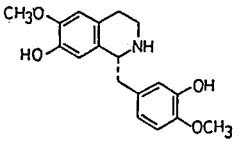

7

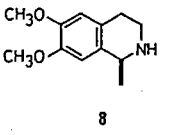

8

VII-C-3 Highly Enantioselective Hydrogenation of Allylic Alcohols by the Use of BINAP-Based Ru(II) Complexes

Hidemasa TAKAYA, Tetsuo OHTA *(IMS)*, **Shin-ichi INOUE, and Ryoji NOYORI** *(Nagoya Univ.)*

[*J. Am. Chem. Soc.*, in press]

Some selected Rh^+ and Ir^+ complexes are known to catalyze the hydroxyl-directed diastereoselective hydrogenation of *chiral* allylic and homoallylic alcohols. This methodology presents considerable synthetic potential, but highly enantioselective hydrogenation of the *prochiral* substrates is still elusive. We disclose here a highly enantioselective hydrogenation of allylic alcohols catalyzed by the newly synthesized Ru(II) dicarboxylate complexes of BINAP and *p*-TolBINAP, which brings about a breakthrough in this important but yet unsolved problem.

Geraniol (**2**) or nerol (**3**) was hydrogenated by 40-100 atm of hydrogen in the presence of a catalytic amount of Ru(*(S)*-binap)$(OCOCH_3)_2$ [*(S)*-**1**] at room temperature for 2~3 h to give *(R)*- or *(S)*-citronellol (**4**), respectively, in 96~98% ee. The yield of **4** is nearly quantitative. The allylic and nonallylic double bonds in **2** and **3** can be clearly differentiated; the product was accompanied by less than 0.5%, if any, of dihydrocitronellol (**5**). The substrate/catalyst ratio is extremely high (up to 50,000). The stereochemical relationship of the catalytic reaction is shown in Scheme I. The present result marks the first example of highly enantioselective hydrogenation of the simple prochiral unsaturated alcohols, providing a new, powerful, and potentially general means in synthesis of optically active terpenes and related compounds. Indeed, this procedure has been successfully applied to the asymmetirc sysnthesis of the alcohol **8**, the C_{15} side chain of vitamin E (**6**), from **7**. The diastereomeric purity of **8** thus obtained was determined to be 98%.

Scheme I

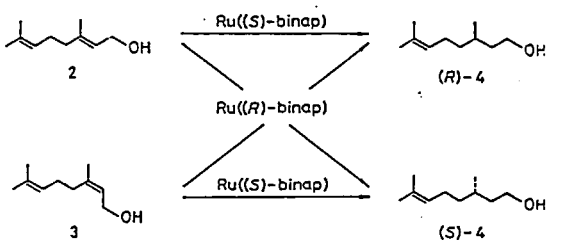

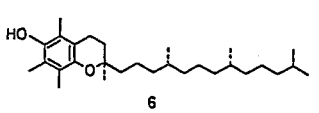

6

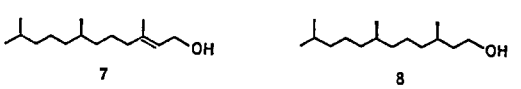

7 8

Instrument Center

VII–D Excitation-Energy Transport in Organized Molecular Assemblies

The present study is concerned with multilayered molecular assemblies such as Langmuir-Blodgett films and phospholipid bilayers in which the long-distance excitation energy transport (Förster type) takes place in two- and three-dimensional architectures. The dynamical characteristics are investigated by means of a picosecond time-resolved fluorescence spectrophotometer.[1] The focus has been directed to (1) fundamentals of energy migration and collection in multilayered architectures and (2) photochemical reactions under the highly-ordered molecular assemblies. The goal of our work is to develop new electrooptic devices capable of spatial control and switching of photonic-energy transport.

Reference

1) I. Yamazaki, N. Tamai, H. Kume, H. Tsuchiya, and K. Oba, *Rev. Sci. Instrum.*, **56**, 1187 (1985).

VII-D-1 Sequential Excitation-Energy Transport in Stacked Multilayers of Langmuir-Blodgett Type

Iwao YAMAZAKI, Naoto TAMAI, Tomoko YAMAZAKI, and Katsuhiro SUMI

The Langmuir-Blodgett (LB) film is an ordered molecular assembly in which one can build up in a desired structure with different kinds of monolayers. The LB film provides us with an artificial multilayered structure analogous to an antenna pigment system of the photosynthetic organism in plants, in particular, analogous to the accessary pigment system of phycobilin-chlorophyll complex in algae.[1] The present study has been initiated with a view to investigating kinetics of Förster-type excitation-energy transfer in multilayered architectures in a comparative study through biological and artificial systems. Figure 1 shows the time-resolved fluorescence spectra of the LB film consisting of a sequence of donor (CC) and acceptor (DC). When the outer surface layer is excited at 540 nm laser pulses, two fluorescence bands due to the donor monomer and dimer (λ_{max} = 570 and 640 nm, respectively) appear in the initial time region. In longer time region, the fluorescence band due to the acceptor is grown up (λ_{max} = 665 nm), indicating that the photonic energy is transferred sequentially among the layers of donor and acceptor. We can deduce kinetics of sequential energy transport as a function of distance between the layers.

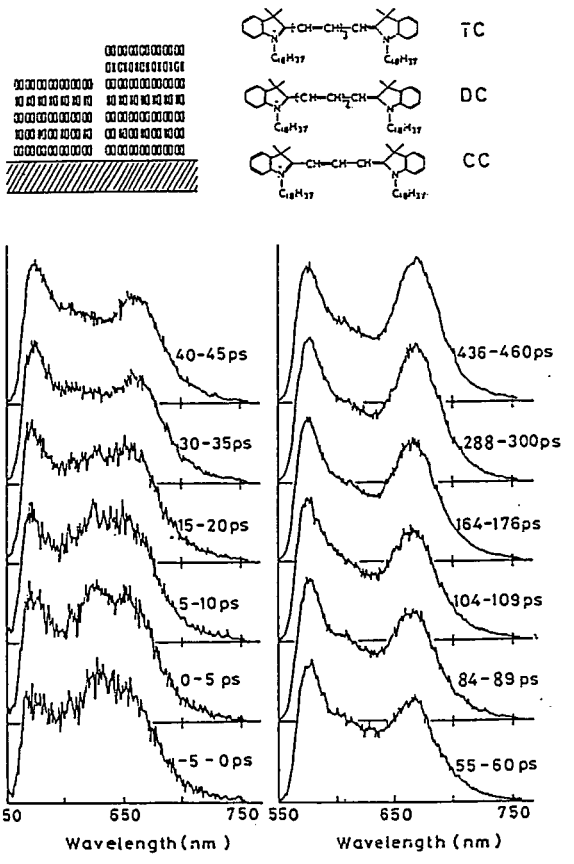

Figure 1. Schematic illustration of LB multilayer film containing three kinds of cyanine dyes in each monolayer, and time-resolved fluorescence spectra of the LB film.

Reference

1) I. Yamazaki, M. Mimuro, T. Murao, T. Yamazaki, K.

Yoshihara, and Y. Fujita, *Photochem. Photobiol.*, **39**, 233 (1984).

VII-D-2 Two-Dimensional Excitation-Energy Transfer in Langmuir-Blodgett Monolayers

Naoto TAMAI, Tomoko YAMAZAKI, and Iwao YAMAZAKI

[*J. Phys. Chem.*, in press]

The two-dimensional excitation-energy transfer of Förster type has been studied with Langmuir-Blodgett monolayers containing 11-(N-carbazolyl) undecanoic acid (CU, donor) and 16-(9-anthroyloxy) parmitic acid (AP, acceptor). Fluorescence decay curves of donor (1.5 mol%) in the presence of acceptors (1.5-8.5 mol%) were measured with a picosecond time-correlated, single-photon counting apparatus. The decay curves (Figure 1) were analyzed in terms of time-dependent equation of excited-state survival in the two-dimensional energy transfer system. At substantially higher concentrations of acceptor (5 mol%), the fluorescence decay follows an equation of the two-dimensional energy transfer kinetics plus an exponential decay term:

$$\varrho(t) = A_1\exp[-t/\tau_D - 2\gamma_A(t/\tau_D)^{1/3}] + A_2\exp(-t/\tau_D)$$

At lower concentrations, the energy transfer competes with the fluorescence quenching due to the electron transfer from a photo-excited carbazole chromophore to carboxyl groups of stearic acid of the LB film. A non-exponential decay curve of carbazole chromophore without acceptor, which is independent of the concentration, is found to be consistent with a theoretical decay function of the electron transfering quenching.

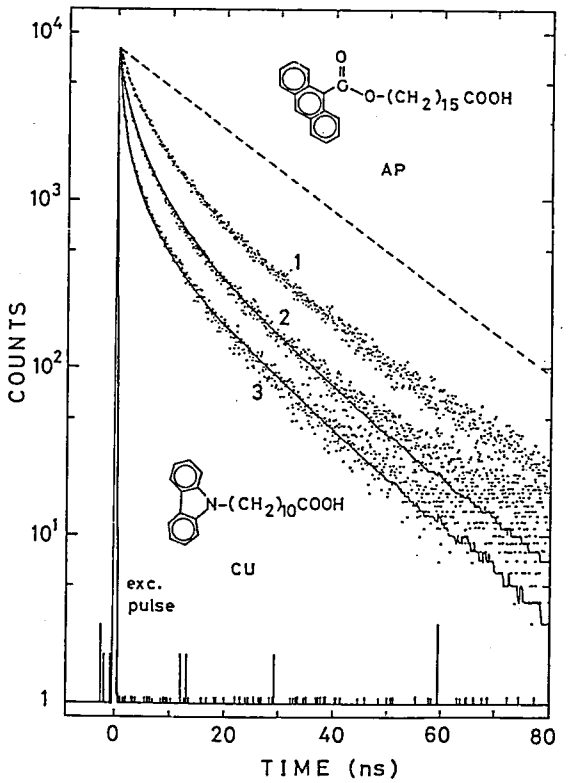

Figure 1. Fluorescence decay curves of donor CU in LB film in the presence of acceptor AP. A broken line is the exponential decay curve obtained for CU in ethanol solution; the lifetime is 20 ns. The solid lines depicted on the experimental curves are the best fit curve obtained with simulating calculation.

References

1) M. Hauser, U.K.A. Klein, and U. Gosele, *Z. Physik. Chem. NF*, **101**, S255 (1976).

VII-D-3 Fractal Structures and Excitation Energy Transfer in Molecular Organizates

Naoto TAMAI, Iwao YAMAZAKI, Tomoko YAMAZAKI, and Noboru MATAGA *(Osaka Univ. and IMS)*

Statistical self-similar structures, which are referred to as fractals, are emerging as an essential concept underlying the behavior of disordered systems.[1] In cases of the Förster-type energy transfer, the decay function of the donor fluorescence is given by a equation characterized by the fractal dimension, $\bar{d}$, which generally differs from the dimension of the embedding Euclidean space.[2] We have studied on the two-dimensional excitation energy transfer with vesicles and Langmuir-Blodgett films on the basis of the fractal analysis as well as the classical statistics.

The fluorescence decays of rhodamine 6G (donor) in the presence of malachite green (acceptor) adsorbed on anionic DHP vesicle surface were analyzed in terms of the fractal theory. The analysis gives the fractal dimension $\bar{d} = 1.31 \pm 0.087$ which is constant irrespective of the acceptor concentration. Provided that the correlation function of dye distribution is following an equation $P(r) \propto r^{-\bar{d}}$, the fractal pattern were obtained for $\bar{d} = 1.3$ along with $\bar{d} = 1.9$ and 1.1. The results are shown in Figure 1 indicating that the dye molecules are not randomly distributed on the vesicle surface, and its

distribution forms a fractal structure.

References

1) B.B. Mandelbrot, "*The Fractal Geometry of Nature*", Freeman, San Francisco, 1982.
2) J. klafter and A. Blumen, *J. Chem. Phys.* **80**, 875 (1985).

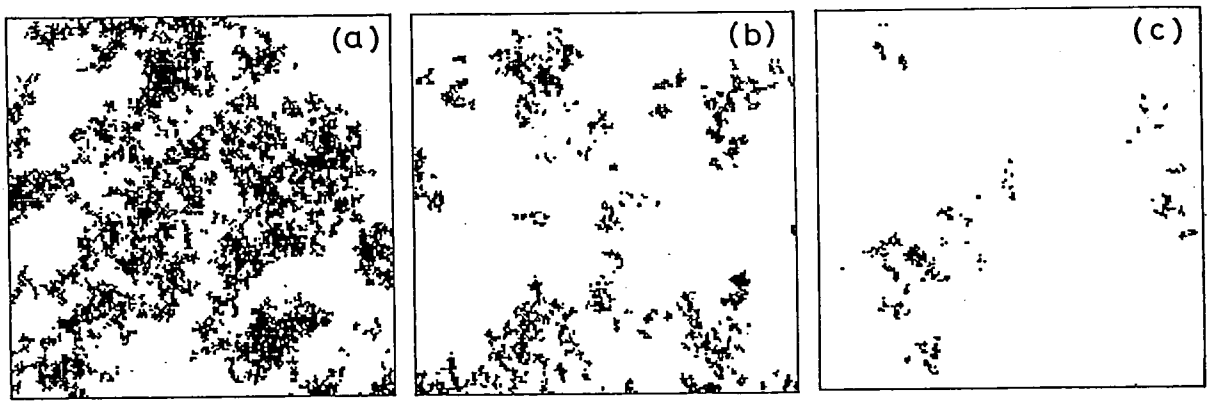

Figure 1. Fractal patterns obtained from simulation calculation based on a correlation function $P(r) \propto r^{-\bar{d}}$; (a) $\bar{d} = 1.8$, (b) $\bar{d} = 1.3$ and (c) $\bar{d} = 1.1$.

VII–E Picosecond Time-Resolved Fluorescence Spectroscopy on Photophysical Processes in Organized Molecular Assemblies

In ordered molecular assemblies such as polymers, Langmuir-Blodgett films and oriented vapor-deposited films, one can expect to observe new aspects of photochemical and photophysical processes because one-dimensional polymers or uniform thin layers with the two-dimensional order might show configurational and dynamical behaviors quite different from those of homogeneous solution. In this research project, excimer formation and ground-state molecular association in the highly anisotropic media are investigated by means of a picosecond time-resolved fluorescence spectroscopy. To examine the layered structures with a spatial resolution we have developed a new experimental technique capable of monitoring selectively the emission at particular depth in the multilayered structure.

VII-E-1 Molecular Association in Langmuir-Blodgett Multilayers

Iwao YAMAZAKI, Katsuhiro SUMI, Naoto TAMAI, and Tomoko YAMAZAKI

[*Chem. Phys. Lett.*, **124**, 326 (1986)]

Molecular association of chromophoric pyrene has been studied with the Langmuir-Blodgett (LB) monolayer film consisting of stearic acid and 16-(1-pyrenyl) hexadecanoic acid. Picosecond time-resolved fluorescence spectra (Figure 1) have shown four fluorescence bands with its intensities depending on the time regions: a ground-state dimer (F_1), a isolated monomer (F_2) and two kinds of excimers (E_1 and E_2). The excimer of E_2 fluorescence band corresponds to the well-known sandwich-type (or two-center type) excimer. On the other hand, another excimer of a new type of excimer band E_1 was assigned as a one-center type excimer in parallel with those known in cases of perylene single crystals.[1] In the initial time region (0-100 ps), F_1 band is dominant, and its decay is associated with a rise of E_2 band. The fluorescence band E_1 forms much more faster than that of E_1. The fluorescence decay curves of isolated monomers are analyzed in terms of the two-dimensional energy transfer and trapping, leading to a conclusion that the LB monolayer film has an irregular distribution of chromophores.

Reference

1) A. Matsui, K. Mizuno, and H. Nishimura, *J. Phys. Soc. Jpn.*, **53**, 2821 (1984).

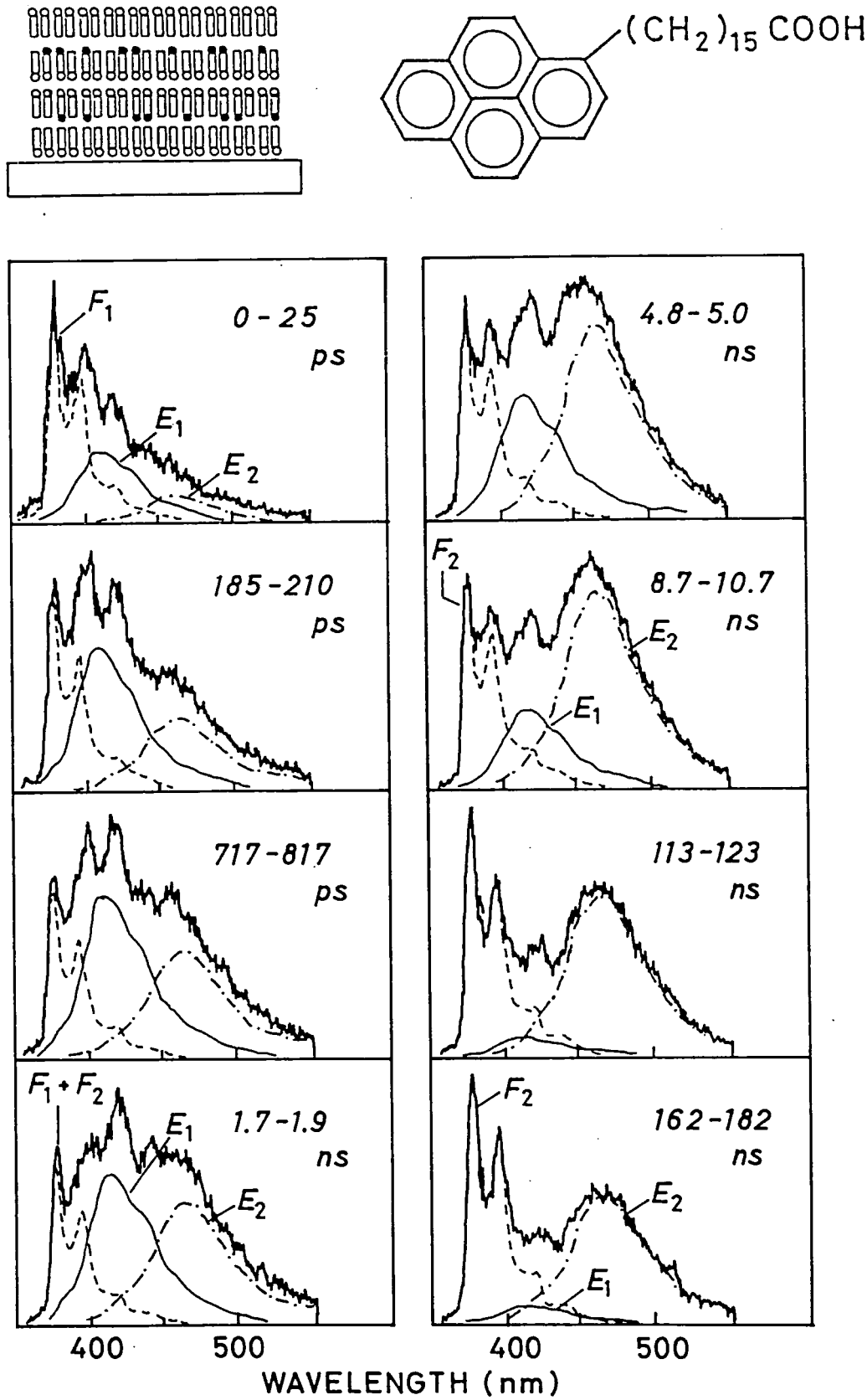

Figure 1. Time-resolved fluorescence spectra of the LB film and spectral analysis into components. Concentration of PHA is 13.9 mol%. The excitaiton wavelength is 315 nm. The structure of the LB film is illustrated; solid circles stand for pyrene ring, open circles for carboxyl group, and rods for hydrocarbon chain.

VII-E-2 Picosecond Fluorescence Spectroscopy of Vacuum-Deposited Films of ω-(1-Pyrenyl) alkanoic Acids

Hiroshi MASUHARA *(Kyoto Inst. Tech.)*, **Yoshio TANIGUCHI, Munehisa MITSUYA** *(Hitachi Adv. Res. Lab.)*, **Naoto TAMAI, and Iwao YAMAZAKI**

[*Chem. Phys. Lett.*, in press]

Compared to aromatic hydrocarbons, the present compound is more easily deposited at room temperature and the formed thin film is more stable. The fluorescence spectrum and behavior are quite different from those of its powders, dilute solution, and films prepared by evaporating the solvent. The fluorescence bands were observed at 423, 448, 478 and 510 nm in addition to the pyrene monomer fluorescence. Co-depositions of this molecules and stearic acid change the relative intensity of these new bands and monomer fluorescence. Analyzing ps time-resolved spectra of these films, microscopic structures around the pyrenyl chromophore and their dynamics were discussed.

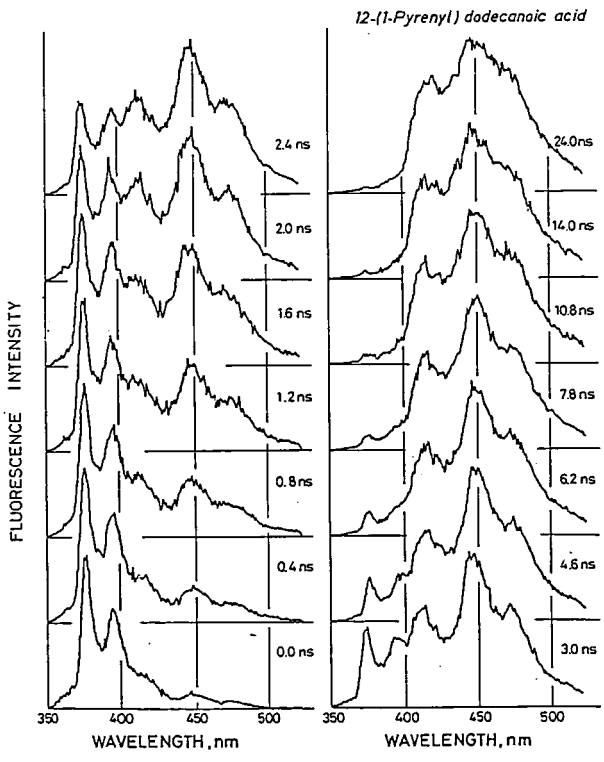

Figure 1. Time-resolved fluorescence spectra of a vacuum-deposited film of PyC_8. The time zero corresponds to the time in which the excitation laser pulse reaches maximum intensity.

VII-E-3 Formation and Relaxation of an Excited Complex in a Polymer

Shigeo TAZUKE, Yuko HIGUCHI, Nobuo TAMAI, Noboru KITAMURA *(Tokyo Inst. Tech.)*, **Naoto TAMAI, and Iwao YAMAZAKI**

[*Macromolecules*, **19**, 603 (1986)]

The dynamic fluorescence spectroscopy of an excimer-forming polymer (I) and an exciplex-forming polymer (II) is studied in comparison with the corresponding dimer model (III) and monomer model (IV), respectively, in dilute solution. Figure 1 shows the time-resolved fluorescence spectra for I-IV. The rise profile of intrapolymer excimer in I is faster than that of III, although diffusion of polymer-bonded chromophores is slower than for the small molecule. The reason is believed to be the high local concentration of chromophores in I. In the case of exciplex formation by II, the mode of excited-state interaction is mostly interpolymer and the formation of the exciplex is completed within a time of the order of 100 ps. The corresponding monomer model (IV) forms the exciplex more slowly. Loose polymer association prior to excitaiton accounts for the fast rise of the exciplex emission in II. The time-resolved fluorescence of II shows a gradual red shift of the exciplex emission beyond 100 ns, whereas IV does not exhibit this shift. This is an indication that solvation and other relaxation processes forming the stable exciplex state in II are slow. Also, excimer formation by I does not show a time-dependent wavelength shift since the relaxation of the excimer is less than that of the exciplex.

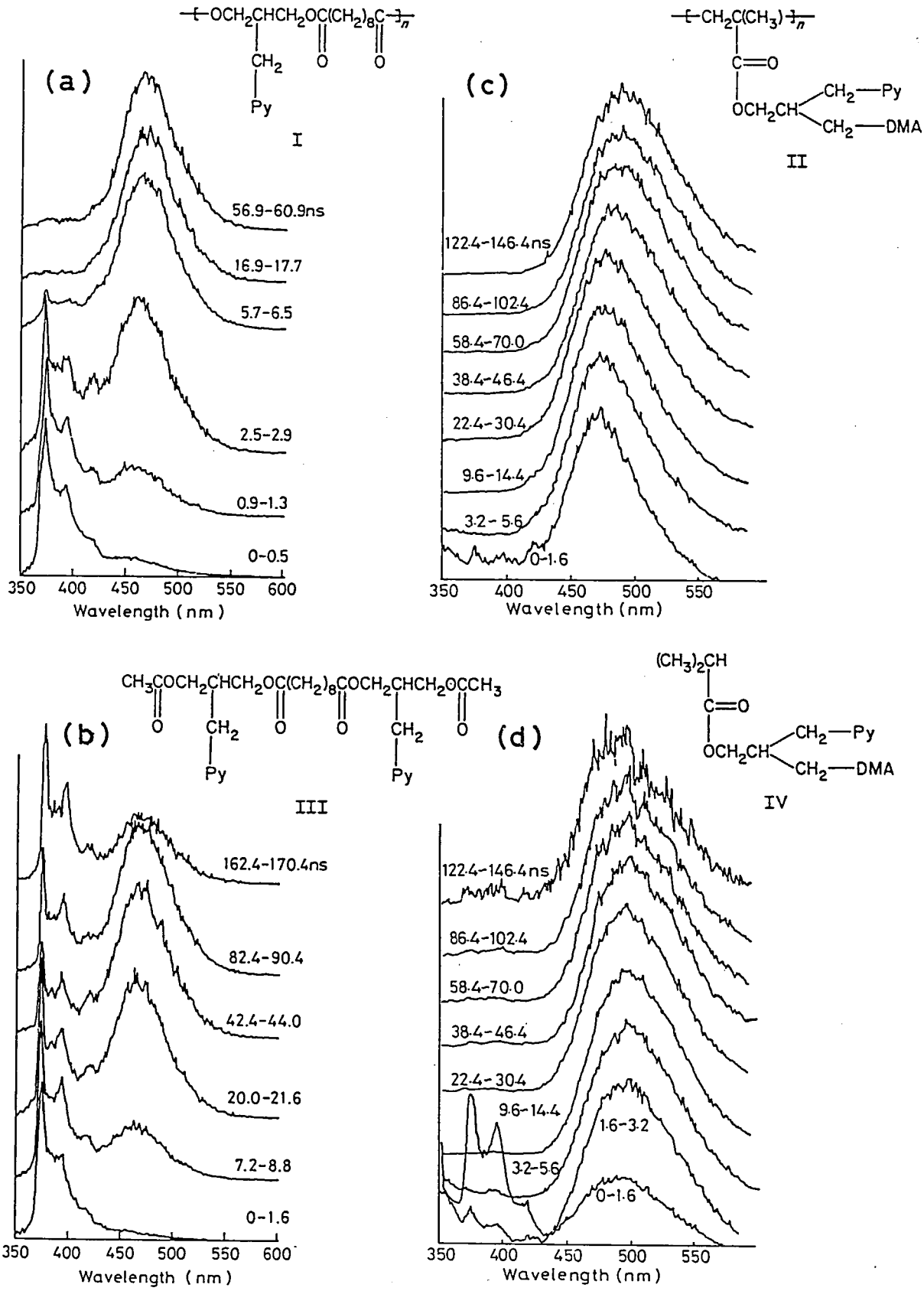

Figure 1. Time-resolved fluorescence spectra of I (a) and III (b) in toluene, and II (C) and IV (d) in MTHF. Excitation wavelength is 315 nm.

VII-E-4 Transient Free-Exciton Luminescence and Exciton-Lattice Interaction in Pyrene Crystals

Atsuo MATSUI, Ken-ichi MIZUNO *(Konan Univ.)*, **Naoto TAMAI, and Iwao YAMAZAKI**

Time-resolved spectra and luminescence decay time in pyrene crystals have been studied by a time-correlated, photon-counting technique over the temperature range 295-136 K (above the phase-transition point). Figure 1 shows an example of the time-resolved spectra. Transient free-exciton luminescence is observed as well as thermally-activated, free-exciton luminescence. Figure 1 shows an example of time-resolved spectra. The rate of decay of transient free-exciton luminescence σ is proportional to $\exp(-E_B/kT)$, where k is the Boltzmann constant and T the temperature.

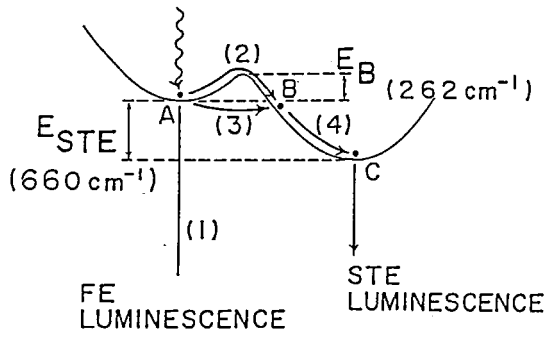

The ST barrier height E_B is found to be 260 cm^{-1}. The lattice relaxation time after tunneling is estimated to be of the order of 4 ps. The lower bound of the time required for excitons to tunnel through the ST barrier is estimated to be 36 ps. The ratio of the ST barrier height against the exciton bandwidth is found to be 0.1.

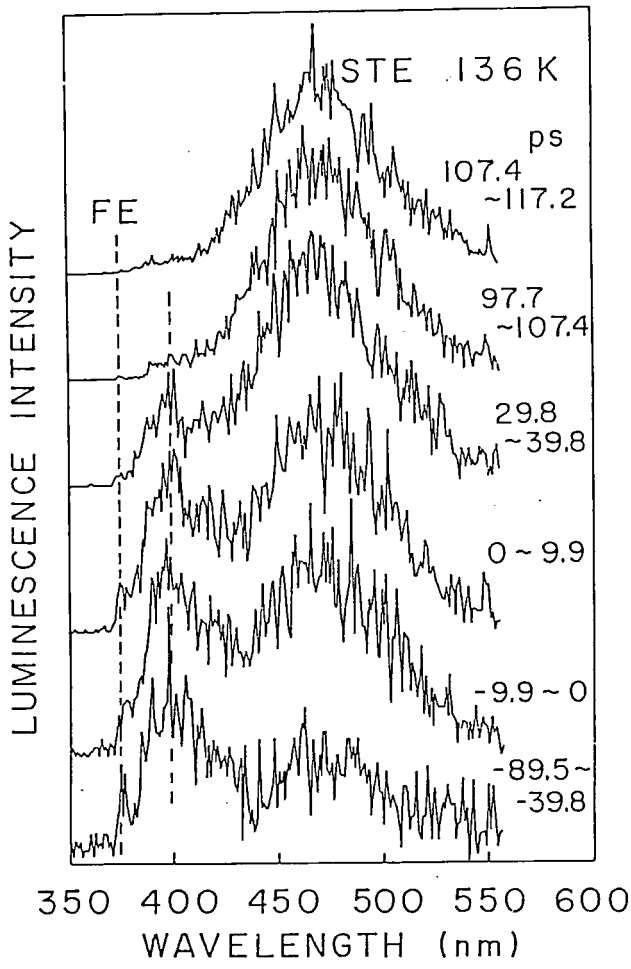

Figure 1. Time-resolved luminescence spectra of pyrene single crystal measured at 293 K. The excitation wavelength is 316 nm.

VII-F Photonic Energy Transport and Primary Reaction in Biological Photoreceptors

Primary processes in biological photoreceptors such as photosynthetic pigments and phytochrome are characterized by highly efficient absorption and subsequent transfer of photo-excitation energy to the reaction centers. These ultrafast processes of the energy transport and the primary photochemical reaction have studied on the basis of picosecond time-resolved fluorescence spectroscopy.

VII-F-1 Picosecond Fluorescence Spectroscopy on Photosynthetic Pigment System I in Plants

Mamomu MIMURO, Yoshihiko FUJITA *(NIBB)*, **Naoto TAMAI, Tomoko YAMAZAKI, and Iwao YAMAZAKI**

Kinetics of the photonic energy transport and the

primary reaction in pigment system I (PS I) chl a has been studied with PS I enriched particles from spinach chloroplasts. Time-resolved fluorescence spectra of PS I chl a system at room temperature (Figure 1), which were measured by means of a picosecond time-resolved, photon-counting apparatus,[1] showed a fluorescence band with the maximum at 688 nm in a short time range (0 to 25 ps) after an excitation. In the wavelength region around 720 nm, an additional fluorescence band was clearly observed. The rise time of the 688-nm component was faster than that of the 720-nm component. The fluorescence decay time of the PS I enriched particles was faster than those of thylakoid membranes and the PS II particles. These results indicates that the PS I chl a system exhibits two fluorescence components: one has the maximum at 699 nm and is closely related to RCI, and the other is the band around 720 nm, which corresponds to an energy sink of PS I and to a well-known fluorescence band observed at low temperature. These results were compared with our previous study for corresponding particles from a green alga chlorella pyrenoidosa.[2]

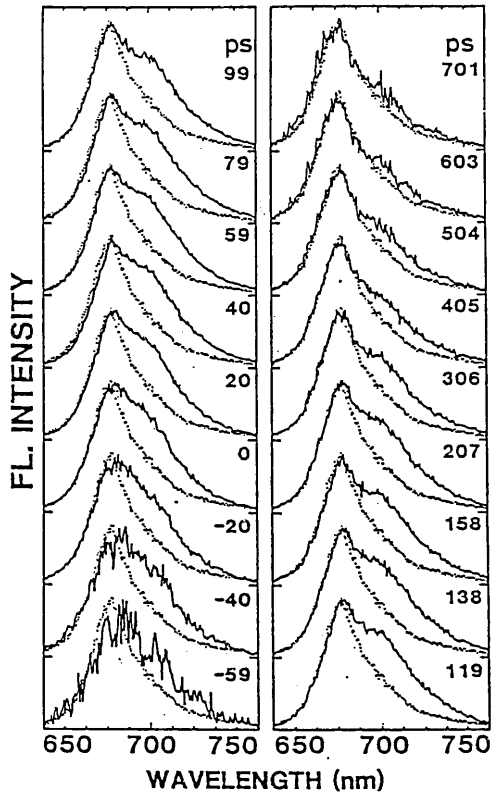

Figure 1. Time-resolved fluorescence spectra of PS I particles. The delay times after excitation are indicated in the figure. Dotted lines show the spectra at about 1 ns after excitation.

References

1) I. Yamazaki, N. Tamai, H. Kume, H. Tsuchiya, and K. Oba, *Rev. Sci. Instrum.*, **56**, 1187 (1985).
2) I. Yamazaki, M. Mimuro, N. Tamai, T. Yamazaki, and Y. Fujita, *FEBS Letters*, **179**, 65 (1985).

VII-F-2 Primary Photoprocess of 124 kDalton Phytochrome

Pill-Soon SONG *(Texas Tech Univ.)*, **Naoto TAMAI, and Iwao YAMAZAKI**

[*Biophys. J.*, **49**, 645 (1986)]

To characterize the nature of primary photoprocesses of phytochrome which serves as the red-far red reversible photoreceptor for photomorphogenesis in plants, viscosity dependence of the fluorescence lifetimes of phytochrome isolated from etiolated oat seedling (Avena sativa L.) has been investigated. The fluorescence decay of phytochrome exhibited approximately two components; one with lifetimes in the range of 50~70 ps and another with 1.1~1.2 ns in phosphate buffer with or without 40~67% glycerol. However, relative amplitudes of these decay components were found to be strongly viscosity dependent. Thus the longer decay component increased from 2~5% in phosphoate buffer to about 20% in 67% glycerol-phosphate buffer. These results have been interpreted in terms of primary reaction from the excited singlet state of phytochrome, yielding a photoreversible intermediate whose rates of formation and decay were apparently viscosity-dependent. Further, the viscosity depnedence is consistent with the primary reaction involving conformational changes of the chromophore and its apoprotein environment (Figure 1).

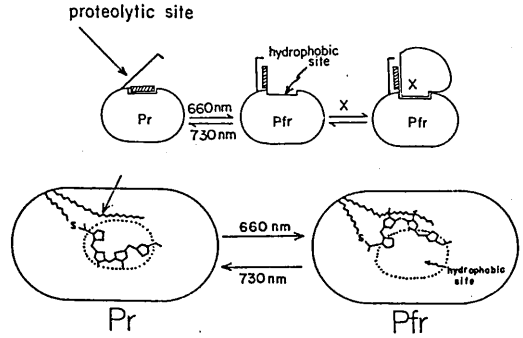

Figure 1. A model for the phototransformation of phytochrome from Pr to Pfr form. Top panel: side view; X, membrane or different binding site. Lower panel: top view; Proteolytic digestion of Pr yields a 6000-dalton molecular mass peptide (arrow).

VII–G Electron Transfer in Hydrogenase and Cytochrome c_3

Hydrogenase is an enzyme for hydrogen cleaverage reaction and cytochrome c_3 is a native electron carrier for this reaction. The active center and the reaction mechanism for hydrogenase have been studied by ESR spectroscopy. Cytochrome c_3 is well known as a multiheme protein. The intermolecular and intramolecular electron transfer mechanisms were studied by ^{1}H-NMR method. AC Electrical conductivity of anhydrous cytochrome c_3 film was also measured as functions of frequency and temperature.

VII–H The Study of Metal Fine Particles Prepared by Means of Gas Evaporation Technique

Fine particles whose sizes are less than ten nm, are characterized by the quantum size effect, surface effect on the bulk properties and also a fluctuation of a thermodynamical properties by its low dimensionality. These effects were studied as functions of metal species, organic solvents and ambient gas purity.

VII-H-1 Size Distribution as a Function of Preparation Method

Keisaku KIMURA

We have developed new preparation techniques for metal fine particles in organic solvents.[1] These are the matrix isolation method, the gas-flow cold trap method and the gas-flow solution trap method. We have applied these methods to indium small particles dispersed in acetone. The diameter of particles were determined by electron micrograph. Figure 1 shows the size distribution of In small particles made by gas-flow cold trap method. The total gas pressure(Ar+He) was 3 kPa. The size distribution was well fitted by the log normal distribution function which was shown by a broken line in the Figure. The median diameter was 19 nm which was about twice of the peak radius.

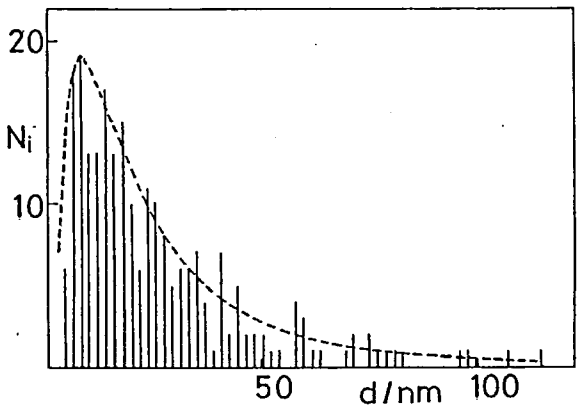

Figure 1. Size distribution of In small particles in acetone by gas-flow cold trap method.

When we applied the gas-flow solution trap method with the other conditions being the same, the peak radius shifted to 6 nm and the size distribution gave double peaks (peak positions were 6 nm and 40 nm). It was suggested that the secondary particles were formed by the coarescence growth of 6 nm particles. A sort of gases also affected the size distribution. A sharp peak (radius 3 nm) was obtained under 1.3 kPa He gas in the gas-flow solution trap method, in contrast to the 6 nm and 40 nm double peak distribution stated above.

Reference

1) K. Kimura and S. Bandow, *Bull. Chem. Soc. Jpn.*, **56**, 3578 (1983).

VII-H-2 Dispersibility of Metal Fine Particles in Organic Solvents

Keisaku KIMURA and Shunji BANDOW

A highly pure colloidal system, composed of metal ultrafine paritcles and an organic solvent, was produced by means of gas evaporation method combined with matrix isolation technique. This system is free from colloidal stabilizers. The dispersibility of the colloids were examined as a function of kinds of metal species and solvents. A strong correlation between the state of colloids and a dielectric constant of a solvent was found

and shown in Figure 1 as a two dimensional correlation diagram. It should be noted that there is a systematic tendency among more than a hundred different combination between metal species and a kind of organic solvent. In a solvent with a large dielectric constant, many metal particles were well dispersed. On the other hand, none of metal particles was dispersed in the solvent with a small dielectric constant, resulting in coagulation. The dispersibility of colloidal system was also dependent on a kind of metals which was classified by the standard electrode potential E'_0. Taking into account the fact that the heat of formation from metal halide, metal oxide and metal sulfide has strong correlation with E'_0, the reactivity of metal small particles towards a solvent probably affects the dispersibility.

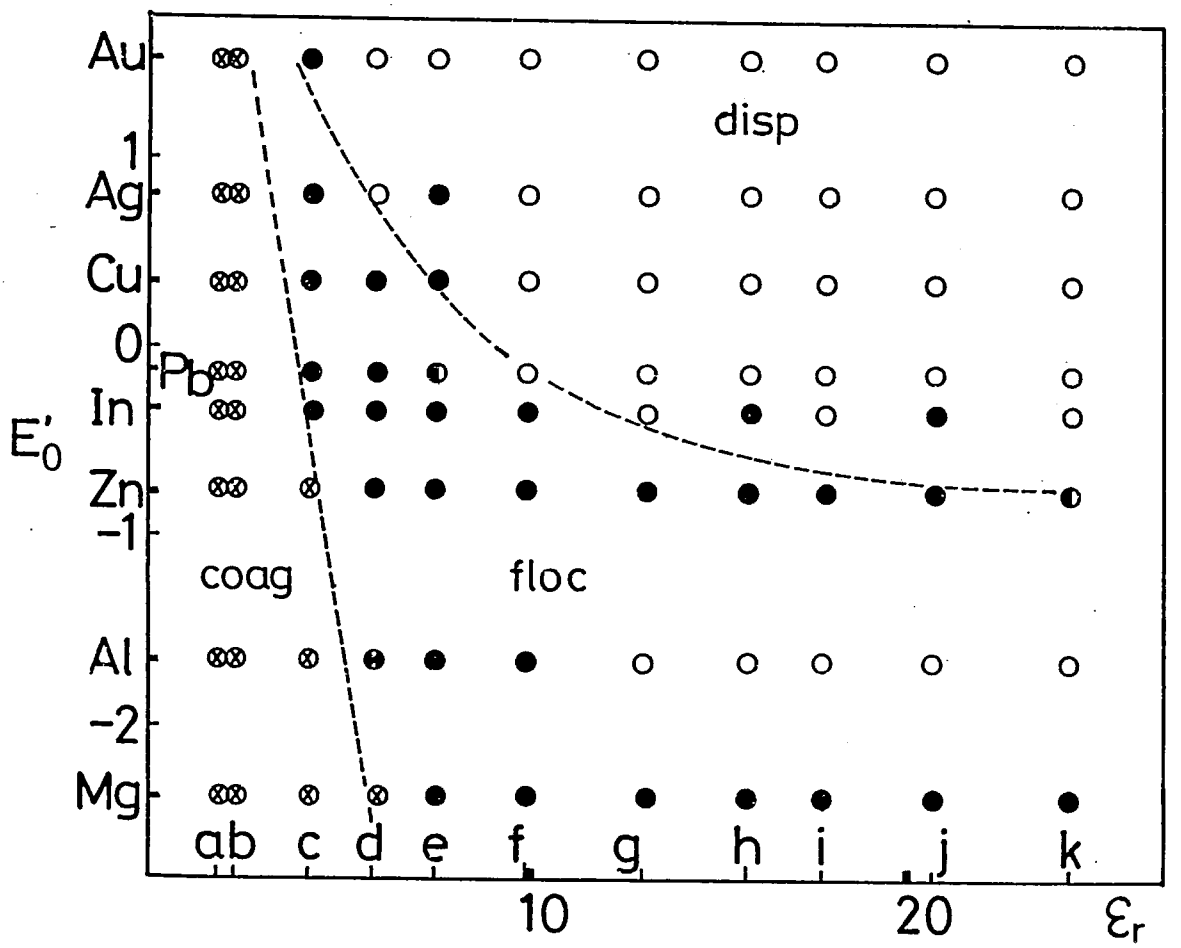

Figure 1. Dispersibility of colloidal system as functions of metal species and a kind of solvent.
disp: dispersion, floc: flocculation, coag; coagulation
a) hexane b) benzene c) ether d) ethylacetate e) tetrahydrofuran f) dichloroethane g) benzyl alcohol h) 2-butanol i) butanol j) acetone k) ethanol

VII-H-3 Paramagnetic Enhancement in the Magnetic Susceptibility of Magnesium Ultrafine Particles

Keisaku KIMURA and Shunji BANDOW

Magnesium small particles were produced by the matrix isolation method combined with the gas evaporation technique. Magnetic susceptibility of samples (typically 5 mg Mg UFPs in 100 μℓ liquid paraffin) was measured by a high-sensitivity Faraday-type magnetic balance system with a superconducting magnet (5 T) and with a microprocessor aided data logging system. The magnetic susceptibilities of the samples were obtained after subtraction of the values of the control experiments. The susceptibilities at high temperature (χ_{UFP}) were nearly constant above 200 K. Figure 1

shows the constant paramagnetic susceptibility normalized to the bulk value (x_b) as a function of the inverse of the number of atoms in a particle.

Since the atomic contribution to magnetic susceptibility is independent of particle size and the spin contribution is also independent of particle size at high temperature, it is reasonable to consider that the linearity between x_{UFP}/x_b and 1/n reflects the orbital contribution. It is known that the orbital motion of perfectly free electron gives Landau diamagnetism, but does not give paramagnetism within a framework of the single band model. However, when there is overlapping of bands as is the case of divalent metals, an applied magnetic field induces a non-zero interband matrix element. This term will add a paramagnetic contribution in addition to the intraband Landau diamagnetism.

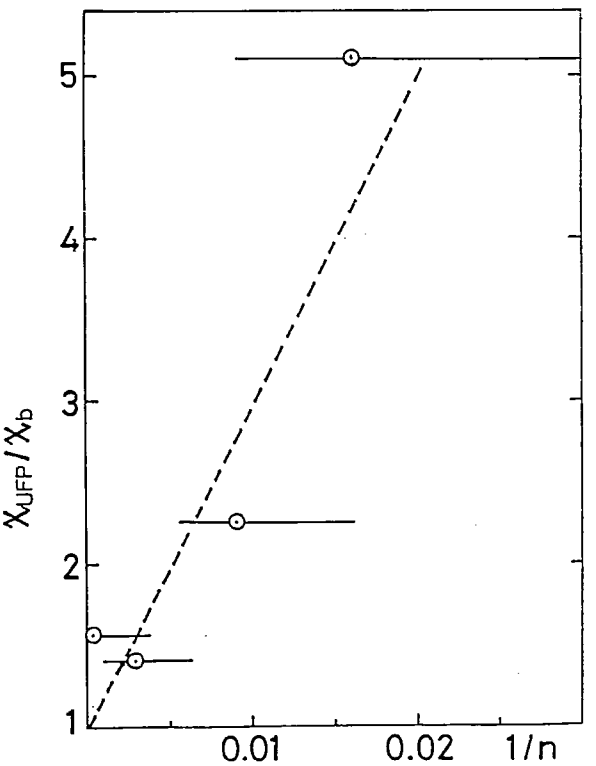

Figure 1. Normalized magnetic susceptibilities of UFP as a function of the inverse number of atoms in a particle. Horizontal bars in the Figure reflect the particle size distribution.

VII-H-4 Origin of the ESR Spectrum from the Ultrafine Particles of Magnesium: Quantum Size Effect?

Shunji BANDOW and Keisaku KIMURA

We have prepared the ultrafine particles of Mg by using the matrix isolation method[1] (purified hexane was used as a solvent) under the ultrahigh vacuum (the oxygen partial pressure was less than 10^{-7}Pa), and have measured the X-band ESR at 3K. As a result, very weak ESR signal was detected near g = 2 (Figure 1A). Upon exposing the oxgen to this sample, spectrum A changed to spectrum B. From an analysis of the XPS spectrum, only a few layer of the surface was oxidized. The g-value of spectrum B approximately agreed with that of the O_2^- ion on the MgO surface.[2] This (B) spectrum also agreed with that by Millet et al.[3] which was reported as the quantum size effect. If our ESR spectrum (B) is originated from conduction electrons, the intensity must be independent of an atomosphere. Therefore we can not conclude that spectrum B is due to the quantum size effect. This spectrum is probably due to the O_2^- ion. Spectrum C was observed under the condition of leaking the oxygen gas (10^{-1} Pa·l/sec) during the sample preparation. Magnetic susceptibilities from the spectra B and C are estimated to be in the order of 10^{-8} – 10^{-9} emu/g at 3K.

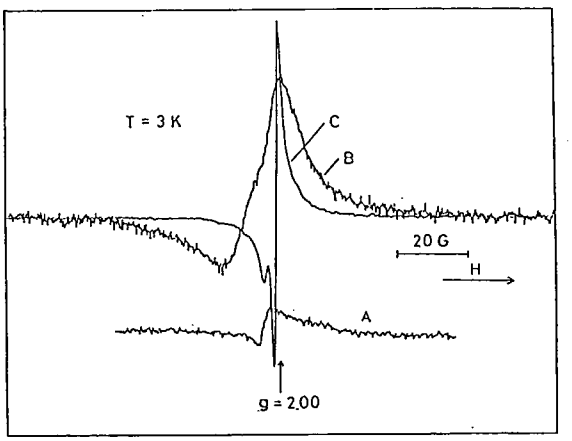

Figure 1. ESR spectra from Mg ultrafine particles (average size is ca. 3 nm). A; sample was prepared under the condition of ultrahigh vacuum. B; after O_2 exposure, spectrum A changes to spectrum B. C; sample preparation with leaking the O_2 gas.

References

1) K. Kimura and S. Bandow, *Bull. Chem. Soc. Jpn.*, **56**, 3578 (1983).
2) J.H. Lunsford and J.P. Jayne, *J. Chem. Phys.*, **44**, 1487 (1966).
3) J.L. Millet and J.P. Borel, *Solid State Commun.*, **43**, 217 (1982).

VII-H-5 Analysis of the Magnetization Curve of the Ultrafine Particles of Magnetite Prepared by Using a W/O Microemulsion

Shunji BANDOW, Keisaku KIMURA, Kijiro KON-NO *(Sci. Univ. of Tokyo)*, **and Ayao KITAHARA** *(Sci. Univ. of Tokyo)*

Measurement of the magnetization curve was performed on the colloidal system of iron-oxide prepared by using a W/O microemulsion.[1] From an electron microscopic photograph, the size distribution of the particles was revealed to be a log-normal type; the mean diameter is 3.6 nm with standard deviation σ = 1.28. Iron-oxide particles are Fe_3O_4 (magnetite) from the analysis of electron diffraction patterns and the chemical analysis. This colloidal system showed a superparamagnetism above ca. 50K. However, the magnetization curves were not represented by a simple Langevin function (Figure 1A). Therefore we assume a model that the paramagnetic Fe ions exist on the each particle surfaces. The result of the magnetization curve of this model shown in Figure 1B. In this case, the distance of the surface Fe ions is about 1.2 nm. The agreement is good between the temperature range from 50 K to 200 K. The magnetization curves under 50 K is different from the curve B. That is caused from an effect of the blocking temperature of the superparamagnetism.

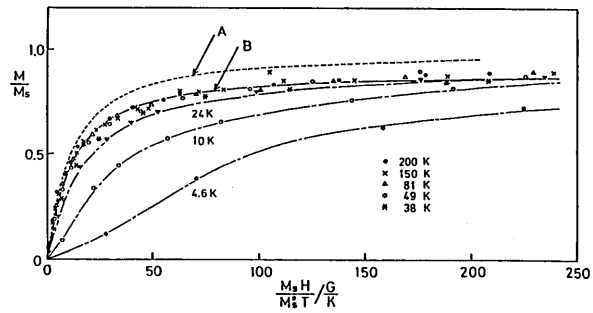

Figure 1. Magnetization curves of the magnetite colloid at various temperatures. Curve A is calculated from a simple Langevin function taking account of a size distribution. Curve B is calculated by a model explained in the text. Here M is a magnetization, M_S is a saturation magnetization at various temperatures and M_S^O is M_S at T = 0 K.

Reference

1) M. Gobe., K. Kandori, K. Kon-no, and A. Kitahara, *J. Jpn. Soc. Col. Mater.*, **57**, 380 (1984).

Low Temperature Center

VII-I A Transfer Tube Lift

VII-I-1 A Transfer Tube Lift

Kiyonori KATO, Kohichi SUZUI, and Keiichi HAYASAKA

We developed a Transfer Tube Lift, which was equipped to a 1000ℓ liquid helium reservoir. A Transfer Tube (abbreviated as TT) is an adiabatic-insulated metal tube for liquid helium transfer from the reservoir to another low temperature vessel or an experimental apparatus. The Transfer Tube Lift is used to move TT automatically upward or downward for liquid helium transfer. The system consists of an arm which fixes TT, a motored ball screw which can move the arm, a seal which is attached to the top port of the reservoir to prevent helium gas from leakage, and an electric control panel with two micro-switches and safety equipments.

The features are as follows;

(1) We can easily move TT up and down with the operation of one push button through remote control. This makes an operator free from troublesome work on the top of the reservoir.

(2) Damage caused by frozen water drops is avoided by means of slow moving speed of TT (140 mm/min.), which can keep the seal at room temperature and dry during the operation.

(3) Inserting TT at about 300K into liquid helium (at 4.21K) is accompanied by only negligible pressure increase (below 0.01 Kg/cm^2).

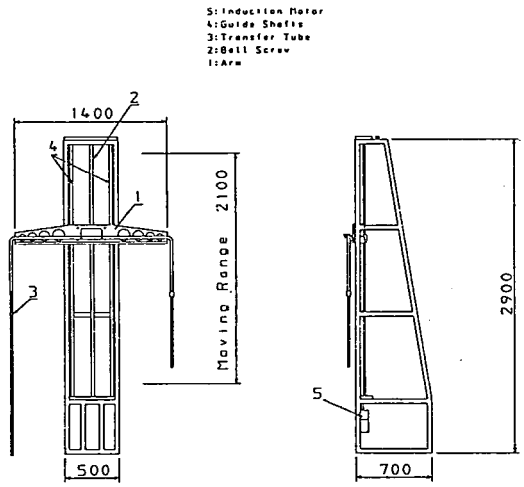

Figure General View

VII–J Alkali Metal-Hydrogen-Graphite Ternary Intercalation Compounds

Graphite-alkali metal intercalation compounds absorb hydrogen chemisorptively, leading to the occlusion of hydrogen in intercalate layers. The introduction of hydrogen gives effects on the electronic and lattice properties of the compounds due to the strong electron affinity of hydrogen and the occupation of the sites by hydrogen species in the intercalate layers.

We investigate the properties of the alkali metal-hydrogen-graphite ternary intercalation compounds by means of specific heat, Shubnikov de Haas effects, electron microscope and positron annihilation. (See also IV-D).

VII-J-1 Specific Heat of Hydrogen-Alkali Metal Ternary Graphite Intercalation Compounds

T. ENOKI, M. SANO *(Kumamoto Univ.)*, **and H. INOKUCHI**

[*Synth. Metals* **12**, 207 (1986)]

Low temperature specific heat has been investigated for hydrogen-alkali metal ternary graphite intercalation compounds, C_8MH_X(M=K, Rb). The electronic structures depending on x are discussed in relation to the effects of dissolved hydrogen on the superconductivity. The parameters of the lattice energies, the electronic states and superconductivity are summarized in Table I; Θ_D, Debye temperatures; T_E, Einstein temperature; $N(E_F)$, the density of states at the Fermi level; T_C, superconductive transition temperature; λ, the electron-phonon couping constant; V, the attractive interaction.

Table I. The parameters of the lattice energies, the electronic states and superconductivity

	θ_D / K	T_E / K	$N(E_F)$ / states/eV atom of C	T_C / K	λ	$N(E_F)V$
C_8K	393.5	82.2	0.40	0.15	0.30	0.13
$C_8KH_{0.0547}$	403.0	90.7	0.38	(0.19[a])	0.31	0.13
$C_8KH_{0.6485}$	350.3	58.1	0.20	<0.05		
C_8Rb	245.4	60.3	0.35	0.026	0.27	0.11
$C_8RbH_{0.0546}$	319.1	56.2	0.33			

(a) The value is expected from T_C=0.22K for $C_8KH_{0.19}$ after Kaneiwa et al.

VII-J-2 Shunbnikov-de Haas Experiments on Potassium -Hydrogen Graphite Intercalation Compounds (KH_x-GIC's)

T. ENOKI, N. -C. YEH *(MIT)*, **S. -T. CHEN** *(MIT)*, **and M.S. DRESSELHAUS** *(MIT)*

[*Phys. Rev.* **B33**, 1292 (1986)]

Potassium-hydrogen-graphite ternary compounds (KH_x-GIC, $0<x<1$) are donor-type compounds containing an ionic intercalant K^+H^-. Basically the effect of hydrogen addition is the uptake of electrons from the potassium so that fewer electrons are available for conduction in the graphite π bands. To obtain Fermi-surface information directly, Shubnikov-de Haas (SdH) measurements were carried out on stage-1, -2, and -4 KH_x-GIC's. The results (Table I) are compared with the electronic properties of K-GIC's and KHg_x-GIC's. The observed oscillations are qualitatively modeled using the three-dimensional dilute-limit model. These Fermi-surface results are related to other experiments on KH_x-GIC's, such as magnetic susceptibility, electronic specific heat, Raman scattering, and superconductivity. For example, it is found that because of the strong electron affinity of hydrogen, the charge transfer to hydrogen and graphite in stage-2 KH_x-GIC's completely depletes the electrons in the potassium conduction band, consistent with the experimental specific-heat results. The basic conclusion that the uptake of hydrogen results in a lower electron concentration in the graphite π bands is supported by all experiments.

Table I. The fractional charge transfer coefficients f_C, f_K (or f_{KHg}), and f_H on the C, K (or KHg), and H atoms are tabulated in units of charge per atom. The density of states at the Fermi level $N(E_F)$ is in units of states/eV atom of C.

GIC	f_C	f_H	f_K(or f_{KHg})	E_F (eV)	$N(E_F)$
$C_4KH_{0.8}$	−0.020	−1	+0.88	0.65	0.24
$C_8KH_{0.8}$	−0.033	−1	+1	1.15	0.06
C_4KHg_x	−0.094[a]		+0.38	1.53[a]	
C_8KHg_x	−0.064[a]		+0.51	1.0[a]	
C_8K	−0.075[b]		+0.6	1.4[b]	
$C_{24}K$	−0.042[c]		+1		

a, b, c, the results in literatures.

VII-J-3 High-Resolution Transmission Electron Microscopy on KH_x-GIC's

L. SALAMANCA-RIBA *(MIT)*, **N. -C. YEH** *(MIT)*, **M.S. DRESSELHAUS** *(MIT)*, **M. ENDO** *(Shinshu Univ.)*, **and T. ENOKI**

[*J. Mater. Res.* **1**, 177 (1986)]

The in-plane and c-axis structure of KH_x-GIC's and KD_y-GIC's studied using transmission electron microscopy (TEM) and x-ray diffraction as a function of intercalation temperature and time. With the TEM, two commensurate in-plane phases are found to coexist in these compounds with relative concentrations depending on intercalation conditions. When the direct intercalation method is used, the first step of intercalation is the formation of a stage n potassium-GIC and the final compound is a state n KH_x-GIC (or KD_y-GIC). High-resolution (001) lattice images show direct evidence for intermediate phases in the intercalation process. These intermediate phases are hydrogen (deuterium) deficient and are found at the boundary between pure potassium regions and regions with high hydrogen (deuterium) content. A comparison of the structure for the two methods of intercalation of KH is also presented.

Equipment Development Center

VII−K Studies of Quasi-One-Dimensional Materials

VII-K-1 A Phase Diagram of Neutral-to-Ionic Phase Transition in TTF-p-chloranil Crystal

Tadaoki MITANI, Yoshinori TOKURA*, Takao KODA*, and Gunji SAITO* *(*Univ. of Tokyo)*

[*Synth Metals.* (in press)]

A phase diagram of mixed-stack charge-transfer crystal, TTF-p-chloranil, as a function of temperature and pressure has been determined on the basis of electric conductivity and infrared molecular vibration spectroscopy under pressure.

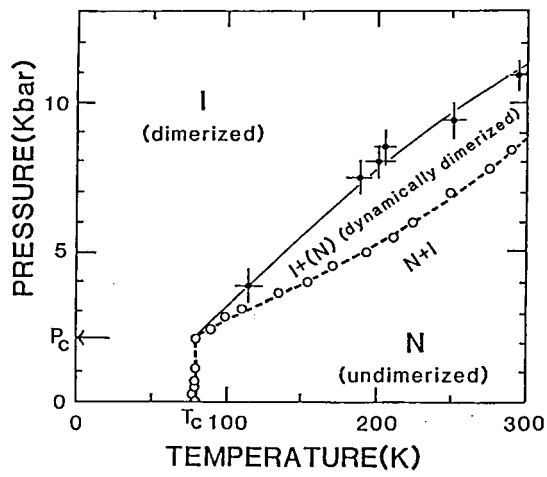

Figure 1. Experimental phase diagram for neutral-to-ionic (NI) transition in TTF-p-chloranil crystal. Solid curve (filled circles) represents the phase boundary between the dimerized ionic phase and the weakly (or dynamically) dimerized ionic phase determined from infrared molecular vibration spectra. Dashed curve (open circles) represents the maximum positions of electrical conductivity, indicating the maximum densities of the NI domain walls.

VII-K-2 Pressure-Induced Neutral-to-Ionic Phase Transition in TTF-p-chloranil Studied by Infrared Vibrational Spectroscopy

Yoshinori TOKURA*, Hiroshi OKAMOTO*, Takao KODA*, Tadaoki MITANI, and Gunji SAITO* *(*Univ. of Tokyo)*

[*Solid State Commun.* **57** 607 (1986)]

Pressure-induced neutral-to-ionic (NI) phase transition in TTF-p-chloranil has been investigated by means of infrared vibrational spectroscopy. Below 10 Kbar, the ionisity of molecules increases continuously with increasing pressure, in contrast with the first-order-like behavior at the thermally induced NI phase transition. At about 11 Kbar, however, the ionisity shows a sharp increase indicating an onset of the first-order-transition to the more ionic phase. At the same time, the lattice undergoes a large dimeric distortion as evidenced by a strong enhancement of the normally infrared-inactive (a_g) molecular vibration.

VII-K-3 Study of Inter-Molecular Proton-Transfer in Quinhydrone Charge-Transfer Crystals

Tadaoki MITANI, Yoshiki WADA, and Gunji SAITO *(Univ. of Tokyo)*

Applying hydrostatic pressure on quinhydrone crystal, the degree of charge-transfer from donor (hydroquinone) to acceptor (benzoquinone) molecules increases in a similar way as observed in usual charge-transfer complexes. At the same time, the O-H streching vibrational mode shifts to a lower frequency, and its intensity becomes unobservable, indicating the presence of the strong electron-proton coupling in this system. At about 40 Kbar, the C=O streching vibrational mode is found discontinuously to shift to a low frequency. This phase transition is considered to arise from the competition between and the electron-proton (lattice) interaction and the electron -electron interaction, that is, it suggests a new phase transition from the CDW state to the SDW state.

VII-K-4 Optical Properties of Halogen-Bridged Mixed-Valent Complexes, $[Pt(en)_2X_2]$ $[M(en)_2]$ $(ClO_4)_4$, (M=Pt, Pd and Ni, X=Cl, Br and I): The Effect of Metal-Alternation

Yoshiki WADA, Tadaoki MITANI, and Masahiro YAMASHITA *(Kyushu Univ.)*

The effect of metal alternation (Pt and M) in linear-chain halogen-bridged mixed-valent complexes, $[Pt(en)_2X_2]$ $[M(en)_2]$ $(ClO_4)_4$, (X=Cl, Br and I, M=Pt, Pd and Ni, en=ethylenediamine), has been investigated by the polarized reflection measurements. Thier electronic spectra transformed by the Kramers-Kronig relation from the reflectivity spectra are characterized by two charge-transfer (CT) excitons associated with the inter-metal transitions, "M-Pt"[1], and the transitions from halogen ions to metal ions, "X-Pt". By replacement of metal ions (M=Pt, Pd and Ni), an enhancement of absorption intensity is observed for the "X-Pt" excitons in contrast to the reduction for the "M-Pt" excitons. The intensity transfer between these two excitons is considered, to be due to the super-transfer mechanism of the d_{z^2} electrons of metal ions via the halogen ions. These characteristic features of CT excitons, including the large Stokes shifts of luminescence band, can be explained in the framework of the extended Peierls-Hubbard model.

Reference

1) Y. Wada, T. Mitani, M. Yamashita, and T. Koda, *Synthetic Metals*, (in press).

VII-L Optical Spin Orientation in Condensed Matter and Spectroscopic Measurements Using a Novel Optical Gating Technique

VII-L-1 Optical Spin Orientation in Aqueous Solution of Manganese (II) Sulfate

Yoshihiro TAKAGI

[*Opt. Commun.*, **59**, 122 (1986)]

Optically induced magnetization has been directly observed in aqueous solutions of $MnSO_4$ at room temperature using picosecond and nanosecond lasers. The induced magnetization has been associated with the electron-spin orientation in the ground state $^6A_{1g}$ of Mn^{2+} ions. The spin-relaxation time was measured to be approximately 0.6ns when there was no magnetic field. This value increased with an increasing magnetic field. The excitation spectrum of the intensity of the optical spin orientation was measured by scanning the laser frequency. The polarity of the spin orientation depended on the absorption bands. This could be explained using a group-theoretical argument that took into account the spin-orbit coupling.

VII-L-2 Application of Three and Four-Wave Optical Parametric Mixings to High Gain and High Time-Resolution Spectroscopy

Yoshihiro TAKAGI and Keitaro YOSHIHARA

Transient spectra of fast luminescence from short-lived excited states has been detected with a temporal resolution as short as excitation laser pulse and also with a gain as high as 10^3 using three-wave optical parametric conversion with a nonlinear crystal. This technique yields a high gain in detection of weak light signal in contrast to the conventional up or down conversion technique in time-resolved spectroscopy. Figure 1 shows a fluorescence decay profile of a laser dye solution at 360 nm. The signal was detected as a difference frequency wave (idler) at 1018 nm generated in KD*P crystal pumped by a fourth-harmonic of a mode-locked Nd:YAG laser. The data were scattered almost uniformly from zero due to fluctuations of the pump power and exponential dependence. Stabilization of the laser and a suitable normalization would improve the data. Practical application to time-resolved spectroscopic measurements are being progressed.

Four-wave optical mixing, specially CARS scheme, was also applied to the optically gated spectroscopy. Under high pump radiation (ω_1), weak signal pulse (ω_2) was amplified as a stokes wave through a pressurized hydrogen gas and an antistokes wave ($2\omega_1$-ω_2) was stimulated giving rise to simultaneous signal sampling in time and spectrum.

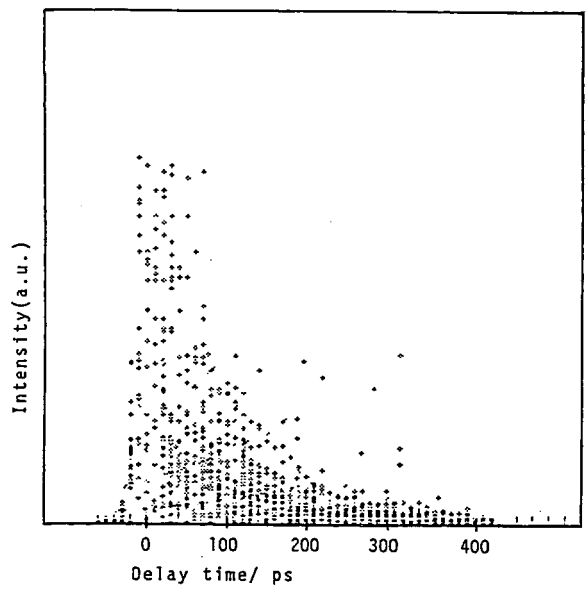

Figure 1. Laser dye fluorescence decay optically gated as a difference wave at 1018 nm.

VII-M Development of Experimental Devices

VII-M-1 Efficient Operation of a Simple Home-Built Nd:YAG Laser as a Picosecond Widely Tunable Light Source

Yoshihiro TAKAGI, Kazuo HAYAKAWA, Hisashi YOSHIDA, Toshio HORIGOME, Norio OKADA, Mitsukazu SUZUI, Shinji KATO, Nobuo MIZUTANI, Masaaki NAGATA, and Tadaoki MITANI

Picosecond tunable lasers are usually not easy to handle compared with nanosecond lasers for those who are not familiar with lase technique. And also the infrared picosecond spectroscopic technique including the method of generation of light source has not been well developed compared with that in the visible and uv regions. Keeping these points in mind, we have constructed a passively mode-locked Nd: YAG laser as a pump source of picosecond continuously tunable laser (Figure 1). The system has several features: ease of operation, high power (0.1-100 mJ), widely tunable (0.2-10μ), high rep. rate (40Hz), and good stability. The oscillator constitution is as follows: Resonator frame with six invar rods. Saturable dye circulator (a part of a thin cell is an end mirror). Output coupler (50% reflecting mirror). YAG rod (4 mmϕ×100 mm, Brewster) and flash lamp positioned close to the focal lines of an elliptical cylinder (CVI Type #2 pump reflector). Cooled water circulator (±0.1°C). Power supply (resonant charging, 40 Hz rep. rate, 40μF and 1.5 kV). A single-pulse selector consisted of a pockels cell and a Klytron pulser.

We are designing amplifiers and frequency conversion system (various harmonics, optical parametric converter, short-cavity dye laser, stimulated Raman, etc.). This tunable laser system is commonly applied to a variety of practical uses.

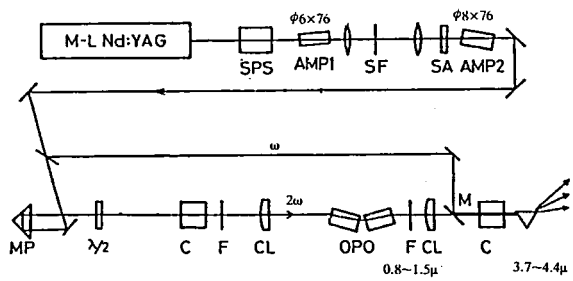

Figure 1. Optical arrangement for generation of picosecond continuously tunable infrared radiation. SPS: single-pulse selector, SF: spatial filter, SA: soft aperture, MP: movable prism, C: crystal, F: filter, CL: cylindrical lens, OPO: optical parametric oscillator.

VII-M-2 Time-Resolved Fluorescence Spectroscopy Using the Synchrotron Radiation Light Source

Mitsukazu SUZUI, Takaya YAMANAKA, Toshio HORIGOME, Kazuo HAYAKAWA, Iwao YAMAZAKI, and Tadaoki MITANI

By using a improved 1 m Seya-Namioka type monochromator, which has been constructed by the staff of Equipments Development Center, we have

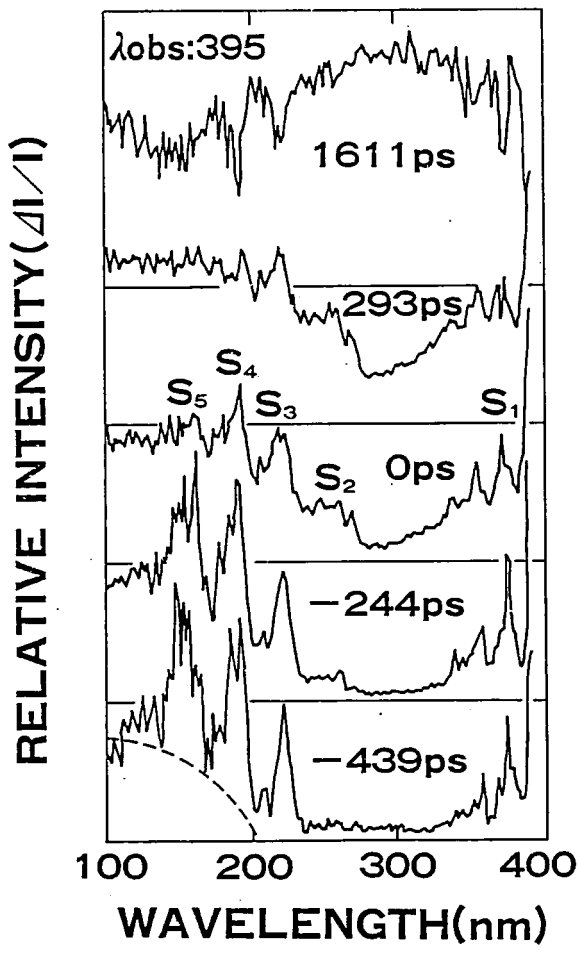

Figure 1. The normalized time-resolved fluorescence excitation spectra of anthracene crystal at 77 K at various time range.

elaborated a computer-aided time-resolved fluorescence spectrometer as the UVSOR facility for common use. The time jitter of the pulse light from the UVSOR electron storage-ring is fairly small (less than 50 psec), so that the time-resolved measurements can be made with a time-resolution of about 100 psec uitlizing the fast-raised time structure of the light. In Figure 1, the normalized time-resolved fluorescence excitation spectra of anthracene crystal at 77 K at various time stages. The fluorescence intensity was monitored at the lowest singlet S_1 exciton band. The spectrum at the initial stage shows a resonance behavior with the highly excited singlet excitons. These characteristic features of the time-resolved spectra can be interpreted by the excitonic polariton model. It is worthy to note that such a resonant internal conversion has been revealed by the time-resolved spectroscopy, although its conversion rate is considerably smaller than other complicated conversion processes in anthracene crystal.

VII-M-3 Time-resolved Photo-emission Spectroscopy Using the Synchrotron Radiation Light Source

Takaya YAMANAKA, Kazuo HAYAKAWA, Hisashi YOSHIDA, Iwao YAMAZAKI, and Tadaoki MITANI

The pulsed characteristic of synchrotron radiation from the UVSOR electron storage ring provides an good time base for the time-of-flight (TOF) analysis in the photo-emission spectroscopy. Compared with electrostatic deflection electron analyzers usually employed, the TOF analysis has a much higher counting efficiency of electron, since the counting permits the entire energy spectrum region within a time window of the pulse train to be analyzed simultaneously. Furthermore, it is expected to obtain an unique information of the dynamics of photo-generated electrons in the surface state separated from the bulk excitations in the time-resolved excitation spectra with a short-time resolution of about 100 psec. From the preliminary experimental results of the TOF analysis and the time-resolved excitation spectra, the usefulness of the short-pulsed synchrotron radiation in a single-bunch mode operation for the study of the energy structures in molecular crystals has been confirmed.

Ultraviolet Synchrotron Orbital Radiation Facility

VII–N Construction of UVSOR Light Source

The UVSOR storage ring is operated stably at the electron energy of 750 MeV and the initial beam current of 85 mA. The single bunch operation of the ring is successfully tried. Arrangements for the free electron laser (FEL) are being made.

VII-N-1 Performance of Light Source

Toshio KASUGA, Hiroto YONEHARA, Toshio KINOSHITA, and Masami HASUMOTO

The vacuum system of the UVSOR storage ring is slightly improved in March 1986, i.e. gate valves were installed on both sides of the r.f. cavity and a longitudinal kicker was set to cure the longitudinal coupled bunch instability caused by the higher mode resonances of the cavity. It is aged with the electron beam for 4 weeks after the improvements. Researches using the UVSOR were started again in the middle of April. The light source was operated at the electron energy of 600 MeV from April through the first decade of June and 750 MeV thereafter. The initial current in the routine operation is 85 mA, and the e-folding lifetime of the beam is about 2 hr at the current. The single bunch operation mode was tried. The current of 50 mA was achieved in this mode, however the lifetime decreased to 50 min at 40 mA due to the Touschek effect. The light source is quite reliable. The ratio of the failure time to the scheduled one was less than 1%.

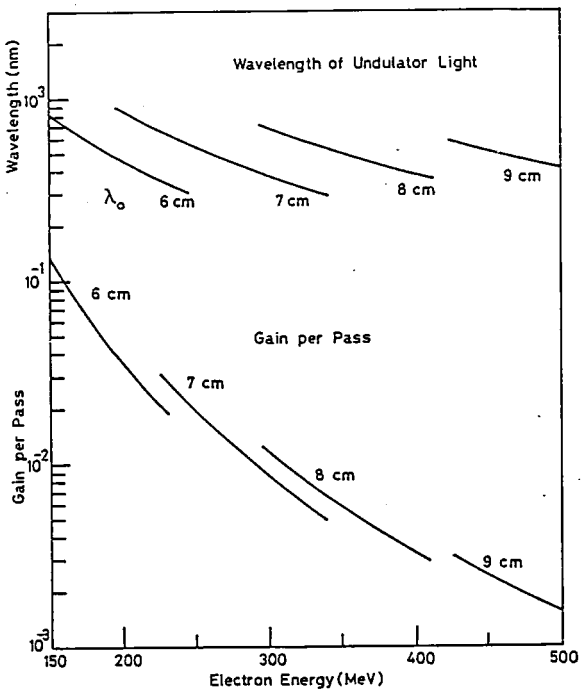

Figure 1. FEL gain estimation to the electron energy with some periods of plane undulator. λ_0 shows the period length of undulator of which total length should be less than 2.5 m.

VII-N-2 Undulator for Free Electron Laser Experiment

Hiroto YONEHARA, Toshio KASUGA, Toshio KINOSHITA, and Masami HASUMOTO

A free electron laser (FEL) experiment using the UVSOR storage ring is planned. The wavelength of 488 nm was selected for simplicity of the experiment especially for accomplishment of an optical cavity. The inner height of the vacuum chamber must be wider than 20 mm as it determines the lifetime due to the scattering with the residual gas. The free space of 2.5 m is available for the experiment in the ring. The gain of the FEL is estimated as a function of the electron energy and the length λ_0 of a unit cell of the undulator. The results are shown in Figure 1. The gain is large when λ_0 is short, however the energy must be low. Generally speaking, beam properties is bad at low energy. The λ_0 of 7.4 cm and the electron energy of 285 MeV are chosen. The undulator with these parameters was already installed in the ring. The influence of it on the beam properties is small and will be reduced moreover by the fine alignment.

VII–O Development of Measurement Systems for UVSOR

VII-O-1 Far Infrared Radiation Port

Takao NANBA*, Yasuhito URASHIMA*, Mikihiko IKEZAWA*, Makoto WATANABE, Eiken NAKAMURA, Kazutoshi FUKUI, and Hiroo INOKUCHI *(*: Tohoku Univ.)*

[*Int. J. Infrared & Millimeter Waves*, in press]

Synchrotron orbital radiation (SOR) is useful not only in vacuum ultraviolet but also in far infrared.[1] BL6A1 is a beam line for far infrared radiation. It is designed to match to absorption and reflection measurements on small samples. SOR of 80 mrad × 60 mrad is collected by collector mirrors, made parallel by collimator mirrors and introduced to a Martin-Puplett interferometer. For comparison parallel light from a high pressure mercury lamp can also be introduced to the interferometer. The light beam is focussed on the sample. Si and polyethylene windows are used to separate the vaccum of the interferometer from those of the light source and the sample chamber, respectively. Figure 1 shows the intensity distribution of the far

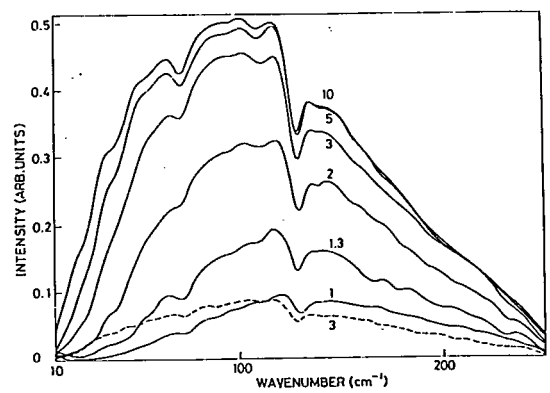

Figure 1. Far infrared spectra obtained at BL6A1. The solid curve shows the spectra of the synchrotron radiation at the ring current of 45 mA. The dashed curve shows that of a high pressure mercury arc lamp. The light passes through an aperture placed at the sample position. The diameters of the aperture are given in mm. The detector is a Golay cell.

infrared radiation from the UVSOR passing through an aperture with variable diameter place at the sample position (solid curve) and that from the mercury lamp (dashed curve). This result indicates that the diameter of far infrared radiation from the UVSOR at the sample position is about 3 mm and that the far infrared radiation with diameter of 3 mm from the UVSOR at the ring current of 45 mA is about five times more intense than that from the mercury lamp.

Reference

1) J. Yarwood, T. Shuttleworth, J.B. Hasted, and T. Nanba, Nature **312**, 742 (1984).

VII–P Researches by the Use of UVSOR

Researches of IMS staff other than UVSOR staff are reported in IV-G-1, IV-I-1, IV-M-1, IV-M-2, IV-M-3, IV-P-1, IV-P-2, IV-P-3, IV-P-4, IV-P-5, IV-P-6, IV-P-7, IV-P-8, VII-M-2 and VII-M-3 in this issue. Details of all researches performed by inside and outside users will be reported in UVSOR Activity Report 1986.

VII-P-1 Polarized Reflection Spectra of Orthorhombic Indium Bromide in 2 – 30 eV Region

Kaizo NAKAMURA*, Yasuo SASAKI, Makoto WATANABE, and Masami FUJITA***** *(*: Kyoto Univ. and IMS, **: Kyoto Univ., ***: Maritime Safety Academy)*

[*Physica Scripta*, in press]

Reflection spectra of orthorhombic indium bromide crystal (InBr: space group D_{2h}^{17}) have been investigated in the energy region between 2 and 30 eV by the use of PGM at BL6A2. The single crystal was cleaved into thin slabs with ac-surface.

Figure 1 shows the spectra at liquid helium temperature. Curve (a) represents the spectrum for the polarization parallel to the c-axis (E//c) and (b) to the a-axis (E//a). In the low energy region (2 – 4 eV), both spectra are consistent with the previous results.[1] The first exciton peak at 2.33 eV is due to the transition from the top valence band, which consists mainly of In 5s orbital, to In 5p conduction band bottom. This transition is allowed for E//c. Structure between 3 and 15 eV is classified into 2 groups: One from Br 4p valence band and the other from In 5s valence band.[2] At about 20 eV sharp doublet structures are observed in both spectra. These are due to the In 4d core exciton. The multiplet was analyzed with an atomic picture.[2]

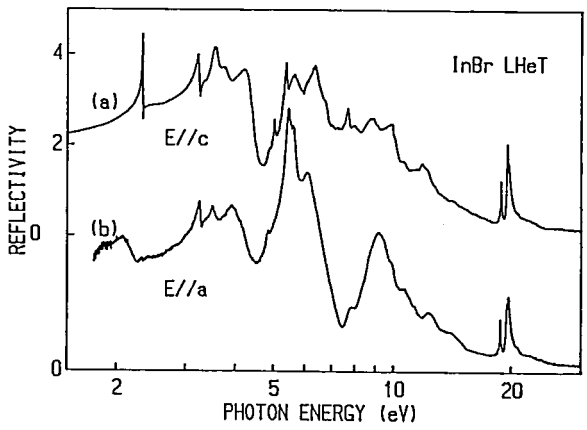

Figure 1. Reflection spectra of orthorhombic InBr at liquid helium temperature in the energy region 2-30 eV. Scale of the photon energy is logarithmic. Curve (a) represents the spectrum for the polarization parallel to the c-axis (E//c). Curve (b) for E//a.

References

1) M. Yoshida, N. Ohno, H. Watanabe, K. Nakamura, and Y. Nakai, *J. Phys. Soc. Jpn*, **53**, 408 (1984).
2) K. Nakamura, Y. Sasaki, M. Watanabe, and M. Fujita, Abstracts of 8th Int. Conf. on Vacuum Ultraviolet Radiation Physics, Lund, p.413 (1986).

VII-P-2 Reflection and Luminescence Excitation Spectra of Cadmium Halide Crystals

Hideyuki NAKAGAWA*, Yukio SHIMAMOTO, Hiroaki MATSUMOTO**, Masami FUJITA***, Takeshi MIYANAGA****, Kazutoshi FUKUI, and Makoto WATANABE** *(*: Fukui Univ. and IMS, **: Fukui Univ., ***: Maritime Safety Academy, ****: Wakayama Univ.)*

Reflection and luminescence excitation spectra in cadmium bromide and iodide crystals were measured at 5 K and 78 K up to 30 eV. The SR was monochromatized with a plane grating monochromator. Monochromatized light was incident on the crystal surface

nearly along the c-axis.

Figure 1 shows nearly normal incidence reflectivity spectra of $CdBr_2$ at 5 K. Structures are almost the same as those previously reported by Kondo *et al.* [1] and by Pollini *et al.* [2] Doublet structures observed around 15 – 17 eV region are due to core exciton transition from the $Cd^{2+}N_{IV,V}$ levels.

Luminescence excitation spectra were also measured at 5 K. Ultraviolet emission was detected. In the excitation spectra below 20 eV are observed sharp dips corresponding to the peaks in the reflection spectra. Relative intensity of luminescence is enhanced with increase of the excitation energy in the region 10 to 20 eV. A multiple exciton production process was suggested.

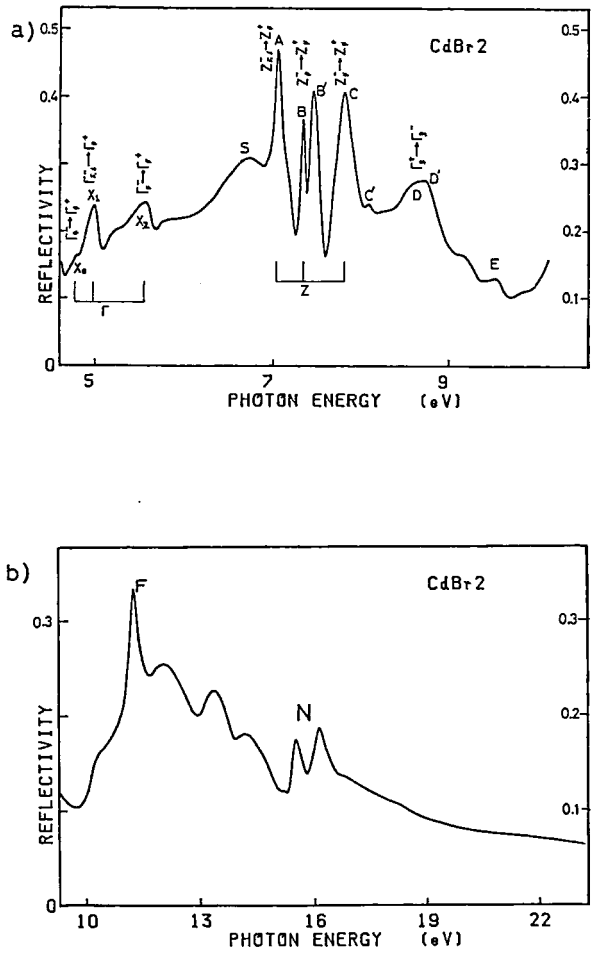

Figure 1. Nearly normal incidence optical reflectivity spectra of the cleaved surface of $CdBr_2$ single crystals measured at 5 K. a) below 10 eV, b) from 10 to 22 eV.

References

1) S. Kondo and H. Matsumoto, *J. Phys. Sol. Jpn.*, **51**, 1441 (1982).
2) I. Pollini, J. Thomas, R. Coehoorn, and C. Haas. *Phys. Rev.*, B **33**, 8 (1986).

VII-P-3 Absorption Spectra of SnTe Thin Films in the 2 – 100 eV Region

Kazutoshi FUKUI, Eiken NAKAMURA, Osamu MATSUDO, Tadaaki SAITO*, Shin-ichi KONDO*, and Makoto WATANABE (*: *Fukui Univ.*)

SnTe film is known to be amorphous when evaporated onto substrate held at near liquid nitrogen temperature (LNT).[1] Irreversible amorphous – crystalline transformation occurs at the temperature T_C of about 200 K. When the temperature rises and it goes over T_C, electrical conductivity abruptly changes from insulator-like to metal-like.[1),2)] In this experiment, the effect of amorphous – crystalline transformation on optical spectra was investigated. The absorption measurements of SnTe films of both phases were carried out in the 2 – 100 eV energy range by using plane grating monochromator. The substrates were thin collodion films.

Figure 1 shows the optical density of amorphous (as-deposited) and crystalline phase (annealed) of the same film at LNT between 20 and 55 eV. Doublet

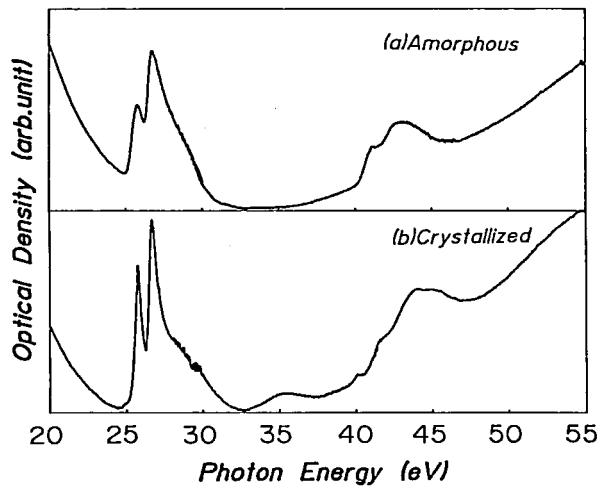

Figure 1. Absorption spectra of SnTe thin film at the liquid nitrogen temperature. (a) for amorphous phase (as=deposited) (b) for crystalline phase (annealed).

structure at about 26 eV are due to the transition from Sn 4d core level. As the peaks are sharp, they are likely to be due to the excitonic transition. After amorphous-crystalline transformation, these peaks become more sharp. At about 44 eV, one can find a structure due to the transition from Te 4d core level. As the structure is broad, it does not seem to be due to the excitonic transition in contrast with the transition from Sn 4d level.

References

1) R.W. Brown *et al.* Thin Solid Films **5**, 157 (1970).
2) K. Fukui *et al. Jpn. J. Appl. Phys.*, **23**, 1141 (1984).

RESEARCH FACILITIES

For the sake of brevity of the present issue are included only the newly installed facilities and the activities since September 1985. Concerning the activities and facilities before September 1985, please refer to IMS Annual Review (1978～1985).

Computer Center

A new computer system consisting of a supercomputer HITAC S-810/10 and a general purpose computer HITAC M-680H was introduced in the last December. The Computer Center began its computational services in January 1986. The maximum speed of S-810 is 315 MFLOPS. S-810 has 128 mega byte main memory and 1 giga byte extended storage. The CPU speed of M-680H is about 14 MFLOPS and it has 64 mega byte main memory. Both computers can access 85 giga byte disk memory and optical disk memory whose maximum content is 86 giga byte. Two kinds of high speed IO facilities are equipped. Although the extended storage is used only for working files, it is 88 times as fast as usual disk. The other is a parallel IO disk set which consists of 16 channels for each computer and 40 giga byte disk memory. Its observed speed is 46 times as fast as usual disk speed. The computer system can be accessed from every place in Japan through the telephone line and DDX network. In the campus of IMS, an optical fiber local area network supports high speed data transfer.

The computers are used not only by the research staff at IMS but also by the staff at nearby National Institutes as well as by scientists outside the Institutes in the related fields. The number of project groups was 244 consisting of 594 users in March 1986. In the twelve month period ending March 1986, 274421 jobs were processed with about 12000 hours of CPU time in the M-200H base.

Supercomputer HITAC S-810/10

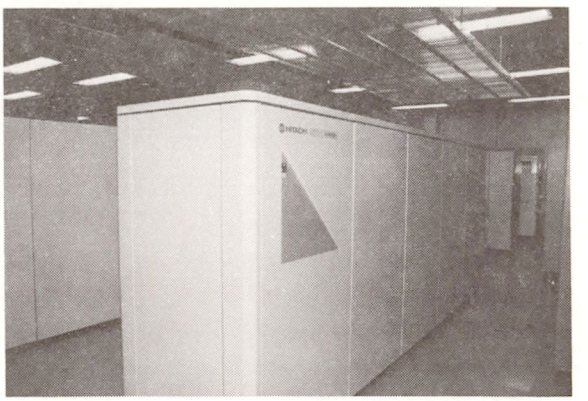

General purpose computer HITAC M-680H

Chemical Materials Center

The Chemical Materials Center plays an important role in the synthesis and purification of chemical substances in IMS. The scientists and technical associates of this facility support other people in IMS to carry out the above works. They also carry out their own researches on synthesis of new interesting compounds, developments of new selective chemical transformations, elucidation of reaction mechanisms, and application of new methodologies developed in IMS to the analysis of chemical substances and reactions. Parts of the scientific activities are presented in the Section VI.

Instrument Center

For the effecient use of instruments, the Center is equipped with various types of instruments for general use.[1] Two instruments have been newly installed in 1985.

1) **ESCA Surface Analyzer System** (VG Scientific, ESCALAB MKII)
Chemical analyses of surfaces of organic and inorganic materials can be performed under ultrahigh vacuum by means of an X-ray photoelectron spectrometric technique. The system is composed of an MgAl dual anode, a triple channeltron for electron counting, an Ar-ion etching gun and two Apple II microcomputers as foreground and background processors.

2) **High Vacuum Evaporator** (ULVAC EBV-6DH)
The new instrument has been introduced as an advanced version of the existing evaporator (ULVAC EBH-6). A chamber elevating mechanism will enables us to handle the system easily and rapidly.

1) *List of Instruments*, No.6, IMS Instrument Center (1986).

Low Temperature Center

The amount of liquid helium supplied in 1985 was about 12000 l. A manual of high pressure gases was published for beginners who start to use high pressure gases. A handbook of cryogenic technical terms was also published according to the discussion at the meeting of technical staffs held at IMS, 1984.

Equipment Development Center

A number of research instruments have been designed and constructed by making use of the mechanical, electric and glass-blowing technologies available at this Facility. Representative instruments developed during this fiscal year of 1985 are listed below.

- Large-sized gate valve (12″ viton O-ring seal) for Molecular Beam UVSOR Fluoresence Apparatus.
- Zero dispersion double-prism monocrometor for Raman measurements.
- In-situ cell for EXAFS measurements.
- Bakable Raman cell for Catalyst study.
- Vacuum system of double-crystal spectrometer.
- Cryostat for electrical conductivity measurements under pressure.
- Electric circuit of high-power flash mercury lamp.
- Two channel timer for T.O.F. measurements.
- Differential electric circuit for detection of tunneling current.
- Fast video digitizer system using CCD video camera.
- Interface for OMA-3.
- Interface for MCPD.
- Interface & software for mass spectrometer.
- Cylindrical quartz dewar.
- Thin-glass cell for X-ray diffraction measurements.
- Optical glass-cryostat.

Ultraviolet Synchrotron Orbital Radiation Facility

The UVSOR light source is usually operated at the electron energy of 750 MeV. The usual initial current is 100 mA, and the lifetime at this current is about 2 hours. (The maximum current at 600 MeV attained so far is 500 mA.) Single bunch operation was carried out several times for time resolved spectroscopy. The pulse width is about 0.4 ns. Two beam lines are newly opened to users. They are BL3A1 using undulator radiation without a monochromator and BL6A1 for solid state spectroscopy in the far infrared region. At present, BL1B and BL8B1 are being set up, and they will be opened in October. In the fiscal year 1985, 3 research projects of "Joint Studies", 14 researches of "Cooperative Research" and 32 researches of "Use of Facility" were performed, besides those of the staff at Department of Molecular Assemblies. A user's meeting and workshop on beam dynamics were held. Activity Report 1984/85 was published.

SPECIAL RESEARCH PROJECTS

IMS has special research projects supported by national funds. Two projects presently in progress under the third year plan (1985–1989) are:

(1) Development and evaluation of molecular synergistic systems and their application to chemical energy conversion.

(2) Fundamental research of molecular devices.

The third project started in the 1982 fiscal year is:

(3) Molecular science of primordial chemical evolution.

These projects are being carried out with close collaboration between research divisions and facilities. Collaborators from outside also make important contributions. Research fellows join these projects. In this report, the results in 1985 are reviewed.

(1) Development and Evaluation of Molecular Synergistic Systems and their Application to Chemical Energy Conversion

Synthesis of Highly Functional Transition Metal Complexes and Their Use in Catalytic Reactions

Hidemasa TAKAYA*, Kazushi MASHIMA, and Tetsuo OHTA

We have been studying synthesis of various chiral transition metal complexes and their use in asymmetric catalytic reactions. We reported previously the synthesis of 2,2′-bis(diphenylphosphino)-1,1′-binaphthyl (BINAP) and its Rh complexes. They have been successfully used as catalysts for asymmetric hydrogenation of α-acylaminoacrylic acids and asymmetric isomerization of allylamines into enamines. This time, we have prepared new BINAP-based Ru(II) complexes of the type Ru(binap)$(OCOR)_2$ and have found that these complexes are extremely efficient catalysts for asymmetric hydrogenations of olefinic substrates. For example, the above complexes catalyze the asymmetric hydrogenation of *N*-acyl-1-alkylidenetetrahydroisoquinolines to give 1-alkyltetrahydroisoquinolines in 95–100% ee. The above catalysts have also been successfully applied to the asymmetric hydrogenation of allylic alcohols. Thus, citronellol with 96–98% enantiometric purity, which is difficultly accessible from natural products, has been prepared from geraniol or nerol in nearly quantitative yields. The C_{15} side chain of vitamin E has been synthesized in 98% enantiomeric excess. Parts of these results are presented in the Section VII-C.

Dynamical Molecular Structure and Control of Reactive Molecules

Eizi HIROTA*, Shuji SAITO, Chikashi YAMADA, Yasuki ENDO, Kentarou KAWAGUCHI, Tetsuo SUZUKI, and Hideto KANAMORI

Infrared laser kinetic spectroscopy combined with excimer laser photolysis has been extended to observe Doppler profiles of infrared transitions. This method has been successfully applied to determine the branching ratio of the $CS_2 \rightarrow CS+S$ reaction (II-A-3). Kinetic spectroscopy has also been applied to an interesting system of the acetylene photodecomposition reaction (II-A-13, II-A-25). It has also been extended to the millimeter- and submillimeter-wave regions (II-B-1), where the O+ethylene (II-A-6) and O+acetylene reactions have been examined in detail.

Optical-optical double resonance spectroscopy using two cw dye lasers as sources has been developed to detect highly excited vibrational states and metastable states. It has been successfully applied to the HCF molecule, and four vibrational states, (010), (020), (100), and (011), have been detected and analyzed in detail (II-A-17).

Excited-State Photoelectron Spectroscopy for Studying Photophysical and Photochemical Behaviors of Molecules and van der Waals Complexes in Supersonic Jets

Katsumi KIMURA*, Yohji ACHIBA, Kenji SATO, and Haruo SHIROMARU

Excited-state photoelectron spectroscopy using a UV/visible pulse laser technique and a supersonic molecular beam technique has been developed in this Institute since 1980 (IMS Annual Review, 1980–84). This method has made it possible to study dynamic behavior of excited-state species which include non-radiative ones, if they are ionized by the laser photons. Photoelectron signals from various molecular excited states have been investigated from photophysical and photochemical points of view. The information deduced from excited-state photoelectron spectra have been found to be unique.

In this project, not only single molecules but also van der Waals molecules produced in supersonic jets have been studied with laser photoelectron spectroscopy, and several typical applications have been demonstrated in the following several subjects: (1) ionization selectivity, (2) autoionization, (3) intramolecular vibrational redistribution, (4) photodissociation, and (5) excited states of van der Waals molecules (See IV-I).

Hot Molecule Mechanism of Photodissociation

Nobuaki NAKASHIMA and Keitaro YOSHIHARA

Several years ago we found that primary intermediates of photochemistry of gaseous benzene was hot molecule (S_0^{**}: highly excited vibrational states in the ground electronic states) by nanosecond flash photolysis. This has been immediately extended to fluorobenzene. The same mechanism is now applicable to dissociation reaction of many olefins and alkylbenzenes. Since the internal energy of this state is determined by photon energy and unique, we can directly obtain the specific rate constants ($k_{diss}(E)$) of S_0^{**}. We showed that the dissociation rate constants of olefins could be predicted on the basis of RRKM theory. Deuterium isotope effect on the rate constants of alkylbenzenes suggests that intramolecular vibrational redistribution is completed before the dissociation reaction. Details are given in III-A.

Photocatalytic Effects of Semiconductors and Dyes

Masahiro HIRAMOTO, Kazuhito HASHIMOTO and Tadayoshi SAKATA

In order to solve the photocorrosion of small band gap semiconductors, we have developed a mosaic coating method by use of photolithography. For n-Si with a MIS structure, a microstructured electrode was found to improve the efficiency of oxygen evolution.

Relating with photoelectrode reactions, electrochemical reactions at a semiconductor electrode with a pn-junction were investigated in dark. In the case of n-Fe_2O_3/p-Si, a fairly large anodic current flowed without deterioration and bubbles of oxygen evolved vigorously from the iron oxide surface, indicating that holes are injected from the p-Si to n-Fe_2O_3. This result suggests that the pn-junction electrode held in dark can do the same work with the semiconductor electrode under irradiation.

In order to investigate the dynamical processes of electron transfer between semiconductor and adsorbed molecules, we have measured luminescence decay and time resolved spectra. In the case of red luminescence of CdS, the quenching is static. SA (Self-Activated) center model was proposed to explain the results. In the case of TiO_2, the luminescence intensity of a broad emission with a peak at 500nm was found to be quite sensitive to various adsorbed molecules. Adsorbed hydrogen atom, a photocatalytic reaction product, was suggested to be involved in the luminescence process. In the case of Ru complexes on various semiconductors, the effects of water vapor, solvents, temperature and energy levels were investigated precisely. Related studies are reported in III-E.

External Magnetic Field Effects upon Chemical Reactions

Hisaharu HAYASHI *(Inst. of Phys. and Chem. Res. and IMS)*, **Hirochika SAKURAGI** *(Univ. of Tsukuba and IMS)*, **Ryoichi NAKAGAKI, Takashi IMAMURA, Haruo ABE** *(Inst. of Phys. and Chem. Res. and IMS)*, **Yoshio FUKUDA** *(Inst. of Phys. and Chem. Res. and IMS)*, **and Saburo NAGAKURA**

External magnetic field effects on chemical reactions can provides us with an excellent probe for elucidating the mechanism of reactions involving radical pairs and biradicals. In the present project, we have studied the magnetic field effects on inter- and intramolecular photo-induced electron transfer reactions. It has been shown that the magnetic field effects can be used for controlling the relative yield of escape and cage products in the case of some bichromophoric species containing electron donor and acceptor moieties. We have also examined the external magnetic field effects upon gaseous chemiluminescence produced by a microwave discharge and the mechanism of magnetic quenching of CS_2 fluorescence.

An Improvement in EXAFS Measurement by a Feedback to the X-ray Source

Takanori MIZUSHIMA and Yasuo UDAGAWA

What makes in-house EXAFS measurement difficult most is a counting loss or non-linearity of detectors and electronics. It causes a serious distortion in the spectra when background intensity changes a lot, which is often the case in the conventional x-ray generator due to the presence of many characteristic lines of tungsten from filament. In order to overcome this difficulty, a feedback system was constructed to keep x-ray intensity constant.

An ionization chamber monitors I_0, and if I_0 changes very much, the target current is adjusted in such a way that the fluctuation in x-ray intensity is within 5% of the average of the previous several points. Figure 1 shows the performance of the feedback system. The middle trace is the background intensity when the target current is constant and the lower one is with the feedback to the current. The ordinate is normalized in such a way that the intensity of the first point is unity. Therefore, it is evident that over an order of magnitude difference in background intensity has been reduced to be within a few percent. The upper curve is the spectrum of Ni foil with feedback, and no trace of distortions due to characteristic lines is seen.

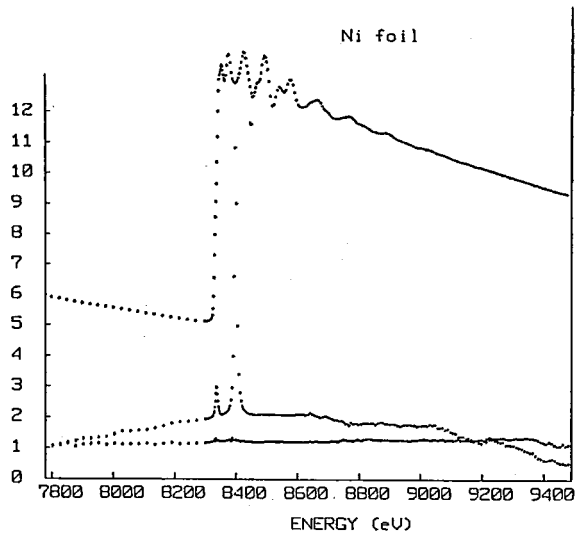

Figure 1. A performance of the feedback system

Molecular Beams Study of Photoassisted Surface Reactions

Kosuke SHOBATAKE, Kiyohiko TABAYASHI, and Atsunari AHIRAYA

Photoassisted surface reactions are studied using our molecular beam chemistry apparatus (Model MBC-I) with a rotatary mass spectrometer detector. Figure 1a) shows a schematic diagram of the apparatus, used for photoassisted etching of solid Si by F_2 molecules in a continuous beam. Experiments were also done when a continuous effusive flow of F_2 (10%) in He was directly applied to the Si surface instead of the collimated F_2 beam shown in Figure 1a). The time evolution of intensity of the chemical species produced upon irradiation of mildly focused pulsed excimer 1a (308 nm) was monitored at mass number m/e = 28 (Si^+), 47 (SiF^+), 66 (SiF_2^+), 85 (SiF_3^+), and 44 (SiO^+). A typical time-of-flight (TOF) spectrum (flight length = 23.7 cm) is shown in Figure 1b). From the analysis of all TOF spectra obtained under different experimental conditions such as laser repetition rate, temperature of solid Si, and F_2 intensity, we conclude that (1) when the F_2 density is low, the velocity distribution f(u) of the products (with mass m) formed in the etching reaction obeys the Maxwell-Boltzmann (M-B) type distribution: $f(u) \propto u^n \exp[-mu^2/(2kT_0)]$, where n is an exponent ranging from 1 to 3, and T_0 an effective temperature, and the present etching processes are essentially due to evaporation of fluorides from solid Si surface heated by laser irradiation, and (2) when the F_2 density is high, the product velocity distributions appreciably deviate from the M-B type, which indicates the occurrence of the secondary reactions between the species emitted from the surface and F_2 molecules in the beam.

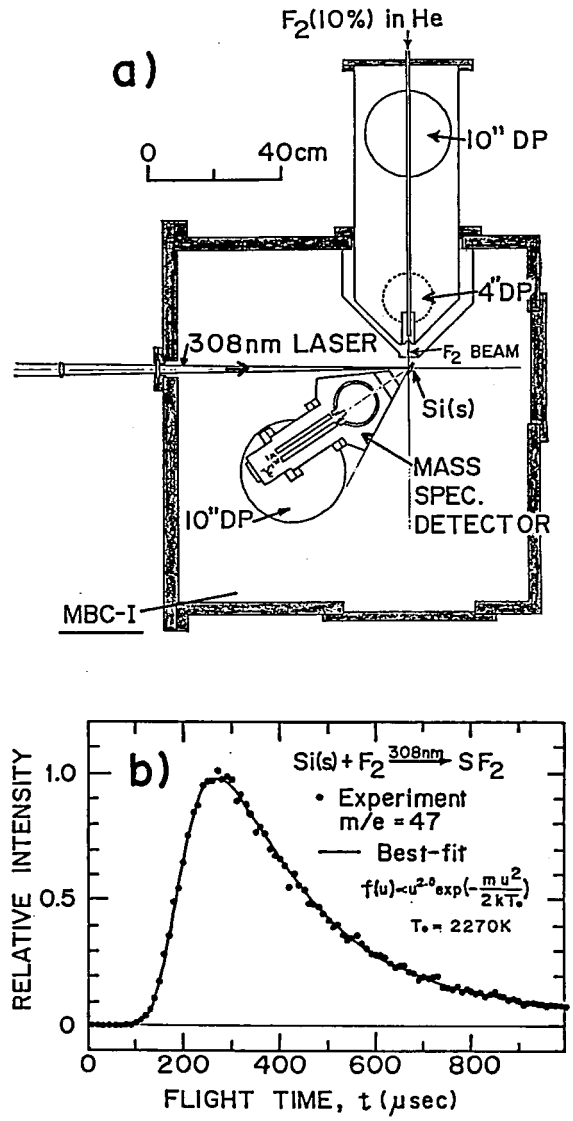

Figure 1

(2) Fundamental Research of Molecular Devices

Study of Electron Transfer Through Proteins: Detection of an Electron Transfer Intermediate for Cytochrome *c* Oxidase

Takashi OGURA, Shinya YOSHIKAWA *(Konan Univ.)* **and Teizo KITAGAWA**

Cytochrome oxidase is a terminal enzyme of the respiratory chain which catalyzes dioxygen reduction coupled with proton translocation. By using difference absorption spectra and oxygen consumption measurements, we confirmed occurrence of photoreduction for the bovine cytochrome oxidase irradiated with laser light at 406.7, 441.6, and 590 nm. The resonance Raman spectra were obtained under the same experimental conditions as those adopted for the measurements of oxygen consumption and difference absorption spectra. It was found that aerobic laser irradiation produces a photo-steady state of the catalytic dioxygen reduction and that the Raman scattering from this photo-steady state probes cytochrome a^{2+} and cytochrome a_3^{3+} separately upon excitations at 441.6 and 406.7 nm, respectively. The enzyme was apparently protected from the photo reduction in the

spinning cell with the spinning speed between 1 and 1500 rpm. These results suggested the maximum rate constant for the electron transfer from cytochrome *a* to cytochrome a_3 to be 0.5 s^{-1}, in agreement with the reported value of 0.58 s^{-1}. On the other hand, the electron transfer from cytochrome a_3 to dioxygen was investigated with the mixed flow transient Raman apparatus constructed to detect an intermediate. The Raman spectrum of an intermediate formed within 450 μs after mixing of the reduced enzyme with molecular oxygen was obtained with high S/N ratios. To obtain the transient Raman spectra with higher time resolution, we constructed an artificial cardiovascular device involving the enzyme reproduction system and now are going to measure the reaction intermediate.

Picosecond Dynamics of Excitation-Energy Transport in Organized Molecular Assemblies

Iwao YAMAZAKI, Naoto TAMAI, Katsuhiko SUMI and Tomoko YAMAZAKI

Dynamics of two- and three-dimensional excitation energy transports are investigated by means of a picosecond time-resolved fluorescence spectrophotometer with several kinds of multilayered architectures:

(1) Langmuir-Blodgett multilayer films,
(2) oriented vapor-deposited films,
(3) photosynthetic antenna pigment systems.

In the multilayer systems (1) and (2) in which different monolayer of chromophore are stacked, the light energy absorbed by the outer surface is transferred sequentially among the layers, and finally trapped to the reaction center. In the course of the energy transfer, fluorescence is emitted from each layer, and is used as a probe for investigating kinetics of the energy transport. These multilayers are analogues to the so-called "antenna pigment" system in the photosynthetic organisms, in particular, the accessary pigment system in blue-green and red algae, in which different kinds of phycobiliproteins are stacked like the artificial multilayers. The results have been presented in the 5th *International Conference on Ultrafast Phenomena* (Snowmass, Colorado, 1986). The final goal of our study is to develop a electrooptic device in molecular scale that controls the light energy transport in the two- and three-dimensional architectures.

Study of Functionalized Ultrafine Particles

Keisaku KIMURA

Metal small particles whose size is less than 5 nm were produced by several methods (see VII-H). The ratio of the number of atoms at surface to the total atoms in these small particles exceeds 50% resulting in the enhanced surface effect. Various kinds of organic dyes including rhodamine derivatives and cyanine derivatives were examined to modify the surface of metal small particle. Chemical modification of surfaces was studied by X-ray photoelectron spectroscopy and by X-ray diffraction. As for tin and lead fine particles, the superconducting transition temperature were measured by the electrical conductivity and AC magnetic susceptibility methods.

Design, Construction and Analyses of High-Spin Organic Molecules and Molecular Assemblies

Hiizu IWAMURA*, Tadashi SUGAWARA, Akira IZUOKA, and Shigeru MURATA

As a subject for the fundamental research of molecular devices, the alignment and storage of spins are as important as the mobility of electrons in organic solids. High-spin polycarbenes $PhC(m\text{-}C_6H_4C)_{n-1}Ph$ and $1,3,5\text{-}C_6H_3[PhC(m\text{-}C_6H_4C)_{\frac{n}{3}-1}]_3$ have been found to have $S=n$ and the spin multiplicity of $2n + 1$ in the ground state. In addition to these systems, a new series of high-spin polymers that have the origin of the spins residing on the side chain of a mainframe conjugate system have been designed. Synthetic efforts have been made to construct polyacetylenes $(p\text{-}PhCC_6H_4\overset{\|}{C}\text{-}C{\equiv}C\text{-}\underset{\|}{C})_n$ and polyphenoxy radicals $(4\text{-}\dot{O}\text{-}3,5\text{-}(t\text{-}C_4H_9)_2C_6H_2\text{-}\overset{|}{C}\text{=}\underset{|}{C})_n$. Model experiments on the dimers have shown that the spin alignment is governed by the regioisomeric connectivity as predicted by theory (V-A-3).

Time Resolved ESR Study on the Excited Triplet States of Coordination Compounds

Shozo TERO and Tasuku ITO

Time resolved ESR technique is a powerful means

to investigate an excited triplet state. The usefulness of this method is enhanced by using helium cryostat, since electron spin relaxation of coordination compounds is normally very short. Effects of molecular structure and configuration on zero-field splitting parameters are our main interest. Excited d-d or d-π CT state, which has very short relaxation time of electron spin, has been studied at very low temperatuers. Parts of our results are presented in the Section VI-I.

Construction of a On-Line Controlled Calorimetry System for Studying Complex Formation Reactions of Metal Ions in Solution

Shin-ichi ISIGURO

Calorimetry is one of the most useful techniques for studying complex formation equilibria between metal ions and ligands in solution. Both formation constants and enthalpies can be simultaneously determined by analyzing a large number of calorimetric data obtained with high accuracy and over the wide range of concentration ratio of ligand to metal ion in solution. The titration method is widely used for the purpose and we developed a fully automatic on-line system for titration calorimetry. The system is based on measurement of a set of temperature-changes ranging 0–0.02°C with a certainty ± 0.00005°C over a certain period of time. The amount of heat accompanying reactions at each titration point is immediately determined by analyzing the set of temperature-change data. Whole titration procedure including 20–30 titration points is automatically carried out according to the computer program developed in our laboratory. Typical results thus obtained using the calorimetry system are given in Section VI-C. A similar system aiming at determining heats of solution of salts in various solvents has been also constructed.

Construction of High-Power Picosecond-Pulsed Laser System Being Tunable from Infrared to Ultraviolet Wavelength Region

Tadaoki MITANI, Yoshihiro TAKAGI, Kazuo HAYAKAWA, Toshio HORIGOME

The time-correlated spectroscopy using picosecond pulsed-lasers is an attractive tool for the investigation of the dynamical properties of the excited states in molecular assemblies. Particularly, the picosecond spectroscopy for study of the strong electron-lattice coupling system, such as structural phase transition in quasi-one-dimensional materials, increasingly attracted attention. To improve optical techniques required for such a wide-frequency picosecond spectroscopy, the staff of Equipment Development Center has designed a high-power picosecond-pulsed laser system, which is composed of a passively mode-locked Nd:YAG laser, a single-pulse selecter, amplifiers (I,II), SHG, THG, FHG, optical parametric generators, and a frequency-down converter (see VII-M-1). This system permits various kinds of the instrumentations, such as optically induced transient absorption measurements and optical gating technique for infrared emission measurement using two picosecond lasers in a spectral region of 266-4400 nm.

Search for New Type Superconductivity in Transition Metal Oxides and Bronzes

Masatoshi SATO, Masashige ONODA, Yuji MATSUDA and Shin-ichi SHAMOTO

There seem two different but closely related ways in the recent studies on superconductivity. One is, more or less, the direct trial to find high-T_c superconductors. Various materials are introduced in this kind of studies. Another way is the search for superconductors which cannot be explained by the traditional BCS type theory. We have adopted transition metal oxides and bronzes as the suitable systems for the latter type studies or for the search for superconductors with very strong electron phonon coupling. So far, various compounds have been prepared and characterized. Among these compounds, rather detailed studies on the anomalous resistivity upturn with decreasing temperature followed by the occurrence of the superconductivity in $Li_{0.9}Mo_6O_{17}$ have been carried out and it can be concluded that $Li_{0.9}Mo_6O_{17}$ is quite unique compound which clearly exhibits both behaviors of superconductivity and electron localization. Detailed studies of CDW-superconductivity competition in Mo_nO_{3n-1} and $A_{0.9}Mo_6O_{17}$ (A = Li, Na and K) have also been carried out. All the compounds have similar layers formed with the corner-linked MoO_6 octahedra

and they exhibit CDW transitions except for $Li_{0.9}Mo_6O_{17}$ which is a superconductor. The condensed modes at the CDW transitions in these compounds are found to be quite similar; that is they can be described as the rotational modes of the octahedra. The coupling of the electrons to this type phonon modes increases with decreasing conduction electron density. Present results give us various informations on the nature of the electron phonon coupling near metal-insulator boundary which seem to be important for the search for high-T_c superconductors.

Reference
M. Sato, *Proc. 15th Yamada Conf.* 1986 Lake Kawaguchi; *Physica B*

Fabrication of Novel Organic Molecular Assemblies with the Use of Molecular Beam Epitaxy Technique

Yusei MARUYAMA, Hajime HOSHI, and Tamotsu INABE

In order to prepare new materials which could be useful for molecular devices elements, we have started to design and fabricate ultra-thin organic multi-layered systems. As the first candidate for this strategy, we have chosen a combination of charge transfer donor and acceptor molecules, e.g. TTF and TCNQ. Sequence of donor and acceptor in the order of monomolecular thickness in each may result in new structure materials which presumably realize new properties. There are many experimental difficulties to obtain a significant size of highly organized 2-dimensional thin-layers. Epitaxial growth deposition of well-regulated molecular beams is now under taken for TCNQ molecules. Technical development for 3-dimensional ordering of multi-layers is also in progress.

Coupled Proton and Electron Transfer in the Crystals of Salicylidenaniline and its Analogues

Tamotsu INABE, Naomi HOSHINO, Tadaoki MITANI, Yoshiki WADA, and Yusei MARUYAMA

It has been well known that the intramolecular proton transfer through the hydrogen bonds in the molecules of salicylidenaniline and its anologues makes a trigger for photochromism and/or thermochromism revealed in the crystalline state of these compounds. After the proton transfer, the lowest excited state could be an intramolecular charge transfer state in which the quinoid structure after releasing proton may be an electron acceptor moiety. These characters may be useful for memory or switching elements of molecular devices. Moreover if we can incorporate significant intermolecular electronic interactions in these crystals, such proton vibration could provide a unique electron-phonon coupling which might result in somewhat novel electron transport behaviors.

At first stage in this work, we have concentrated to prepare a series of new compounds which could have strong intramolecular charge transfer character, some of which are shown in the figure. Optical and electrical properties of these compounds as functions of temperature and pressue are now being pursued.

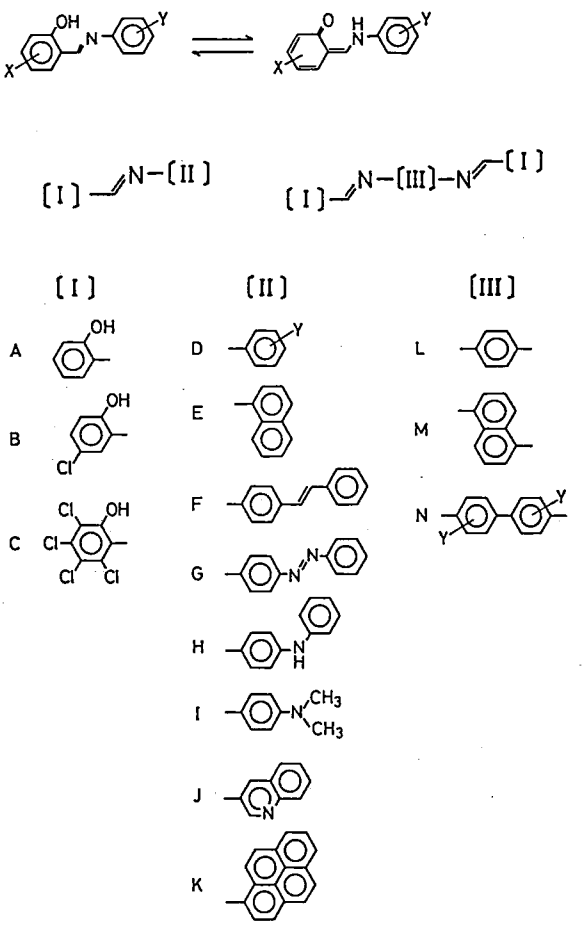

Figure 1

(3) Molecular Science of Primordial Chemical Evolution

Study on Condensation of Interstellar Molecules Forming Icy Dusts and Reactions Induced by Photons and Electrons

Nobuyuki NISHI, Hisanori SHINOHARA, and Kazunori YAMAMOTO

Clustering and aggregation of simple molecules from low temperature gas mixture have been studied by supersonic expansion of molecular beams in order to know possible chemical compositions of icy dusts. Chemical composition of aggregates has been found to be highly dependent on condensation temperature. The systems studied are binary gas mixtures of H_2O+NH_3, H_2O+CO_2, H_2O+CH_3CN, H_2O+CH_3NH_2, H_2O+C_2H_2, H_2O+Ar, and CO_2+CS_2. Due to the very high stabilization energy of water cyclic pentamer (ΔE = −56 kcal/mol at STO-3G level), H_2O molecules in gas mixture tend to condense avoiding the inclusion of foreign molecules, even such hydrophilic molecules as ammonia, which may condense outside of a stable water cluster unit. On the other hand, the ions of the molecular species can form clathrate compounds. Based on the experimental results, two different models of icy dust structure are presented. One is mosaic-microcrystalline model which will be seen for the dusts formed at very low pressure and low temperature region. The other is homogeneously-layered mantle model where inner core is formed around 100 K (depend on the partial pressure) and other molecular species condensate one after another on the temperature decrease. The outermost shell of the dust is expected to consist of hydrophobic molecules such as acetylene, ethylene, allene, cyanoacetylene etc. Those molecules has been found to be converted to highly unsaturated large molecules by photochemical surface reactions. This kind of brownish photoproducts may be the origin of the Halley's black skin.

A Computer Simulation Study of the Formation of Interstellar Molecules by Ion-Molecule Reactions

Hideo YAMAZAKI *(Tokyo Inst. of Tech.)* **and Inosuke KOYANO**

A computer simulation of the molecular syntheses in the interstellar clouds has been performed based on a gas-phase ion-molecule reaction model which incorporates 282 chemical reactions with 104 chemical species. Time evolution of these species was followed from 10^3 to 10^{14} sec by solving the coupled rate equations numerically by use of a quasi-steady state method. The quasi-steady state method has the explicit and semi-implicit forms. The latter is more suitable for the numerical integration of the simultaneous differential equations for reactions, in which rate constants ranging over several orders of magnitude are involved. The semi-implicit method showed perfect stability up to 10^{19} sec. It has been found that about a half of the species attain quasi-steady state at 10^{14} sec, although all species are not in quasi-steady state at the initial stage. In many of these species, the time dependence of the concentration was found to be approximated by the equation $\log C_i(t) = A_i \log t/(1 + B_i \log t)$, where C_i is the concentration of the *i*th chemical species, A_i and B_i are constants, and t is the time.

A sensitivity test was performed for all rate constants involved by changing the value of each rate constant k_j by 10% successively and examining the quantity $(k_j/C_i)(\Delta C_i/\Delta k_j)$ for all i. It has been found that the increase by 10% in a rate constant sometimes yeilds more than 100% increase in the concentration of some species at 10^{11} sec. This stresses the importance of using correct rate data in the reaction model.

OKAZAKI CONFERENCES

"Okazaki Conferences" are principal symposia at IMS, which are held on the subjects related to the "Special Research Projects." They are held two or three times a year, with a moderate number of participants around 50, including several invited foreign speakers. The formal language for the conference is English. Outlines of the twenty-fourth to twenty-sixth conferences are as follows.

The Twenty-fourth Okazaki Conference

Future Prospect in Quasi-One-Dimensional Systems – Charge Transfer and Electron-Phonon Interaction –
(December 12–14, 1985)

Organizers: I. Tsujikawa *(Kyoto Univ.)*, **Y. Maruyama** *(IMS)*, **T. Mitani** *(IMS)* **and K. Nasu** *(IMS)*
Invited Speakers: P. Day *(Univ. Oxford)*, **T.J. Marks** *(Univ. Northwestern)*, **A.J. Heeger** *(Univ. California)*, **M.H. Whangbo** *(Univ. North Carolina)*, **B.K. Chakraverty** *(CNRS, Grenoble)*

This conference was organized so as to discuss various problems concerning with low-dimensional materials such as halogen-bridged mixed-valence metal complexes, BEDT-TTF, polyacetylene and transition metal bronzes. Besides the invited speakers and the organizers listed above, the following domestic participants also gave talks: H. Inokuchi (IMS), M. Yamashita (Univ. Kyushu), K. Toriumi (IMS), H. Tanino (Electrotechnical Laboratory), Y. Wada (IMS), S. Kurita (National Univ. Yokohama), T. Inabe (IMS), G. Saito (ISSP, Univ. Tokyo), H. Kobayashi (Univ. Toho), H. Fukuyama (ISSP, Univ. Tokyo), J. Takimoto (IMS), Y. Tokura (Univ. Tokyo), T. Goto (Univ. Tohoku), K. Yoshino (Univ. Osaka), T. Yamabe (Univ. Kyoto), R. Aoki (Univ. Kyushu), H. Nagasawa

(Univ. Tsukuba), M. Sato (IMS) and K. Kobayashi (Univ. Toyama). Each talk summarized recent developments in the theoretical and experimental studies for low-dimensional materials with some future prospects of this field.

The Twenty-fifth Okazaki Conference

Dynamic Processes of Photoisomerizations
(Jan. 16–18, 1986)

Organizers: M. Itoh *(Kanazawa Univ.)*, **N. Hirota** *(Kyoto Univ.)*, **H. Shizuka** *(Gunma Univ.)* **and K. Yoshihara** *(IMS)*
Invited Speakers: M.A. El-Sayed *(Univ. California, Los Angeles)*, **H.P. Trommsdorff** *(Univ. Scien. Med. Grenoble)*, **R. Mathies** *(Univ. California, Berkeley)*, **P.F. Barbara** *(Univ. Minnesota)* **and J.C. Scaiano** *(NRC Canada)*

This conference was held to discuss about dynamic processes of photoisomerization reactions in the orgnaic molecules. The topics included are as follows: (1) The excited state proton or hydrogen atom transfer, (2) The cis-trans photoisomerizations and related phenomena, and (3) The detection and reaction of photochemical transient species.

Twenty one talks including plenary and invited talks were presented and about 80 people participated to discuss about recent results of these fields especially laser photochemistry of the photoisomerizations.

The Twenty-sixth Okazaki Conference

Molecular Processes in Interstellar Space and Cometary Atmosphere
(June 26–28, 1986)

Organizers: I. Hanazaki *(IMS)*, **I. Koyano** *(IMS)*, **S. Saito** *(Nagoya Univ. and IMS)*, **and N. Nishi** *(IMS)*
Invited Speakers: J. Mayo Greenberg *(Univ. of Leiden)*, **D. Smith** *(Univ. of Birmingham)*, **A. Hjalmarson** *(Onsala Space Obs.)*, **and Adams** *(Univ. of Birmingham)*

"Molecules" are now known as very important elementary substances in accounting for astronomical

phenomena, such as primary processes of star formation or evolution of proto-solar nebulae. As predicted by Prof. Greenberg in the early 1960s, interstellar dusts are also understood as condensates of molecules which form cometary nuclei in some cases. In recent spacecraft encounters with comet Halley, Giotto, Suisei and Vega provided highly conclusive evidence for this idea.

Dr. Hjalmarson talked about the distribution of molecular species and its relation to physical processes and structures of interstellar space from a viewpoint of radioastronomy. Prof. Hayakawa introduced a historical survey of the study of interstellar dusts. Special emphasis was put on the grain size in relation to the formation circumstances, in the stellar wind of cool stars or in shock waves triggered by supernovae.

Prof. Greenberg presented his new idea of molecular formation on interestellar dusts and proposed that the original materials of the most of organic compounds on earth were carried by comets. Prof Shimizu reported the observation of hydrogen-atom emission distribution around Halley by Japanese spacecraft Suisei and attributed its origin partly to organic substances on cometary dusts ejected from nucleus.

Prof. Smith discussed the molecular formation processes in diffuse and dense molecular clouds from a point of view of ion-molecule reactions. He particularly emphasized the importance of radiative association mechanism as demonstrated by the formation of $C_3H_3^+$. Dr. Adams talked about the laboratory measurements of ion-molecule reaction rates at low temperatures. As can be seen in the program, many impressive presentations were also given by other Japanese speakers and the participants were convinced that the field of "astrochemistry" or "molecular astrophysics" is growing quite rapidly with the cooperation of astronomers, physicists, and physical chemists.

JOINT STUDIES PROGRAMS

As one of the important functions of an inter-university research institution, IMS undertakes joint studies programs for which funds are available to cover research expenses as well as travel and living expenses of individuals. The proposals from domestic scientists are reviewed and controlled by the inter-university committee. The programs are carried out under one of five categories:

1) Joint studies on Special Projects (a special project of significant relevance to the advancement of molecular science can be carried out by a team of several groups of scientists).
2) Research Symposia (on timely topics in collaboration with both outside and IMS scientists).
3) Cooperative Research (carried out in collaboration with both outside and IMS scientists).
4) Use of Facility (the Computer Center, Instrument Center and other research facilities at IMS are open to all researchers throughout the country).
5) Joint studies programs using UVSOR facilities have started in the fiscal year 1985.

In the fiscal year 1985, number of joint studies programs accepted amounted to 4, 8, 170 and 214 for categories 1)–4), respectively.

1) Special Projects

Magnetic Field Effects Upon Dynamic Behavior of Excited Species

Coordinators: **Hisaharu HAYASHI** *(Inst. of Phys. and Chem. Research and IMS)*
Hirochika SAKURAGI *(Univ. of Tsukuba and IMS)*
Yoshifumi TANIMOTO *(Kanazawa Univ.)*
Hajime KATO *(Kobe Univ.)*

Recently, we have found magnetic field effects in many chemical reactions and many energy transfer processes. The effects have provided us with new aspects in dynamic behavior of excited species. However, for some of the effects, their mechanisms have not yet been clarified well. Therefore, one of the aims of this joint study is to investigate the mechanisms. Indeed, we have studied the effects on the gas-phase-emission of CS_2 and Cs_2 with ns and ps dye lasers. On the other hand, we would like to challenge to discover new magnetic field effects. In actuality, we have found the effects on the reactions of excited species (NO and CH) generated by microwave discharge in the gas phase and the intra-molecular hydrogen abstraction and electron-transfer reactions of chained molecules ($A\text{-}(CH_2)_n\text{-}D$) in solution. This joint study was started from April, 1985.

The other members of the program are N. Mataga *(Osaka Univ. and IMS)*, K. Mutai *(Univ. of Tokyo)*, I. Yamazaki *(Instrument Center)*, R. Nakagaki *(Electronic Structure)*, T. Imamura *(Electronic Structure)*, H. Abe *(Inst. of Phys. and Chem. Res.)*, K. Iwai *(Nara Women's Univ.)* and Y. Hirata *(Osaka Univ.)*.

Near Infrared Raman Spectroscopy of Doped Polyacetylene

Coordinators: **Iwao YAMAZAKI** *(Instrument Center)*
Teizo KITAGAWA *(Department of Molecular Structure)*
Jiro TANAKA *(Nagoya University)*

The mechanism of the electrical conduction in the doped polyacetylene is still a problem of open question and the structure of the charged soliton defect has attracted many attention. The electronic transition of the charged soliton defect is characterized by the so-called the mid-gap band which appeared in the near infrared region and it has been desired to measure the Raman spectra of doped polyacetylene by a resonance excitation of the near infrared light. The Raman instrument which utilizes the near infrared excitation will be set up and a quantitative measurement on the doping level and the Raman spectra will be performed. This study will be extended to include many dopant, transient Raman spectral studies and to other kind of conducting polymers.

Cooperators: Masaaki Shimizu, Masashi Tanaka and Kimihiko Hirao *(Nagoya University)*, Takayoshi Kobayashi *(University of Tokyo and IMS)*

Molecular Mechanism of the Electron and Proton Transfers by Proteins and Their Coupling

Coordinator: **Teizo KITAGAWA** *(Department of Molecular Dynamics)*

The vectorial proton translocation through biological membrane against the concentration-gradient is known to be essential to biological energy production, but its mechanism remains to be solved. This project aims to elucidate a molecular mechanism of the proton translocation for three representative cases. The first is the electron-driven proton pump seen in the respiratory chain of aerobic organisms. Among the three pumping sites, we pick up only site III where cytochrome oxidase pumps protons. The electron transfer between two heme groups in this enzyme and the reduction of molecular oxygen by the transfered electrons will be investigated mainly with transient resonance Raman spectroscopy. The timing of the proton translocation induced by the electron transfer will be determined by time resolved fluorescence spectra of an appropriate pH indicator. Drs. Y. Orii (Kyoto Univ.) and Y. Sone (Jichi Medical School) join in discussion. The second system to be treated is a light-driven proton pump seen in bactriorhodopsin. In this case photo-induced cis-trans isomerization of the retinal Schiff's base is the primary process. We intend to observe transient resonance Raman spectra in μs region of the protein as well as of the chromophore. Drs. A. Maeda (Kyoto Univ.) and K. Ohno (Jichi Medical School) actively join in this subject. The third system is a passive proton translocation along the concentration-gradient by H^+-ATPase, which catalyzes the formation of ATP from ADP and P_i upon the proton translocation. Drs. M. Futai (Osaka Univ.) and N. Sone (Jichi Medical School) join in this subject as biochemists.

Dynamics of Excited Molecules in the Gas Phase Produced by Collisions with Metastable Atoms

Kozo KUCHITSU *(University of Tokyo)*, **Eizi HIROTA, Kosuke SHOBATAKE, Tamotsu KONDOW** *(University of Tokyo)*, **Kaoru SUZUKI** *(University of Tokyo)*, **Takashi NAGATA** *(University of Tokyo)*, **Hiromichi UEHARA** *(Josai University)*, **and Hiroki NAKAMURA**

Reaction dynamics of rare gas metastable atoms, Rg^m, and highly excited Rydberg atoms, Rg**, with molecules and clusters has been studied. The velocity dependence of the cross section for the following reaction was measured using an arc-heated molecular beam apparatus in order to obtain information on the potential surface:

$$Rg^m + BrCN \rightarrow Rg + Br + CN(B^2\Sigma^+), \quad (1)$$

where Rg^m is $Ar(^3P_{0,2})$ or $Kr(^3P_{0,2})$. The results suggest the importance of the interaction in the entrance channel, where the covalent (Ar/Kr, BrCN) potential crosses the ionic (Ar^+/Kr^+, $BrCN^-$) potential. In the case of $Ar(^3P_{0,2})$ the reaction at thermal energy region was investigated using a flowing afterglow apparatus. The nascent rovibrational distribution of $CN(B^2\Sigma^+)$ in reaction (1) was measured. A surprisal analysis of the result suggests the energy transfer mechanism for reaction (1). This conclusion is consistent with the above-mentioned molecular-beam experiment as well as the Xe^m+BrCN/ClCN experiment at thermal energy and for the polarization study at higher collision energy.[1] When He^m was used, the target molecule such as H_2O, H_2S, NH_3, CH_3Cl, and CH_3OH, could be excited to high Rydberg states.[2] Some of these Rydberg states may be produced via double excitation, for which the reaction of metastable atoms is shown to be efficient.

The quartet states of CN are also produced in the reaction of metastable rare gas atoms with BrCN. Collisional relaxation of the $^4\Pi$ state was studied. Ar and He were chosen as collision partners. The results confirm that the polarizability of the collision partner is important in the collisional relaxation. In reaction (1) $CN(B^2\Sigma^+)$ is produced in vibrational states up to 20. An analysis of the band intensities of the $B^2\Sigma^+ - X^2\Sigma^+$ transition leads to the determination of the dependence of the electronic transition moment on the internuclear distance. The dependence reflects the mixing of higher electronic states. Other potential sources of similar information are electronic terms of various interactions. A perturbation analysis between the $A^2\Pi_i$ and $B^2\Sigma^+$ states was also made in this context.

Negative cluster ions were formed in reactions of high Rydberg rare gas atoms with van der Waals clusters. The size dependence of the electron affinity, evaporation of the constituent, intracluster reactions and hydration of the clusters were obtained for various molecular systems such as CO_2, OCS, CS_2,[3] SF_6,[4]

CH_3CN,[5] pyridine, NO, N_2O, and CCl_4. Negative cluster ions of water, $(H_2O)_n^-$, were detected in this reaction in contrast to $(H_2O)_mOH^-$ reported in previous papers.

References

1) T. Nagata, T. Kondow, K. Kuchitsu, T. Tabayashi and K. Shobatake, *J. Phys. Chem.*, **89**, 2916 (1985).
2) K. Someda, T. Kondow and K. Kuchitsu, *J. Phys. Chem.*, **90**, 4044 (1986).
3) T. Kondow and K. Mitsuke, *J. Chem. Phys.*, **83**, 2612 (1985).
4) K. Mitsuke, T. Kondow and K. Kuchitsu, *J. Phys. Chem.*, **90**, 1552 (1986).
5) K. Mitsuke, T. Kondow and K. Kuchitsu, *J. Phys. Chem.*, **90**, 1505 (1986).

2) Research Symposia

1. Molecular Fields Made by Cage-Shaped Organic Molecules and Their Novel Functions
   (December 2nd – 3rd, 1985)
   Organizer: S. Misumi (IMS)
2. Relationship between Catalytic Actions of Multinuclear Metal Complexes and Metal Clusters
   (January 10th – 11th, 1986)
   Organizer: A. Nakamura (IMS)
3. New Aspects of Electron Spectroscopy
   (March 7th, 1986)
   Organizer: K. Kimura (IMS)
4. Conducting Single Component Organic Solids –Molecular Fastner–
   (March 13th – 14th, 1986)
   Organizer: H. Inokuchi (IMS)
5. Formation of Metastable Atoms and Their Dynamical Behavior
   (March 24th, 1986)
   Organizer: K. Kuchitsu (Univ. of Tokyo)
6. Theory of Molecular Dynamic Processes
   (March 25th – 27th, 1986)
   Organizer: H. Nakamura (IMS)
7. Recent Progress in Chemical Reaction Dynamics Research
   (May 23rd – 24th, 1986)
   Organizer: K. Shobatake (IMS)
8. Electrochemical and Catalytic Processes of Carbon Dioxide Reduction and Nitrogen Fixation
   (August 18th – 19th, 1986)
   Organizer: K. Ito (Nagoya Inst. Tech.)

3) Cooperative Research

This is one of the most important programs IMS undertakes for conducting its own research of the common interest to both outside and IMS scientists by using the facilities at IMS. During the first half of fiscal year of 1985 ending on September 30, 88 outside scientists including 5 invited collaborated with IMS scientists; and during the second half of the fiscal year, 82 outside scientists including 7 invited worked in collaboration with IMS scientists, the names and the affiliations of these collaborators are found in the Research Activities.

4) Use of Facility

The number of projects accepted for the Use of Facility Program of the Computer Center during the fiscal year of 1985 amounted to 152 (427 users), and the computer time spent for these projects is 5075 hours (55% of the total annual CPU time).

Sixty two projects (102 users) were accepted for the Use of Facility Program of the Instrument Center during the fiscal year of 1985.

5) UVSOR

Joint studies programs using UVSOR facilities are carried out under one of three categories: 5-a) UVSOR Special Project, 5-b) UVSOR Cooperative Research, and 5-c) Use of UVSOR Facility.

The 7th UVSOR Research Symposium, organized by H. Inokuchi (IMS), was held during December 3rd – 4th, 1985.

5-a) UVSOR Special Project

Studies of Negative Ion Formation by Two-Electron Capture of Positive Molecular Ions from Alkali Atoms

Coordinators: **Toshio SUGIURA** *(Univ. of Osaka Prefecture)*
Inosuke KOYANO *(Department of Molecular Assemblies)*

The neutral beam injection (NBI) into a magnetically-confined fusion reactor is an issue of current concern as a means of auxiliary heating of

fusion plasma. One of the most promising techniques for producing the fast (E $\gtrsim$ 100 keV) neutral beams required for this purpose is the generation and subsequent neutralization of fast negative ion beams. Basic studies of processes producing negative ions are urgently required for the development of the fast beam sources.

In the present project, we study the production of the H^- ions from H_2^+ by two-step charge exchange with Cs. Preliminary experiments with electron impact ionization indicated that the vibrationally excited H_2^+ ions might play an important role in this exchange process. Thus the main objective of the present study is the determination of the H^- production efficiency for the individual vibrational states of H_2^+. For this purpose we utilize the TEPSICO-II apparatus,[1,2] which is installed in the BL3B beam line of the UVSOR, with some modification. The primary H_2^+ ions are produced by photoionization of H_2 at the threshold wavelengths for the individual vibrational states of interest. H^- ions produced are counted in coincidence with the threshold electrons. The main point of modification is the replacement of the dodecapole reaction region of the TEPSICO-II by a heated charge-exchange chamber combined with a cesium oven. Fabrication and installation of these systems have been completed and experiments are going on.

References

1) K. Tanaka, T. Kato, and I. Koyano, *IMS Ann. Rev.*, 85 (1984).
2) I. Koyano, K. Tanaka, T. Kato, S. Suzuki, and E. Ishiguro, *Nucl. Instrum. Meth.*, **A246**, 507 (1986).

Synchrotron Radiation Photoionization Spectroscopy of Molecules and Molecular Clusters in Supersonic Jets

Katsumi KIMURA

The supersonic molecular beam apparatus constructed in the Beam Line BL2B2 [UVSOR-13, p.27] has further been improved during the past one year in several points mainly by H. Shiromaru and Y. Achiba in cooperation with several other collaborators who join in this project. The improvements recently made are as follows: (1) the alignment of molecular beam, (2) the preparation of a sample cooling system, (3) the removal of the second-order radiation by introducing helium gas into the monochromator, (4) the monitor of the stagnation pressure, (5) the manipulation of a LiF plate from outside of the chamber, (6) the computer control of injector pulse, etc. Several kinds of experiments of photoionization threshold measurements with a quadrupole mass filter and photoabsorption measurements are now proceeding for various cooled molecules and molecular clusters. Photoelectron measurements are also included in this project.

Fluorescence Studies of Photochemical Reactions Using Synchrotron Radiation as a Light Source

Coordinator: **Kosuke SHOBATAKE** *(Department of Molecular Assemblies)*

This group project is to organize the research efforts aimed at studying the photochemical reactions initiated by UV and vacuum uv light using a vapor phase fluorescence apparatus installed on the beam line BL2A at the UVSOR synchrotron radiation facility. The brief description of the fluorescence apparatus and some of the results obtained last year are presented in the Research Activities IV-O of IMS Annual Review, 1985 (pp.95-98). For the last one year fluorescence studies of gaseous chemical reactions using this apparatus have been continued. One can now routinely measure absorption, fluorescence excitation, and dispersed fluorescence spectra of gaseous samples in the wavelength region above 1050 Å. Some part of the results are presented in the Research Activities IV-O of this issue (IV-O-1~7). Recently a progress has been made in measuring time-resolved fluorescence decay spectra using the pulsed nature of synchrotron radiation (see IV-O-8). Although the single bunch mode operation of the machine is not carried out very often, this new technique is expected to provide dynamic information about photochemical reactions.

5-b) UVSOR Cooperative Research

During the first half of fiscal year of 1985, 13 outside scientists including 6 invited collaborated with IMS scientists; and during the second half of the fiscal year, 11 outside scientists including 4 invited worked in collaboration with IMS scientists.

5-c) Use of UVSOR Facility

The number of projects accepted for the Use of UVSOR Facility Program during the fiscal year of 1985 amounted to 32.

FOREIGN SCHOLARS

Visitors from abroad play an important role in research activities and are always welcome at IMS. The following is the list of foreign scientists who visited IMS in the past year (Aug. 1985 – July 1986). The sign *1 indicates an attendant to an Okazaki Conference, *2 an IMS or Japan Society for the Promotion of Science Invited Foreign Scholar, *3 an IMS councillor, *4 an IMS visiting scientist and *5 an IMS adjunct professor or associate Professor from abroad.

Prof. R.J. Donovan	Univ. of Edinburgh	(UK)	Jul. – Aug. 1985
Prof. C.B. Moore	Univ. of California, Berkeley	(USA)	Jul. – Aug. 1985
Prof. T. Gillbro	Univ. Umeå	(Sweden)	Jul. – Aug. 1985
Prof. V. Sundström	Univ. Umeå	(Sweden)	Jul. – Aug. 1985
Prof. V.S. Letokhov	Inst. Spectroscopy	(USSR)	Jul. – Aug. 1985
Dr. A.J. Rest	Univ. of Southampton	(UK)	Jul. – Aug. 1985
Prof. L.M. Venanzi*2	ETH	(Switzerland)	Jul. – Aug. 1985
Prof. B.J. Yoon	Kangreung Natl. Univ.	(Korea)	Jul. – Aug. 1985
Prof. K.T. No	Soon Jun Univ.	(Korea)	Jul. – Aug. 1985
Prof. M.C. Chang*2·4	Sun Cheon Natl. Univ.	(Korea)	Jul. – Aug. 1985
			Dec. 1985 – Jan. 1986
			Jun. – Jul. 1986
Prof. H. Okabe*4	Howard Univ.	(USA)	Jul. – Sep. 1985
Prof. A.H. Kalantar	Univ. of Alberta	(Canada)	Aug. 1985
Prof. P. Tseng	Natl. Taiwan Univ.	(Taiwan)	Aug. 1985
Prof. E.W. Schlag	Tech. Univ. München	(FRG)	Aug. 1985
Prof. E.K.C. Lee	Univ. of California, Irvine	(USA)	Aug. 1985
Prof. R.N. Dixon	Univ. of Bristol	(UK)	Aug. 1985
Prof. W.M. Jackson	Howard Univ.	(USA)	Aug. 1985
Prof. K.Y. Choo	Seoul Natl. Univ.	(Korea)	Aug. 1985
Prof. D. Phillips	Royal Inst.	(UK)	Aug. 1985
Prof. F. Stuhl	Ruhr Univ.	(FRG)	Aug. 1985
Prof. C. Wittig	Univ. of South. California	(USA)	Aug. 1985
Dr. H.H. Nelson	Nav. Res. Lab.	(USA)	Aug. 1985
Dr. J.E. Butler	Nav. Res. Lab.	(USA)	Aug. 1985
Prof. E.C. Lim	Wayne State Univ.	(USA)	Aug. 1985
Prof. K.H. Becker	Berg. Univ.	(FRG)	Aug. 1985
Prof. F. Lahmani	Univ. Paris-Sud	(France)	Aug. 1985
Dr. W.L. Faust	Nav. Res. Lab.	(USA)	Aug. 1985
Dr. A. Auty	Royal Inst.	(UK)	Aug. 1985
Prof. G.B. Sergeev	Mosk. Gos. Univ.	(USSR)	Aug. 1985
Prof. H. Meier	Univ. Mainz	(FRG)	Aug. 1985
Dr. H.E. Hunziker	Res. Lab., IBM, San Jose	(USA)	Aug. 1985
Dr. H. Petek	Univ. of California, Berkeley	(USA)	Aug. 1985 – Jul. 1987
Dr. N. Boens*4	Kathol. Univ. Leuven	(Belgium)	Aug. – Sep. 1985
Prof. H.D. Bist*5	Indian Inst. Tech., Kanpur	(India)	Aug. 1985 – May 1986
Prof. X. Zhao*2	Kankai Univ.	(China)	Sep. 1985
Prof. W.A. Lester	Univ. of California, Berkeley	(USA)	Sep. 1985
Dr. R.R. Ries	Natl. Sci. Found. (NSF)	(USA)	Sep. 1985

Mr. C.T. Owens	Natl. Sci. Found. (NSF) Tokyo Office	(USA)	Sep. 1985
Prof. D.B. McLay	Queen's Univ.	(Canada)	Sep. 1985
Dr. J.B. Hunt	Natl. Sci. Found. (NSF)	(USA)	Sep. 1985
Dr. W.C. Harris	Res. Lab., IBM, San Jose	(USA)	Sep. 1985
Prof. C.E. Schäffer*[2]	Univ. Copenhagen	(Denmark)	Sep. 1985
Prof. M.A. Robb	Queen Elizabeth Coll.	(UK)	Sep. 1985
Dr. V.R. Saunders	Daresbury Lab., SERC	(UK)	Sep. 1985
Prof. N.C. Handy	Univ. of Cambridge	(UK)	Sep. 1985
Dr. J.N.L. Connor	Univ. of Manchester	(UK)	Sep. 1985
Dr. D.C. Clary	Univ. of Cambridge	(UK)	Sep. 1985
Prof. D.F. Fincham	Univ. of York	(UK)	Sep. 1985
Prof. K. Singer	Univ. of London	(UK)	Sep. 1985
Prof. J. Gerratt	Univ. of Bristol	(UK)	Sep. 1985
Dr. P. Monceau	CNRS Grenoble	(France)	Sep. 1985
Prof. E.A. Silinish*[2]	Physico-energ. Inst., Ratvian Acad. Sci.	(USSR)	Sep. – Dec. 1985
Prof. R. Chen*[2]	Dalian Inst. Chem. Phys.	(China)	Sep. – Nov. 1985
Prof. M. Baer*[5]	Soreq Nucl. Res. Cent.	(Israel)	Sep. 1985 – Jun. 1986
Mr. M.J.J. Vrakking*[4]	Eindhoven Univ. Tech.	(Netherlands)	Sep. 1985 – Mar. 1986
Dr. V.M. Donnely	AT & T Bell Lab.	(USA)	Oct. 1985
Prof. M.A.J. Rodgers	Univ. of Texas, Austin	(USA)	Oct. 1985
Prof. L.T. Scott	Univ. of Nevada	(USA)	Oct. 1985
Prof. H. Taube*[2]	Stanford Univ.	(USA)	Oct. 1985
D.A.A. MacDowell	Daresbury Lab., SERC	(UK)	Oct. 1985
Prof. F. Bickelhaupt	Vrije Univ.	(Netherlands)	Oct. 1985
Prof. I. Bertini*[2]	Univ. Firenze	(Italy)	Nov. 1985
Prof. A. Magnéli*[2]	Univ. Stockholm	(Sweden)	Nov. 1985
Dr. H. Jucker	Lonza Ltd.	(Switzerland)	Nov. 1985
Dr. K. Yoshino	Harvard-Smithonian Cent. Astrophys.	(USA)	Nov. 1985
Prof. P.E. Eaton	Univ. of Chicago	(USA)	Nov. 1985
Prof. H. Winick	Stanford Synch. Rad. Lab., Stanford Univ.	(USA)	Dec. 1985
Prof. R. Kaptein	Univ. Groningen	(Netherlands)	Dec. 1985
Prof. T.K. Sham	Chinese Univ.	(Hong Kong)	Dec. 1985
Dr. H. Roth	AT & T Bell Lab.	(USA)	Dec. 1985
Prof. K.H. Jung	Korea Adv. Inst. Sci. Tech. (KAIST)	(Korea)	Dec. 1985 – Feb. 1986
Dr. Z. Chen	Hefei Natl. Synch. Rad. Lab., Univ. Sci. Tech. China	(China)	Jan. 1986
Dr. Y. Zhang	Hefei Natl. Synch. Rad. Lab., Univ. Sci. Tech. China	(China)	Jan. 1986
Dr. Y. Pei	Hefei Natl. Synch. Rad. Lab., Univ. Sci. Tech. China	(China)	Jan. 1986
Prof. G. Li	Hefei Natl. Synch. Rad. Lab., Univ. Sci. Tech. China	(China)	Jan. 1986
Dr. R. Xie	Hefei Natl. Synch. Rad. Lab., Univ. Sci. Tech. China	(China)	Jan. 1986

Prof. G.C. Wang	Hefei Natl. Synch. Rad. Lab., Univ. Sci. Tech. China	(China)	Jan. 1986
Dr. Y. Yamaguchi	Univ. of California, Berkeley	(USA)	Jan. 1986
Prof. H.P. Trommsdorff*[1]	Univ. Sci. Med. Grenoble	(France)	Jan. 1986
Prof. P.F. Barbara*[1]	Univ. of Minnesota	(USA)	Jan. 1986
Dr. J.C. Scaiano*[1]	Natl. Res. Counc. (NRC)	(Canada)	Jan. 1986
Prof. R. Mathies*[1]	Univ. of California, Berkeley	(USA)	Jan. 1986
Prof. M.A. El-Sayed*[1]	Univ. of California, Los Angeles	(USA)	Jan. 1986
Prof. B.S. Lee*[2]	Inha Univ.	(Korea)	Jan. – Mar. 1986
Dr. T.A. Claxton	Univ. of Leicester	(UK)	Mar. 1986
Prof. K. Siegbahn*[2]	Uppsala Univ.	(Sweden)	Mar. 1986
Prof. Y.T. Lee*[2]	Univ. of California, Berkeley	(USA)	Mar. – Jun. 1986
Prof. E. Fluck*[2]	Gmelin-Inst. Anorg. Chem., Max-Planck-Ges.	(FRG)	Mar. 1986
Dr. D.E. Fenton*[2]	Univ. of Sheffield	(UK)	Mar. 1986
Prof. A.S. Kende	Univ. of Rochester	(USA)	Mar. 1986
Dr. J.-L. Birbaum	Inst. Chim. Org. l'Univ.	(France)	Mar. 1986
Prof. G.L. Closs	Univ. of Chicago	(USA)	Mar. 1986
Mr. A. Campen	Univ. of Southampton	(UK)	Mar. – Jun. 1986
Prof. M. Vala	Univ. of Florida	(USA)	Apr. 1986
Prof. A.G. Sykes*[2]	Univ. of Newcastle upon Tyne	(UK)	Apr. 1986
Mr. S.J. Cox	Royal Soc.	(UK)	Apr. 1986
Prof. L. Skattebol	Univ. Oslo	(Norway)	Apr. 1986
Prof. J.M. Lee*[5]	Chonbuk Natl. Univ.	(Korea)	Apr. – Nov. 1986
Prof. G.A. Crosby	Washington State Univ.	(USA)	May 1986
Prof. L.I. Simándi*[2]	Univ. Budapest	(Hungary)	May 1986
Prof. M.A. Hoffman	Boston Univ.	(USA)	May 1986
Dr. L. Nogy	A. Jozsef Univ.	(Hungary)	May 1986
Dr. P. Delhaes	Cent. Rech. Paul Pascal, Univ. Bordeaux	(France)	May 1986
Prof. P.O. Löwdin*[3]	Univ. of Florida	(USA)	May 1986
Prof. E. Fischer	Weizmann Inst.	(Israel)	May 1986
Prof. B.L. Crawford, Jr.	Univ. Minnesota	(USA)	May 1986
Prof. L.D. Kispert	Univ. of Alabama	(USA)	May 1986
Dr. J. Dumas	CNRS Grenoble	(France)	May 1986
Mr. Z. Tian*[4]	Fudan Univ.	(China)	May – Oct. 1986
Dr. C. Daniel*[2]	Univ. Strasbourg	(France)	May – Nov. 1986
Dr. J.K. Jeszka*[5]	Cent. Mol. Macromol. Stud., Pol. Acad. Sci.	(Poland)	May – Nov. 1986
Prof. K. Nakamoto	Marquette Univ.	(USA)	Jun. 1986
Prof. C.E. Brion*[2]	Univ. of British Columbia	(Canada)	Jun. 1986
Prof. K.W. Hanck	North Carolina State Univ.	(USA)	Jun. 1986
Prof. M.K. DeArmond	North Carolina State Univ.	(USA)	Jun. 1986
Prof. D. Smith*[1]	Univ. of Birmingham	(UK)	Jun. 1986
Dr. N.G. Adams*[1]	Univ. of Birmingham	(UK)	Jun. 1986
Dr. A.G. Hjalmarson*[1]	Onsala Space Obs.	(Sweden)	Jun. 1986
Prof. J.M. Greenberg*[1]	Univ. of Leiden	(Netherlands)	Jun. 1986
Dr. T. Matsubara	Photogr. Res. Lab., Eastman Kodak Co.	(USA)	Jun. 1986

Dr. M.F.Guest	Daresbury Lab., SERC	(UK)	Jun. 1986
Prof. S.O. Oh*2	Kyungpook Natl. Univ.	(Korea)	Jun. – Aug. 1986
Prof. H.-S. Yoo*2	Chungbuk Natl. Univ.	(Korea)	Jun. – Aug. 1986
Dr. M.R. Willis*2	Univ. of Nottingham	(UK)	Jun. – Sep. 1986
Prof. E. Tiemann*5	Inst. At. Molekulphys., Univ. Hannover	(FRG)	Jun. 1986 – Mar. 1987
Dr. J.R. Grover*5	Brookhaven Natl. Lab.	(USA)	Jun. 1986 – Apr. 1987
Prof. M. Randic	Drake Univ.	(USA)	Jul. 1986
Mr. H.K. Kang	Korea Adv. Inst. Sci. Tech. (KAIST)	(Korea)	Jul. 1986
Prof. B.Y. Lee*4	Gyeongsang Natl. Univ.	(Korea)	Jul. 1986
Dr. J.A. Richards	British Counc., Tokyo	(UK)	Jul. 1986
Prof. B.T. Newbold	Moncton Univ.	(Canada)	Jul. 1986
Prof. F.K. Tittel	Rice Univ.	(USA)	Jul. 1986
Dr. J.P. Pouget	Lab. Phys. Solids, Univ. Paris-Sud	(France)	Jul. 1986
Prof. X. Sun*2	Fudan Univ.	(China)	Jul. – Nov. 1986
Mr. Chang-qin Wu	Fudan Univ.	(China)	Jul. – Oct. 1986

AWARD

The Cultural Achievements of Professor Nagakura

Professor Saburo Nagakura, the Director General of IMS, was honored as a Person of Cultural Merit by the Government for his contributions to culture through his achievements in molecular science. Person of Cultural Merit is the most distinguished title that can be awarded to scientists and artists in Japan. Among his important research achievements, the following are the most widely recognized: the concept of charge-transfer in molecules and its experimental proof, and studies of the effect of magnetic fields on chemical reactivity and the concomitant creation of the new field of spin chemistry.

Prof. Kida's Scientific Achievement

Prof. Sigeo Kida received the Award of the Chemical Society of Japan in 1986 for his contribution to "Studies on Binuclear and Polynuclear Metal Complexes".

Since 1970, Prof. Kida continues his original works on the syntheses of various kinds of binuclear complexes such as alkoxo-bridged, hetero-metal, face-to-face and hetero-bridged complexes. Especially, from magnetic properties of a series of hetero-metal binuclear complexes, it was revealed that spin exchange interactions within these complesxes are mainly ascribed to the overlap between orbitals of the bridged atoms and d-orbitals of metal ions occupied with unpaired electrons. He also experimentally demonstrated the existence of the orbital complementary and counter complementary effects in superexchange interaction within the hetero-bridged binuclear complexes.

He found that binuclear copper (II) complexes exhibit two-electron redox properties, and then used them as oxidative catalysts of 3,5-di-*tert*-butylcatechol, ascorbic acid and etc. The binuclear copper (II) complexes showed a significantly high catalytic ability as compared with that of the corresponding mononuclear complexes.

Prof. Kida was also interested in a variety of one-dimensional mixed valence complexes of Pt(II, IV), Pd(II, IV) and Ni(II, IV), and investigated their physico-chemical properties. Nowadays, these works became a basis of those of related one-dimensional mixed valence complexes that are widely studied in our country.

Prof. Mataga's Scientific Achievements

Prof. Noboru Mataga, an adjunct professor from Osaka University, received the Award of the Chemical Society of Japan in 1986 for his contributions to "Studies on Molecular Interactions in Excited Electronic States and Photochemical Primary Processes".

Since 1950's he has been a pioneer in the study of the primary photochemical reactions in solution. The focus of his research has been to the various kinds of intermolecular interactions of excited molecules. His contributions includes: 1) solvent effects on fluorescence spectra, 2) hydrogen bonding interactions in the electronically excited states, 3) photo-induced electron transfer, 4) intermolecular energy transfer, 5) intermolecular interactions, and 6) photochemical reactions in molecular assembries. Much of this work was made possible by Professor Mataga's improvements on nanosecond and picosecond flash photolysis techniques.

Mr. Hayasaka's Contribution

Mr. Kei-ichi Hayasaka received the Chemical Society of Japan Award for Distinguished Technical Achievements for 1985 for "Development of Production Techniques and Utilization of Liquid Helium".

This award is presented to a person who contributed a great deal to the development of techniques needed in chemical and chemical engineering research in Japan. Mr. Hayasaka remarkably improved efficiency for producing liquid helium and greatly shortened the waiting period between the starting time of liquidifier and that of liquidification by technical improvements involving modification of a heat exchanger. For efficient use of liquid helium, it is well known that a high recovery rate of used helium gas is essential. In fact Mr. Hayasaka designed and made new gas balloons made of far less permiable synthetic rubber and installed high-quality gas recovery lines. Owing to Mr. Hayasaka's perpetual improvements of helium gas recovery processes, a remarkably high recovery rate of 95% has been successfully achieved at the Low-Temperature Center of the Institute for Molecular Science.

LIST OF PUBLICATIONS

K. MOROKUMA, K. OHTA, N. KOGA, S. OBARA, and E.R. DAVIDSON, "Potential-energy Surfaces for Chemical Reactions. Dimerization of CH_2 and SiH_2, the S_N2 Reaction in Gas-phase Clusters and CH Activation in Transition-metal Complexes.", *Faraday Symp. Chem. Soc.*, **19**, 49 (1985).

N. KOGA and K. MOROKUMA, "Determination of the Lowest Energy Point on the Crossing Seam between Two Potential Surfaces Using the Energy Gradient.", *Chem. Phys. Lett.*, **119**, 371 (1985).

K. ABE, M. HIROTA, and K. MOROKUMA, "Preferred Conformation of 1-Phenyl-2-propanol. Ab initio and Molecular Mechanics Calculations with Geometry Optimization.", *Bull. Chem. Soc. Jpn.*, **58**, 2713 (1985).

N. KOGA, S. OBARA, K. KITAURA, and K. MOROKUMA, "Role of Agostic Interaction in β-Elimination of Pd and Ni Complexes. An Ab Initio MO Study.", *J. Am. Chem. Soc.*, **107**, 7109 (1985).

N. KOGA and K. MOROKUMA, "Alkyl Migration or Carbonyl Migration? Ab Initio MO Study of Reaction Mechanism for Carbonyl Insertion of Pd Complex.", *J. Am. Chem. Soc.*, **107**, 7230 (1985).

K. OHTA and K. MOROKUMA, "An MO Study of S_N2 Reactions in Hydraged Gas Clusters: $(H_2O)_nOH^- + CH_3Cl(H_2O)_m \rightarrow HOCH_3 + Cl^- + (n+m)H_2O$.", *J. Phys. Chem.*, **89**, 5845 (1985).

S. SAKAKI, H. SATO, Y. IMAI, K. MOROKUMA, and K. OHKUBO, "Comparison of Electronic Structure, Stereochemistry, and Coordinate Bonds Between Ni(0)–SO_2 Complexes and Nonmetal SO_2 Complexes. An MO Study.", *Inorg. Chem.*, **24**, 4538 (1985).

K. KAMIYA and K. MOROKUMA, "Potential Energy Surface and Reaction Mechanism for the Ion-Molecule Reaction: $CH_4 + CH_4^+ \rightarrow CH_3 + CH_5^+$", *Chem. Phys. Lett.*, **123**, 331 (1986).

Z. LATAJKA, W.B. PERSON, and K. MOROUMA, "An Ab Initio Calculation of the Infrared Spectrum and Tautomerism of Guanine.", *J. Mol. Str.*, **135**, 253 (1986).

Z. LATAJKA, K. MOROKUMA, H. RATAJCZAK, and W.J. ORVILLE-THOMAS, "Stretching Force Constants of the $H_3N\cdots LiF$ Lithium Bonded and $H_3N\cdots HF$ Hydrogen-Bonded Complexes: Comparison Study at the SCF Level.", *J. Mol. Str.*, **135**, 429 (1986).

I. KUSUNOKI, K. YAMASHITA, and K. MOROKUMA, "Ab Initio Calculations of Doublet States of NH^+.", *Chem. Phys. Lett.*, **123**, 533 (1986).

K. OHTA, G.L. CLOSS, K. MOROKUMA, and N.J. GREEN, "Stereoelectronic Effects in Intramolecular Long-Distance Electron Transfer in Radical Anions as Predicted by Ab Initio MO Calculations.", *J. Am. Chem. Soc.*, **108**, 1319 (1986).

Y. SUGAWARA, A.Y. HIRAKAWA, M. TSUBOI, S. KATO, and K. MOROKUMA, "Ab Initio SCF MO Study on the Force Field of Amides.", *J. Mol. Spectr.*, **115**, 21 (1986).

J.G. YU, X.Y. FU, R.Z. LIU, K. YAMASHITA, N. KOGA, and K. MOROKUMA, "Theoretical Study of Structures and Energies of $[HCOO]^+$ and $[COOH]^+$ and their Rearrangement.", *Chem. Phys. Lett.*, **125**, 438 (1986).

S. NAGAOKA, T. TAKEMURA, H. BABA, N. KOGA, and K. MOROKUMA, "Ab Initio Study on the Low-Lying Triplet States of Chlorobenzene.", *J. Phys. Chem.*, **90**, 759 (1986).

M. TSUKADA, and C. SATOKO, "Electronic Structure of the Pyramidal Cluster Model of the Si(111)7 7 Surface", *Surface Science*, **161**, 289 (1985).

S. SAITO, S. OHNISHI, C. SATOKO, and S. SUGANO, "LCAO-Xα-Force Study on Stable Structures of Si_6 and Si_{10}", *J. Phys. Soc. of Japan*, **55**, 1791 (1986).

J. KAWAI, C. SATOKO, K. FUJISHIMA, and Y. GOHSHI, "Many-electron effects in the shape of the $ClK\alpha_{1,2}$ x-ray emmision lines", *Phys. Rev. Letters*, **57**, 988 (1986).

I. OHMINE, "Mechanism of Nonadiabatic Transitions in Photoisomerization Processes of Conjugated Molecules; Role of Hydrogen Migrations.", *J. Chem. Phys.*, **83**, 2348 (1985).

M. SASAI and H. FUKUTOME, "Coulomb Effects on the Carbon 1s XPS in Doped Polyacetylene.", *Solid State Commun.*, **58**, 735 (1986).

K. TAKATSUKA and H. NAKAMURA, "Semiclassical Theory in Phase Space for Molecular Processes: Scattering Matrix as a Special Case of Phase Space Distribution Function.", *J. Chem. Phys.*, **83**, 3491 (1985).

H. TAKAGI and H. NAKAMURA, "Dissociative Recombination of H_2^+ by Collisions with Slow Electrons.", *J. Chem. Phys.*, **84**, 2431 (1986).

K. SATO, Y. ACHIBA, H. NAKAMURA, and K. KIMURA, "Anomalous Rotational-state Distribution of NO A State in UV Photodissociation of Rare gas-NO Van der Waals Complexes. Rotational Rainbow Effect.", *J. Chem. Phys.*, **85**, 1418 (1986).

M. BAER, S. SUZUKI, K. TANAKA, I. KOYANO, H. NAKAMURA, Z. HERMAN, and D.J. KOURI, "$He+H_2^+$ Ion-molecule Reaction: A Comparison between Experimental and Quantum-mechanical Results.", *Phys. Rev.*, **A34**, 1748 (1986).

M. BAER, H. NAKAMURA, and D.J. KOURI, "Quantum Infinite Order Sudden Approximation for Ion-Molecule Reactions: Treatment of the He + H_2^+ System.", *Intern. J. Quantum. Chem.*: Symposium, **20** (1986).

T. TONUMA, H. SHIBATA, S.H. BE, H. KUMAGAI, M. KASE, T. KANBARA, I. KOHNO, A. OHSAKI, and H. TAWARA, "Production of Highly Charged Slow Ar Ions Recoiled in 1.05-MeV/amu Ne^{q+} (q = 2, 7–10) and Ar^{q+} (q = 4, 6, 10–14)-ion Bombardment.", *Phys. Rev.*, **A33**, 3047 (1986).

S. MURAMATSU, M. AIHARA, and K. NASU, "Depolarization Dynamics of Hot Luminescence: The Time-resolved Spectrum under Pulse-excitation.", *J. Phys. C: Solid State Phys.*, **19**, 2585 (1986).

H. HAYASHI and K. NASU, "Effect of Electron Correlation on The Ground State, The Single-Exciton States, and the Triplet-Exciton States of Trans-Polyacetylene.", *Phys. Rev.*, **B32**, 5295 (1985).

K. NASU, "Periodic Kondo-Hubbard Model for a Quasi-One-dimensional Organic Ferromagnet m-Polydiphenylcarbene: Cooperation between Electron Correlation and Topological Structure.", *Phys. Rev.*, **B33**, 330 (1986).

K. SAKURAI, K. KITAURA, and K. NISHIMOTO, "Partial Structure Analysis of Conjugated Systems. I. Benzene Character," *Theor. Chim. Acta*, **69**, 23 (1986).

Y. KASHIMORI, F. CHIEN, and K. NISHIMOTO, "Theoretical Study of Soliton Dynamics of a Finite One Dimensional Hydrogen-Bonded System", *Chem. Phys.*, **107**, 389 (1986).

Y. OHTA, H. TANAKA, Y. BABA, A. KAGEMOTO, and K. NISHIMOTO, "Solvent Effect on the Hydrogen-Bonding Interaction between Adenine and Uracil", *J. Phys. Chem.*, **90**, 4438 (1986).

K. NAKANISHI, "Effect of Pressure on the Internal Energy of Lennard-Jones Mixtures", *Physica*, **139&140**, 148 (1986).

K. KAWAGUCHI, S. SAITO, and E. HIROTA, "Microwave Spectroscopy of the NCO Radical in the v_2=0 $^2\Pi$, v_2=1 $^2\Delta$, and v_2=2 $^2\Phi$ Vibronic States.", *Mol. Phys.*, **55**, 341 (1985).

Y. ENDO, S. SAITO, and E. HIROTA, "The Microwave Spectrum of the Vinoxy Radical.", *J. Chem. Phys.*, **83**, 2026 (1985).

H. KANAMORI, J.E. BUTLER, K. KAWAGUCHI, C. YAMADA, and E. HIROTA, "Infrared Diode Laser Kinetic Spectroscopy of Transient Molecules Produced by Excimer Laser Photolysis: Application to the SO Radical.", *J. Mol. Spectrosc.*, **113**, 262 (1985).

H. KANAMORI, J.E. BUTLER, T. MINOWA, K. KAWAGUCHI, C. YAMADA, and E. HIROTA, "Infrared Laser Kinetic Spectroscopy.", in "Laser Spectroscopy VII.", T.W. Hänsch and Y.R. Shen Ed., Springer, pp.115-117 (1985).

T. SUZUKI, S. SAITO, and E. HIROTA, "Doppler-Limited Dye Laser Excitation Spectrum of the C_2 Swan Band ($v'-v''$=1–0).", *J. Mol. Spectrosc.*, **113**, 399 (1985).

T. MINOWA, S. SAITO, and E. HIROTA, "The Microwave Spectrum of the PCl Radical in the $X^3\Sigma^-$ State.", *J. Chem. Phys.*, **93**, 4939 (1985).

H. KANAMORI, C. YAMADA, J.E. BUTLER, K. KAWAGUCHI, and E. HIROTA, "Infrared Diode Laser Spectroscopy of the PCl Radical.", *J. Chem. Phys.*, **83**, 4945 (1985).

H. UEHARA, K. KAWAGUCHI, and E. HIROTA, "Diode Laser Spectroscopy of the v_2 and v_3 Fundamental Bands of DO_2.", *J. Chem. Phys.*, **83**, 5479 (1985).

T. SUZUKI, S. SAITO, and E. HIROTA, "Hyperfine Coupling Constants of the CCN Radical in the $\widetilde{A}^2\Delta$(000) State by Microwave-Optical Double Resonance Spectroscopy.", *J. Chem. Phys.*, **83**, 6154 (1985).

K. KAWAGUCHI and E. HIROTA, "Magnetic-Field-Modulated Infrared Laser Spectroscopy of the HBF^+ v_3

Band.", *Chem. Phys. Lett.*, **123**, 1 (1986).

K. KAWAGUCHI, A.R.W. McKELLAR, and E. HIROTA, "Magnetic Field Modulated Infrared Laser Spectroscopy of Molecular Ions: The ν_1 Band of DCO^+.", *J. Chem. Phys.*, **84**, 1146 (1986).

S. SAITO, Y. ENDO, and E. HIROTA, "The Microwave Spectrum of an Unstable Molecule, HPO.", *J. Chem. Phys.*, **84**, 1157 (1986).

M. TANIMOTO, S. SAITO, and E. HIROTA, "Microwave Spectrum of the Boron Monoxide Radical, BO.", *J. Chem. Phys.*, **84**, 1210 (1986).

K. TAKAGI, S. SAITO, T. SUZUKI, and E. HIROTA, "Microwave-Optical Double Resonance of HNO. II. Rotational Spectrum in $\tilde{A}^1A''(020)$.", *J. Chem. Phys.*, **84**, 1317 (1986).

C. YAMADA, Y. ENDO, and E. HIROTA, "Infrared Diode Laser and Millimeter-Wave Spectroscopy of the NCl Radical: Vibrational and Isotopic Dependences of Molecular Constants.", *J. Mol. Spectrosc.*, **115**, 105 (1986).

C. YAMADA, H. KANAMORI, H. HORIGUCHI, S. TSUCHIYA, and E. HIROTA, "Infrared Diode Laser Kinetic Spectroscopy of the CCO Radical in the $\tilde{X}^3\Sigma^-$ State Generated by the Excimer Laser Photolysis of Carbon Suboxide.", *J. Chem. Phys.*, **84**, 2573 (1986).

K. KAWAGUCHI and E. HIROTA, "Infrared Diode Laser Study of the Hydrogen Bifluoride Anion: FHF^- and FDF^-.", *J. Chem. Phys.*, **84**, 2953 (1986).

C. YAMADA and E. HIROTA, "Infrared Diode Laser Spectroscopy of the ν_3 Band of the Fluoromethyl Radical, CH_2F.", *J. Mol. Spectrosc.*, **116**, 101 (1986).

C. YAMADA and E. HIROTA, "Detection of the Silyl Radical SiH_3 by Infrared Diode-Laser Spectroscopy.", *Phys. Rev. Lett.*, **56**, 923 (1986).

C. YAMADA, J.E. BUTLER, K. KAWAGUCHI, H. KANAMORI, and E. HIROTA, "Infrared Diode Laser Spectroscopy of the SCl Radical in the $X^2\Pi_{3/2}$ State.", *J. Mol. Spectrosc.*, **116**, 108 (1986).

K. KAWAGUCHI and E. HIROTA, "Diode Laser Spectroscopy of the BO_2 Radical: The $\varkappa^2\Sigma \leftarrow {}^2\Pi_{3/2}$ Transition of the ν_2 Fundamental Band.", *J. Mol. Spectrosc.*, **116**, 450 (1986).

M. TANIMOTO, S. SAITO, Y. ENDO, and E. HIROTA, "Microwave Spectroscopic Study of the GeF Radical.", *J. Mol. Spectrosc.*, **116**, 499 (1986).

C. YAMADA, Y. ENDO, and E. HIROTA, "Submillimeter-Wave Spectroscopy of the ^{15}NCl Radical: Determination of Born-Oppenheimer Constants.", *J. Mol. Spectrosc.*, **117**, 134 (1986).

K. TANAKA, K. KAWAGUCHI, and E. HIROTA, "Diode Laser Spectroscopy of the ν_4 (HCN Bend) Band of $HCNH^+$.", *J. Mol. Spectrosc.*, **117**, 408 (1986).

T. OGURA, S. YOSHIKAWA, and T. KITAGAWA, "Resonance Raman Study on Photoreduction of Cytochrome c Oxidase; Distinction of the a and a_3-Hemes in the Intermediates.", *Biochemistry*, **24**, 7746 (1985).

T. OGURA, S. YOSHIKAWA, and T. KITAGAWA, "Resonance Raman Spectra of Oxygenated Intermediates of Cytochrome c Oxidase Detected with a Mixed Flow Transient Raman Apparatus.", *Biochim. Biophys. Acta*, **832**, 220 (1985).

S. HASHIMOTO, Y. TATSUNO, and T. KITAGAWA, "Resonance Raman Evidence for Oxygen-Exchange between the Fe^{IV}=0 Heme of Compound II of Horseradish Peroxidase and Bulk Water and Its Relation with the Heme-Linked Ionization.", *Proc. Natl. Acad. Sci. U.S.A.*, **83**, 2417 (1986).

K. KAMOGAWA and T. KITAGAWA, "Raman Difference Spectroscopy of the C-H Stretching Vibrations: Frequency Shifts and Excess Quantities for Acetone/Water and Acetonitrile/Water Solutions.", *J. Phys. Chem.*, **90**, 1077 (1986).

A. MAEDA, T. OGURA, and T. KITAGAWA, "Resonance Raman Study on Proton Dissociated State of Bacteriorhodopsin: Stabilization of L-like Intermediate Having the All-trans Chromophore.", *Biochemistry*, **25**, 2798 (1986).

N. SONE, T. OGURA, and T. KITAGAWA, "Iron-Histidine Stretching Raman Line and Enzymic Activities of Beef- and Bacterium Cytochrome c Oxidase.", *Biochim Biophys. Acta*, **850**, 139 (1986).

T. KITAGAWA, S. HASHIMOTO, and T. OGURA, "Resonance Raman Spectra of Reaction Intermediates of Heme Enzymes." in *"Time Resolved Vibrational Spectroscopy"* (A. Leabreau and M. Stockburger eds.) p.211, Springer-Verlag, Heidelberg (1985).

H. HAMAGUCHI, and K. KAMOGAWA, "A Convenient Line Elimination Optical Filter for Multi-channel Raman Spectroscopy." *Appl. Spectrosc.*, **40**, 564 (1986).

K. TOHJI, Y. UDAGAWA, T. MIZUSHIMA, and A. UENO, "The Structure of the Cu/ZnO Catalyst by an in-situ EXAFS Study", *J. Phys. Chem.*, **89**, 5671 (1985).

K. OZUTSUMI, T. YAMAGUCHI, H. OHTAKI, K. TOHJI, and Y. UDAGAWA, "Structure of Ni(II)- and Zn(II) Glycinato Complexes in Aqueous Solution Determined by EXAFS Spectroscopy", *Bull. Chem. Soc. Jpn.*, **58**, 2786 (1985).

D.M. HANSON, Y. UDAGAWA, and K. TOHJI, "Chemistry of Acetylene Exposed to Alumina and Alumina Supported Rhodium Catalyst", *J. Am. Chem. Soc.*, **108**, 3884 (1986).

K. TOHJI and Y. UDAGAWA, "Present Aspect of X-ray Raman Scattering Measurement", *Bunko Kenkyu*, **35**, 10 (1986).

T. OSUKA, H. MORIKAWA, F. MARUMO, K. TOHJI, Y. UDAGAWA, A. YASUMORI, and M. YAMANE, "Changes in Zr Coordinaiton Number during the Pyrolysis of a SiO_2-ZrO_2 Gel", *J. Noncrystl. Solids*, **82**, 154 (1986).

M. HARADA, K. ONO, A UENO, T. MIZUSHIMA, and Y. UDAGAWA, "Preparation of Fine Fe-Ni Alloy Particles Dispersed in Silica", *Chem. Lett.*, **1986**, 1569.

N. SHIMO, N. NAKASHIMA, and K. YOSHIHARA, "The UV Absorption Spectrum of Trimethylsilyl Radical in the Gas Phase.", *Chem. Phys. Lett.*, **125**, 303 (1986).

N. SHIMO, N. NAKASHIMA, N. IKEDA, and K. YOSHIHARA, "Laser Flash Photolysis of 1-Alkenes at 193 nm in the Gas Phsae: Effect of Molecular Size on the Formation yield of Allyl Radical.", *J. Photochem.*, **33**, 279 (1986).

J. N. MOORE, D. PHILLIPS, N. NAKASHIMA, and K. YOSHIHARA, "Photochemistry of 9,10-Anthraquinone-2,6-disulphonate.", *J. Chem. Soc., Faraday Trans. 2*, **82**, 745 (1986).

T. ICHIMURA, K. NAHARA, Y. MORI, M. SUMITANI, and K. YOSHIHARA, "Triplet Lifetime of Dichlorobenzenes in the Vapour Phase Studied by Time-Resolved and Stationary Observations of Photo-sensitized Phosphorescence.", *J. Photochem.*, **33**, 173 (1986).

T. ICHIMURA, Y. MORI, M. SUMITANI, and K. YOSHIHARA, "Intramolecular Hydrogen Transfer in the o-Tolyl Radical Studied by Time Resolved Absorption Measurement.", *J. Chem. Phys.*, **84**, 1943 (1986).

P.H. BONG, S.C. SHIM, K.H. CHAE, N. NAKASHIMA, and K. YOSHIHARA, "Nanosecond Laser Flash Photolysis Study of 1,2-Bispyrazylethylene.", *J. Photochem.*, **31**, 223 (1985).

P.H. BONG, H.J. KIM, K.H. CHAE, S.C. SHIM, N. NAKASHIMA, and K. YOSHIHARA, "Photochemical Trans $\rightleftarrows$ cis Isomerization of 1,2-Bis(heteroaryl)ethylenes: 1,2-Bis(pyrazyl)ethylene.", *J. Am. Chem. Soc.*, **108**, 1008 (1986).

N. NAKASHIMA, S.R. MEECH, A.R. AUTY, A. JONES, and D. PHILLIPS, "Fluorescence Properties of Provitamin D_2.", *J. Photochem.*, **30**, 207 (1985).

T. SAKATA and K. HASHIMOTO, "Highly Efficient Photocatalytic Production of Amino Acids from Organic Acids-Ammonia-Water by Use of Dyes", *Nouv. J. Chim.*, **9**, 699 (1985).

H. TAKEMURA, T. SAJI, M. FUJIHARA, S. AOYAGUI, K. HASHIMOTO, and T. SAKATA, "Luminsecence Dynamics of Ru(II) Complexes Chemically Immobilized on Semiconductor Particles in Water", *Chem. Phys. Lett.*, **122**, 496 (1986).

T. SAKATA, E. JANATA, W. JAEGERMANN, and H. TRIBUTSCH, "Time-Resolved Photocurrent of WSe_2 Photoanode Studied with a Nanosecond Pulse Laser", *J. Electrochem. Soc.*, **133**, 399 (1986).

M. HIRAMOTO, K. HASHIMOTO, and T. SAKATA, "Visible-Light Induced Water Splitting on New Semiconductor Electrodes Made by Photolithography", *Chem. Lett.*, 899 (1986).

S. OHSHIMA, T. KAJIWARA, M. HIRAMOTO, K. HASHIMOTO, and T. SAKATA, "Excited Tetraphenylporphine on a Silver Surface: Fluorescence Quenching and Interference Effects", *J. Phys. Chem.*, **90**, 4214 (1986).

M. BABA, "Spectroscopic Study of 2-Indanone; The $T_1(n,\pi^*)$ and $S_1(n,\pi^*)$ States", *J. Chem. Phys.*, **83**, 3318 (1985).

I. HANAZAKI, M. BABA, and U. NAGASHIMA, "Orientational Site Splitting of Methyl C-H Overtones in Acetone and Acetaldehyde", *J. Phys. Chem.*, **89**, 5637 (1985).

M. BABA, U. NAGASHIMA, and I. HANAZAKI, "Ab initio Study of the Methyl Internal Rotation of Acetaldehyde in the $S_1(n,\pi^*)$ State", *J. Chem. Phys.*, **83**, 3514 (1985).

R. NAKAGAKI and I. HANAZAKI, "Overtone spectroscopy of Acetyl Compounds. Inequivalent Oscillators and Substituent Effects of the Carbonyl Group", *Chem. Phys. Lett.*, **128**, 432 (1986).

H. SHINOHARA, U. NAGASHIMA, H. TANAKA, and N. NISHI, "Magic Numbers for Water-Ammonia Clusters: Enhanced Stability of Ion Clathrate Structures", *J. Chem. Phys.*, **83**, 4183 (1985).

N. WASHIDA, H. SHINOHARA, U. NAGASHIMA, and N. NISHI, "Ionization of NO_2 Clusters in a Supersonic Nozzle Beam: Appearance of the odd-number cluster ions of NO_2", *Chem. Phys. Lett.*, **121**, 223-227 (1985).

T. ICHIMURA, Y. MORI, H. SHINOHARA, and N. NISHI, "Fast Photodecomposition of Chlorobenzene and m-Chlorotoluene in Molecular Beams at 193 nm", *Chem. Phys. Lett.*, **122**, 51-54 (1985).

T. ICHIMURA, Y. MORI, H. SHINOHARA, and N. NISHI, "Three Dissociation Channels for p-Dichlorobenzene at 193 nm in Molecular Beams", *Chem. Phys. Lett.*, **122**, 55-58 (1985).

N. NISHI, K. YAMAMOTO, H. SHINOHARA, U. NAGASHIMA, and T. OKUYAMA, "A Mass Spectrometric Study of Water Association in Acetonitrile by a New Liquid Expansion Method", *Chem. Phys. Lett.*, **122**, 599-604 (1985).

T. ICHIMURA, Y. MORI, H. SHINOHARA, and N. NISHI, "Photodissociation Channels for Pentafluorobenzene Excited at 193 nm in Molecular Beams", *Chem. Phys. Lett.*, **125**, *263-266 (1986).*

U. NAGASHIMA, H. SHINOHARA, N. NISHI, and H. TANAKA, "Enhanced stability of ion-clathrate structures for magic number water clusters", *J. Chem. Phys.*, **84**, 209-214 (1986).

K. YAMAMOTO and N. NISHI, "Generation of Molecular Beams by the Expansion of Liquid Jet", *J. Spectrosc. Soc. Japan* (in Japanese), **35**, 164-166 (1986).

H. SHINOHARA, N. NISHI, and N. WASHIDA, "Photoionization of Water Clusters at 11.83 eV: Observation of Unprotonated Cluster Ions $(H_2O)_n^+$ $(2 \leq n \leq 10)$", *J. Chem. Soc.*, **84**, 5561-5567 (1986).

K. SEKI, N. NAKASHIMA, N. NISHI, and M. KINOSHITA, "Photochemistry of Acetylene at 193 nm: Two Pathways for Diacetylene Formation", *J. Chem. Phys.*, **85**, 274-279 (1986).

Y. FUKUDA, H. HAYASHI, and S. NAGAKURA, "External Magnetic Field Effects on the Emission Intensities of the $NO(B^2\Pi_r\text{-}X^2\Pi_r)$ Bands in an Afterglow Produced by a Microwave Discharge", *Chem. Phys. Lett.*, **119**, 480 (1985).

R. NAKAGAKI, M. HIRAMATSU, K. MUTAI, and S. NAGAKURA, "Photochemistry of Bichromophoric Chain Molecules Containing Electron Donor and Acceptor Moieties. Dependence of Reaction Pathways on the Chain Length and Mechanism of Photoredox Reaction of N-[ω-(*p*-Nitrophenoxy)alkyl]anilines", *Chem. Phys. Lett.*, **121**, 262 (1985).

K. MUTAI, R. NAKAGAKI, and H. TUKUDA, "A Rationalization of Orientation in Nucleophilic Aromatic Photosubstitution", *Bull. Chem. Soc. Jpn.*, **58**, 2066 (1985).

K. MUTAI and R. NAKAGAKI, "Further Evidence for the Regioselectivity Rules in Nucleophilic Aromatic Photosubstitution", *Bull. Chem. Soc. Jpn.*, **58**, 3663 (1985).

Y. FUKUDA, H. ABE, H. HAYASHI, T. IMAMURA, and S. NAGAKURA, "External Magnetic Field Effects on the Emission Intensities of the OH(A-X) and CH(A-X) Bands in Low Pressure C_2H_2/O_2 and C_3H_8/O_2 Flames", *Chem. Lett.*, **1986**, 777.

M. SANO, I. KANAZAWA, H. MURAKAMI, Y. SAKURAI, T. ENOKI, and H. INOKUCHI, "Position Annihilation in a Hydrogen-Physisorbed Graphite-Caesium Intercalation Compounds.", *Chem. Phys. Letters*, **122**, 143 (1985).

I. KANAZAWA, M. SANO, T. ENOKI, H. MURAKAMI, Y. SAKURAI, and H. INOKUCHI, "Positron Annihilation in Graphite-Alkali Metal-Hydrogen Ternary Systems.", *Synth. Metals*, **12**, 225 (1985).

M. KOBAYASHI, T. ENOKI, H. INOKUCHI, M. SANO, A. SUMIYAMA, Y. ODA, and H. NAGANO, "Superconductivity in The First Stage Rubidium Graphite Intercalation Compounds C_8Rb", *Synth. Metals*, **12**, 341 (1985).

T. ENOKI, K. IMAEDA, M. KOBAYASHI, and H. INOKUCHI, "ESR Studies of Organic Conductors with Bis(ethylenedithio)tetrathiafulvalene(BEDT-TTF), $(BEDT\text{-}TTF)_2ClO_4(C_2H_3Cl_3)_{0.5}$, and $(BEDT\text{-}TTF)_3$

$(ClO_4)_2$, and their Two-Dimensionality.", *Phys. Rev.* **B33**, 1553 (1986).

H. INOKUCHI, G. SAITO, P. WU, K. SEKI, T.B. TANG, T. MORI, K. IMAEDA, T. ENOKI, Y. HIGUCHI, K. INAKA, and N. YASUOKA, "A Novel Type of Organic Semiconductors Molecular Fastener.", *Chem. Lett.*, 1263 (1986).

P. WU, T. MORI, T. ENOKI, K. IMAEDA, G. SAITO, and H. INOKUCHI, "Crystal Structure and Physical Properties of (TTM-TTF)$I_{2.47}$," *Bull. Chem. Soc. Jpn.*, **59**, 127 (1986).

T. MORI, F. SAKAI, G. SAITO, and H. INOKUCHI, "Crystal and Band Structures of β''-(BEDT-TTF)$_2AuBr_2$," *Chem. Lett.*, 1037 (1986).

T. MORI, F. SAKAI, G. SAITO, and H. INOKUCHI, "Crystal Structure and Electrical Properties of an Organic Conductor δ-(BEDT-TTF)$_2AuBr_2$," *Chem. Lett.*, 1589 (1986).

T. MORI and H. INOKUCHI, "Structural and Electrical Properties of (BEDT-TTF)(TCNQ)," *Solid State Commun.*, **59**, 355 (1986).

M. MITSUYA, Y. TANIGUCHI, N. SATO, K. SEKI, and H. INOKUCHI, "An Ultraviolet Photoelectron Spectroscopic Study of Oriented Carboxylic Acid Films Prepared by Vacuum Deposition", *Chem. Phys. Lett.*, **119**, 431 (1985).

N. UENO, K. SUGITA, K. SEKI, and H. INOKUCHI, "Electron Affinities of Polystyrene and Poly(2-vinylpyridine) by Means of Low-energy Electron Inelastic Scattering", *Jpn. J. Appl. Phys.*, **24**, 1156 (1985).

T.B. TANG, K. SEKI, H. INOKUCHI, and T. TANI, "Ionization Thresholds of Merocyanine Dyes in the Solid State", *J. Appl. Phys.*, **59**, 5 (1986).

K. SEKI, H. NAKAGAWA, K. FUKUI, E. ISHIGURO, R. KATO, T. MORI, S. SAKAI, and M. WATANABE, "A Plane-Grating Monochromator for 2 eV ≤ hν ≤ 150 eV", *Nucl. Instrum. Methods Phys. Res.*, **A246**, 264 (1986).

K. SEKI, N. UENO, U.O. KARLSSON, R. ENGELHARDT, and E.-E. KOCH, "Valence Bands of Oriented Finite Linear Chain Molecular Solids as Model Compounds of Polyethylene Studied by Angle-Resolved Photoemission", *Chem. Phys.*, **105**, 247 (1986).

K. SEKI, T.B. TANG, T. MORI, P. WU, G. SAITO, and H. INOKUCHI, "Valence Electronic Structures of Tetrakis(alkylthio)-tetrathiafulvalenes", *J. Chem. Soc. Faraday Trans. 2*, **82**, 1067 (1986).

K. TANAKA, T. KATO, and I. KOYANO, "State Selected Ion-Molecule Reactions by a TESICO Technique. X. $O_2^+(v) + CH_4$.", *J. Chem. Phys.*, **84**, 750 (1986).

I. KOYANO, K. TANAKA, T. KATO, S. SUZUKI, and E. ISHIGURO, "The TEPSICO-II Apparatus for Use with UVSOR Synchrotron Radiation.", *Nucl. Instrum. Methods*, **A246**, 507 (1986).

I. KOYANO, K. TANAKA, and T. KATO, "State Selected Ion-Molecule Reactions by TESICO.", in "*Electronic and Atomic Collisions.*", D.C. Lorents, W.E. Meyerhof, and J.R. Peterson, Eds., Elsevier, pp.529-540 (1986).

M. ITOU, T. HARADA, K. HASUMI, I. KOYANO, and K. TANAKA, "A Normal Incidence Monochromator with an Aberration-Corrected Concave Grating for Synchrotron Radiation.", *Appl. Opt.*, **25**, 2240 (1986).

S. SUZUKI, S. NAGAOKA, I. KOYANO, K. TANAKA, and T. KATO, "The TEPSICO-II Apparatus at UVSOR and Threshold Electron Spectra of Some Molecules over the Wavelength Range 35–120 nm.", *Z. Physik D*, **4**, 111 (1986).

M. BAER, S. SUZUKI, K. TANAKA, I. KOYANO, H. NAKAMURA, Z. HERMAN, and D.J. KOURI, "He + H_2^+ Ion-Molecule Reaction: A Comparison between Experimental and Quantum-Mechanical Results.", *Phys. Rev. A*, **34**, 1748 (1986).

S. NAGAOKA, M. FUJITA, T. TAKEMURA, and H. BABA, "Fluorescence from an Upper Excited State of o-Hydroxybenzaldehyde in the Vapor Phase.", *Chem. Phys. Lett.*, **123**, 489 (1986).

S. NAGAOKA, E.T. Harrigan, M. NODA, N. HIROTA, and J. HIGUCHI, "A Study on the Zero Field Splittings of the Lowest Excited Triplet States of Substituted Benzenes and Related Molecules by Optical Detection of Magnetic Resonance, Electron Paramagnetic Resonance, and Molecular Orbital Calculations.", *Bull. Chem. Soc. Jpn.*, **59**, 355 (1986).

S. NAGAOKA, T. TAKEMURA, H. BABA, N. KOGA, and K. MOROKUMA, "Ab Initio Study on Low-Lying Triplet States of Chlorobenzene.", *J. Phys. Chem.*, **90**, 759 (1986).

T. TAKEMURA, M. FUJITA, and S. NAGAOKA, "Electronic Structures and Energy Relaxation in Low-Lying

Triplet States of Chlorobenzene in Rigid Matrices.", *Chem. Phys. Lett.*, **130**, 39 (1986).

S. TOMODA and K. KIMURA, "Equilibrium Structure and the Two Kinds of Dissociation Energies of the Ammonia Dimer Cation $H_3NH^+...NH_2$", *Chem. Phys. Lett.*, **121** 159 (1985).

Y. NAGANO, Y. ACHIBA, and K. KIMURA, "Laser Photoelectron Spectroscopic Determination of Electronic States of Fe Atoms Produced in Multiphoton Dissociation of $Fe(CO)_5$ in the Gas Phase", *J. Chem. Phys.*, **84**, 1063 (1986).

Y. NAGANO, Y. ACHIBA, and K. KIMURA, "Photoelectron Spectroscopic Interpretation on Background Signal Observed in Multiphoton Ionization Ion-Current Spectrum of Iron Pentacarbonyl", *J. Phys. Chem.*, **90**, 615 (1986).

Y. NAGANO, Y. ACHIBA, and K. KIMURA, "Multiphoton Dissociation of Volatile Iron Complexes, as Revealed by MPI Ion-Current and Photoelectron Spectroscopy", *J. Phys. Chem.*, **90**, 1288 (1986).

K. SATO, Y. ACHIBA, and K. KIMURA, "Photoelectron Spectroscopic Evidence for Photodissociation of the Nitrogen Oxide Dimer in Supersonic Jet", *Chem. Phys. Lett.*, **126**, 306 (1986).

K. SATO, Y. ACHIBA, H. NAKAMURA, and K. KIMURA, "Anomalous Rotational-State Distribution of NO A State in UV Photodissociation of Rare Gas-NO van der Waals Complexes. Rotational Rainbow Effect", *J. Chem. Phys.*, **85**, 1418 (1986).

K. TABAYASHI and K. SHOBATAKE, "Collision Energy Dependence of the Cross Sections for the Electronic Excitation Transfer Reactions: $Rg(^3P_{0,2}) + N_2(X^1\Sigma_g) \rightarrow Rg(^1S_0) + N_2(C^3\Pi_u)$, (Rg = Ar, Kr).", *J. Chem. Phys.*, **84**, 4919 (1986).

K. TABAYASHI and K. SHOBATAKE, "Collision Energy Dependence of the Cross Sections for the Dissociative Excitation Reactions: $Rg(^3P_{0,2}) + NH_3 \rightarrow Rg + NH(A^3\Pi, c^1\Pi) + H_2$, (Rg = Ar, Kr).", *J. Chem. Phys.*, **84**, 4930 (1986).

S. HIRAYAMA, K. SHOBATAKE, and K. TABAYASHI, "Lack of Heavy Atom Effect on the Fluorescence Lifetimes of 9-Cyanoanthracene-Rare Gas Clusters in a Supersonic Free Jet.", *Chem. Phys. Lett.*, **121**, 229 (1985).

F. TANAKA, S. HIRAYAMA, S. YAMASHITA, and K. SHOBATAKE, "Fluorescence Lifetimes of 9-Methylanthracene in Supersonic Free Jets. A Level Invrsion between S_1 and T_2 states upon the Phase Change from Solution to Gas.", *Bull. Chem. Soc. Jpn.*, **59**, 2011 (1986).

R.J. DONOVAN, B.V. O'GRADY, K. SHOBATAKE, and A. HIRAYA, "Fluorescence from Ion-pair and Rydberg states of I_2," *Chem. Phys. Lett.*, **122**, 612 (1985).

T. INABE, S. NAKAMURA, W.-B. LIANG, T.J. MARKS, R.L. BURTON, C.R. KANNEWURF, and K. IMAEDA, "Highly Conductive Metallomacrocyclic Assemblies. Synthesis via Electrocrystallization and Single-Crystal Properties of a Phthalocyanine "Molecular Metal" without Halogen Counterions.", *J. Am. Chem. Soc.*, **107**, 7224 (1985).

T. INABE, W.-B. LIANG, J.F. LOMAX, S. NAKAMURA, J.W. LYDING, W.J. MCCARTHY, S.H. CARR, C.R. KANNEWURF, and T.J. MARKS, "Phthalocyanine-Based Electrically Conductive, Processible Molecular/ Macromolecular Hybrid Materials.", *Synthetic Metals*, **13**, 219 (1986).

K. OHTA, A. TAKAGI, H. MUROKI, I. YAMAMOTO, K. MATSUZAKI, T. INABE, and Y. MARUYAMA, "Novel Discotic Liquid Crystals Obtained from Substituted Bis(dithiolene)nickel Complexes.", *J. Chem. Soc., Chem. Commun.*, **1986**, 883.

Y.I. DOLZHENKO, T. INABE, and Y. MARUYAMA, "In Situ X-Ray Observation on the Intercalation of Weak Interaction Molecules into Perovskite-Type Layered Crystals $(C_9H_{19}NH_3)_2PbI_4$ and $(C_{10}H_{21}NH_3)_2CdCl_4$.", *Bull. Chem. Soc. Jpn.*, **59** 563 (1986).

Y. MARUYAMA, S. SUZUKI, T. OSAKI, H. YAMAGUCHI, S. SAKAI, K. NAGASATO, and I. SHIROTANI, "Electronic Properties of Black Phosphorus Single Crystals and Intercalation Compounds.", *Bull. Chem. Soc. Jpn.*, **59**, 1067 (1986).

S. SUGAI, M. SATO, and S. KURIHARA, "Interphonon interaction at the CDW Phase Transitions in $(TaSe_4)_2I$ and $(NbSe_4)_2I$", *Phys. Rev.*, **B32**, 3004 (1985).

M. SATO, H. FUJISHITA, S. SATO, and S. HOSHINO, "Structural Transitions in Mo_8O_{23}", *J. Phys.*, **C19**, 3059

(1986).

K. NOMURA, K. KUME, and M. SATO, "NMR Study of $Rb_{0.3}MoO_3$: Static Structure and Dynamic Behavior of CDW", *European Workshop on Charge Density Waves in Solids*, p.8 (1986) Zagreb.

T. TAMEGAI, K. TSUTSUMI, S. KAGOSHIMA, Y. KANAI, H. TOMOZAWA, M. TANI, Y. NOGAMI, and M. SATO, "X-ray Study of Field Induced Deformation of Sliding CDW in $K_{0.3}MoO_3$", *Solid State Commun.*, **56**, 13 (1986).

T. TAMEGAI, K. TSUTSUMI, S. KAGOSHIMA, and M. SATO, "Time-Resolved X-ray Study of Sliding CDW in Quasi One-Dimensional Conductor $K_{0.3}MoO_3$", *Nuclear Instruments and Methods in Phys. Research,* **A246**, 801 (1986).

H. FUJISHITA, S.M. SHAPIRO, M. SATO, and S. HOSHINO, "Neutron Scattering Study of the Quasi-One-Dimensional Conductor $(TaSe_4)_2I$", *J. Phys.*, **C19**, 3049 (1986).

K. NOMURA, K. KUME, and M. SATO, "Incommensurate CDW in $Rb_{0.3}MoO_3$: ^{87}Rb NMR", *Solid State Commun.*, **57**, 611 (1986).

K. NOMURA, K. KUME, and M. SATO, "Direct Evidence of Sliding Motion of CDW in $Rb_{0.3}MoO_3$", *J. Phys.*, **C19**, L289 (1986).

T. SUGAWARA, S. MURATA, K. KIMURA, H. IWAMURA, Y. SUGAWARA, and H. IWASAKI, "Design of Molecular Assembly of Diphenylcarbenes Having Ferromagnetic Intermolecular Interactions", *J. Am. Chem. Soc.*, **107**, 5293 (1985).

S. MURATA, T. SUGAWARA, and H. IWAMURA, "Reactivities of Rotameric *ap*- and *sp*-3,5-Dimethyl-2-(9-fluorenyl)phenylnitrenes", *J. Am. Chem. Soc.*, **107**, 6317 (1985).

T. SUGAWARA, S. BANDOW, K. KIMURA, H. IWAMURA, and K. ITOH, "Magnetic Behavior of Nonet Tetracarbene as a Model for One-Dimensional Organic Ferromagnets", *J. Am. Chem. Soc.*, **108**, 368 (1986).

Y. TEKI, T. TAKUI, K. ITOH, H. IWAMURA, and K. KOBAYASHI, "Preparation and ESR Detection of a Ground-State Nonet Hydrocarbon as a Model for One-Dimensional Organic Ferromagnets", *J. Am. Chem. Soc.*, **108**, 2147 (1986).

T. SUGAWARA, H. TUKADA, A. IZUOKA, S. MURATA, and H. IWAMURA, "Magnetic Interaction among Diphenylmethylene Molecules Generated in Crystals of Some Diphenyldiazomethanes", *J. Am. Chem. Soc.*, **108**, 4272 (1986).

N. KOGA, Y. KAWADA, and H. IWAMURA, "Synthesis of 9,10-Bis(9-triptycyloxy)triptycenes; Molecular Design of a System with Doubly Correlated Internal Rotation", *Tetrahedron*, **42**, 1679 (1986).

N. KOGA and H. IWAMURA, "A Kinetic Study of Coupled Internal Rotation in Racemic 2,3-Benzo-9-triptycyl 2-(Dimethylaminomethyl)-9-triptycyl Ether by Means of Exciplex Fluorescence Dynamics", *Chemistry Lett.*, 247 (1986).

H. TUKADA, T. SUGAWARA, S. MURATA, and H. IWAMURA, "An Irreversible Structural Change Observed for Di-(9-naphthyl)methylene in Organic Rigid Glass", *Tetrahedron Lett.*, **27**, 235 (1986).

Y. KAWADA, H. YAMAZAKI, G. KOGA, S. MURATA, and H. IWAMURA, "Bis(9-triptycyl)amines, a Missing Link between the Corresponding Methanes and Ethers. An Unconventional Synthesis and Influence of Nitrogen Inversion on the Coupled Disrotatory Trajectory", *J. Org. Chem.*, **51**, 1472 (1986).

S. ONAKA, T. SUGAWARA, Y. KAWADA, Y. YOKOYAMA, and H. IWAMURA, "^{17}O-NMR Studies on a Series of Manganese Carbonyl Derivatives with Sn-Mn Bonds", *Bull. Chem. Soc. Jpn.*, **59**, 3079 (1986).

H. ITO and T. ITO, "Structures of Monomethylcarbonato- and Hydrogencarbonato(1,4,8,11-tetramethyl-1,4,8,11-tetraazacyclotetradecane)cadmium(II) Perchlorate, $[Cd(O_2COCH_3)(Me_4[14]aneN_4)](ClO_4)$ (I) and $[Cd(O_2COH)(Me_4[14]aneN_4)](ClO_4)$ (II)", *Acta Cryst.*, **C41**, 1598 (1985).

M. YAMASHITA, K. TORIUMI, and T. ITO, "Structure of Bis(isothiocyanato)(1,4,8,11-tetraazacyclotetradecane)nickel(III) Perchlorate", *Acta Cryst.*, **C41**, 1607 (1985).

T. ITO, M. KATO, M. YAMASHITA, and H. ITO, "Utilization of Chemical and Structural Characteristics of Tetraazacycloalkane Complexes.", *J. Cood. Chem.*, **B15**, 29 (1985).

Y. KATO, H. ISAGO, H. OGINO, K. TORIUMI, and T. ITO, "Structural Studies of Thiocyanato and Isothiocyanato Cobalt(III) Complexes Ligating Diamine-N,N′-polycarboxylates", *Bull. Chem. Soc. Jpn.*, **58**, 3506 (1985).

T. TSUBOMURA, S. YANO, K. TORIUMI, T. ITO, and S. YOSHIKAWA, "Structure and Circular Dichroism of Nickel(II) Complexes Containing a Glycosylamine Derived from Ketoses", *Inorg. Chem.*, **24**, 3218 (1985).

M. KATO and T. ITO, "Syntheses, Characterization, and Structures of (Monomethylcarbonato)-Nickel(II), -Copper(II), and -Cobalt(II) Complexes with Tetraazacycloalkanes Obtained from CO_2 Uptake", *Bull. Chem. Soc. Jpn.*, **59**, 285 (1986).

U. SAKAGUCHI and T. ITO, "The Crystal and Molecular Structure of Δ-(8-Methyl-1,3,6,10,13,16,19-heptaazabicyclo[6.6.6]icosane)cobalt(III) Perchlorate Monohydrate", *Bull. Chem. Soc. Jpn.*, **59**, 635 (1986).

N. MATSUMURA, M. TOMURA, S. YONEDA, and K. TORIUMI, "2,3,4,5-Tetrahydro-1,6-diethyl-3,4-propano-6a-thia(S^{IV})-1,3,4,6-tetraazapentalene-2,5-dithione", *Chem. Lett.*, **1986**, 1047.

K. AKIYAMA, T. ISHII, S. TERO-KUBOTA, and Y. IKEGAMI, "Photolytic Generation and the Substituted Dimerizatin of 4-Alkyl-1-methypyridinyl Radicals in Solution as Studied by Steady-state and Kinetic ESR Spectroscopy", *Bull. Chem. Soc. Jpn.*, **58**, 3535 (1985).

N. TOYOTA, T. ITOH, M. KATAOKA, T. FUKASE, H. TAKEI, and Y. MUTO, "Magnetic Field Effect on the Martensitic Transformation Temperature in Nb_3Sn", *Physica*, **135B**, 364 (1985).

E. TORIKAI, A. ITO, Y. TAKADA, K. NAGAMINE, K. NISHIYAMA, Y. SYONO, and H. TAKEI, "Spin Dynamics in Mixed Antiferromagnet with Competing Anisotropies $Fe_{0.6}Co_{0.3}TiO_3$ Proved by Positive Muons", *Solid State Commun.*, **58**, 839 (1986).

H. TAKEI, "Single Crystals of Compound-Superconductors", *Kinzoku*, **56**, 17 (1986), in Japanese.

M. KIKUCHI, K. HIRAGA, Y. SYONO, and H. TAKEI, "Observation of Shocked and Unshocked $BaZnGeO_4$ by Means of Electron Microscopy", *J. Solid State Chem.*, **56**, 390 (1985).

S. TSUNEKAWA, Y. SUZUKI, and H. TAKEI, "Mechanical Properties of Sintered Ultra-fine Al Products", *Trans. Jpn. Inst. Metals*, **26**, 61 (1985).

N. MOMOZAWA, Y. YAMAGUCHI, H. TAKEI, and M. MITA, "Magnetic Structure of $(Ba_{1-x}Sr_x)_2Zn_2Fe_{12}O_{22}$ (x=0–1.0)", *J. Phys. Soc. Jpn.*, **54**, 771 (1985).

L. PINTSCHOVIUS, H. TAKEI, and N. TOYOTA, "Phonon Anomalies in Nb_3Sn", *Phys. Rev. Letters.* **54**, 35 (1985).

H. TAKEI and S. HOSOYA, "Growth of $MnSiO_3$ and $(Mn,Mg)SiO_3$ Crystals by the Floatingzone Method", *J. Crystal Growth*, **71**, 17 (1985).

Y. ISHIKAWA, N. SAITO, M. ARAI, Y. WATANABE, and H. TAKEI, "A New Oxide Spin Glass System of $(1-x)FeTiO_3$–xFe_2O_3 (I), Magnetic Properties", *J. Phys. Soc. Jpn.*, **54**, 312 (1985).

M. ARAI, Y. ISHIKAWA, N. SAITO, and H. TAKEI, "A New Oxide Spin Glass System of $(1-x)FeTiO_3$–xFe_2O_3 (II), Neutron Scattering Studies of a Cluster Type Spin Glass of $90FeTiO_3$–$10Fe_2O_3$", *J. Phys. Soc. Jpn.*, **54**, 781 (1985).

M. ARAI, Y. ISHIKAWA, and H. TAKEI, "A New Oxide Spin Glass System of $(1-x)FeTiO_3$–xFe_2O_3 (IV), Neutron Scattering Studies on a Reentrant Spin Glass of $79FeTiO_3$–$21Fe_2O_3$ Single Crystal", *J. Phys. Soc. Jpn.*, **54**, 2279 (1985).

T. SHISHIDO and H. TAKEI, "Crystal Growth of CsCl-Type $Rh_{50}Al_{50-x}Cu_x$ from Cu Solution", *J. Less Common Metals*, **119**, 75 (1986).

J.M. NEWSAM, Y. ENDOH, Y. ISHIKAWA, and H. TAKEI, "Power Neutron Diffraction Studies of the Mixed Ilumenite System $Fe_{0.6}Co_{0.4}TiO_3$", *J. Phys. C*, **19**, 1273 (1986).

S. HOSOYA, H. TAKEI, Y. KOIKE, N. KOBAYASHI, and T. MUTO, "Growth and Superconducting Properties of $HoMo_6S_8$ Single Crystals", *Jpn. J. Appl. Phys.*, **25**, 115, (1986).

N. SATO, M. KOHGI, T. SATOH, Y. ISHIKAWA, H. HIROYOSHI, and H. TAKEI, "Magnetic States of the Kondo Lattice $CeSi_{1.70}$", *J. Mag. Mag. Materials.* **52**, 360 (1985).

N. MOMOZAWA, Y. YAMAGUCHI, H. TAKEI, and M. MITA, "Modification of Helix in $(Ba_{1-x}Sr_x)_2Zn_2Fe_{12}O_{22}$ due to Applied Magnetic Field", *J. Phys. Soc. Jpn.*, **54**, 3859 (1985).

M. EBIHARA, Y. SASAKI, and K. SAITO, "Mechanism of Acid-catalysed Decomposition of the (Δ,Δ)-(μ-Hydroxo)(μ-preoxo)bis[bis(ethylenediamine)cobalt(III)] Ion", *Inorg. Chem.*, **24**, 3831 (1985).

M. KIKKAWA, Y. SASAKI, S. KAWATA, Y. HATAKEYAMA, F.B. UENO, and K. SAITO, "Photochemical and

Thermal Decomposition of (ΔΔ,ΛΛ)-(μ-Hydroxo)(μ-peroxo)bis[bis(ethylenediamine)cobalt(III)] Ions in Basic Solution", *Inorg. Chem.*, **24**, 4096 (1985).

Y. SASAKI, K. MEGURO, and K. SAITO, "Selectivity Induced by an Optically Active Cationic Cobalt(III) Complex Ion on the Outer-sphere Redox Reaction between Hexachloroiridate(IV) and Racemic Binuclear Molybdenum(V) Anions in Water", *Inorg. Chem.*, **25**, 2277 (1986).

K. OHNO, K. MOROKUMA, F. HIROTA, H. HOSOYA, S. IWATA, Y. OSAMURA, H. KASHIWAGI, S. YAMAMOTO, K. KITAURA, N. KOSUGI, H. NAKATSUJI, S. OBARA, K. TANAKA, M. TOGASHI, and S. YAMABE, "Quantum Chemistry Literature Data Base – Bibliography of Ab Initio Calculations for 1984", *J. Mole. Struct.* (Theochem), **134**, 1 (1985).

Y. WATANABE, Y. SAKAI, and H. KASHIWAGI, "Model Potential Method in As_2 and As_4 Molecular Calculations", *Chem. Phys. Letters,* **120**, 363 (1985).

T. YAMAZAKI, N. TAMAI, and I. YAMAZAKI, "Molecular Association of Pyrene in Langmuir-Blodgett Monolayer Film: Analysis of Picosecond Time-Resolved Fluorescence Spectra.", *Chem. Phys. Lett.*, **124**, 326 (1986).

S. TAZUKE, Y. HIGUCHI, N. TAMAI, N. KITAMURA, N. TAMAI, and I. YAMAZAKI, "Formation and Relaxation of an Excited Complex in a Polymer.", *Macromolecules,* **19**, 603 (1986).

P.-S. SONG, N. TAMAI, and I. YAMAZAKI, "Viscosity Dependence of Primary Photoprocesses of 124 kDalton Phytochrom.", *Biophys. J.*, **49**, 645 (1986).

H. MASUHARA, S. TAZUKE, N. TAMAI, and I. YAMAZAKI, "Time-Resolved Internal Reflection Fluorescence Spectroscopy for Surface Photophysics studies.", *J. Phys. Chem.*, **90**, 5830 (1986).

M. MITSUYA, Y. TANIGUCHI, N. TAMAI, I. YAMAZAKI, and H. MASUHARA, "Fluorescence Spectra of Vacuum-Deposited Films of ω-(1-Pyrenyl)alkanoic Acids.", *Thin Solid Films,* **129**, L45 (1985).

T. ENOKI, M. SANO, and H. INOKUCHI, "Specific Heat of Hydrogen-Alkali Metal Ternary Graphite Intercalation Compounds.", *Synth. Metals,* **12**, 207 (1985).

T. ENOKI, N.-C. YEH, S.-T. CHEN, and M.S. DRESSELHAUS, "Shubnikov-de Haas Experiments on Potassium-Hydrogen Graphite Intercalation Compounds (KH_x-GIC's).", *Phys. Rev.*, **B33** 1292 (1986).

L. SALAMANCA-RIBA, N.-C. YEH, M.S. DRESSELHAUS, M. ENDO, and T. ENOKI, "High-Resolution Transition Electron Microscopy on KH_x-GIC's.", *J. Mater. Res.*, **1**, 177 (1986).

H. TAKAYA, K. MASHIMA, K. KOYANO, M. YAGI, H. KUMOBAYASHI, T. TAKETOMI, S. AKUTAGAWA, and R. NOYORI, "Practical Synthesis of (*R*)- or (*S*)-2,2'-Bis(diarylphosphino)-1,1'-binaphthyls (BINAPs).", *J. Org. Chem.*, **51**, 629-635 (1986).

K. MASHIMA, K. JYODOI, A. OHYOSHI, and H. TAKAYA, "Synthesis of New Fischer-Type Carbene Complexes: Characterization and Reactions of Titanoxycarbene Metal Complexes Derived from $(\eta^5\text{-}C_5Me_5)_2Ti(C_2H_4)$ and Metal Carbonyls.", *J. Chem. Soc., Chem. Commun.*, 1145-1146 (1986).

R. NOYORI, M. OHTA, Y. HSIAO, M. KITAMURA, T. OHTA, and H. TAKAYA, "Asymmetric Synthesis of Isoquinoline Alkaloids by Homogeneous Catalysis.", *J. Am. Chem. Soc.*, **108**, 7117-7119 (1986).

T. MITANI, "Application of Pulse Characteristics of the Synchrotron Radiation", *Optics* (in Japanese), **15**, 336 (1986).

Y. TOKURA, T. KODA, G. SAITO, and T. MITANI, "Pressure-Induced Neutral-to-Ionic Phase Transition in TTF-p-chloranil Studied by Infrared Vibrational Spectroscopy", *Solid State Commun.*, **57**, 607 (1986).

H. YOSHIOKA, S. KAZAMA, T. MITANI, and T. HORIGOME, "Construction of a High-Pressure Electron Spin Resonance Spectrometer Using a Helix Resonator", *Anal. Chem.*, **57**, 2517 (1985).

Y. TAKAGI, "Optical Spin Orientation in Aqueous Solution of Manganese (II) Sulfate", *Opt. Commun.*, **59**, 122 (1986).

Review Articles and Textbooks

I. OHMINE, "Methods for the Electron Correlations; Configuration Interaction and Many Body Perturbation

Theory.", *Monograph Series in Molecular Science,* **2**, Kyoritsu Press (in Japanese) 1986.

H. NAKAMURA, "Semiclassical Theory of Nonadiabatic Transitions", *Butsuri* (in Japanese), **41**, 413 (1986).

R.R. LUCCHESE, K. TAKATSUKA, and V. MCKOY, "Applications of the Schwinger Variational Principle to Electron-Molecule Collisions and Molecular Photoionization", *Phys. Rep.*, **131**, 148 (1986).

K. NASU, M. YAMASHITA, T. MITANI, and S. KURITA, "Optical Excitation and Lattice Relaxation in CDW: Halogen Bridged One-Dimensional Metal Complexes", *Butsuri,* (in Japanese) **41**, 317 (1986).

E. HIROTA, "Molecular Structure of Chemical Reaction Intermediates by High-Resolution Laser Spectroscopy.", *Rev. Laser Eng.* (in Japanese), **13**, 674 (1985).

E. HIROTA and K. KAWAGUCHI, "High Resolution Infrared Studies of Molecular Dynamics.", *Ann. Rev. Phys. Chem.*, **36**, 53 (1985).

E. HIROTA, "Analysis of Molecular Structure by High-Resolution Infrared Spectroscopy.", in "Techniques of Super LSI 9, Semiconductor Process 3, Studies on Semiconductor.", (in Japanese), **22**, J. Nishizawa Ed., Kogyo Chosakai, pp.171-187 (1985).

E. HIROTA, "High Resolution Laser Spectroscopy of Small Molecules.", in "Vibrational Spectra and Structure.", **14**, J.R. Durig Ed., Elsevier, pp.1-67 (1985).

E. HIROTA, "Five Strange Carbon Compounds.", *Chemistry* (in Japanese), **41**, 534 (1986).

T. KITAGAWA, "Resonance Raman Spectra of Reaction Intermediates of Heme Enzymes" in "Advances in Infrared and Raman Spectroscopy", **13**, R.J.H. Clark and R.E. Hester, eds., John Wiley & Sons, 443-481 (1986).

Y. UDAGAWA, "Measurement and Analysis for Catalysis Study (8), EXAFS", *Shokubai*, **28**, 322 (1986).

K. YOSHIHARA, "Flash Photolysis and Chemical Intermediates" in "Molecular Science Series", **7** (in Japanese), S. Nagakura ed., Kyoritsu Publ. Co., pp.261-281.

K. YOSHIHARA, "Laser", *Chem. Education* (in Japanese), **32**, 405 (1984).

K. YOSHIHARA, "Chemistry and Laser", *Chem. Tody* (in Japanese), **181**, 36 (1986).

K. HASHIMOTO, "Photocatalytic Reaction: A New Field in Chemistry", *Kagaku to Kogyo* (in Japanese), **38**, 954 (1985).

T. SAKATA, "Hydrogen Production by Photon Energy", *J. Hydrogen Energy Systems Soc. Japan* (in Japanese), **11**, 17 (1986).

T. SAKATA, "Photocatalytic Organic Synthesis by Use of Semiconductor or Dyes" in "Homogeneous and Heterogeneous Photocatalysis", NATO ASI Series, ed. by E. Pelizetti and N. Serpone, D. Reidel Publishing Company, pp.397-413 (1986).

R. NAKAGAKI, "Photochemistry of Bichromophoric Chain Molecules Containing Electron Donor and Acceptor Moieties", *Kagaku to Kogyo* (in Japanese), **38**, 902 (1985).

R. NAKAGAKI, "Magnetic Field Effects upon Photochemistry Involving Radical Pairs and Biradicals", *Bunko Kenkyu* (in Japanese), **35**, 326 (1986).

H. INOKUCHI, K. SHOBATAKE, and M. WATANABE, "UVSOR and Its Application to Molecular Science.", *Kasokuki Kagaku* (in Japanese), **1**, 15 (1986).

K. SEKI, "Application of Synchrotron Radiation to the Study of Organic Polymers", *Hyomenkagaku* (in Japanese), **7**, 121 (1986).

K. SEKI and H. INOKUCHI, "Electron Spectroscopy", in "Langmuir-Blodgett Films and Electronics" (in Japanese) in (*CMC*, Tokyo, 1986).

K. SEKI, "UV Photoelectron Spectroscopy" in "Organic Materials in Electronics" (in Japanese), (*Science Forum,* Tokyo, 1986).

M. WATANABE, I. KOYANO, and K. SEKI, "The UVSOR Facility at IMS.", *Shinku* (in Japanese), **28**, 729 (1985).

I. KOYANO, "State-to-State Chemistry in Ion-Molecule Reactions: the TESICO Study at the Institute for Molecular Science (IMS).", *ONR Scientific bulletin,* **11**, 86 (1986).

K. KIMURA, "Multiphoton Ionization Photoelectron Spectroscopy for Excited-State Atoms and Molecules", in "Multiphoton Processes" eds. by P. Lambropoulos and S.J. Smith (Springer-Verlag, Berlin, 1984), p.164.

K. KIMURA, "Photoelectron Spectroscopy of Excited States", *Adv. Chem. Phys.*, **60**, 161 (1985).

H. IWAMURA, "High-Spin Polycarbenes as Models for Organic Ferromagnets", *Pure Appl. Chem.,* **58**, 187-196 (1986).

H. IWAMURA, ""Superparamagnetic" Polycarbenes", in "Studies in Organic Chemistry 25, New Synthetic Methodology and Functionally Interesting Compounds", Z. Yoshida, Ed., Kodansha/Elsevier, pp.403-420 (1986).

H. IWAMURA, "Multi-Nuclear NMR", *Kagaku Sosetsu* (in Japanese), **49**, 50-61 (1986).

K. SAITO, "Chemistry of Modern Coordination Chemistry" (in Japanese), Dainippon Tosho Co. (1986).

H. KASHIWAGI et al. (ed. C. NAGATA et al.), "Biomolecules – Electronic Aspects –", *Japan Sci. Soc. Press,*

H. KASHIWAGI and K. MOROKUMA, "Research for World of Molecules by Computer", *Suurikagaku* in Japanese), No.268, 61 (Science Co. Tokko, 1985).

H. KASHIWAGI et al. (ed. T. KAMINUMA), "Biotechnology and Computer Use" (in Japanese), CMC Ltd. Tokyo, 1985.

H. KASHIWAGI et al. (ed. Phys. Soc. Japan), "Supercomputer" (in Japanese), Baifukan, Tokyo, 1985.

H. KASHIWAGI, "Computer Aided Chemistry", ELAN (in Japanese), 1986-MARCH, 28 (Bunkahoso Brain, Tokyo, 1986).

H. KASHIWAGI and S. INA, "Ionization and Charge Transfer in Iron-Porphine", *Kagaku* (in Japanese), No.4 (Kagakudozin, Kyoto 1986).

K. NASU, M. YAMASHITA, T. MITANI, and S. KURITA, "Optical Excitations and Lattice Relaxations in the CDW State.", *Nippon Butsuri Gakkaishi* (in Japanese), **41**, 317 (1986).

T. ENOKI and H. INOKUCHI, "Ternary Graphite Intercalation Compounds.", *Physics,* 7, 203 (1986) (in Japanese).

T. KASUGA, H. YONEHARA, T. KINOSHITA, and M. HASUMOTO, "Beam Properties of UVSOR Storage Ring", *IEEE Trans. Nucl. Sci.,* **NS-32**, 2550 (1985).

T. KASUGA, H. YONEHARA, T. KINOSHITA, and M. HASUMOTO, "Present Status of UVSOR", *IEEE Trans. Nucl. Sci.,* **NS-32**, 3409 (1985).

H. YONEHARA, T. KASUGA, O. MATSUDO, T. KINOSHITA, M. HASUMOTO, J. YAMAZAKI, T. KATO, and T. YAMAKAWA, "Undulator and Wiggler of UVSOR", *IEEE Trans. Nucl. Sci.,* **NS-32**, 3412 (1985).

M. WATANABE, "The UVSOR Facility: Status in 1985", *Nucl. Instr. and Meth.,* **A246**, 15 (1986).

M. WATANABE, I. KOYANO, and K. SEKI, "The UVSOR Facility at IMS", *J. Vac. Soc. Jpn* (in Japanese), **28**, 729 (1985).

H. INOKUCHI, K. SHOBATAKE, and M. WATANABE, "UVSOR and Its Application to Molecular Science", *J. Accel. Sci. and Tech.* (in Japanese), **1**, 15 (1986).

Institute for Molecular Science, Myodaiji, Okazaki 444, Japan